

**EFFECTS OF IRBESARTAN AND DRONEDARONE ON *IN VIVO* GENE
EXPRESSION SIGNATURES OF LEFT ATRIAL TISSUE IN A PORCINE
MODEL OF ACUTE RAPID PACING**

INAUGURAL DISSERTATION

zur
Erlangung des akademischen Grades
Doctor rerum naturalium (Dr. rer. nat.)
an der
Mathematisch-Naturwissenschaftlichen Fakultät
der
Ernst-Moritz-Arndt-Universität Greifswald

vorgelegt von
Ravi Kumar Chilukoti
geboren am 20.11.1978
in Peteru, India

Greifswald, [21.08.2014]

Dekan: Prof. Dr. rer. nat. Klaus Fesser

Erstgutachter: Prof. Dr. rer. nat. Uwe Völker

Zweitgutachter: Prof. Dr. rer. nat. Jens Kockskämper

Tag der Promotion: 10.12.2014

TABLE OF CONTENTS

Abbreviations	5
Summary.....	8
Zusammenfassung	12
1. Introduction.....	18
1.1. ATRIAL FIBRILLATION: CLINICAL RELEVANCE	18
1.2. ATRIAL FIBRILLATION: CLINICAL RISK FACTORS	19
1.3. ATRIAL FIBRILLATION: REMODELING	21
1.4. ATRIAL FIBRILLATION: ELECTRICAL REMODELING	21
1.5. ATRIAL FIBRILLATION: CONTRACTILE DYSFUNCTION (REMODELING).....	25
1.6. ATRIAL FIBRILLATION: ENDOTHELIAL/ ENDOCARDIAL/INFLAMMATORY REMODELING	27
1.7. ATRIAL FIBRILLATION: STRUCTURAL REMODELING.....	28
1.8. ATRIAL FIBRILLATION: ROLE OF THE RENIN- ANGIOTENSIN SYSTEM (RAS)	30
1.9. ATRIAL FIBRILLATION: ROLE OF THE NITRIC OXIDE (NO) IN BLOOD PRESSURE REGULATION.....	31
1.10. NON-ARRHYTHMIC & ANTI-ARRHYTHMIC AGENTS: USE OF IRBESARTAN AND DRONEDARONE IN PREVENTING THE PERPETUATION OF ATRIAL FIBRILLATION	31
2. Aims of the Study	33
3. Materials & Methods.....	34

3.1. MATERIALS	34
3.1.1. Chemicals and kits.....	34
3.1.2. Media for HL-1 and MCF Culturing	35
3.1.3. Buffers	36
3.1.4. Equipment and accessories.....	38
3.1.5. Software used for data analysis.....	38
3.1.6. Primers used for RT q-PCR (Irbesartan study)	38
3.1.7. Primers used for RT-qPCR (oxidative stress/ischaemia-related genes, Dronedarone study)	39
3.1.8. Antibodies used for Immunoblotting.....	40
3.1.9. Rapid Atrial Pacing (RAP) Model.....	41
3.1.10. Cardiomyocyte cell culture	42
3.1.11. RNA Isolation and Quality Control.....	43
3.1.12. Clean-up and concentration of isolated total RNA.....	43
3.1.13. Assessing the purified RNA quantity using an ND-1000 spectrophotometer.....	44
3.1.14. Assessing the purified RNA quality using a Bio-analyzer 2100 44	
3.1.15. Transcriptome analysis	45
3.1.16. Transcriptome Data Analysis	46
3.1.17. <i>In silico</i> pathway- and functional analysis of transcriptome data 52	
3.1.18. Reverse Transcription quantitative PCR (RT-qPCR)	52
3.1.19. Protein extraction and Immuno-blot analysis.....	53
4. Results	55
4.1. HAEMODYNAMICS AND PHYSIOLOGY.....	55
4.2. ARRAY QUALITY AND PRINCIPLE COMPONENT ANALYSIS	57
4.3. IMPACT OF RAP, RAP/I AND RAP/D ON LEFT ATRIAL GENE EXPRESSION.....	59
4.4. IMPACT OF IRBESARTAN AND DRONEDARONE: PARTIAL ATTENUATION OF RAP-INDUCED GLOBAL GENE EXPRESSION CHANGES BY IRBESARTAN AND DRONEDARONE	61

4.5. FUNCTIONAL CATEGORIZATION OF IMPORTANT GENE EXPRESSION SIGNATURES IN RESPONSE TO RAP AND RAP/I.....	64
4.6. DRONEDARONE PREVENTS RAP-INDUCED MICROCIRCULATORY ABNORMALITIES AND OXIDATIVE STRESS/ISCHAEMIA-RELATED GENE EXPRESSION.....	68
4.6.1. Dronedarone prevents RAP-induced oxidative stress	68
4.6.2. Effect of Dronedarone on the RAP-induced redox-sensitive transcription factor NFκB	71
4.6.3. Dronedarone attenuates RAP-induced changes in ischaemia/oxidative stress-related gene expression of left ventricular tissue samples	72
4.7. CANONICAL PATHWAYS INFLUENCED BY IRBESARTAN.....	76
4.8. IMPACT OF RAPID ATRIAL PACING (RAP) ON EXPRESSION OF <i>CTGF</i>	82
4.9. RAP-DEPENDENT REGULATION OF <i>EDN1</i> AND <i>SGK1</i>	84
4.10. RAP-INDUCED SGK1 PHOSPHORYLATION IS PARTLY PREVENTED BY IRBESARTAN	86
4.11. EXPRESSION OF RAS COMPONENTS DURING RAP	88
4.12. CONFIRMATORY EXPERIMENTS WITH THE MURINE HL-1 CARDIOMYOCYTE-LIKE CELL LINE	90
4.12.1. RAP-induced ERK1/2 phosphorylation is partially prevented by irbesartan in the HL-1 cell line.....	90
4.12.2. Frequency-dependent down-regulation of <i>CACNA1C</i> mRNA amounts in HL-1 cells subjected to rapid pacing <i>in vitro</i>	91
4.12.3. Comparison of <i>in vivo</i> transcriptome results from the irbesartan study with previous transcriptome data of paced HL-1 cells reveals similar regulation of most prominent genes.....	92
4.12.4. <i>CTGF</i> expression is transiently induced in HL-1 cells by exogenous administration of ET1.	96
4.12.5. Rapid pacing of HL-1 cells induces <i>CTGF</i> expression <i>via</i> the ET1-SGK1-axis.....	97
5. Discussion	99

5.1. DRONEDARONE PREVENTS AF-(RAP)-INDUCED MICROCIRCULATORY FLOW ABNORMALITIES	101
5.2. “OXIDATIVE STRESS” AND AF: IMPACT OF DRONEDARONE AND IRBESARTAN	102
5.2.1. Panel of oxidative stress-related genes: Mechanistic insights into the actions of dronedarone and irbesartan	103
5.3. ENERGY DEPLETION	107
5.4. TISSUE REMODELING	111
5.5. REGULATION OF <i>CTGF</i>	117
6. References	121
7. Appendix	144
7.1. PUBLICATIONS	144
7.2. CONTRIBUTIONS TO SCIENTIFIC MEETINGS	146
7.3. ORIGINAL ARTICLES	147
7.4. AFFIDAVIT	148
7.5. CURRICULUM VITAE	149
7.6. ACKNOWLEDGEMENTS	151
7.7. SUPPLEMENTARY TABLES OF IRBESARTAN STUDY	153
7.7.1. Supplementary table 1 (RAP)	153
7.7.2. Supplementary table 2 (RAP/I)	153
7.7.3. Supplementary table 3 (Overlap)	153
7.7.4. Supplementary table 4 (genes affected by Irbesartan)	153

ABBREVIATIONS

AF	Atrial fibrillation
ACE	Angiotensin-converting enzyme
ACS	Acute coronary syndromes
ADAM	A disintegrin and metalloproteinase
AGT	Angiotensinogen
ANG II	Angiotensin II
AP	Action potential
AT1R	Angiotensin II type 1 receptor
ATP	Atrial tachypacing
AV	Atrioventricular node
ATHENA	Prevention of Cardiovascular Hospitalization or Death From Any Cause in Patients with Atrial Fibrillation/Atrial Flutter
CaMKII	Ca ²⁺ /calmodulin-dependent protein kinases II
CFR	Coronary flow reserve
CHF	Congestive heart failure
CTGF	Connective tissue growth factor
CVR	Coronary vascular resistance
DAD	Delayed afterdepolarization
EAD	Early afterdepolarization
ECM	Extracellular matrix
ECV	Electrical cardioversion
EDN1/ET1	Endothelin 1
eNOS	Endothelial nitricoxide synthase
ERK 1/2	Extracellular signal regulated kinase 1/2
FFR	Fractional flow reserve
Fn14	FGF-inducible 14-kDa protein
HIF1 α	Hypoxia-inducible factor-1 α

I _{CaL}	L-type Ca ²⁺ current
I _{KCa}	Ca ²⁺ -activated potassium channels
I _{Na}	Na ⁺ -current
I _{Kr}	Rapid delayed rectifier current
I _{Ks}	Slow delayed rectifier current
I _{Kur}	Ultrarapid delayed rectifier current
IP3R	Inositol trisphosphate receptor
MAPK	Mitogen-activated protein kinase
MBF	Myocardial blood flow
MKK3	Mitogen-activated protein kinase kinase 3
MMP	Matrix metalloproteinases
NCX	Na ⁺ /Ca ²⁺ exchanger
NFκB	Nuclear factor kappa-light-chain-enhancer of activated B cells
NOX	NADPH oxidase subunits 1, 2 and 4
NO	Nitric Oxide
PCV	Pharmacological cardioversion
PLN	Phospholamban
PPARGC1	PPARγ coactivator 1-α
PRKAG2	PKA subunit γ-2
RAA	Right atrial appendage
RAP	Rapid atrial pacing
RAP/D	Rapid atrial pacing with dronedarone
RAP/I	Rapid atrial pacing with irbesartan
RAS	Renin-angiotensin system
ROS	Reactive oxygen species
RYR	Ryanodine receptor
SERCA	Sarcoplasmic reticulum Ca ²⁺ -ATPase
SGK1	Serum-and-glucocorticoid-inducible-kinase-1
Sham	Sham operated animal (baseline)

TGF- β	Transforming growth factor beta
TNFRSF12A	Tumor necrosis factor receptor superfamily member 12A
TWEAK	Tumor necrosis factor-like WEAK inducer of apoptosis
VTP	Ventricular tachypacing

SUMMARY

Atrial fibrillation (AF) is the most common sustained cardiac arrhythmia in clinical practice, causing an increasing number of complications and deaths in humans. AF can markedly impair quality of life through symptoms such as palpitations, fatigue and dyspnoea and is independently associated with an increased risk of stroke, heart failure and death. However, AF remains an enigmatic disease arising from multiple, mutually interacting mechanisms. The pathophysiology of AF is very complex and incompletely understood. Though the management of AF has improved greatly in the past few years, therapeutic success rates in AF patients treated with either antiarrhythmic drug therapy or catheter-based ablation, or both remain highly variable, in part because of incomplete understanding of the mechanisms underlying AF.

AF is characterised by electrical and structural remodelling of the atria with atrial fibrosis being one hallmark. ANG-II is a major contributing factor and blockade of its type I receptor AT1R prevents remodelling to some extent. In the present study, the effects of the AT1R antagonist irbesartan and the antiarrhythmic drug dronedarone on left atrial gene expression and profibrotic signalling pathways were explored *in vivo* using a porcine rapid atrial pacing (RAP) model.

The results of the current study demonstrate that acute RAP *in vivo* for 7 h results in profound changes in the global gene expression pattern of left atrial tissue. Microarray-based gene expression profiling of left atrial (LA) tissue specimens revealed substantial changes in atrial gene expression provoked by RAP, which could be partly reversed by irbesartan. Altogether 1134 gene-specific probe sets corresponding to 1001 genes indicated RAP-induced significant expression changes. A total of 585 gene-specific probe sets indicated common (overlapping) changes in expression in RAP and RAP/I when compared with Sham as baseline. Of these 585 probe sets, 151 (25.8% of the overlap) showed a minimum of 15% attenuation of RAP-induced expression change in RAP/I group due to Irbesartan treatment. The transcriptome analysis revealed a RAP-induced overall expression profile reflecting increased ROS production and induction of redox-regulated pathways, tissue remodeling, and energy depletion. Most of these signatures largely reflect RAP-induced increased tissue levels of ANG-II. Previous studies have also clearly demonstrated that AF triggers increases in systemic ANG-II levels, indicating a potential link between AF and AF-induced maladaptive changes such as increased CVR/decreased MBF/LV malperfusion. Blockade of AT1R with irbesartan partially attenuated these maladaptive alterations emphasizing the key role of ANG II-signaling as a major underlying pathomechanism.

The dronedarone study focused on RAP-induced microvascular flow abnormalities. The results show that 6 h of RAP reduced the CFR indicating partial myocardial ischemia but not

the FFR, an indicator of coronary artery stenosis. This demonstrated that there was a ventricular microcirculatory flow disturbance during RAP without significant obstruction of blood flow. The effect was abolished by dronedarone by increasing the CFR, suggesting that the drug prevents RAP-induced microcirculatory flow disturbances. As oxidative stress and calcium overload appeared to be the major underlying mechanisms of microcirculatory flow abnormalities, expression of the oxidative stress molecular markers NOX1/2/4 (members of the NADPH oxidase family) was assessed by Western blotting. Compared with sham levels, expression of these NADPH oxidases was induced 6h after RAP, suggesting ROS production (oxidative stress) during RAP. The ANGII-dependent activation of NADPH oxidase with subsequent increase in cardiac ROS was further confirmed by the demonstration of increased phosphorylation of PKC α and elevated levels of F₂-isoprostanes, the most reliable index of *in vivo* oxidative stress, after RAP. PKC is regulating calcium and potassium channels and phosphorylates the p47^{phox} regulatory NOX subunit. When physically bound to the regulatory NOX subunit p67^{phox}, phosphorylated p47^{phox} plays a pivotal role in the activation of the NOX protein family. Furthermore, RAP induced expression of the redox-sensitive transcription factor NF- κ B. Disturbance of the vascular microcirculation was further associated with RAP-induced significantly increased mRNA amounts of genes related to ischaemia, energy metabolism, and oxidative stress (*VEGF-A*, *PRKAG2*, *DNAJB9*, *PRX3*, *PPARGC1*, *CCL2* and *HIF-1 α*). Finally, these results were confirmed *in vitro* using HL-1 cells by the demonstration of increased amounts of phospho-PKC α in response to RAP. Dronedarone reduced the microvascular flow abnormalities as well as RAP-induced oxidative stress. The drug furthermore caused significantly reduced expression of genes encoding ROS-generating enzymes (NADPH oxidase) and oxidative stress response proteins (PKC, NF- κ B). Dronedarone was therefore capable of attenuating most of the RAP-induced changes in ischaemia/oxidative stress-related gene expression.

Oxidative stress has been closely associated with AF and implicated as playing a critical role in the pathophysiology of heart and other cardiovascular diseases. Previous studies have demonstrated that irbesartan also prevents RAP-induced increased ventricular F₂-isoprostane concentrations. This increase in cardiac ROS levels was further supported by results of the transcriptome analysis from the irbesartan study, which showed significantly elevated mRNA amounts of several prominent genes known to be induced by increased ROS levels (*HMOX1*, *MAFF*, *MAFG*, *SOD2*, *TXNRD1*, *TXNDC1*, *MAP2K3*, and *CP*). With the exception of MKK3 encoded by *MAP2K3* which is part of a phosphorylation cascade involved in transcriptional activation of *HMOX1*, all the encoded proteins mediate protection against increased amounts of ROS. In addition, induction of the heat-shock genes *DNAJA4*, *DNAJB9*, *DNAJC1*, *DNAJC3*, *HSPA4*, *HSPA13*, *HSPA14* and *HSPH1* encoding molecular co-chaperones and chaperones pointed towards ROS production, as it has been

demonstrated that the common regulatory transcription factor of those genes, HSF1, is not only activated by temperature up-shift but also by oxidative stress.

A number of *in vivo* and *in vitro* studies demonstrated association of AF with a higher demand of energy in cardiomyocytes, resulting in transiently decreased concentrations of high-energy phosphates and mitochondrial NADH. Consequently, a high ADP/ATP or AMP/ATP ratio during AF implies reduced energy charge, resulting in the activation of pathways that restore energy homeostasis. The depletion of energy during RAP/AF was indeed clearly indicated by significant increases in *PRKAG2*- and *PPARGC1A*-specific mRNAs under RAP-conditions. Both genes encode key proteins involved in regulation of cellular energy balance, namely a γ -subunit of the AMP-activated protein kinase (AMPK) and the transcriptional co-activator proliferator-activated receptor γ co-activator (PGC)-1 α , respectively. Expression of *SOD2* which is regulated by PGC-1 α and encodes mitochondrial superoxide dismutase 2 was also detected to be up-regulated during RAP. Similarly, the up-regulation of *SLC25A25* encoding mitochondrial ATP-Mg/P_i carrier protein (phosphate carrier), thought to be involved in the control of ATP homeostasis, also indicates the onset of energy depletion.

Alterations in atrial tissue structure (tissue/structural remodeling) have been proposed as a “second factor” after electrical remodeling contributing to the high susceptibility to self-perpetuation of arrhythmia in patients with AF. In response to a variety of stimuli including oxidative stress, cardiac fibroblasts proliferate, differentiate, and synthesize extracellular matrix (ECM) proteins. Furthermore, they produce cytokines that in turn stimulate the fibroblasts, thereby providing positive feedback and perpetuating the fibrogenesis cascade. The resulting ECM accumulation causes fibrosis that favors occurrence and maintenance of AF. Activation of the TWEAK/Fn14-axis has been shown to mediate transcriptional regulation of several genes encoding matrix metalloproteinases involved in remodeling of the extracellular matrix. Consistently, the transcriptome analysis showed pronounced induction of *TNFRSF12A* (*Fn14*) with subsequent down-regulation of *ADAMTS6*, *MMP2*, and *MMP11* as well as up-regulation of *MMP8* and *ADAMTS9*. Additional matrix metalloproteinase encoding genes, namely *ADAMTS7* and *ADAMTS20* turned out to be down-regulated under RAP conditions. The differential regulation of these genes, together with the observed down-regulation of collagen structural genes (*COL1A1*, *COL5A1*, *COL11A1*, *COL14A1*, and *COL15A1*), and genes encoding extracellular matrix component proteins, in particular laminins (*LAMA2* and *LAMB2*) under conditions of RAP might indicate the onset of structural cardiac remodeling, a hallmark of atrial fibrillation.

In addition, the results indicate specific positive regulation of *CTGF* via the axis ANG II-ET-1-SGK1. The present study demonstrated that concomitant to the RAP-dependent increase in *CTGF* mRNA amounts there is a sequential transcriptional induction of *ET-1* and *SGK1*. This

suggests that ET-1, after or in addition to ANG II-mediated transcriptional up-regulation, modulates *CTGF* induction in an auto- and paracrine fashion *via* SGK1 activation by increased transcription of its encoding gene and by specific phosphorylation of the protein. Interestingly, the observed RAP-dependent changes in gene expression were not restricted to the LA, but could often be observed in RA and LV samples too, although to different extents. These specific expression changes were additionally validated by RT-qPCR or immunoblot analyses in LA (left atrium), RA (right atrium), and partly in LV (left ventricle) samples. In support of the proposed hypothesis, the *in vivo* results were further confirmed by exposing HL-1 cardiomyocytes to RAP *in vitro*. Furthermore, exogenously added endothelin-1 (ET-1) induced *CTGF* expression concomitant to the transcriptional activation of *SGK1* in HL-1 cells. Thus, these results add another piece of evidence by demonstrating the efficacy of *ET-1* to induce both *SGK1* and *CTGF* expression.

In summary, the transcriptome data demonstrated that acute RAP for 7h induces significant changes in the expression of several left atrial genes, including those reflecting ANG II-mediated oxidative stress, tissue remodeling, and energy depletion. Furthermore, the results from the dronedarone study demonstrated that this drug is capable of attenuating most of RAP-induced changes in oxidative stress-related gene expression. Accordingly, the haemodynamic parameters also showed that dronedarone reduced RAP-induced microvascular flow abnormalities. This view is supported by the observation that in the used porcine model of acute AF, dronedarone decreased RAP-dependent PKC phosphorylation, NADPH isoform expression, F₂-isoprostane release and IκBα phosphorylation. Additionally, the results of the irbesartan study indicate that *ET-1* contributes to AF-dependent atrial fibrosis by synergistic activity with ANG-II to stimulate *SGK1* expression and enhance phosphorylation of the SGK1 protein which, in turn, induces *CTGF*. The latter has been consistently associated with tissue fibrosis. In support of this view, *in vitro* analyses using HL-1 cells verified *CTGF* induction after short episodes of RAP and additionally in response to exogenous addition of ET-1. Accordingly, irbesartan was shown to attenuate most of the RAP-dependent changes in atrial or ventricular gene expression.

ZUSAMMENFASSUNG

Vorhofflimmern (VHF) stellt die häufigste bedeutsame kardiale Arrhythmie in der klinischen Praxis dar und verursacht eine zunehmende Zahl von Komplikationen und Todesfällen. VHF kann durch Symptome wie Herzrasen, Ermüdung und Atemnot die Lebensqualität erheblich beeinträchtigen und ist mit einem erhöhten Risiko für Schlaganfall und Herzversagen assoziiert. Dennoch sind zahlreiche Aspekte der Entstehung des VHF, die offensichtlich durch mehrere, teilweise miteinander wechselwirkende Mechanismen bedingt wird, immer noch unklar. Die Pathophysiologie des VHF erscheint folglich gegenwärtig als sehr komplex und nur unvollständig verstanden. Obgleich in der Behandlung des VHF in den letzten Jahren insgesamt erhebliche Fortschritte erzielt wurden, haben sich die Erfolgsraten bei Patienten, die entweder durch Medikation mit Antiarrhythmika oder mittels Katheterablation oder mit beiden Therapieformen behandelt wurden als sehr variabel erwiesen, was sich zum Teil auf das nicht hinreichende Verständnis jener Mechanismen zurückführen lässt, welche dem VHF zugrunde liegen. Anhalten des VHF führt zu elektrischem und strukturellem Umbau (*Remodelling*) der Atrien, wobei die atriale Fibrose ein typisches Charakteristikum darstellt. Angiotensin II (ANG II) trägt wesentlich zu diesen Prozessen bei, weshalb die pharmakologische Blockade des ANG II-Typ 1-Rezeptors AT1R das *Remodelling* teilweise abschwächt. In der vorliegenden Arbeit wurden die Auswirkungen des AT1R-Antagonisten *Irbesartan* sowie des Antiarrhythmikums *Dronedaron* auf das globale Genexpressionsprofil sowie auf pro-fibrotische Signalwege im linken Atrium unter den Bedingungen induzierter schneller Vorhofstimulation (*Rapid Atrial Pacing; RAP*) anhand eines porcinen *in vivo*-Modells analysiert.

Die Ergebnisse der *Irbesartan*-Studie zeigten, dass akutes *RAP in vivo* für 7 h umfängliche Veränderungen des linksatrialen Genexpressionsprofils zur Folge hat: Die Mikroarray-basierte Transkriptom-Analyse linksatrialer Gewebeproben detektierte umfangreiche *RAP*-induzierte Veränderungen in den Abundanzan zahlreicher Gen-spezifischer Transkripte, die teilweise in Gegenwart von *Irbesartan* abgeschwächt wurden. Insgesamt 1134 Gen-spezifische Sonden-Gruppen (*Probe Sets*), die 1001 Genen zugeordnet werden konnten, zeigten beim Vergleich mit der Kontrollgruppe (*SHAM*) signifikante, durch *RAP* ausgelöste Expressions-Änderungen an. Der Vergleich der Expressionsprofile *RAP versus SHAM* und *RAP plus Irbesartan versus SHAM* ergab 585 *Probe Sets*, die signifikante überlappende *RAP*-bedingte Genexpressions-Änderungen indizierten. Davon zeigten 151 *Probe Sets*, also 25,8%, eine mindestens 15% ige Veränderung des jeweiligen Faktors der differentiellen Genexpression, die durch *Irbesartan* bedingt war. Die Transkriptom-Analyse in der *Irbesartan*-Studie demonstrierte ein *RAP*-induziertes linksatriales Genexpressions-Profil, das

eine verstärkte Produktion reaktiver Sauerstoff-Spezies (*Reactive Oxygen Species; ROS*), die Induktion Redox-regulierter Signalwege, beginnenden Gewebeumbau (*Remodelling*) und bereits eingesetzte Energieverknappung im betroffenen Gewebe reflektierte. Die meisten dieser Signaturen lassen sich auf *RAP*-induzierte erhöhte ANG II-Gewebekonzentrationen zurückführen. Frühere Studien hatten eindeutig den Nachweis erbracht, dass VHF einen Anstieg der systemischen ANG II-Konzentration bewirkt, was eine mechanistische Verbindung zwischen VHF und dadurch ausgelösten pathologischen Konsequenzen wie erhöhtem koronaren Gefäßwiderstand, verringertem myokardialen Blutfluss und linksventrikulärer Malperfusion darstellen könnte. Pharmakologische Blockade von AT1R mittels *Irbesartan* bewirkte auch eine Abschwächung dieser pathologischen Veränderungen, was bereits die Schlüsselrolle der ANG II-vermittelten Signaltransduktion in diesem Kontext unterstrich.

Oxidativer Stress ist nicht nur sehr stark mit VHF korreliert, sondern es wird auch angenommen, dass er eine Schlüsselrolle in der Pathophysiologie anderer kardiovaskulärer Erkrankungen spielt. Frühere Arbeiten haben bereits überzeugend gezeigt, dass *Irbesartan* unter anderem einen *RAP*-induzierten Anstieg der ventrikulären F₂-Isoprostan-Konzentration abschwächt. F₂-Isoprostane gelten als die verlässlichsten *in vivo*-Indikatoren für oxidativen Stress. Der *RAP*-induzierte Anstieg der kardialen ROS-Konzentrationen spiegelte sich auch in den Ergebnissen der Transkriptom-Analyse in der vorliegenden Arbeit wieder, die signifikant erhöhte mRNA-Mengen mehrerer ROS-responsiver Indikator-Gene zeigten (*HMOX1*, *MAFF*, *MAFG*, *SOD2*, *TXNRD1*, *TXNDC1*, *MAP2K3* und *CP*). Mit Ausnahme der *MAP2K3*-kodierten MKK3-Kinase, die Teil einer Phosphorylierungskaskade ist, welche in die transkriptionelle Aktivierung von *HMOX1* involviert ist, vermitteln alle kodierten Proteine Schutz gegen ROS. Zusätzlich belegte auch die Induktion der Hitzeschock-Gene *DNAJA4*, *DNAJB9*, *DNAJC1*, *DNAJC3*, *HSPA4*, *HSPA13*, *HSPA14* und *HSPH1*, welche für molekulare Ko-Chaperone und Chaperone kodieren, verstärkten oxidativen Stress, da bereits früher gezeigt wurde, dass der diesen Genen gemeinsame Transkriptionsfaktor HSF1 nicht nur durch Temperaturerhöhung, sondern auch durch erhöhte ROS-Konzentrationen aktiviert wird.

Eine große Zahl von *in vivo*- und *in vitro*-Studien demonstrierte bereits früher, dass VHF mit einem erhöhten Energiebedarf der Kardiomyozyten einhergeht, was sich in verringerten Konzentrationen zellulärer Energie- und Reduktionsäquivalente niederschlägt. Erhöhte VHF-bedingte ADP/ATP-bzw. AMP/ATP-Quotienten signalisieren dabei eine reduzierte zelluläre Energieladung, was zur Aktivierung von Signalwegen führt, welche die Wiederherstellung der Energie-Homöostase zum Ziel haben. Der Energiemangel während VHF bzw. *RAP* schlug sich in der Transkriptomanalyse der vorliegenden Arbeit deutlich in signifikanten Anstiegen der *PRKAG2*- und *PPARGC1A*-spezifischen mRNA-Mengen unter *RAP*-Bedingungen

nieder. Beide Gene kodieren Schlüsselproteine, die in die Regulation des zellulären Energiegleichgewichts involviert sind, namentlich eine γ -Untereinheit der AMP-aktivierten Proteinkinase (AMPK) und den Transkriptions-Ko-Aktivator *proliferator-activated receptor γ co-activator* (PGC)-1 α . Die Expression von *SOD2*, welches durch PGC-1 α positiv reguliert wird und die mitochondriale Superoxid-Dismutase 2 kodiert, wurde ebenfalls durch *RAP* induziert. In ähnlicher Weise demonstrierte die verstärkte Expression von *SLC25A25*, welches ein mitochondriales ATP-Mg/Pi Carrier-Protein (einen Phosphat-Carrier) kodiert, von dem angenommen wird, dass er in die Kontrolle der ATP-Homöostase involviert ist, die bestehende *RAP*-bedingte Energieverknappung.

Ein Umbau der atrialen Gewebestruktur (strukturelles *Remodelling*) war bereits früher als „zweiter Faktor“ nach dem elektrischen *Remodelling* vorgeschlagen worden, welcher zu der hohen Anfälligkeit zur Selbstverstärkung und Verstetigung der Arrhythmie bei VHF-Patienten beiträgt. Als Antwort auf eine Vielzahl von Stimuli, darunter oxidativer Stress, beginnen kardiale Fibroblasten zu proliferieren, zu differenzieren und verstärkt Proteine der extrazellulären Matrix (*Extracellular Matrix*, *ECM*) zu synthetisieren. Außerdem produzieren sie Zytokine, die ihrerseits wiederum stimulierend auf die Fibroblasten zurückwirken, wodurch diese positive Rückkopplung eine Selbst-Verstärkung der Fibrogenese-Kaskade zur Folge hat. Die daraus resultierende ECM-Akkumulation führt zu Fibrose, welche die Verstetigung des VHF begünstigt. In diesem Zusammenhang vermittelt die Aktivierung der sogenannten TWEAK/Fn14-Achse die transkriptionelle Regulation mehrerer Gene, die für den Umbau (das *Remodelling*) der ECM involvierte Matrix-Metalloproteinasen kodieren. In Übereinstimmung hiermit zeigte die Transkriptom-Analyse der vorliegenden Arbeit eine deutliche *RAP*-abhängige Induktion von *TNFRSF12A* (*Fn14*) sowie, mit großer Wahrscheinlichkeit als deren Konsequenz, Repression von *ADAMTS6*, *MMP2* und *MMP11* und Induktion von *MMP8* und *ADAMTS9*. Weitere für Matrix-Metalloproteinasen kodierende Gene, namentlich *ADAMTS7* und *ADAMTS20*, zeigten eine *RAP*-induzierte Repression. Die differentielle Regulation der genannten Gene, zusammen mit der ebenfalls beobachteten Repression mehrerer Kollagen-Strukturgene (*COL1A1*, *COL5A1*, *COL11A1*, *COL14A1* und *COL15A1*) und für Laminin-Komponenten der ECM kodierender Gene (*LAMA2* und *LAMB2*) unter *RAP*-Bedingungen lässt sich als Signatur für das strukturelle kardiale *Remodelling*, ein wesentliches Merkmal des VHF, interpretieren.

Zusätzlich zu den beschriebenen Mikroarray-basierten globalen Genexpressions-Signaturen konnte im Rahmen der vorliegenden Arbeit eine spezifische positive Regulation des Gens *CTGF* über die Signaltransduktions-Achse ANG II- Endothelin-1 (ET-1) -Stress/ Glukokortikoid-regulierte Kinase 1 (SGK1) experimentell demonstriert werden. Demnach geht der *RAP*-induzierten Zunahme an *CTGF*-spezifischer mRNA eine sequentielle transkriptionelle Induktion der Gene *ET-1* und *SGK1* voraus. Dies legte ein Modell nahe,

demzufolge nach ANG II-vermittelter transkriptioneller *ET-1*-Induktion das resultierende ET-1-Protein nach Sekretion und Bindung an seinen Rezeptor eine auto- und parakrine Aktivierung von SGK1 mittels verstärkter *SGK1*-Transkription und aktivierender Phosphorylierung von SGK1 bewirkt. Dieses aus den *in vivo*-Analysen abgeleitete Modell wurde *in vitro* unter Nutzung der murinen kardialen Herzmuskel-Zelllinie HL-1 validiert: Exogene Zugabe von ET-1 zu HL-1-Zellen resultierte in transkriptioneller *CTGF*-Induktion, und die HL-1-Zellen reagierten auf elektrische Hochfrequenz-Stimulation mit der postulierten sequentiellen transkriptionellen Induktion von *ET-1*, *SGK1* und *CTGF*. Interessanterweise waren die insgesamt detektierten *RAP*-abhängigen Genexpressions-Änderungen häufig nicht auf das linke Atrium beschränkt, sondern konnten auch in Gewebeproben des rechten Atriums sowie des linken Ventrikels mittels RT-qPCR oder Western-Blotting nachgewiesen werden, wenngleich in unterschiedlichem Ausmaß.

Im Zentrum der im Rahmen der vorliegenden Arbeit durchgeführten Analysen zur Wirkungsweise des Antiarrhythmikums *Dronedaron* standen zunächst *RAP*-induzierte mikrovaskuläre Durchblutungsstörungen. Die Ergebnisse der *Dronedaron*-Studie zeigten, dass akutes *RAP in vivo* für 6 h die koronare Flussreserve (*Coronary Flow Reserve; CFR*) reduzierte, was auf eine partielle myokardiale Ischämie hinwies, während die fraktionale Flussreserve (*Fractional Flow Reserve; FFR*), die einen Indikator für eine Stenose der Koronararterien darstellt, unverändert blieb. Dies belegte eine *RAP*-bedingte Störung der ventrikulären Mikrozirkulation, die jedoch keine deutliche Beeinträchtigung der Durchblutung zur Folge hatte. Dieser Effekt wurde durch *Dronedaron* aufgehoben, welches eine Erhöhung der *CFR* bewirkte, was den Schluss zulässt, dass das Antiarrhythmikum *RAP*-induzierte mikrozirkulatorische Durchblutungsstörungen verhindert. Da oxidativer Stress und zelluläre Calcium-Überladung die wichtigsten bekannten Faktoren darstellen, die mikrozirkulatorischen Durchblutungsstörungen zu Grunde liegen, wurden nachfolgend die Gewebe-spezifischen Abundanzen der Proteine NOX1, NOX2 und NOX3 mittels Western-Blotting bestimmt. Alle drei Proteine gehören der Familie der ROS-generierenden NADPH-Oxidasen an und stellen damit Indikatoren für oxidativen Stress dar. Im Vergleich mit der *SHAM*-Bedingung zeigten die drei Proteine erhöhte Mengen nach 6 h *RAP*, was auf eine dadurch bedingte erhöhte Menge an ROS und damit auf *RAP*-induzierten oxidativen Stress schließen ließ. Weiterhin wurde die aus der Literatur bekannte ANG II-abhängige Aktivierung der NADPH-Oxidasen durch den Nachweis verstärkter aktivierender Phosphorylierung der PKC α -Kinase sowie durch den direkten Nachweis erhöhter Mengen an F₂-Isoprostanen im betroffenen Gewebe belegt. Aktivierte PKC reguliert durch Phosphorylierung Calcium- und Kalium-Kanäle und katalysiert insbesondere eine aktivierende Phosphorylierung der regulatorischen NOX-Untereinheit p47^{phox}. Phosphoryliertes p47^{phox} bindet an die regulatorische NOX-Untereinheit p47^{phox}, was einen wesentlichen Schritt im Rahmen der

Aktivierung der Mitglieder der NOX-Protein-Familie darstellt. Darüber hinaus wurde der Nachweis geführt, dass *RAP* die Expression des Redox-sensitiven Transkriptionsfaktors NF- κ B induziert, und es konnten signifikant erhöhte mRNA-Mengen der Gene *VEGFA*, *PRKAG2*, *DNAJB9*, *PRX3*, *PPARGC1*, *CCL2* und *HIF1A* unter *RAP*-Bedingungen detektiert werden. Die von diesen Genen kodierten Proteine erfüllen zelluläre Funktionen, die sich den Kategorien *Ischämie*, *Energiestoffwechsel* und *Oxidativer Stress* zuordnen lassen. Abschließend wurden einige der *in vivo* erzielten Ergebnisse *in vitro* unter Nutzung der HL-1-Zelllinie bestätigt: Auch die HL-1-Zellen reagierten auf elektrische Hochfrequenz-Stimulation durch verstärkte Phosphorylierung von PKC α .

Insgesamt konnte in der *Dronedaron*-Studie gezeigt werden, dass das Antiarrhythmikum *RAP*-induzierten oxidativen Stress sowie wahrscheinlich dadurch bedingte mikrovaskuläre Durchblutungsstörungen reduziert. Dies wurde durch die signifikant geringere Expression von Genen, die für ROS-generierende Enzyme (NAPDH-Oxidasen) sowie für ROS-induzierte Proteine (NF- κ B) kodieren, sowie durch abgeschwächte aktivierende PKC-Phosphorylierung deutlich. *Dronedaron* schwächte insgesamt einen großen Teil jener *RAP*-induzierten Genexpressionsmuster ab, die in den funktionellen Kontext von Ischämie und oxidativem Stress einzuordnen waren.

Zusammenfassend lässt sich aus der *Irbesartan*- und der *Dronedaron*-Studie schließen, dass akutes *RAP* für 7 h signifikante Änderungen in der linksatrialen Genexpression bewirkt, darunter solche, die indikativ sind für ANG II-vermittelten oxidativen Stress, atrialen Gewebeumbau (*Remodeling*) und zelluläre Energieverknappung. Darüberhinaus zeigen die Ergebnisse der *Dronedaron*-Studie, dass das Antiarrhythmikum eine große Zahl der *RAP*-induzierten Genexpressions-Änderungen, die durch oxidativen Stress bedingt sind, reduziert. In Übereinstimmung hiermit demonstrierten die haemodynamischen Parameter ebenfalls eine Verringerung *RAP*-induzierter mikrovaskulärer Durchblutungsstörungen durch *Dronedaron*. Das Antiarrhythmikum schwächte außerdem weitere *RAP*-abhängige Effekte ab, namentlich die Phosphorylierung von PKC und I κ B α , die Induktion der Expression verschiedener NAPDH-Oxidasen, und die Erhöhung der Gewebekonzentration von F₂-Isoprostanen. Diese Ergebnisse sind konsistent mit der Vorstellung, dass ein großer Teil der Änderungen der *RAP*-induzierten linksatrialen Genexpression sowie der damit verbundenen pathologischen Effekte durch ANG II-induzierten oxidativen Stress vermittelt werden. Konsistent hiermit schwächte *Irbesartan*, welches den ANG II-Typ 1-Rezeptor AT1R blockiert, seinerseits die meisten *RAP*-induzierten linksatrialen Genexpressionsänderungen ab. Ein weiteres wesentliches Ergebnis besteht darin, dass ET-1 zur VHF-bedingten atrialen Fibrose beiträgt, indem es nach ANG II-vermittelter transkriptioneller Aktivierung seines Strukturgens sowohl die Expression von *SGK1* als auch die Phosphorylierung der davon kodierten Kinase stimuliert, die dann ihrerseits die Expression von *CTGF* induziert. Vom

CTGF-Protein wird schon seit längerer Zeit angenommen, dass es pro-fibrotisch wirkt. An HL-1-Zellen durchgeführte *in vitro*-Analysen bestätigen diese Folgerungen: Hochfrequenz-Stimulation induziert die sequentielle transkriptionelle Induktion von *ET-1*, *SGK1* und *CTGF*, und exogenes ET-1 führt zur Induktion der *CTGF*-Expression.

1. INTRODUCTION

1.1. ATRIAL FIBRILLATION: CLINICAL RELEVANCE

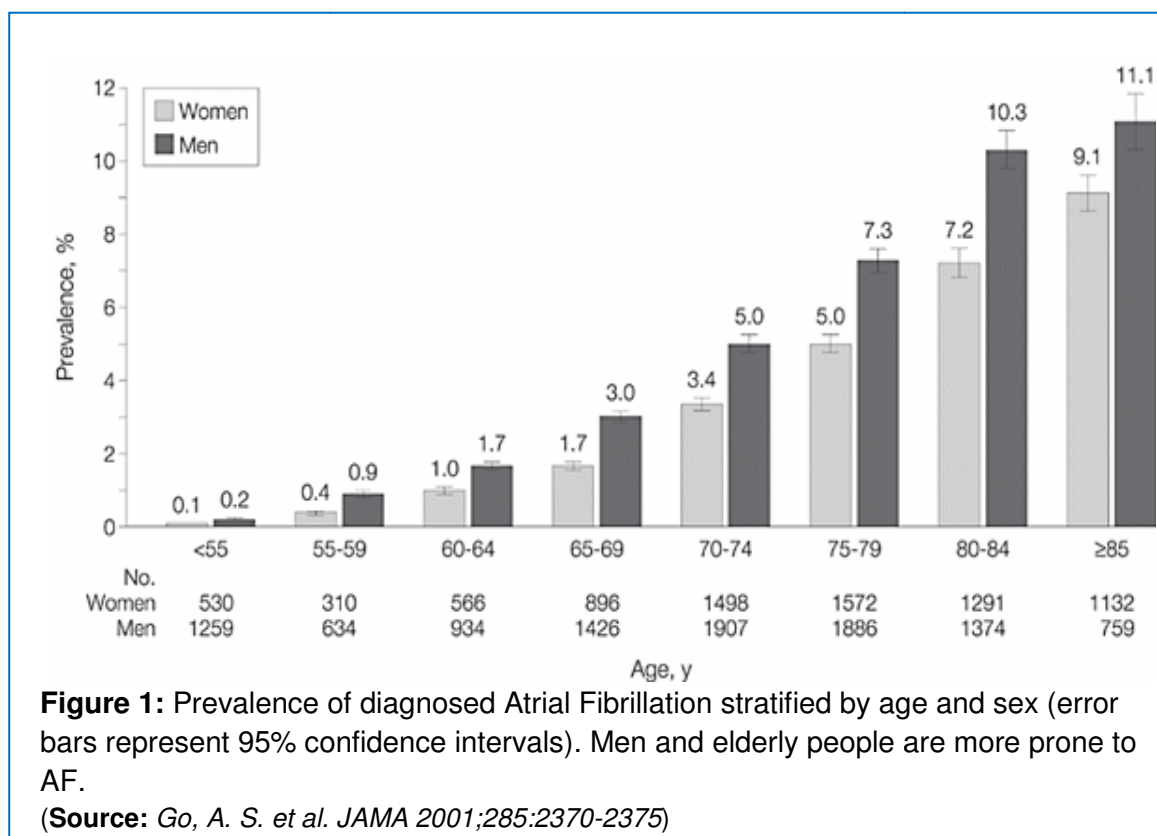
Atrial fibrillation (**AF**) is the most common form of serious cardiac arrhythmia in humans, causing an increasing number of potential complications such as stroke and heart failure and contributing significantly to population morbidity and mortality (Fuster et al., 2006; Gaborit et al., 2005; Nattel et al., 2008; Schotten et al., 2011). Normal cardiac rhythm is initiated in the sino-atrial (SA) node of the right atrium. From there, electrical excitation spreads through the atria, finally causing their activation. Subsequently, excitation is transmitted to the ventricles *via* the atrio-ventricular (AV) node, located centrally between atria and ventricles, and further through the His-Purkinje conducting system leading to ventricular activation. The AV node acts as a frequency filter preventing excessive ventricular rates (ventricular arrhythmia). Thus, the coordinated conduction of the electrical signal ensures regular (rhythmic) sequential activation and contraction of atria and ventricles.

During AF, rapid irregular electrical activation of the atria causes their rapid incomplete contraction, resulting in insufficient pre-loading of the ventricles, and a subsequently decreased ventricular ejection fraction, which finally generates clinical symptoms such as palpitations, shortness of breath, fatigue, and chest discomfort (Wakili et al., 2011). To restore the normal rhythm of the heart, clinicians generally perform cardioversion in two ways: either by using drugs (pharmacological cardioversion, PCV) or therapeutic dosing of electrical impulses (electrical cardioversion, ECV).

AF may be classified as first diagnosed AF, paroxysmal, persistent, longstanding persistent AF and permanent AF. If a patient is presenting with AF for the first time irrespective of the duration of the arrhythmia or the presence and severity of AF-related symptoms that patient is considered as first diagnosed AF patient. Paroxysmal AF is characterized by self-terminating episodes of ≤ 48 hours. In persistent AF, the episodes last longer than seven days or require cardioversion to restore sinus rhythm. Longstanding persistent AF is defined as lasting longer than 1 year. Permanent AF is refractory to cardioversion or when attempts at establishing sinus rhythm are no longer pursued (European Heart Rhythm Association et al., 2010).

Incidence and prevalence of AF are increasing worldwide and electrocardiogram (ECG)-based surveys suggest that ~ 1 -2% of the total population is affected (Go et al., 2001; Kannel et al., 1998). The prevalence of AF increases with advancing age. Hence, AF is frequent in the elderly, with a prevalence of $\sim 20\%$ in patients >85 years of age (Heeringa et al., 2006).

The number of patients with AF is likely to double or triple within the next two to three decades due to the increasing average age in the human population (Developed with the special contribution of the European Heart Rhythm Association (EHRA) et al., 2010; Go et al., 2001; Hobbs et al., 2005).



The prevalence of AF is also sex dependent, as men are more prone to AF than women in the similar age group (Go et al., 2001; Heeringa et al., 2006). As indicated by epidemiological and other observational studies, AF is associated with high mortality and approximately doubles the mortality rate, independent of other known cardiovascular conditions. The major reason for the high mortality rate associated with AF is an increased risk for atrial thrombus formation and subsequent thromboembolic events finally causing ischemic stroke. Out of all ischemic strokes, AF accounts for 30% and recent data indicate that it has already reached 50%. Strokes due to AF are more severe than strokes of other origin (Benjamin et al., 1998; Miyasaka, 2005; Nieuwlaat et al., 2008).

1.2. ATRIAL FIBRILLATION: CLINICAL RISK FACTORS

Most AF episodes are asymptomatic and usually self-terminated after a very short duration. When the frequency increases over time, typically progressing over decades, the individual episodes are extended, and eventually permanent forms of AF develop, which may become resistant to cardioversion (Israel et al., 2004; Ulrich Schotten et al., 2011). As shown in *figure*

2, AF progresses from undiagnosed to first diagnosed, paroxysmal, persistent and permanent forms (typical pattern of time in AF (black) and sinus rhythm (gray) over time on x-axis) (Schotten et al., 2011). This progression of AF- to become chronic is partly caused by AF itself, which can be conceived as “AF begets AF”. The time course of AF stabilization is more rapid in patients with structural heart disease, than in “lone AF” patients (Kato et al., 2004).

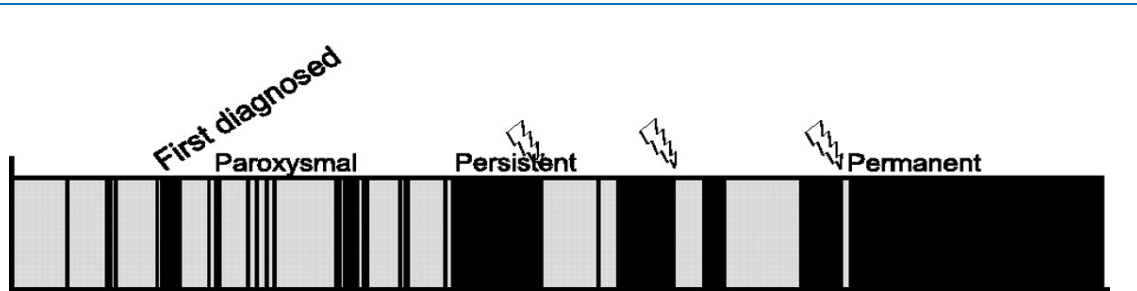


Figure 2: The “natural” course of the arrhythmia progression in an atrial fibrillation (AF) patient. Black coloring indicates AF, gray coloring indicates sinus rhythm. The undiagnosed AF events become more and more frequent and finally progress to permanently stabilized AF.

(Source: Schotten U et al. *Physiol Rev* 91: 265-325, 2011)

There are numerous clinical conditions associated with the initiation of AF. They are likely due to the changes in the atrial myocardium, also referred to as remodeling. Most of these factors contribute to a gradual and progressive process of atrial remodeling characterized by changes in ion channel expression and function, Ca^{2+} homeostasis, and atrial structure such as cellular hypertrophy, activation of fibroblasts, and tissue fibrosis. The mechanisms or clinical conditions that initiate episodes of the arrhythmia have not been fully elucidated. One reason could be that the majority of patients with the above-mentioned AF-causing factors never experience AF in their lifetime. The factors shown to be associated with lone AF, like abnormal calcium handling and stretch-activated automaticity, favor the inducibility of prolonged AF episodes. Also, focal ectopic beats originating in the pulmonary veins initiate AF in many patients. Although some experimental studies have attempted to identify arrhythmogenic mechanisms in these ectopic foci i.e. pulmonary veins and adjacent myocardium, the prominent role of the pulmonary veins in AF remains poorly understood (Bode et al., 2001; Haïssaguerre et al., 1998, 1998; Patterson et al., 2007; Rostock et al., 2008).

The cardiac and non-cardiac clinical conditions associated with the development of a substrate for AF are as follows:

- Hypertension (Pathologically increased blood pressure associated with 60-80% of AF patients)
- hyper- aldosteronemia (12x increased risk)
- Coronary Artery Diseases (25-33% of AF patients)
- Heart failure (30%-40% of AF patients)
- Mitral valve defects
- Insulin resistance & diabetes (~20% of AF patients)
- Hyperthyroidism
- Alcohol, Smoking
- Obesity
- Inflammation
- COPD (Chronic obstructive pulmonary disease)
- Genetic predisposition& familial history

The predominant risk factor associated with AF is hypertension, which causes atrial hypertrophy (increased left atrial diameter) due to increased systemic resistance (Cuspidi et al., 2013; Takaoka et al., 2013; Watanabe et al., 2013). AF and hypertension are both associated with elevated levels of serum- and local AngII, which in turn stimulates production of the adrenocorticoide, aldosterone, resulting in its increased blood levels (hyper-aldosteronemia). Hyper-aldosteronemia is in turn associated with an increased prevalence of AF due to increased blood pressure (Reil et al., 2012; Watson et al., 2009). The other risk factors such as insulin resistance, smoking and obesity are indirectly associated with AF as they strongly contribute to the development of hypertension (Targher et al., 2013). These clinical conditions seem to enhance the inducibility of AF in an additive manner, as the studies indicate that the risk of persistent AF gradually increases depending on the number of such conditions present (Cleland, 2003; Nabauer et al., 2008; Nieuwlaet, 2005).

1.3. ATRIAL FIBRILLATION: REMODELING

The progressive nature of AF is due to many changes in the atria, which are also referred to as remodeling. AF-mediated atrial remodeling can be further categorized as electrical, contractile, endothelial/endocardial (inflammatory) and structural remodeling.

1.4. ATRIAL FIBRILLATION: ELECTRICAL REMODELING

The main ionic currents underlying atrial or ventricular action potential (AP) are *Inward/depolarizing* currents and *outward/repolarizing* currents. In sinus rhythm, the shape of

the atrial AP is triangular with a gradual repolarization (outward) phase that is less pronounced compared to that of left ventricular myocytes. The main depolarizing currents in atria and ventricles, the Na^+ -current (I_{Na}), and the L-type Ca^{2+} current (I_{CaL}), are both activated and inactivated by rapid opening and closing of specific cytoplasmic membrane channels, namely the *SCN5a* encoded NaV1.5 Na^+ -channel and the *CACNA1C* encoded CaV1.2 Ca^{2+} -channel, where the latter shows a somewhat slower kinetic (Greiser et al., 2011; Nattel, 2002; Schotten et al., 2011). The $\text{Na}^+/\text{Ca}^{2+}$ exchange current I_{NCX} is mediated by the cytoplasmic membrane $\text{Na}^+/\text{Ca}^{2+}$ -ion exchange system encoded by *NCX* and serves as both depolarizing and repolarizing current, depending on the actual intra- and extracellular concentrations of Na^+ and Ca^{2+} . In the context of membrane repolarization, the ultra-rapid delayed rectifier current I_{Kur} , the rapid delayed rectifier current I_{Kr} , the transient outward current I_{to} , the slow delayed rectifier current I_{Ks} , and the inward rectifier K^+ current I_{K1} are mediated by opening of the cytoplasmic membrane channels Kv1.5 (encoded by *KCNA5*), Kv11.1 (encoded by *KCNH2*), Kv4.3 (encoded by *KCND3*), Kv7.1 (encoded by *KCNQ1*), and Kir2.1 (encoded by *KCNJ2*), respectively. Atria exhibit ion channel compositions and densities that differ partially from those of ventricles, resulting in atrium-specific kinetics of repolarizing currents. Therefore, during sinus rhythm, the triangular shape of the atrial cardiomyocyte AP exhibits a less pronounced gradual repolarization phase as compared to that of ventricular cardiomyocytes. The atria-specific expression of ion channels makes these interesting targets for therapy of AF (Ehrlich et al., 2008; Schotten et al., 2011).

In brief, as shown in *figure 3A*, the cardiomyocyte AP comprises five phases. In **Phase 0**, opening of NaV1.5 channels allow for rapid influx of Na^+ (I_{Na}), resulting in membrane depolarization and maximal AP peak (typically +20 to +35mV). Subsequently, repolarization is initiated in **Phase 1**, by closure of NaV1.5 channels and opening of Kv4.3 channels, causing K^+ efflux. The resulting transient outward I_{Kto} current mediates the observed short and sharp decline in the AP peak. An AP plateau is then sustained in **Phase 2** by the influx of Ca^{2+} due to the opening of CaV1.2 channels, where the inward Ca^{2+} currents (I_{Ca}) in turn triggers release of Ca^{2+} from the sarcoplasmic reticulum (SR) storage. These increased cytoplasmic amounts of Ca^{2+} finally cause cardiomyocyte contraction. At the same time, efflux of K^+ is initiated by opening of the Kv11.1 channels and subsequent outward rapid delayed rectifier K^+ current I_{Kr} . Especially, in the atrial cardiomyocytes, opening of Kv1.5 channels mediates K^+ efflux, resulting in the ultrarapid delayed rectifier current I_{Kur} . Consequently, there is a temporary equilibrium between Ca^{2+} influx and K^+ efflux. **Phase 3** is characterized by repolarization of the cardiomyocyte membrane. This is mediated by continued efflux of K^+ due to activation of slow outward rectifier (I_{Ks}) currents and simultaneous closure of CaV1.2 channels, resulting in termination of the Ca^{2+} influx. Finally, in **Phase 4**, which is also called as resting phase, membrane potential again reaches

between -70mV and -80mV, mediated by inward rectifier K^+ currents (I_{K1}) that are induced by opening of Kir2.1 channels. The Na^+/Ca^{2+} exchanger and the Na^+-K^+ ion exchange pump also contribute to the restoration of the resting membrane potential (de Git et al., 2013; Harkcom and Abbott, 2010; Nerbonne and Kass, 2005).

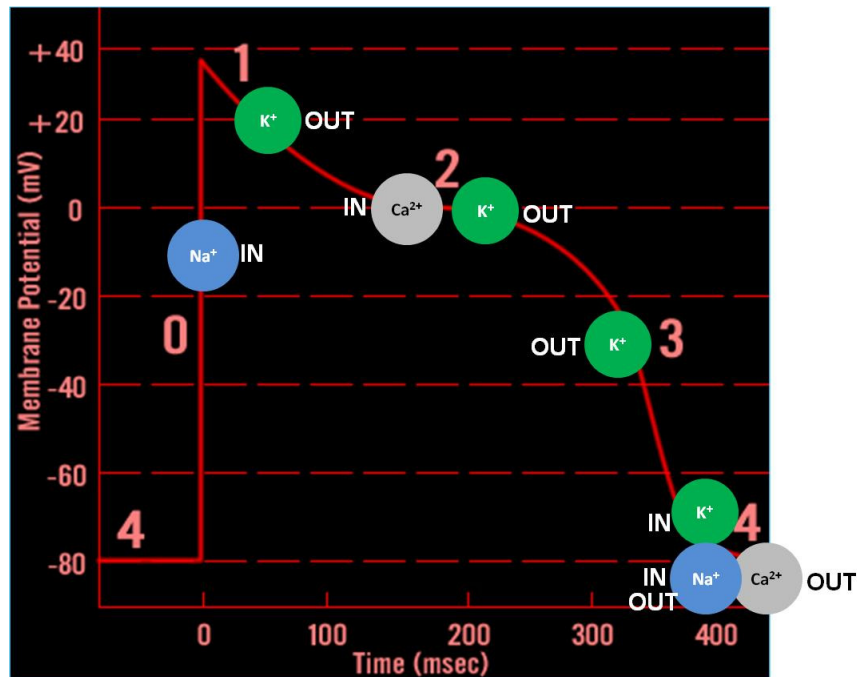


Figure 3A: Efflux and influx of ions during the cardiac action potential (AP) under sinus rhythm conditions. Rapid Na^+ influx in Phase 0 causes depolarization, followed by a short decline of the AP peak due to K^+ efflux in Phase 1. In Phase 2, a plateau is maintained by ongoing Ca^{2+} entry with simultaneous K^+ release. In phase 3, K^+ efflux continues whereas Ca^{2+} influx is terminated, resulting in membrane repolarization. Finally, in Phase 4, the resting membrane potential is restored by exchanging intracellular accumulated Na^+ and Ca^{2+} against K^+ .

(Source: Adopted from Wakili et al., 2011; de Git et al., 2013)

During AF, due to decreased Ca^{2+} influx, there is rapid repolarization after the initial peak without a distinct plateau phase. As a result, the AP is shortened to ~100 msec in contrast to ~200 msec under sinus rhythm conditions (*figure 3B*). Generally, these altered atrial electrophysiological properties favor the development and maintaining the arrhythmia over time, a process called 'electrical remodeling'. The principle mechanisms involved in the onset and maintenance of AF are related to Ca^{2+} metabolism (Greiser et al., 2011; Nattel, 2002). Single nucleotide polymorphisms (SNPs) in genes encoding ion channel subtypes may also contribute to changes in the AP-architecture. Accordingly, SNPs in *SCN5a*, *SCN3B*, *KCNJ5*, and *KCNH2* are associated with an increased AF risk (Chen et al., 2011; Jabbari et al., 2011; Olesen et al., 2011; Sinner et al., 2011, 2008).

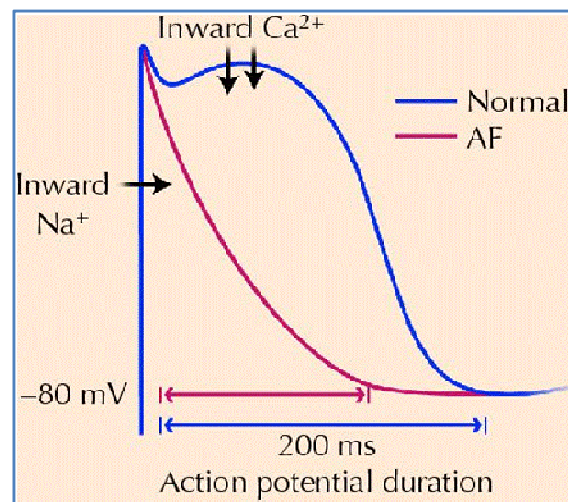
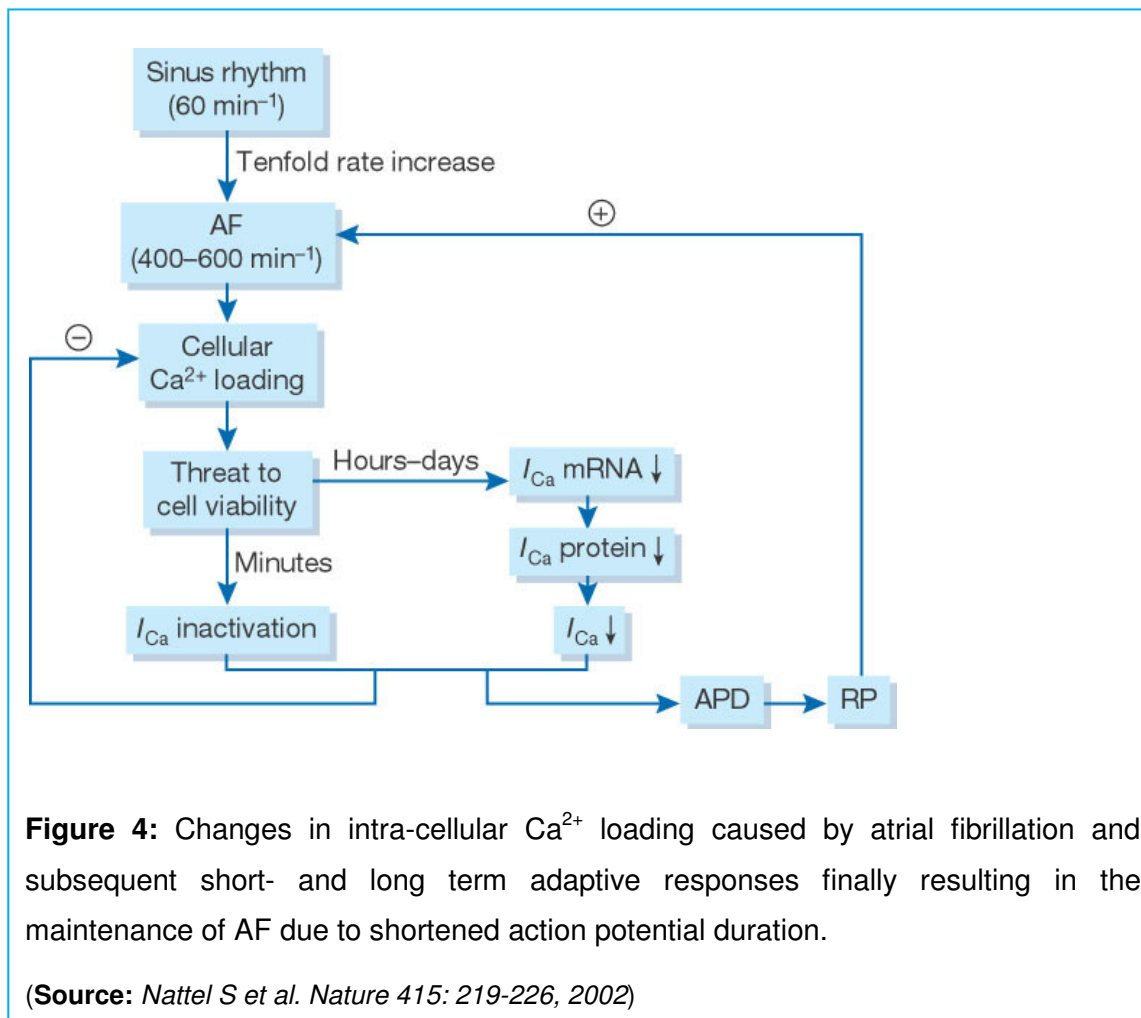


Figure 3B: AP duration: Sinus rhythm versus AF. AP duration and refractory period are shortened as the Ca^{2+} current is reduced. Whereas AP duration in sinus rhythm is about 200ms (blue), it is shortened to ~100ms during AF. The shortened AP duration is caused by reduced Ca^{2+} influx to prevent AF-induced Ca^{2+} overload.

(Source: (Veenhuizen et al., 2004))

As illustrated in *figure 4*, the initial onset of AF causes an increase of the atrial rate roughly by tenfold. This represents the primary remodeling stimulus. Subsequently, the cellular Ca^{2+} load progressively increases due to Ca^{2+} channel activation during each AP. The resulting over-loading of the cell with Ca^{2+} finally threatens cellular viability. Therefore, atrial voltage-dependent Ca^{2+} channels are subsequently inactivated to reduce the influx of Ca^{2+} (Courtemanche et al., 1998). Over the longer term also the mRNA levels of the gene encoding the α -subunit of the pore-forming Ca^{2+} channel are decreased (Brundel et al., 1999; Lai et al., 1999; Yue et al., 1999). Both mechanisms contribute to the prevention of cellular Ca^{2+} overload by reducing I_{Ca} . However, reduced cellular Ca^{2+} influx also causes decreased AP duration and shortened refractory period (RP), factors that promote further AF maintenance by multiple-circuit re-entry (Gaspo et al., 1997; Nattel, 1998).



1.5. ATRIAL FIBRILLATION: CONTRACTILE DYSFUNCTION (REMODELING)

Ca²⁺ represents the mediator of excitation and contraction, ensuring proper contractile function of atria and ventricles during sinus rhythm. Excitation-contraction coupling is initiated by depolarization of the cardiomyocyte cell membrane by an AP which triggers opening of voltage-dependent L-type Ca²⁺ channels (*I_{CaL}*) and causes Ca²⁺ influx. This mediates further release of Ca²⁺ from the sarcoplasmic reticulum (SR) through specific Ca²⁺ release channels (ryanodine receptor channels; **RyR** & inositol trisphosphate channels; **IP₃**) in a process called “**Ca²⁺-induced Ca²⁺ release**”. Cytoplasmic Ca²⁺ binds to troponin C, thereby activating actin-myosin filaments, resulting in cardiomyocyte contraction. Relaxation of cardiomyocytes is initiated by a decline of the cytosolic Ca²⁺ concentration mainly by re-sequestration (reuptake) of Ca²⁺ into the SR by the SR Ca²⁺-ATPase (**SERCA**), which is firmly controlled by its inhibitory protein phospholamban (**PLN**), and also by extrusion to the extracellular space by the Na⁺/Ca²⁺ exchanger (**NCX**). In humans, SERCA mediates ~70% of the Ca²⁺ reuptake,

whereas NCX accounts for ~30% of Ca^{2+} removal from the cytoplasm (Bassani et al., 1994; Bers, 2008; Bootman et al., 2006).

Shortening of the atrial refractoriness under conditions of AF causes changes in the excitation-contraction coupling in atrial cardiomyocytes with subsequent loss of atrial contractility. In the atria, gap junction channels composed by the connexins (Cx40 and Cx43) mediate the cell-to-cell conduction of electric impulses. Generally, in cardiac muscle, strands of cardiomyocytes are organized in bundles named myofibrils which are connected by so-called intercalated discs (IDs) where interlocking membranes of adjacent cardiomyocytes are fixed by desmosomes and directly connected by gap junctions. Myofibrils are separated by a sheath of connective tissue called perimysial fibrous tissue. Gap junctions allow electrical communication between cardiomyocytes *via* electrical communication in the form of ion fluxes. Apart from atrial cardiomyocytes, Cx40 is also present in the sinoatrial and atrioventricular nodes, the Purkinje system, and endothelial cells. An altered Cx40:Cx43 ratio is an important contributor to atrial conduction disturbances and plays a role in forming a substrate for reentry in AF (Burstein et al., 2009; Elenes et al., 1999; van Veen et al., 2006). Altered Ca^{2+} distribution, characterized by decreased I_{CaL} , increased I_{NCX} , and defective release of Ca^{2+} from the SR, is also a major contributor for atrial contractile dysfunction in the context of AF which finally causes shortening of the atrial AP (Greiser et al., 2011, 2009; Yue et al., 1997). The latter is due to the impaired coupling between intracellular Ca^{2+} pump and Ca^{2+} release channel (SERCA and RYR). Therefore, changes in intracellular Ca^{2+} handling are considered to be the major contributors for atrial contractile dysfunction during AF. Apart from this, the so-called “oxidative injury” as well as reduced activity of myofibrillar proteins due to impaired phosphorylation and dephosphorylation of myosin binding protein C was also reported to be associated with reduced performance of the contractile apparatus in patients with AF (El-Armouche et al., 2006; Mihm et al., 2001).

The most important clinical consequence of AF-associated atrial contractile dysfunction is the clearly increased risk of thromboembolic events. Decreased velocity of atrial blood flow under conditions of AF frequently causes atrial thrombus formation, where the thrombi are initially attached to the atrial walls. Sinus rhythm restoration by pharmacological or electrophysiological cardioversion frequently causes displacement of the atrial thrombi and finally ischemic stroke. Reduction of atrial contractility also contributes to further arrhythmia stabilization by enhancing progressive dilatation (Berger and Schweitzer, 1998; Black et al., 1994; Fatkin et al., 1994; Schotten et al., 2004, 2001).

1.6. ATRIAL FIBRILLATION: ENDOTHELIAL/ENDOCARDIAL/INFLAMMATORY REMODELING

AF is further frequently characterized by an inflammatory response and altered endocardial expression of adhesion molecules. These conditions favor atrial thrombogenesis due to increased activity of the clotting system. The inflammatory response is characterized by increased levels of inflammatory markers such as C-reactive protein (CRP), interleukin-6, as well as augmented leukocyte-platelet interactions. Cardiac endocardial amounts of vascular cell adhesion molecule-1 [VCAM-1] and intercellular adhesion molecule-1 [ICAM-1] are also increased. Fibrillating atria cause endothelial dysfunction (“endocardial remodeling”) which activates the plasmonic clotting system. Endocardial remodeling in AF is initiated by decreased availability of nitric oxide (NO), mediated by two different mechanisms: On the one hand, AF-dependent increased systemic amounts of Angiotensin II induce the activity of NADPH oxidase, resulting in increased amounts of reactive oxygen species (ROS). In particular the reaction of superoxide with NO that results in the generation of peroxynitrite reduces the amount of available NO. In addition, expression of endothelial NO synthase (eNOS) is reduced under AF conditions. Reduced NO amounts mediate the up-regulation of adhesion molecules (Cai et al., 2002; Chung et al., 2001; Conway et al., 2004; da Cunha et al., 2005; Dudley et al., 2005; Ferrario and Strawn, 2006; Goette et al., 2009a, 2008a; Mihm et al., 2001; Wang et al., 2001).

NFκB is a key regulator of inflammation and oxidative stress because of its unique ability to respond to both redox and inflammatory signaling and thus contributes to endothelial dysfunction as well. Inflammatory cytokines and ROS trigger NFκB activation. In the presence of these stimuli, inhibitor of κB kinase (IκK) is activated and subsequently mediates phosphorylation and degradation of the inhibitor of NFκB (IκB). This allows translocation of the NFκB heterodimer to the nucleus where it binds to promoters of gene targets, thereby enhancing the expression of genes encoding proteins involved in the defense against oxidative stress such as heme oxygenase 1. Oxidative stress also modulates increased expression of adhesion molecules which promote the adhesion of lymphocytes and monocytes to the endothelial surface. Finally, inflammatory/endothelial/endocardial remodeling triggers initiation and progression of thrombus formation and thereby increases the risk of thromboembolic events as explained in the previous chapter (Conway et al., 2004; de Winther, 2005; Donato et al., 2007; Dudley et al., 2005; Ferrario and Strawn, 2006; Goette et al., 2008a; Pierce et al., 2009).

1.7. ATRIAL FIBRILLATION: STRUCTURAL REMODELING

In addition to electrical remodeling, alterations in atrial tissue structure also contribute to arrhythmia stabilization in AF patients. Various aspects of atrial structural remodeling are associated with AF, like atrial fibrosis, cardiomyocyte hypertrophy, and altered connexin distribution. Pre-existing structural heart disease present in an individual patient also contributes to structural remodeling with similar degree (Frustaci, 1991; Frustaci et al., 1997).

Analysis of biopsies from AF-patients as well as from patients with increased AF-risk with valvular disease, rheumatic heart disease, dilated and hypertrophic cardiomyopathy and of advanced age revealed the presence of atrial fibrosis. Prolonged AF in goats is also reported to result in increased extracellular matrix volume per myocyte (Ausma et al., 2003), and the atria in a dog model for congestive heart failure show larger areas of fibrosis (Li et al., 1999). Therefore, atrial fibrosis was predicted to represent an important factor contributing to AF development by forming a substrate for the latter (Anne et al., 2005; Frustaci, 1991; Frustaci et al., 1997; Kostin, 2002; Lie and Hammond, 1988; Luo et al., 2007; Nattel, 2004; Ohtani et al., 1995; Pham and Fenoglio, 1982; Spach and Boineau, 1997).

The correlation between AF and quantitative atrial fibrosis is primarily due to conduction disturbances. As a consequence of AF, changes in cell-to-cell connections lead to discontinuous conduction at a microscopic scale. This pronounced discontinuous conduction is observed in transverse propagation rather than longitudinal propagation, resulting in delayed activation of adjoining myocytes or myocyte bundles due to poor electrical coupling. It can become more perceptible at short cycle lengths due to incomplete recovery of Na^+ and Ca^{2+} channels, further allowing the reentry to occur in very small circuits, thereby stabilizing the AF.

Development of atrial fibrosis is mediated by Ang-II-dependent and Ang-II-independent mechanisms. In the Ang-II-dependent mechanism, AF stimulates increased tissue expression and activity of angiotensin converting enzyme (ACE), resulting in higher levels of atrial Ang-II. By binding to its type 1 receptor (AT1 receptor), Ang-II subsequently activates the monomeric G protein Ras. Activated Ras in turn causes activation of the Raf-1 kinase which initiates the MEK/ERK dependent phosphorylation cascade, finally causing activating phosphorylation of transcription factors like Elk-1 and c-Fos, which enhance the expression of genes related to atrial fibrosis. The degree of atrial fibrosis is linearly correlated with Ang-II concentration and ERK1/2 activation. In the Ang-II-independent mechanism, TGF β -1 induces fibrosis *via* SMAD signaling (Boldt et al., 2004; Brand and Schneider, 1996; Goette et al., 2000; Kostin, 2002; Li et al., 2001; Shaw and Rudy, 1997; Spach and Boineau, 1997; Spach et al., 2007; Sugden and Clerk, 1997; Zou et al., 1998). Whereas Ang-II and TGF β -1

stimulate activation and proliferation of atrial fibroblasts, less pronounced effects are observed on ventricular fibroblasts. Activation of fibroblasts results in altered expression of genes encoding the matrix metalloproteinases (MMPs) representing a large group of enzymes involved in extracellular matrix remodeling, and the induction of genes encoding ECM (extracellular matrix) proteins like collagen, as well as *CTGF* encoding the Connective Tissue Growth Factor.

CTGF is implicated in various pathophysiological conditions, including AF (Burstein et al., 2008; Ko et al., 2011; Tsai et al., 2011b). Elevated amounts of *CTGF* in the left atrial tissue from AF patients have been associated with increased fibrosis and tissue levels of Ang-II. Ang-II was described to induce *CTGF* via activation of Rac1 and NADPH oxidase, leading to increased expression of specific target genes (Adam et al., 2010). Similarly, AngII induced *CTGF* expression in perfused rat hearts. In a porcine AF model, both the tissue levels of Ang-II and *CTGF* were increased in the left and right atria (Ko et al., 2011). However, recent data suggest that CTGF alone is not sufficient to promote the development of fibrosis. Despite the fact that enhanced *CTGF* expression is regularly associated with fibrosis, *in vivo* evidence clearly demonstrating causality between elevated *CTGF* expression and induction of fibrosis is still lacking. In a rapid pacing-induced model of heart failure, there was no evidence of fibrosis despite of substantially increased CTGF levels (Ahmed et al., 2005). Similarly, over-expression of *CTGF* in cardiomyocytes failed to induce fibrosis (Panek et al., 2009).

In addition to MMPs, ADAMs (“a disintegrin and metalloproteinase”, a large family of membrane-bound glycoproteins), are also reported to influence the interstitial matrix composition. The ADAM15/ β 1-integrin ratio is increased in fibrillating tissue and further correlates with increased left atrial diameter and duration of electrical signal propagation. Thus, altered regulation of MMPs and ADAMs during AF contributes to structural changes and dilatation of the atria and ventricles. Atrial dilatation has been described as a cause as well as a consequence of AF. Left atrial enlargement is a strong independent predictor for the development of AF; on the other hand, several studies suggest that AF causes atrial enlargement and a decrease in the atrial dimension is observed in AF-patients after cardioversion (Anne et al., 2005; Arndt et al., 2002; Benjamin et al., 1994; Henry et al., 1976; Hunt et al., 2002; *Proteases in tissue remodelling of lung and heart*, 2003; Sanfilippo et al., 1990; Schlöndorff and Blobel, 1999; Welikovich et al., 1994; Xu et al., 2004).

Hypertrophy of cardiomyocytes represents another contributing factor for alterations in atrial conduction that has been reported in animal models with rapid atrial pacing (RAP) and atrial dilatation. An increase in cell size and width leads to pronounced delay of electrical conductivity in transverse propagation between myocytes, explaining the role of hypertrophy

in causing conduction disturbances in the absence of atrial fibrosis (Ausma et al., 1997; Boyden and Hoffman, 1981; Spach et al., 2004; Wiegerinck et al., 2006).

1.8. ATRIAL FIBRILLATION: ROLE OF THE RENIN-ANGIOTENSIN SYSTEM (RAS)

One of the most important systems involved in blood pressure regulation, the renin-angiotensin system (RAS), also represents an important mediator in the development of an AF substrate, especially in patients with hypertension and existing heart disease. Elevated expression of genes encoding circulating and/or local tissue components of the RAS as well as increased activity of these components have been reported to be associated with AF. Chronic hyper-activity of the RAS causes hypertension, resulting in left atrial enlargement (Lau et al., 2012).

Under normal conditions, decreased blood pressure stimulates the synthesis of the endopeptidase renin from the juxtaglomerular apparatus of the kidney and its release into the circulation. Here, renin cleaves the inactive pro-hormone angiotensinogen (AGT) which is predominantly produced in the liver, but also locally in several additional tissues, among the myocard. Cleavage of AGT produces the inactive pro-hormone angiotensin I (Ang-I). Subsequently, Ang-I is cleaved by Angiotensin converting enzyme (ACE), resulting in angiotensin II (Ang-II), an active octapeptide hormone. ACE is produced in the vascular endothelium and tissues including heart. Ang-II is a highly potent vasoconstrictor and represents a key factor in blood pressure regulation. Besides the production of Ang-II, ACE inactivates the vasodilator bradykinin (BK). Hence, ACE simultaneously increases the concentration of a vasoconstrictor (Ang-II) and reduces the concentration of a vasodilator (BK).

Binding of Ang-II to its type 1 receptors (AT1R), mediates the vascular smooth muscle contraction, thereby causing vasoconstriction of arterioles. In addition, Ang-II stimulates secretion of the mineralocorticoid hormone aldosterone from the adrenal gland cortex. Aldosterone subsequently stimulates renal re-absorption of sodium and, as a consequence of this of water; the net effects of aldosterone secretion stimulation are therefore increased blood volume and pressure (Carey, 2003; Dostal and Baker, 1999; Dragović et al., 1993; Griendling et al., 1993; Müller et al., 1997; Paul et al., 2006; Soubrier et al., 1993).

Under AF conditions, serum as well as local atrial tissue Ang-II levels are increased due to cardiac specific over-expression of ACE (see 1.7). Of particular importance, the resulting AF-mediated AT1R activation in turn causes activation of the NADPH oxidase (NOX2) and thus the induction of oxidative stress. Inhibition of the endogenous Ang-II prevents the shortening

of atrial effective refractory period in canine RAP model, emphasizing the critical role of cardiac RAS components, especially Ang-II, in the pathogenesis of AF (Caron et al., 2004; Goette et al., 2000; Li et al., 2001; Tsai et al., 2011a, 2008a; Xiao et al., 2004).

1.9. ATRIAL FIBRILLATION: ROLE OF THE NITRIC OXIDE (NO) IN BLOOD PRESSURE REGULATION

Nitric oxide (NO) is a potent vasodilator and therefore represents a further important regulator of blood pressure. In vascular endothelium, NO is synthesized from the amino acid L-arginine by endothelial nitric oxide synthase (eNOS). There are two endothelial NOS, namely constitutive eNOS encoded by *NOS3* (cNOS) and inducible eNOS encoded by *NOS2* (iNOS). Whereas the iNOS activity is Ca^{2+} -independently stimulated by bacterial endotoxins, cytokines and interleukins during inflammation, the Ca^{2+} - and calmodulin-activated cNOS ensures continuous NO production under basal conditions which is additionally stimulated upon binding of variety of ligands (acetylcholine, bradykinin, substance-P, adenosine, and other vasoactive substances) to their endothelial receptors as well as in response to shear from increased blood flow in arteries. NO produced by eNOS in the vascular endothelium rapidly diffuses into adjacent vascular smooth muscle cells where it binds to the heme moiety of the enzyme guanylyl cyclase (GC), resulting in its activation. Active GC catalyzes the conversion of GTP to cGMP which induces smooth muscle relaxation by multiple mechanisms, e. g. dephosphorylation of myosin light chains *via* activation of a cGMP-dependent protein kinase that activates myosin light chain phosphatase (Cabrera and Bohr, 1995; Giles et al., 2012; Stoner et al., 2012).

As described in section 1.8, the availability of NO is reduced under AF-conditions, because AT1R-mediated activation of NOX2 causes the generation of ROS which rapidly react with NO, resulting in peroxynitrite formation. The reduced NO availability has been described to cause endothelial dysfunction and subsequently impaired microcirculation, which may represent key initiator mechanisms of AF-related ventricular remodeling (Goette et al., 2009a).

1.10. NON-ARRHYTHMIC & ANTI-ARRHYTHMIC AGENTS: USE OF IRBESARTAN AND DRONEDARONE IN PREVENTING THE PERPETUATION OF ATRIAL FIBRILLATION

Irbesartan represents a non-arrhythmic anti-hypertensive drug which blocks the AT1R. It was developed by Sanofi Research and jointly marketed by Sanofi-Aventis and Bristol-Myers Squibb, with market names such as Aprovel, Karvea, and Avapro. By blocking AT1R,

irbesartan prevents vascular smooth muscle contraction in response to increased Ang-II concentrations, and thereby attenuates arterial vasoconstriction. Furthermore, renal aldosterone release is suppressed, causing reduced re-absorption of sodium and water. In sum, irbesartan therefore mediates reduction of blood pressure. In the context of AF, blockade of AT1-receptors with irbesartan is predicted to partially attenuate maladaptive AF-mediated alterations which emphasizes the key role of AngII-signaling as a major underlying pathomechanism (Nattel and Carlsson, 2006; Malmqvist et al., 2007; Malishevskii, 2012; Yusuf et al., 2011; Moreno, 2003).

Dronedarone represents an anti-arrhythmic drug belonging to the class of multichannel blockers. It inhibits sodium-, potassium-, and Ca^{2+} -specific channels and is used for treatment of patients whose hearts returned to sinus rhythm after electric cardioversion. Dronedarone has been developed by Sanofi-Aventis with a market name Multaq. Dronedarone's actions at the molecular level are controversially discussed with most studies suggesting an inhibition of multiple outward potassium currents. Dronedarone is also believed to reduce inward rapid Na^+ current and L-type Ca^{2+} - channels. It is used for the treatment of AF in people whose hearts have either returned to normal rhythm or who undergo drug therapy or electric shock treatment i.e. direct current cardioversion to maintain normal rhythm. It causes increased AP duration and increased effective refractory periods, mediating stabilization of the sinus rhythm.

Dronedarone represents a structural analog of its precursor drug amiodarone, but due to the removal of iodine from its benzene ring, it was thought to have a better side effect profile with lower incidences of pulmonary fibrosis, skin photosensitivity, ocular affects and in particular abnormalities in thyroid function. Addition of a methane sulfonyl group to its benzofuran ring decreases the lipophilicity of dronedarone as compared to amiodarone, and thereby results in a markedly shorter half-life (20–40 hours versus 21–47 days) and reduced tissue accumulation (Chahal et al., 2012; Gautier et al., 2003; Hunter et al., 2012; Kathofer et al., 2005; Löbe et al., 2013; Wegener et al., 2006).

2. AIMS OF THE STUDY

The increasing number of hospitalizations because of atrial fibrillation (AF) represents a substantial public health burden. Despite the limited availability of anti-arrhythmic agents by either their modest efficacy or their potential for serious ventricular pro-arrhythmia or extra-cardiac toxic effects, the recent ATHENA (A placebo-controlled, double-blind, parallel-arm Trial to assess the efficacy of dronedarone 400 mg BID for the prevention of cardiovascular Hospitalization or death from any cause in patients with Atrial fibrillation/atrial flutter) clinical trial has shown that dronedarone reduces the incidence of hospitalizations for acute coronary syndromes (ACS) in AF patients (Connolly et al., 2009; Hohnloser et al., 2009). However, the precise mechanism of the cardiovascular protective effects is unclear.

Recently, based on the aforementioned key role of Ang-II in the renin–angiotensin system (RAS), Ang-II receptor blockers have been reported to be beneficial in the prevention of the detrimental consequences of AF. The recent study trial CREATIVE-AF (Impact of Irbesartan on Oxidative Stress and C-Reactive Protein Levels in Patients with Persistent Atrial Fibrillation) indicated that blockade of Ang-II type 1 receptor (AT1R) may help to reduce the risk of thromboembolic events by reducing the levels of circulating adhesion molecules and oxidative stress parameters in patients with persistent AF (Goette et al., 2009a, 2008b). However, such clinical data do not elucidate the cardioprotective molecular mechanisms of these blockers, and therefore further in-depth analyses are required to analyze the efficacy of Ang-II type 1 receptor antagonists at the molecular level.

Hence, the comparative array-based transcriptome analyses described in this work were designed to analyze RAP-induced alterations of the atrial transcriptome. Furthermore, the dronedarone and irbesartan studies additionally demonstrated the impact of these two drugs on the AF (RAP)-induced atrial gene expression profile in order to better understand how these drugs decrease/prevent pathophysiological changes caused by RAP. In both studies, in addition to the porcine *in vivo* standard experimental model, the cardiomyocyte cell line HL-1 subjected to RAP *in vitro* was used for additional analyses such as validation of specific candidate genes as well as determination of time- and frequency-dependency of specific candidate genes.

3. MATERIALS & METHODS

3.1. MATERIALS

3.1.1. Chemicals and kits

<u>Chemicals</u>	<u>Manufacturer</u>
TRIzol reagent (Invitrogen)	Life Technologies
AccuGENE molecular biology grade water	LONZA
Ethanol 99,8%	Roth
RNA 6000 Nano LabChip	Agilent Technologies
RNA 6000 Pico LabChip	Agilent Technologies
RNase-Zap (AMBION)	Life Technologies
One cycle target labeling Kit including: cRNA/ cDNA-CleanUp-Module, Poly-A RNA-controls, Hybridization controls,	Affymetrix
Porcine Genome Array	Affymetrix
3' IVT Express Kit	Affymetrix
Wash and stain kit	Affymetrix
Nuclease free water, AMBION	Life Technologies
RBS T 230 Liquid neutral detergent	RBS (R.Borghgraef S.A.)
RNA Clean-Up and Concentration Micro Kit	Norgen, Canada
RNase-free Microfuge Tubes (1.5 ml, 0.2ml)	AMBION
1.8mL CryoTubes	Thermo Fisher Scientific
Pipette Tips, RNase-free(100 - 1000 µl, 200 µl & 0.1 - 10 µl)	NERBE Plus
Chloroform	Roth
Isopropanol	Roth
Liquid nitrogen or dry ice	

Distilled/Double Distilled water	
Forceps/Scalpel/Spatula, Magnetic Spatula	
Nitrile gloves/Cryogenic gloves/Latex gloves	
Vial Cleaning Brush	
Beakers (~500mL size)	
Protective eye wear	
MicroAmp® Optical 384-Well Reaction Plate	Applied Biosystems
MicroAmp® Optical 96-Well Reaction Plate	Applied Biosystems
MicroAmp® Optical Adhesive Film	Applied Biosystems
MicroAmp® Optical Film Compression Pad	Applied Biosystems
MicroAmp® Adhesive Film Applicator	Applied Biosystems
Countess™ cell counting chamber slides	Invitrogen

3.1.2. Media for HL-1 and MCF Culturing

<u>Medium/Buffer/Chemicals</u>	<u>Manufacturer</u>
HL-1 cell line	Dr. William Claycomb
Claycomb Medium	Sigma Aldrich
Fetal bovine serum	Sigma Aldrich
Penicillin and Streptomycin	Sigma Aldrich
Norepinephrine/L-Ascorbic Acid, Sodium Salt	Sigma Aldrich
DMSO	Sigma Aldrich
L-Glutamine	Sigma Aldrich
Gelatin from bovine skin /Fibronectin	Sigma Aldrich
Distilled Water, cell culture grade	Sigma Aldrich
Cryo vials, 2 ml round bottom	Corning
Sterile Acro disc syringe filters, 0.2µm	Gelman Sciences
Freezing container	Nalgene
Trypsin Inhibitor Type I-S, Soybean	Sigma Aldrich
Dulbecco's PBS (Ca ²⁺ -free and Mg ²⁺ -free)	Sigma Aldrich

Trypsin-EDTA (0.05%trypsin in 0.02% EDTA-Na)	Sigma Aldrich
T25/75 flasks	Sigma Aldrich
6-well plates	BD-Falcon
C57BL/6J mouse cardiac fibroblasts	Cell biologics
Murine Fibroblast Medium /w Kit (M2267)	Cell biologics
Trypan blue stain (0.4 %)	Invitrogen
Countess™ test beads	Invitrogen

3.1.3. Buffers

Buffer	Composition
Wash Buffer B (stringent)	0,1 M MES, 0.1 M [Na ⁺], 0.01% TWEEN-20 83.3 ml 12x MES Stock Buffer 5.2 mL of 5M NaCl 1.0 mL of 10% Tween-20 910.5 mL of water Filter through a 0.2 µm filter Store at 2°C to 8°C and shield from light.
Wash Buffer A (Non-Stringent Wash Buffer)	6X SSPE, 0.01% Tween-20 300 mL of 20X SSPE 1.0 mL of 10% Tween-20 699 mL of water Filter through a 0.2 µm filter. Store at room temperature.
2X Stain Buffer (Final 1X concentration)	100 mM MES, 1 M [Na ⁺], 0.05% Tween-20 41.7 mL of 12X MES Stock Buffer

	92.5 mL of 5M NaCl
	2.5 mL of 10% Tween-20
	113.3 mL of water
	Filter through a 0.2 μ m filter.
	Store at 2°C to 8°C and shield from light.
10 mg/mL Goat IgG Stock	Resuspend 50 mg in 5 mL 150 mM NaCl.
	Store at 4°C.
1 mg/mL Streptavidin Stock	Resuspend 5 mg in 5 mL of PBS.
	Store at 4°C.
12X MES Stock Buffer	1.22M MES, 0.89 M [Na ⁺]
	For 1,000 mL:
	64.61 g of MES hydrate
	193.3 g of MES Sodium Salt
	800 mL of Molecular Biology Grade water
	Mix and adjust volume to 1,000 mL.
	The pH should be between 6.5 and 6.7.
	Filter through a 0.2 μ m filter.
2X Hybridization Buffer (final 1x)	100mM MES, 1 M [Na ⁺], 20 mM EDTA, 0.01% Tween-20
	For 50 mL:
	8.3 mL of 12X MES Stock Buffer
	17.7 mL of 5 M NaCl
	4.0 mL of 0.5 M EDTA
	0.1 mL of 10% Tween-20
	19.9 mL of water
	Store at 2°C to 8°C, and shield from light

3.1.4. Equipment and accessories

<u>Equipment/Accessory</u>	<u>Manufacturer</u>
Mikro-Dismembrators	Sartorius AG
Teflon Vials with grinding metal balls	Sartorius AG
Heat block (Thermomixer)	Eppendorf
Heat block QBT2	Grant
NanoDrop 1000/8000 Spectrophotometer	Thermo Fisher Scientific
2100 Bioanalyzer	Agilent Technologies
7900HT Fast Real-Time PCR System	Applied Biosystems
Hybridization Oven 645, Fluidics Station 450, Scanner 3000 7G	Affymetrix
Thermocycler	Biometra
5%-CO ₂ incubator	
Countess Automated Cell Counter	Invitrogen
Pipettes (2µL, 10µL, 20µL, 100µL, 200µL & 1000µL)	Gilson

3.1.5. Software used for data analysis

<u>Software</u>	<u>Manufacturer</u>
GeneChip Command Console Software (AGCC)	Affymetrix
Expression Console™ Software	Affymetrix
Rosetta Resolver	Rosetta Bio
Rosetta Elucidator	Rosetta Bio
Data Assist	Applied Biosystems
Ingenuity Pathway Analysis	Ingenuity Systems

3.1.6. Primers used for RT q-PCR (Irbesartan study)

Target genes		Sequence 5' → 3'	Product size (bp)
<i>Mus musculus</i>	<i>CTGF</i>	US: CAAAGCAGCTGCAAATACCA DS: GGCCAAATGTGTCTTCCAGT	220

	<i>SGK1</i>	DS: CAAAGTAGAGCTTGTGAGCGGTCTGG US: CCAATGCGCTCGCAAACACGCTG	389
	<i>EDN1</i>	US: CAGCTGTCTTGGGAGCCGAACTC DS: GGTGAGCGCACTGACATCTAACTG	282
	<i>RPLP0</i>	US: GCACTTTTCGCTTTCTGGAGGGTGT DS: TGA CT TGGTTGCTTTGGCGGGTT	344
<i>Susscrofa</i>	<i>CTGF</i>	Probe: TGACGAGCCCAAGGACCACACCG US: GGAAATGCTGCGAGGAGTGG DS: CGTGTCTTCCAGTCGGTAAGC	222
	<i>SGK1</i>	Probe: CTCGGCTGCTTCCTTGACGCTGGC US: ACCCCGAGTTCACCGAAGAG DS: CGTAGGAGAAGCCCAGGAAGG	114
	<i>EDN1</i>	Probe: AGGACCAGCACCTCGCCTGAACA US: GTTCAGACCGTTCCTTACTGC DS: CATCACCGCAAAGGAGGAGAG	150
	<i>GAPDH</i>	Probe: CCTCGGACGCCTGCTTCACCACCT US: TCCGTGTCCCTACTGCCAAC DS: TAGCCCAGGATGCCCTTGAG	130

3.1.7. Primers used for RT-qPCR (oxidative stress/ischaemia-related genes, Dronedarone study)

Gene	Primer sequence	Product size (bp)
US: upstream primer; DS: downstream primer.		
<i>CCL2</i>	US: 5'-CTGCTCACTGCAGCCACCTTC	398
	DS: 5'-GGCATCATGTTTCGTATC	
<i>DNAJB9</i>	US: 5'-CAGGATGGTTCCAGTAGAC	235
	DS: 5'-GTCCTGAACAGTCAGTGTATG	

Gene	Primer sequence	Product size (bp)
<i>HIF-1α</i>	US: 5'- GAGAAGTCTAGAGATGCAGC	255
	DS: 5'- CACCATCATCTGTGAGTACC	
<i>PRKAG2</i>	US: 5'-CTCTTCGATGCTGTACACTC	377
	DS: 5'-GTCACCGTGATGTCTAGGTTG	
<i>Prx1</i>	US: 5'-CTCCGTGGATGAGACTCTGAG	261
	DS: 5'-GTCCCACACATCTGAGCTG	
<i>Prx3</i>	US: 5'-CTTGACAAGTGTGCTGTGGTC	416
	DS: 5'-CTAACAGCACACCGTAGTCTC	
<i>PPARGC1</i>	US: 5'-GATGCACTGACAGATGGAGATG	388
	DS: 5'-GTGCACTTGTCTCTGCTACTG	
<i>PRKCa</i>	US: 5'-GTGACACCTGTGACATGAAC	365
	DS: 5'-GTTCTTGTTGTTCCGGTC	
<i>VEGF-A</i>	US: 5'-CTCCACCATGCCAAGTGGTC	289
	DS: 5'-CTCATCTCTCCTATGTGCTG	
<i>ACTB</i>	US: AAGATGACCCAGATCATGTTTGAG	648
	DS: AGGAGGAGCAATGATCTTGATCTT	

3.1.8. Antibodies used for Immunoblotting

Target proteins	Molecular mass [kD]	Working dilution	Buffer system	Manufacturer	Dilution secondary antibody
CTGF	38	1:200	5% BSA, TBS/T	Santa Cruz	1:10,000
Erk1/2	42/44	1:1,000	5% BSA, TBS/T	Cell Signaling	1:5,000

phospho-Erk (T202/204)	42/44	1:1,000	5% BSA, TBS/T	CellSign aling	1:5,000
SGK1	54	1:1,000	5% BSA, TBS/T	CellSign aling	1:5,000
phospho- SGK1 (S78)	54	1:500	5% BSA, TBS/T	CellSign aling	1:5,000
SGK1	54	1:200	5% BSA, TBS/T	Santa Cruz	1:10,000
phospho- SGK1 (S422)	54	1:200	5% BSA, TBS/T	Santa Cruz	1:5,000
anti-rabbit- HRP	-	-	1×Roti- Block	CellSign aling	-
anti-goat-HRP	-	-	1×Roti- Block	Dianova	-

3.1.9. Rapid Atrial Pacing (RAP) Model

Tissue samples used in the irbesartan analyses were from the same animals used in the study described in *figure 5* (Goette et al., 2009a). The animal experiments were approved by the Institutional Animal Care and Use Committee of the University of Magdeburg. Briefly, a total of 14 pigs were subjected to closed chest, rapid atrial pacing (RAP). In five animals RAP was performed for 7 h at a rate of 600 bpm (twice diastolic threshold, 2-ms pulse duration; RAP-group). In five additional animals RAP was performed in the presence of an irbesartan infusion (1 mg/kg bolus injection followed by $0.3 \text{ mg} \times \text{kg}^{-1} \times \text{h}^{-1}$ i.v.; RAP+Irb-group), and four pigs were instrumented without further intervention (Sham). After the 7h pacing period, the chest and the pericardial sac were opened and the heart was exposed. Tissue samples were immediately frozen in liquid nitrogen and used for RNA profiling and immunoblot analyses as described below.

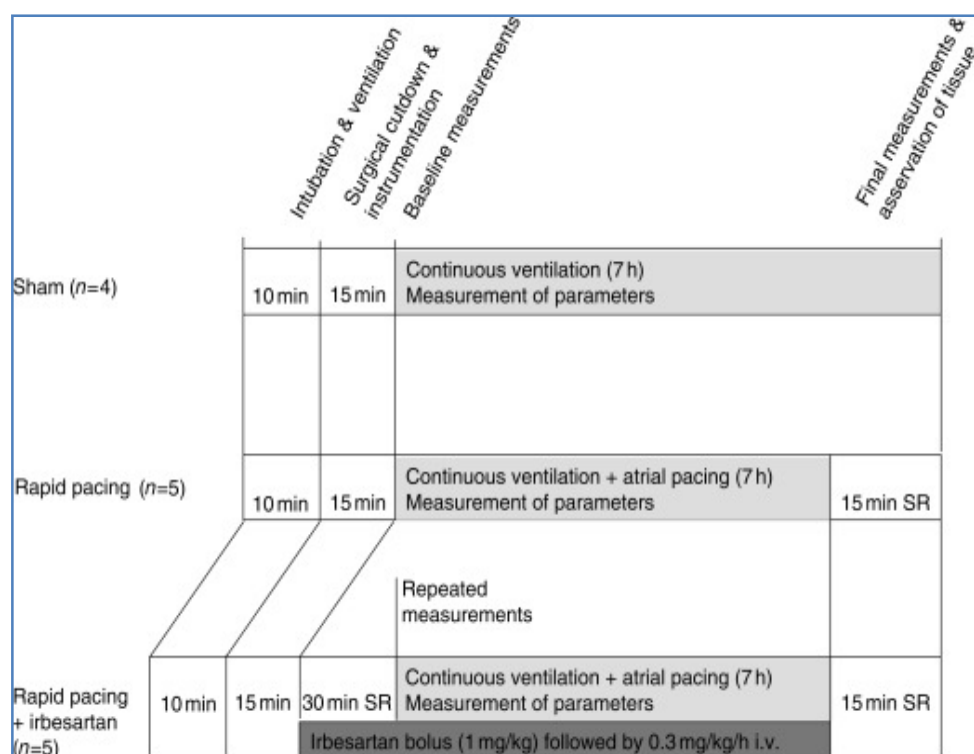


Figure 5: Simulation of AF in pigs using a RAP model as described by Andreas Goette et al., 2009. Sham-operated animals served as control; SR, sinus rhythm (Goette et al., 2009a).

The RAP model in the dronedarone study was designed in a similar way. It included a total of 29 pre-medicated, intubated and instrumented pigs. Of these, RAP was performed in six animals at a rate of 600 beats per minute (twice diastolic threshold, 2 ms pulse duration) for **6 h (RAP group)**. In six animals, RAP was performed after treatment with $10 \text{ mg} \cdot \text{kg}^{-1}$ dronedarone (Sanofi-Aventis, Paris, France; **RAP/D group**). Seven pigs received $10 \text{ mg} \cdot \text{kg}^{-1}$ dronedarone without additional treatment (**D group**). Six pigs were instrumented without any further intervention (**sham group**). Tissue samples were collected in a comparable way to the Irbesartan study (Bukowska et al., 2011).

3.1.10. Cardiomyocyte cell culture

The murine cardiomyocyte cell line HL-1 was kindly provided by Dr William Claycomb (Louisiana State University Health Science Center, New Orleans, LA). Cells were passaged and cultured in Claycomb-Medium (Sigma-Aldrich, Taufkirchen, Germany) as described (Claycomb et al., 1998).

3.1.10.1. Measurement of cell count and viability measurement

A ten μL sample was mixed with $10 \mu\text{L}$ of trypan blue stain gently by pipetting up and down multiple times. $10 \mu\text{L}$ of the sample mixture was then added to one of the chamber ports on

one side of the Countess™ cell counting chamber slide. The slide was inserted into the Countess™ cell counting chamber slide inlet, and cell count was measured after adjusting the image analysis settings in a way that the “Live cells” have bright centres and dark edges, where as “Dead cells” have a uniform blue color throughout the cell with no bright centres.

3.1.10.2. Rapid pacing *in vitro*: murine cardiomyocyte cell line HL-1

For rapid pacing *in vitro*, HL-1 cells were seeded into gelatin/fibronectin-coated 6-well plates at a density of 1×10^6 cells/well/4 ml. Pacing was performed with carbon electrodes using the culture cell pacer system C-Pace EP (IonOptix, Milton, MA). Cells were paced at 20 Hz for 3.5, 7 or 24 hrs (5 V/cm, 4 msec bipolar pulse). Part of this work was done in collaboration with Prof. Dr. Uwe Lendeckel's lab.

3.1.11. RNA Isolation and Quality Control

Total RNA was extracted from frozen specimens of left and right atrium (LA, RA), and left ventricle (LV), and also from cultivated HL-1 cardiomyocytes by performing a modified phenol extraction using Trizol reagent (Invitrogen, Karlsruhe, Germany) (Chomczynski and Sacchi, 1987, p.). For tissue samples, an additional mechanical homogenization of snap-frozen tissue was carried out using a bead mill dismembrator (Braun, Melsungen, Germany) at 2600 rpm for 2 minutes. Phase separation was done using 0.2mL of chloroform per 1.0mL of TRizol reagent. The RNA present in the aqueous phase was transferred to a fresh 1.5mL RNase free tube and precipitation was carried out overnight after addition of 0.5mL of isopropyl alcohol (to 1mL of TRizol reagent used). On the next day, the RNA precipitate was washed 2x with 1 ml of 75% ethanol per 1 ml of TRizol reagent used for the initial homogenization. The RNA pellet was air-dried or dried using a flame until the residual ethanol was completely evaporated. Subsequently, the pellet was re-dissolved in an appropriate amount of RNase-free water by passing the solution a few times through a pipette tip, followed by incubation on ice for 3 hours and 0.5 hours at room temperature.

3.1.12. Clean-up and concentration of isolated total RNA

RNA was further purified using the RNA Clean-Up and Concentration Micro Kit (Norgen, Canada) and concentrations measured using a ND-1000 spectrophotometer (Thermo Fisher Scientific Inc, Wilmington, USA). The kit purifies all sizes of RNA, from large mRNA and ribosomal RNA down to microRNA (miRNA) and small interfering RNA (siRNA). In brief, the total RNA (<35µg) was mixed with Binding Solution, ethanol was added and the RNA was bound to Norgen's proprietary resin containing separation column matrix. The bound RNA was then washed to remove any remaining impurities. Finally, the purified total RNA was

eluted with 20 - 50 μL of the provided Elution Buffer or water.

3.1.13. Assessing the purified RNA quantity using an ND-1000 spectrophotometer

The quantitative measurement of purified total RNA was carried out using $>1.5\mu\text{L}$ volume of appropriate blanking/diluted RNA solution in a NanoDrop ND-1000 spectrophotometer (Thermo Fisher Scientific Inc, Wilmington, USA). The Beer-Lambert equation is used by the software to correlate the calculated absorbance with concentration as follows:

$$c = (A * \epsilon) / b$$

A = the absorbance represented in absorbance units (AU)

ϵ = the wavelength-dependent extinction coefficient in $\text{ng-cm}/\mu\text{L}$ (for RNA: $40\text{ng-cm}/\mu\text{L}$; dsDNA: $50\text{ng-cm}/\mu\text{L}$ and ssDNA: $33\text{ng-cm}/\mu\text{L}$)

b = the pathlength in cm (=1cm, 10mm)

c = the analyte (RNA) concentration in $\text{ng} / \mu\text{L}$.

The ratio of absorbance at 260 nm and 280 (260/280): a ratio of ~ 2.0 is generally accepted as “pure” for RNA. If the ratio is appreciably lower in either case, it may indicate the presence of protein, phenol or other contaminants that absorb strongly at or near 280 nm.

The ratio of 260/230 value: as a secondary measure of nucleic acid purity. Expected 260/230 values are commonly in the range of 2.0-2.2. If the ratio is appreciably lower than expected, it may indicate the presence of contaminants which absorb at 230 nm, such as EDTA, carbohydrates and phenol.

3.1.14. Assessing the purified RNA quality using a Bio-analyzer 2100

The qualitative range for RNA 6000 Nano kit is 5-500 $\text{ng}/\mu\text{L}$. For the RNA 6000 Pico kit, this range is 50-5000 $\text{pg}/\mu\text{L}$. Hence, the quantitated purified total RNA must be diluted to meet the quantitative range of Nano kit or Pico kit. Once the run is finished, the RIN (RNA Integrity Number) is calculated by the software using the entire electrophoretic trace of the RNA sample, including the presence or absence of degradation products. This is a good measure of RNA sample quality and hence, for high quality total RNA samples, RIN will be >9.0 , whereas $\text{RIN} > 6.5 - < 7.5$ may indicate partially degraded RNA. Only RNA samples with a $\text{RIN} > 7.5$ (Schroeder et al., 2006), $A_{260/280} \geq 1.8$ and $A_{260/230} \geq 1.9$ were used for microarray analyses and RT-qPCR experiments.

3.1.15. Transcriptome analysis

The purified total RNA samples from left atrium (LA) were subjected to transcriptome analysis using the GeneChip Porcine Genome Arrays (Affymetrix Inc., Santa Clara, CA, USA). In the irbesartan project, expression profiling was done using the one-cycle target labeling kit at the level of single RNA samples for RAP (n=3), RAP/I (n=5), and sham (n=4). In the dronedarone project, expression profiling was done using the 3' IVT Express Kit at the level of single RNA samples for RAP (n=5), RAP/D (n=4), Sham/D (n=5) and sham (n=4). Target preparation and hybridization were performed according to the manufacturer's instructions (GeneChip® Expression Analysis Technical Manual and 3' IVT Express Kit User Manual, Affymetrix, Inc.).

3.1.15.1. One-cycle labeling kit: Reverse transcription, amplification, *in vitro* transcription, fragmentation and labeling

For each sample, 5 µg of total RNA were reverse transcribed into cDNA using a T7-Oligo (dT) Promoter Primer and reverse transcriptase. The RNA of the resulting cDNA:RNA hybrid was digested into small RNA fragments using RNase H. These RNA fragments then primed second-strand cDNA synthesis by *E. coli* DNA polymerase I with final ligation of remaining gaps by DNA ligase. The double-stranded (ds) cDNA was purified and used as template in the subsequent *in vitro* transcription (IVT) reaction. The IVT reaction was carried out using T7 RNA Polymerase and a biotinylated nucleotide analog/ribonucleotide mix for linear complementary RNA (cRNA) amplification with concomitant biotin labeling. After subsequent *in vitro* transcription and cleaning up, concentration and purity of the resulting biotinylated cRNA were assessed using aND-1000 spectrophotometer (Thermo Fisher Scientific Inc.) and the cRNA pattern was examined by gel electrophoretic separation using a Bioanalyzer 2100 (Agilent Technologies). The biotinylated cRNA targets were then fragmented. Hybridization was achieved by incubating target-filled array cartridges at 45°C for 16 hours. Subsequently, the arrays were washed and stained with streptavidin-phycoerythrin using the standard fluidics protocol for Fluidics Station 450 (Affymetrix Inc.) and scanned with a GeneChip Scanner 3000 (Affymetrix Inc.).

3.1.15.2. Target preparation using 3' IVT Express Kit and subsequent hybridization, washing, staining and scanning of the arrays

For each sample, 200 ng of total RNA were reverse transcribed into cDNA. Following second-strand cDNA synthesis, the double-stranded cDNA was used as template in the subsequent *in vitro* transcription (IVT) reaction. The IVT reaction was carried out using T7 RNA Polymerase and a biotinylated nucleotide analog/ribonucleotide mix for linear

complementary RNA (cRNA) amplification with concomitant biotin labeling. After subsequent *invitro* transcription and magnetic bead based purification, the concentration and purity of resulting biotinylated cRNA were assessed using aND-1000 spectrophotometer (Thermo Fisher Scientific Inc.) and the cRNA pattern was examined by gel electrophoretic separation using a Bioanalyzer 2100 (Agilent Technologies). The biotinylated cRNA targets were then fragmented. Hybridization was achieved by incubating target-filled array cartridges at 45 °C for 16 hours. Subsequently, the arrays were washed and stained with streptavidin-phycoerythrin using the standard fluidics protocol for Fluidics Station 450 (Affymetrix Inc.) and scanned with a GeneChip Scanner 3000 (Affymetrix Inc.).

3.1.16. Transcriptome Data Analysis

First the quality assessment of all hybridizations was carried out by inspecting scan images in the AGCC software for manufacturing defects if any, and by carefully reviewing external and endogenous controls using the Expression Console software (Affymetrix Inc.). The .CEL files were then imported into the Rosetta Resolver software server. Data normalization and statistical tests were performed using pre-written pipelines from the software as described in detail in the following sections.

3.1.16.1. Quality Control Check using Expression Console Software

To monitor assay and data quality control processes for gene expression analyses, Affymetrix has developed several controls which were added at different time points during the assay to check overall assay quality, labeling efficiency, hybridization efficiency etc. These include: hybridization controls, labeling controls and internal control genes.

Labeling Controls: Poly-A RNA controls were used to monitor the entire target labeling process. The porcine genome array contains probe sets from several *B. subtilis* genes that are absent in eukaryotic samples (*lys*, *phe*, *thr*, and *dap*). These Poly-A RNA controls are *in vitro* synthesized, and the poly adenylated transcripts for the *B. subtilis* genes are premixed at staggered concentrations. The Poly-A controls were spiked into all RNA samples, carried through the sample preparation process, and evaluated like the internal control genes. The GeneChip® Poly-A RNA Control Kit (P/N 900433) contains the following four exogenous, premixed control spikes:

Lys: AFFX-r2-Bs-lys (1:100,000)

Phe: AFFX-r2-Bs-phe (1:50,000)

Thr: AFFX-r2-Bs-thr (1:25,000)

Dap: AFFX-r2-Bs-dap (1:6,667)

All of the Poly-A controls should be called “**Present**” with increasing signal values in the order of *lys*, *phe*, *thr*, *dap*.

Internal Control Genes (Housekeeping Genes): Internal control genes or housekeeping genes are gene transcripts that are constitutively expressed in most samples including porcine. These transcripts serve as internal controls, are useful for monitoring the quality of the starting sample, and are subject to any variability in the labeling of the sample and hybridization to the array for 3' Expression Arrays. For Human, Mouse, and Rat 3' Expression Array types, *ACTB* and *GAPDH* are used to assess RNA sample and assay quality. Specifically, the signal values of the 3' probe sets for *ACTB* and *GAPDH* are most informative and, therefore, as a general recommendation, these should be compared to the signal values of the corresponding 5' probe sets. The ratio of the 3' probe set to the 5' probe set should generally be less than 3 for the One Cycle Labeling protocol.

Hybridization Spike-in Controls: The 20x Eukaryotic Hybridization Controls are spiked into the hybridization cocktail, independent of RNA sample preparation, and are therefore used to evaluate sample hybridization efficiency on gene expression arrays. The default spike controls are listed as: AFFX-r2-Ec-BioB, AFFX-r2-Ec-BioC, AFFX-r2-Ec-BioD and AFFX-r2-P1-Cre.

BioB is at the level of assay sensitivity (1:100,000 complexity ratio) and should be called Present at least 70% of the time. **BioC**, **BioD**, and **cre** should always be called Present with increasing signal values.

The Quality assessment of all hybridizations was carried out by inspecting scan images and by carefully reviewing external and endogenous control parameters such as all QC array metrics, signal histograms of all arrays, relative log expression signal values across all arrays using the Expression Console software (Affymetrix Inc.). For all processed arrays, the available control parameters matched the default threshold tests and all arrays were considered to be of good quality.

3.1.16.1. Data extraction, Normalization, identification of differential gene expression profile using Rosetta Resolver Software

In brief, normalized intensity signals were calculated by processing the Affymetrix .CEL files using the Affymetrix Rosetta intensity data summarization. Samples were analyzed based on fold change calculations and signal statistics after direct comparison of different samples (Sham vs. RAP, Sham vs. RAP/I, Sham vs. RP, Sham-Dron vs. RP and Sham vs. RP-Dron). Genes that differed significantly at mRNA level were identified using the following criteria:

- (1) Significant p-value ($p \leq 0.05$) in an one-way analysis of variance with subsequent multiple-testing correction on pair-wise comparisons using the Benjamini and Hochberg false discovery rate,
- (2) Signal correction statistics using the Ratio Builder tool ($p \leq 0.05$) and
- (3) Fold change ≥ 1.5 -fold (for a complete list of significantly regulated genes, see the supplemental material# 7.7.1 and 7.7.2).

A heat map was generated using the k-NN classifier with Euclidean distance similarity measure in order to display specific gene expression signatures including those associated with ROS production and redox-signaling, tissue remodeling, and energy depletion.

As shown in table 1, the factorial design was used to define the animals with their respective groups by grouping into 3 groups in Irbesartan project and 4 groups in Dronedarone project.

Table1: Table showing the groups of animals as defined by the respective levels in the Rosetta Resolver for each treatment factor i.e. Irbesartan project and Dronedarone project.

Factor	Level/Group Name	Level Value
Treatment (Irbesartan Project)	Paced	1.0
	Paced+irbesartan	2.0
	Sham	3.0
Treatment (Dronedarone Project)	Sham	1.0
	Sham-Dronedarone	2.0
	RP	3.0
	RP-Dronedarone	4.0

Based on this factorial design, the normalized signal intensities were calculated as expression summaries from each scan (profile or biological replicate as shown in table 2A and table 2B) using both the perfect-match (PM) and mis-match (MM) probes by the Affymetrix Rosetta - Intensity Profile Builder pipeline.

Table2A: Table showing the biological replicates as defined by the respective levels and grouped according to their treatment in the Rosetta Resolver for the treatment factor: irbesartan.

Treatment Group Name	Profile Name	Biological Replicate	Hyb Name	Barcode
Paced	Ssc_LV_AF_14-c4	BIOSAMPLE - 2444	Ssc_LV_AF_14-c4	001_Ssc_LV_AF
	Ssc_LV_AF_3-c2	BIOSAMPLE - 2445	Ssc_LV_AF_3-c2	002_Ssc_LV_AF
	Ssc_LV_AF_8-c5	BIOSAMPLE - 2446	Ssc_LV_AF_8-c5	003_Ssc_LV_AF
Paced+irbesartan	Ssc_LV_AF_2-c4	BIOSAMPLE - 2447	Ssc_LV_AF_2-c4	004_Ssc_LV_AF
	Ssc_LV_AF_7-c2	BIOSAMPLE - 2448	Ssc_LV_AF_7-c2	005_Ssc_LV_AF
	Ssc_LV_AF_12-c2	BIOSAMPLE - 2449	Ssc_LV_AF_12-c2	006_Ssc_LV_AF
	Ssc_LV_AF_11-c3	BIOSAMPLE - 2450	Ssc_LV_AF_11-c3	007_Ssc_LV_AF
	Ssc_LV_AF_13-c3	BIOSAMPLE - 2451	Ssc_LV_AF_13-c3	008_Ssc_LV_AF
Sham	Ssc_LV_AF_6-c6	BIOSAMPLE - 2452	Ssc_LV_AF_6-c6	009_Ssc_LV_AF
	Ssc_LV_AF_5-c5	BIOSAMPLE - 2453	Ssc_LV_AF_5-c5	010_Ssc_LV_AF
	Ssc_LV_AF_15-c3	BIOSAMPLE - 2454	Ssc_LV_AF_15-c3	011_Ssc_LV_AF
	Ssc_LV_AF_16-c6	BIOSAMPLE - 2455	Ssc_LV_AF_16-c6	012_Ssc_LV_AF

Table2B: Biological replicates as defined by the respective levels and grouped according to their treatment in the Rosetta Resolver for the treatment factor dronedarone

Treatment Group Name	Profile Name	Biological Replicate	Hyb Name	Barcode
Sham	Ssc_LA_AF-Dronedaron_4-LA-Sham	BIOSAMPLE - 3285	Ssc_LA_AF-Dronedaron_4-LA-Sham	001_Ssc_LA_AF-Dronedaron_4-LA-Sham
	Ssc_LA_AF-Dronedaron_7-LA-Sham	BIOSAMPLE - 3309	Ssc_LA_AF-Dronedaron_7-LA-Sham	005_Ssc_LA_AF-Dronedaron_7-LA-Sham
	Ssc_LA_AF-Dronedaron_8-LA-Sham1	BIOSAMPLE - 3310	Ssc_LA_AF-Dronedaron_8-LA-Sham1	006_Ssc_LA_AF-Dronedaron_8-LA-Sham
	Ssc_LA_AF-	BIOSAMPLE	Ssc_LA_AF-	014_Ssc_LA_AF-

Treatment Group Name	Profile Name	Biological Replicate	Hyb Name	Barcode
	Dronedaron_20-LA-Sham	- 3441	Dronedaron_20-LA-Sham	Dronedaron_20-LA-Sham
Sham-Dronedaron	Ssc_LA_AF-Dronedaron_17-LA-Sham-Dronedaron	BIOSAMPLE - 3286	Ssc_LA_AF-Dronedaron_17-LA-Sham-Dronedaron	002_Ssc_LA_AF-Dronedaron_17-LA-Sham-Dronedaron
	Ssc_LA_AF-Dronedaron_23-LA-Sham-Dronedaron	BIOSAMPLE - 3311	Ssc_LA_AF-Dronedaron_23-LA-Sham-Dronedaron	007_Ssc_LA_AF-Dronedaron_23-LA-Sham-Dronedaron
	Ssc_LA_AF-Dronedaron_25-LA-Sham-Dronedaron	BIOSAMPLE - 3312	Ssc_LA_AF-Dronedaron_25-LA-Sham-Dronedaron	008_Ssc_LA_AF-Dronedaron_25-LA-Sham-Dronedaron
	Ssc_LA_AF-Dronedaron_9-LA-Sham-Dronedaron	BIOSAMPLE - 3442	Ssc_LA_AF-Dronedaron_9-LA-Sham-Dronedaron	015_Ssc_LA_AF-Dronedaron_9-LA-Sham-Dronedaron
	Ssc_LA_AF-Dronedaron_14-LA-Sham-Dronedaron	BIOSAMPLE - 3443	Ssc_LA_AF-Dronedaron_14-LA-Sham-Dronedaron	016_Ssc_LA_AF-Dronedaron_14-LA-Sham-Dronedaron
RP	Ssc_LA_AF-Dronedaron_6-LA-RP	BIOSAMPLE - 3287	Ssc_LA_AF-Dronedaron_6-LA-RP	003_Ssc_LA_AF-Dronedaron_6-LA-RP
	Ssc_LA_AF-Dronedaron_18-LA-RP	BIOSAMPLE - 3313	Ssc_LA_AF-Dronedaron_18-LA-RP	009_Ssc_LA_AF-Dronedaron_18-LA-RP
	Ssc_LA_AF-Dronedaron_24-LA-RP	BIOSAMPLE - 3314	Ssc_LA_AF-Dronedaron_24-LA-RP	010_Ssc_LA_AF-Dronedaron_24-LA-RP
	Ssc_LA_AF-Dronedaron_11-LA-RP	BIOSAMPLE - 3444	Ssc_LA_AF-Dronedaron_11-LA-RP	017_Ssc_LA_AF-Dronedaron_11-LA-RP
	Ssc_LA_AF-Dronedaron_12-LA-RP	BIOSAMPLE - 3445	Ssc_LA_AF-Dronedaron_12-LA-RP	018_Ssc_LA_AF-Dronedaron_12-LA-RP
RP-Dronedaron	Ssc_LA_AF-Dronedaron_10-LA-RP-Dronedaron	BIOSAMPLE - 3288	Ssc_LA_AF-Dronedaron_10-LA-RP-Dronedaron	004_Ssc_LA_AF-Dronedaron_10-LA-RP-Dronedaron
	Ssc_LA_AF-Dronedaron_15-LA-RP-Dronedaron	BIOSAMPLE - 3315	Ssc_LA_AF-Dronedaron_15-LA-RP-Dronedaron	011_Ssc_LA_AF-Dronedaron_15-LA-RP-Dronedaron
	Ssc_LA_AF-	BIOSAMPLE	Ssc_LA_AF-	012_Ssc_LA_AF-

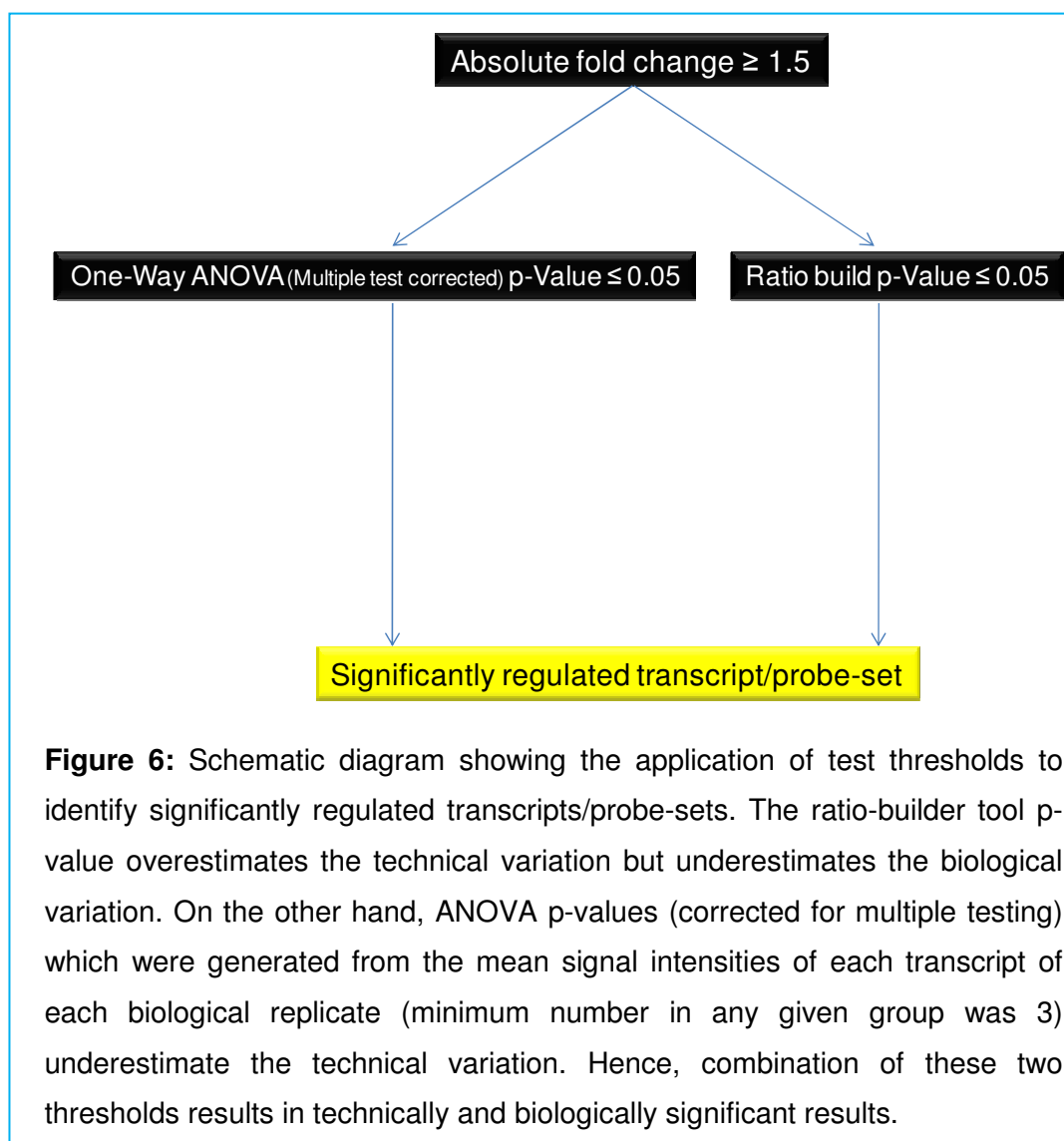
Treatment Group Name	Profile Name	Biological Replicate	Hyb Name	Barcode
	Dronedaron_19 -LA-RP- Dronedaron	- 3316	Dronedaron_19 -LA-RP- Dronedaron	Dronedaron_19-LA- RP-Dronedaron
	Ssc_LA_AF- Dronedaron_13 -LA-RP- Dronedaron	BIOSAMPLE - 3446	Ssc_LA_AF- Dronedaron_13 -LA-RP- Dronedaron	019_Ssc_LA_AF- Dronedaron_13-LA- RP-Dronedaron

Then, the group dependent signal intensity was calculated for each probe-set/gene from the expression values of individual profiles using an error-weighted average. Probe (Reporter)-level data were used to impute missing probes (reporters), if any, and to increase robustness by calculating the averages. All profiles (biological replicates) belonging to one single experiment/level/group were normalized together.

3.1.16.2. Data analysis tools and statistical thresholds to filter the significant data

Rosetta Resolver Ratio Builder tool p-value: The P-values are calculated based on a two-sided, two-sample t-test based on gene-level data. Consequently, the tool is only applicable for comparing gene expression levels/transcript abundances between two groups. This tool considers the gene expression variation within the respective groups at the level of mean signal intensities for each gene. The median number of probes per gene represented on the Affymetrix porcine arrays is 26. Basically, the tool first determines the variance (xdev) of all 26 probe signal intensities of each gene for each group. Subsequently, this variance is considered in the p-value calculation. For example, based on the fold-change, a gene might show spurious differential regulation between two groups because several of the 26 gene-specific probes in one of the groups exhibit very low signal intensities for any reasons (e. g. partial RNA degradation or array artifacts). Such cases can be identified by a high Ratio Builder tool p-value which allows their exclusion from the analysis.

ANOVA and Scheffé post-hoc testing: In addition to the pair wise comparison of the ratio builder, a one-way ANOVA (Error-weighted with Benjamini Hochberg FDR-based multiple test correction) and a Scheffé post-hoc test were applied. The usage of the error-weighted average group mean helps to reduce the number of false positives/negatives compared to a text book ANOVA. The post-hoc test was applied to identify the pair-wise significances for all the groups and factors tested in the ANOVA (here, four groups with one factor i.e. treatment: e. g. dronedarone were present, so the post-hoc test simplifies the visualization of variance with pair-wise comparison).



3.1.17. *In silico* pathway- and functional analysis of transcriptome data

In-silico pathway- and functional analysis of differentially expressed genes (that passed the standard significance threshold $p\text{-value} \leq 0.05$, error weighted with Benjamini Hochberg FDR based multiple test correction) was carried out using the commercial systems biology oriented package Ingenuity Pathways Analysis (Ingenuity Systems, Inc. CA, USA) using the annotation details provided by Christopher K. Tugle (Couture et al., 2009) with their corresponding gene identifiers and expression values.

3.1.18. Reverse Transcription quantitative PCR (RT-qPCR)

To validate several specific candidate genes resulting from the microarray analyses, the fluorescent reporter probe method was used. Specific probes and primers were used as

listed in section 3.1.6 (pig). Probes and primers for qPCR were designed and functionality tested by Microsynth AG (Balgach, Switzerland) on the basis of the appropriate *Sus scrofa* DNA-sequences. All samples were analyzed in duplicate. Briefly, 400 ng of the purified total RNA were converted into cDNA using SuperScript™ II RT kit (Invitrogen, Life Technologies GmbH, Darmstadt, Germany). Gene expression was then measured with the 7900HT Fast Real-Time PCR System (Applied Biosystems, CA, USA). Thermocycling was performed for all samples in 25 µl PCR master-mix containing 2.5 µl cDNA. Initial denaturation at 95°C for 10 min was followed by 50 cycles of denaturation at 95°C for 15s, annealing/elongation at 60°C for 30s. The cDNA content was normalized according to amounts of *GAPDH* specific mRNA. The obtained threshold cycles (Ct values) were then used to calculate relative gene expression differences as fold-change. Significance of gene expression changes was tested using the Mann–Whitney U test (Wilcoxon rank-sum test).

For the HL-1 cell experiments, RT-qPCR was performed using a CFX960 cyclor (BioRad, Munich, Germany). All samples were analysed in triplicate. A 25 µl reaction mixture consisted of 1XSensiMix (Quantace, Bioline, UK), 0.5 µl of SYBR-Green (Quantace, Bioline, UK), 1 µl cDNA, and 0.3 µmol/L specific primers (listed in section 3.1.6 (mouse)). Initial denaturation at 95°C for 10 min was followed by 40 cycles with denaturation at 95°C for 15 s, annealing at 59° for 30 s, and elongation at 72°C for 30 s. Quantities of *RPL* mRNA were used to normalize cDNA contents. The SYBR-Green fluorescence intensity reflected the amount of ds-PCR product actually formed and was determined real-time at the end of each elongation step. The amounts of specific initial template mRNA were calculated by means of the Bio-Rad software by determining the time point at which the linear increase of sample PCR product started, relative to the corresponding points of a standard curve; values are given in arbitrary units. This part of the validation was done in collaboration with Prof. Dr. Uwe Lendeckel's lab.

3.1.19. Protein extraction and Immuno-blot analysis

Tissue samples were frozen in liquid nitrogen and stored at -80°C until use. Samples were homogenized in lysis buffer, containing 50 mmol/L Tris-HCl (pH 7.5), 100 mmol/L NaCl, 5 mmol/L EDTA, 0.5% Triton X-100, 10% glycerol, 10 mmol/L K₂HPO₄, 0.5% NP-40, 1 mmol/L PMSF, 1mmol/L sodium vanadate, 0.5% desoxycholate, 20 mmol/L NaF, 20 mmol/L glycerol-2-phosphate, and a protease inhibitor cocktail (all from Sigma, Heidelberg, Germany). Tissue homogenates were centrifuged at 15,000 rpm for 30 min and the resulting supernatant (total tissue homogenate) was stored at -80°C for further analysis. Twenty micrograms of protein in a final volume of 30 µl 1x Laemmli-buffer were separated by SDS-PAGE and transferred to PVDF membranes. The membranes were incubated with primary antibodies followed by incubation with horseradish peroxidase-conjugated secondary

antibodies (used antibodies are summarized in section 3.1.7). For detection the enhanced chemiluminescence substrate Dura (Pierce, Rockford, USA) was used. The protein levels were quantified using Alpha Ease FC software (Alpha Imager System, Alpha Innotech, CA, USA). This work was done in collaboration with Prof. Dr. Uwe Lendeckel's lab.

4. RESULTS

4.1. HAEMODYNAMICS AND PHYSIOLOGY

Hemodynamic parameters were comparable between the groups RAP, RAP/I, and Sham throughout the experiment as described recently (Bukowska et al., 2011; Goette et al., 2009a). In brief, at baseline the mean ventricular rates were similar, with significant increases in the RAP and RAP/I groups after RAP initiation. Of the two markers for microvascular flow abnormalities, FFR (marker for epicardial flow) and CFR (index of microvascular abnormalities if FFR is normal); FFR was comparable in all groups. In contrast, CFR was decreased in the RAP group, but not in the RAP/I and RAP/D groups, suggesting that the RAP-induced CFR decline was prevented by irbesartan (table 3A) and dronedarone (table 3B).

Table 3A: The parameters analyzed are summarized as mean \pm SEM. Measurements of FFR and CFR were performed during normal sinus rhythm before and 15 min after 7 h pacing (end of experiment). P-values <0.05 are marked in **bold**. **OD**, optical density; **FFR**, fractional flow reserve; **CFR**, coronary flow reserve; **NOX1/2**, NADPH oxidase subunit 1/2, **LOX-1**, lectin-like oxidized low-density lipoprotein receptor-1; **eNOS**, endothelial nitric oxide synthase (Goette et al., 2009a).

	Sham Mean \pm SEM	RAP Mean \pm SEM	RAP/I Mean \pm SEM	P-value of ANOVA
Haemodynamic parameters				
Right atrial pressure (mmHg)	5.3 \pm 0.9	6.2 \pm 0.7	5.8 \pm 0.9	0.816
Systolic right ventricular pressure (mmHg)	23.7 \pm 2.3	26.6 \pm 1.4	24.2 \pm 2.4	0.576
Pulmonary capillary wedge pressure (mmHg)	6.3 \pm 0.3	7.0 \pm 0.9	5.8 \pm 0.7	0.535
Systolic left ventricular pressure (mmHg)	80 \pm 4	74 \pm 4	79 \pm 2	0.375
LV end-diastolic pressure (mmHg)	4.3 \pm 0.3	4.6 \pm 0.8	5.4 \pm 0.7	0.608
Mean heart rate (b.p.m.)	90 \pm 3	83 \pm 7	81 \pm 7	0.659
Mean ventricular rate (b.p.m.)	84 \pm 3	110 \pm 5	114 \pm 4	0.003
Molecular markers				
NOX1 (OD)	0.140 \pm 0.021	0.248 \pm 0.064	0.151 \pm 0.045	0.246
NOX2 (OD)	0.344 \pm 0.049	0.597 \pm 0.096	0.326 \pm 0.053	0.039
p67phOX (OD)	0.380 \pm	0.358 \pm	0.501 \pm	0.305

	Sham Mean±SEM 0.081	RAP Mean±SEM 0.034	RAP/I Mean±SEM 0.073	P-value of ANOVA
F2-isoprostane (pg/mg)	303.67 ± 23.48	445.00 ± 36.25	300.00 ± 17.19	0.008
LOX-1 (%)	100.04 ± 28.59	527.10 ± 140.78	65.10 ± 35.86	0.004
eNOS (%)	100.00 ± 36.35	130.04 ± 33.28	98.52 ± 17.39	0.691
eNOS mRNA (%)	100.00 ± 19.99	20.07 ± 8.56	13.02 ± 2.41	0.002
Flow parameters				
FFR baseline (%)	100.00 ± 0.00	99.96 ± 2.58	101.36 ± 1.37	
7 h		93.40 ± 4.60	96.53 ± 6.64	0.333*
Post	94.27 ± 0.68	96.54 ± 6.18	100.60 ± 3.28	0.327**
CFR baseline (%)	100.00 ± 0.00	100.00 ± 5.97	104.36 ± 10.39	
7 h		62.70 ± 3.68	93.28 ± 5.92	0.004*
Post	97.23 ± 2.77	67.73 ± 7.24	93.16 ± 3.29	0.001**

Table 3B: The flow markers in the dronedarone study. Q1, 1st quartile; Q3, 3rd quartile; LV, left ventricular; FFR, fractional flow reserve; CFR, coronary flow reserve; n.a., not applicable (Bukowska et al., 2011).

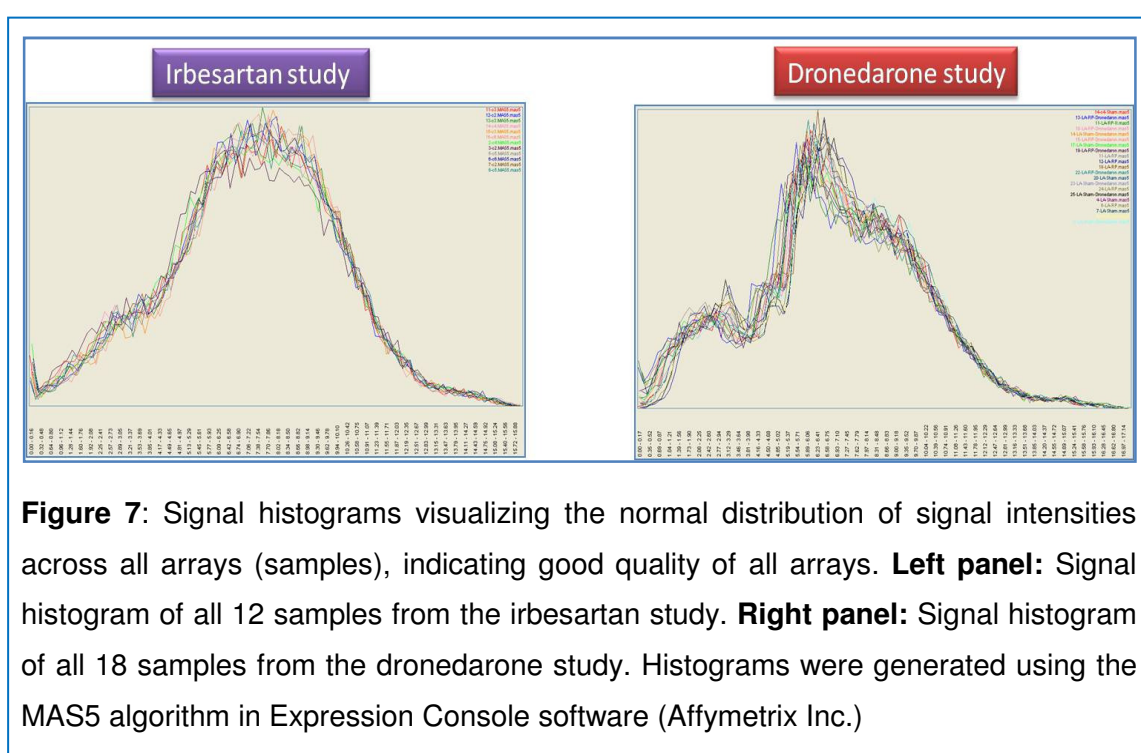
Parameter	Time	Sham (n=6) median (Q ₁ ; Q ₃)	RAP (n=6) median (Q ₁ ; Q ₃)	RAP/D (n=6) median (Q ₁ ; Q ₃)	Sham/D (n=7) median (Q ₁ ; Q ₃)	p-value (Kruskal-Wallis)
FFR absolute	baseline	0.96 (0.94; 1.00)	0.913 (0.90; 0.94)	0.96 (0.94; 1.00)	0.93 (0.87; 0.97)	0.091
	at 6h	0.93 (0.89; 0.98)	0.86 (0.83; 0.90)	0.93 (0.90; 0.96)	0.97 (0.97; 1.00)	0.043
CFR absolute	baseline	1.25 (1.20; 1.30)	1.40 (1.40; 1.50)	1.30 (1.20; 1.60)	1.20 (1.15; 1.35)	0.135
	at 6h	1.30 (1.30; 1.30)	0.80 (0.70; 1.00)	1.35 (1.20; 1.40)	1.30 (1.25; 1.50)	0.007

Expression of NADPH oxidase subunits was elevated in response to RAP, suggesting an increased expression in pathological settings. Besides them, the levels of two additional markers of oxidative stress, i.e. ventricular F₂-isoprostanes and LOX-1 protein were also induced during RAP in both irbesartan and dronedarone studies (Bukowska et al., 2011; Goette et al.,

2009a).

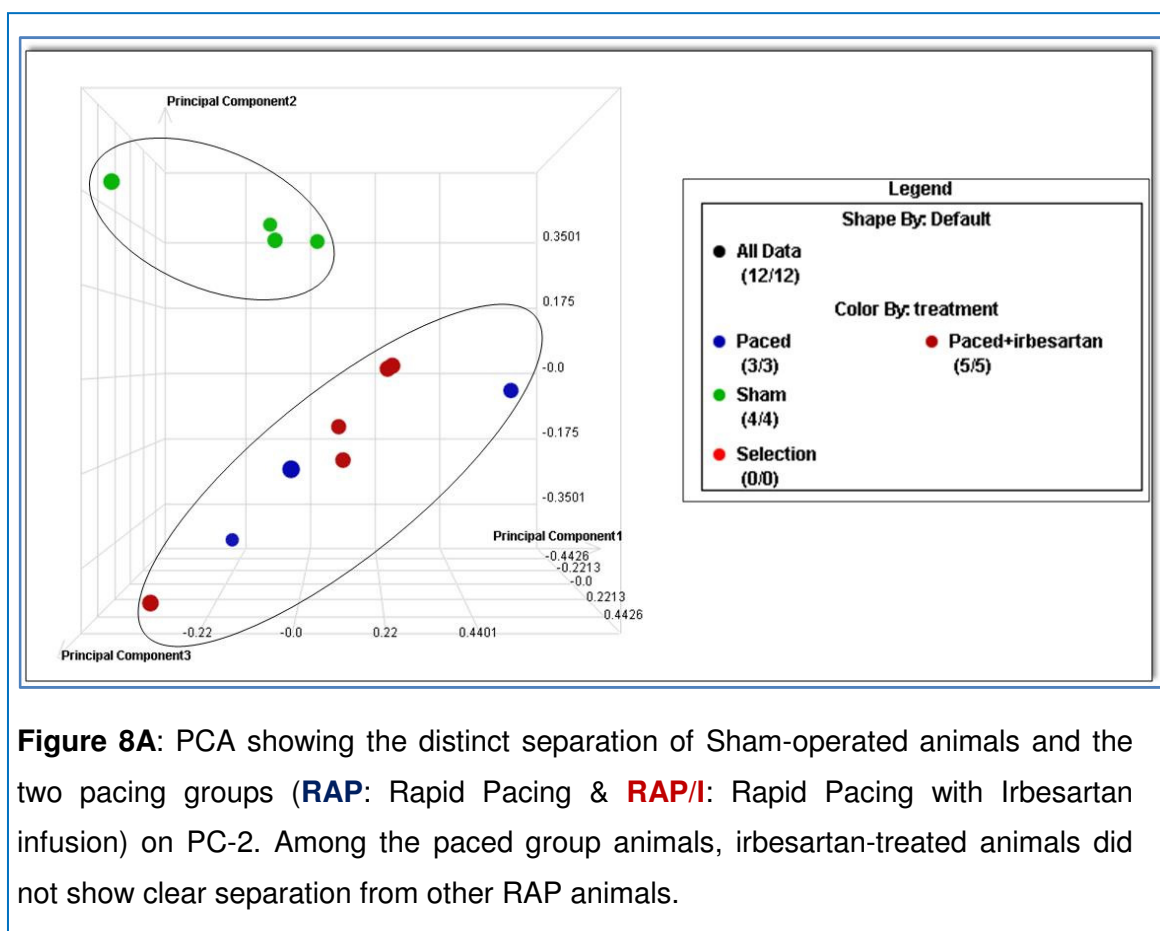
4.2. ARRAY QUALITY AND PRINCIPLE COMPONENT ANALYSIS

To check for technical variation during sample or array processing, signal histograms were generated using all 12 samples from the irbesartan study and 18 samples from the dronedarone study (Expression Console software, Affymetrix Inc.). As shown in *figure 7*, signal intensities were normally distributed across all arrays indicating absence of technical variation in the array processing and good quality of all arrays in both studies.



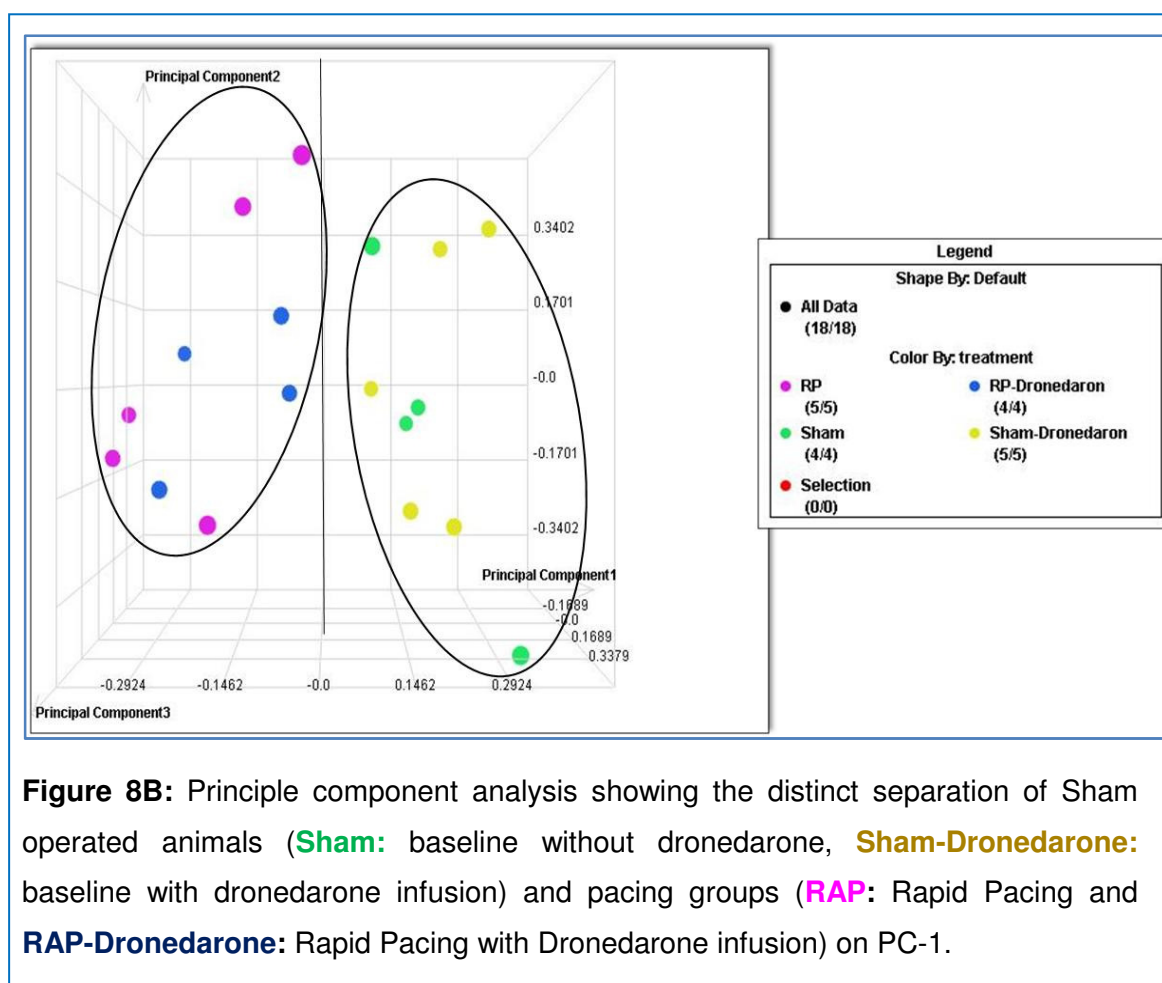
Next, to check for differences among the animals in response to pacing conditions (biological variation) and between the groups (Sham and pacing groups), principle component analysis (PCA) was performed on a global scale using the signal intensities of all probe sets from each array (Rosetta Resolver software, Rosetta Bio Inc.). The basic goal of PCA is to reduce the dimension of the data into principal components, which is a linear combination of two or more observed variables. The first principal component (PC-1) explains the greatest variance in the data, the next principal component (PC-2) represents the next largest variance in the data, and so on. As shown in *figure 8A*, the PCA plot clearly demonstrated the two distinct groups of animals from the irbesartan study, i.e. the sham-operated animals serving as

controls and the two RAP groups (**RAP**: Rapid Pacing and **RAP/I**: Rapid Pacing with Irbesartan infusion).



On a global level, there was no clear separation of irbesartan-treated RAP animals from non-treated RAP animals (**RAP**: Rapid Pacing and **RAP/I**: Rapid Pacing with Irbesartan infusion), which was reflected by the PCA analysis as shown in *figure 8A*.

As shown in *figure 8B*, the PCA plot also clearly showed two distinct groups of animals in the dronedarone study, i.e. sham-operated and paced animals. Sham-operated animals without dronedarone treatment (**Sham**) served as baseline were grouped together with sham-operated animals with dronedarone infusion (**Sham-Dronedarone**) while on the other hand paced animals with (**RAP/D**) or without (**RAP**) dronedarone infusion were grouped. It was clear from the PCA plot that RAP and RAP/D were not separated indicating that dronedarone did not accomplish complete reversion/ prevention of the RAP effects.



4.3. IMPACT OF RAP, RAP/I AND RAP/D ON LEFT ATRIAL GENE EXPRESSION

In the Irbesartan study, the microarray-based profiling of RNA prepared from LA tissue samples from pigs either subjected to RAP or RAP/I allowed detection of 1108 (RAP/I, 4.6% of all probe sets present on the array) and 1134 (RAP, 4.7%) gene-specific probe sets indicating differentially expressed genes when compared with RNA from sham animals, respectively (*figure 9A*). To identify the corresponding differentially expressed genes, the improved annotation information for porcine expressed sequences provided by Tuggle and co-workers (Couture et al., 2009) was used. This allowed identification of 548 and 453 genes exhibiting increased and decreased mRNA amounts, respectively, under RAP conditions, and 542 and 441 genes, respectively, under RAP/I conditions.

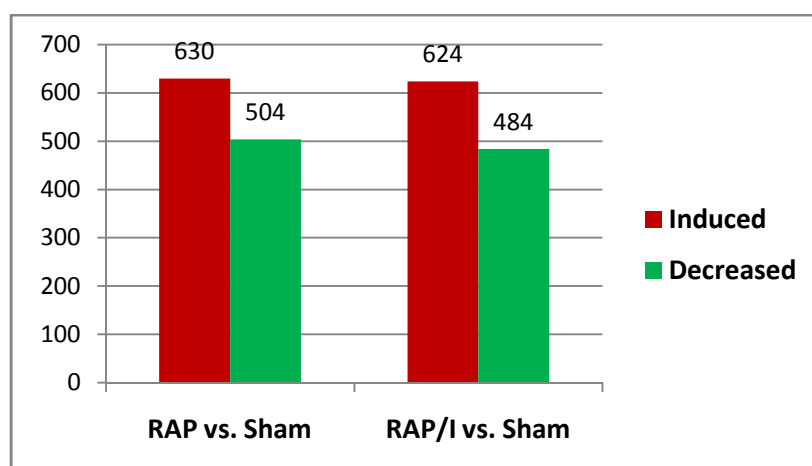


Figure 9A (Irbesartan study): Number of gene-specific probe sets indicating significantly altered gene expression in RAP and RAP/I compared with Sham as baseline. The minimum significance value was ≤ 0.05 after Benjamini Hochberg FDR multiple test correction; A minimum of 1.5-fold absolute expression change relative to Sham animals was considered as induced or decreased either in RAP or RAP/I.

In the dronedarone study, the left atrial expression profiling of animals either subjected to RAP or RAP/D identified 255 (RAP, 1.06% of all probe sets present on the array) and 177 (RAP/D, 0.74%) gene-specific probe sets indicating differentially expressed genes when compared with RNA from sham operated animals, respectively. Interestingly, RAP and RAP/D, when compared with Sham-Dronedarone animals as baseline (i.e. the Sham animals treated with dronedarone, instrumented without any further intervention), allowed identification of 555 (RAP vs. Sham/D, 2.3%) and 378 (RAP/D vs. Sham/D, 1.6%) gene-specific probe sets indicating differentially expressed genes (*figure 9B*). This increase in the number of probesets reflected the negative effect of dronedarone on gene expression in baseline animals (**D** group from section 3.2.1), resulting in a significant increase in the number of identified differentially expressed genes in RAP and RAP/D with Sham/D as the baseline as compared to Sham as the baseline.

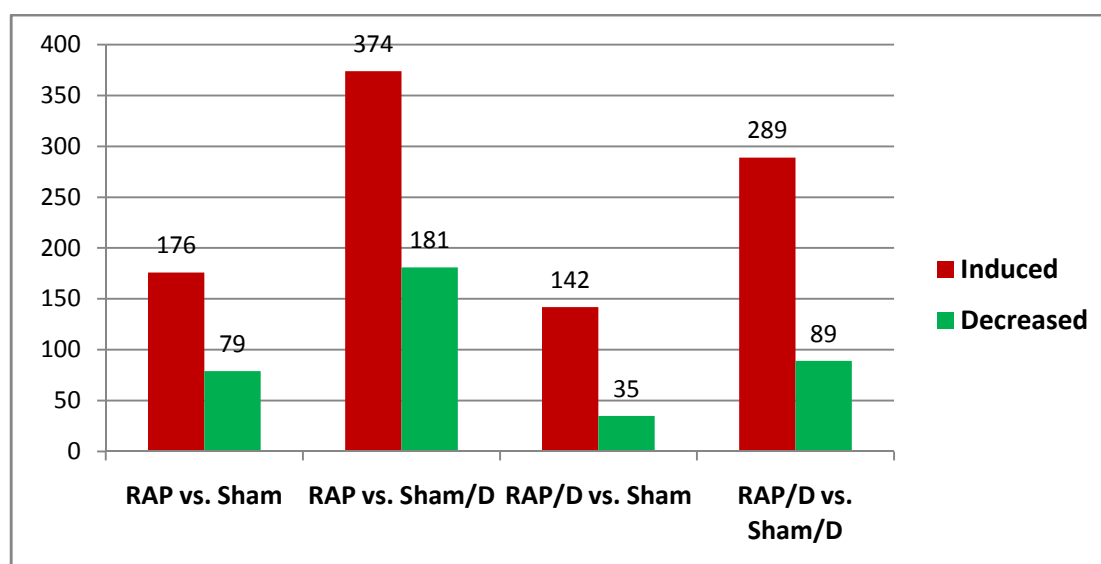


Figure 9B (Dronedarone study): The list of gene specific probe-sets indicating significantly altered gene expression in RAP and RAP/D compared with Sham or Sham/D as baseline. The minimum significance value ≤ 0.05 , after Benjamini Hochberg FDR multiple test correction; A minimum of 1.5 fold absolute change of expression was considered as induced or decreased either in RAP or RAP/D, relative to Sham animals. The maximum number of significant changes was observed when Sham/D was chosen as the baseline, indicating a repressing effect of Dronedarone

4.4. IMPACT OF IRBESARTAN AND DRONEDARONE: PARTIAL ATTENUATION OF RAP-INDUCED GLOBAL GENE EXPRESSION CHANGES BY IRBESARTAN AND DRONEDARONE

In the irbesartan study, as shown in *figure 10A*, a total of 585 significant gene-specific probe sets indicated common (overlap) change of expression in RAP and RAP/I when compared with Sham as baseline.

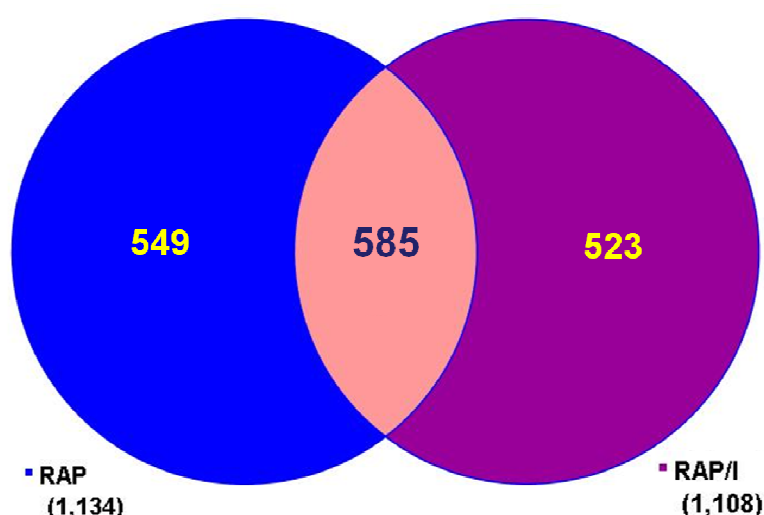


Figure 10A: The number of gene-specific probe sets (585) indicating significantly different gene expression that were commonly regulated in RAP and RAP/I.

Of these 585 common gene-specific probe sets, 151 (25.8%) showed a minimum of 15% irbesartan-mediated attenuation in the RAP/I group due to irbesartan treatment, compared with that of RAP (*figure 10B*). Therefore, the transcriptome data indicated substantial changes in atrial myocardial gene expression provoked by RAP, and most of these RAP-induced expression changes were partly reversed by irbesartan.

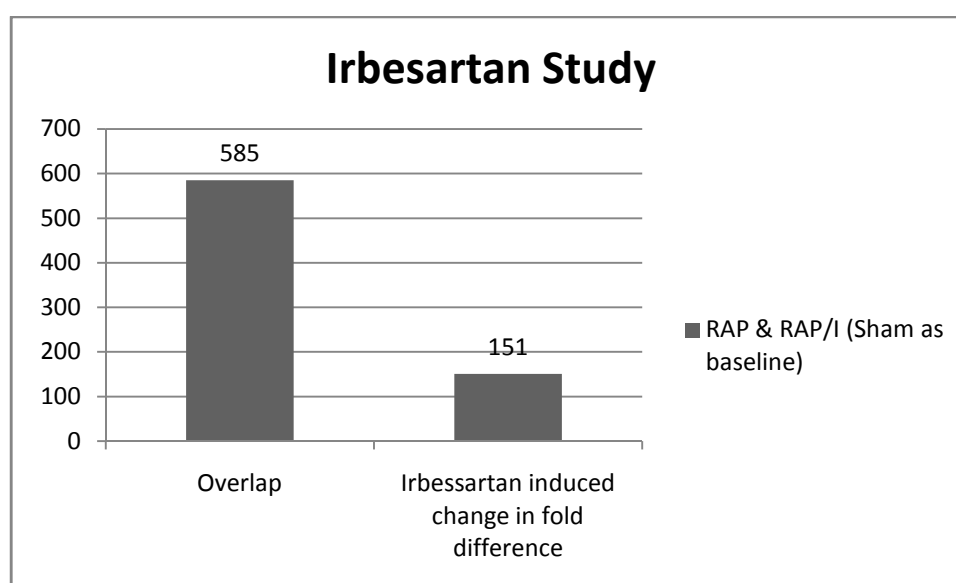


Figure 10B: The number of gene-specific probe sets (151) indicating significantly differential gene expression and showing a minimum of 15% attenuation of RAP-

induced expression change in RAP/I, which can be attributed to irbesartan-dependent effects at the transcriptional level.

In the dronedarone study, due to inter-animal differences in the RAP/D group, the overlap between the groups RAP and RAP/D with Sham as baseline was limited to 92 gene-specific probe sets indicating significantly different gene expression. Of these 92 probe sets, only 17 (18.5% of the overlap) showed a minimum of 15% dronedarone-mediated attenuation in RAP/D, compared with that of RAP. Interestingly, as shown in *figure 10C*, when the analysis was performed with Sham/D as baseline, the overlap between the RAP and RAP/D groups was increased to 266 gene-specific probe sets, and the number of probe sets showing a minimum of 15% dronedarone-mediated attenuation in RAP/D was then increased to 69 (25.8% of the overlap). This increase in the number of affected genes demonstrated the repressing effect of dronedarone at baseline (Sham animals), resulting in a slight increase in the number of dronedarone-mediated attenuation in in RAP/D and an increased overlap between RAP and RAP/D.

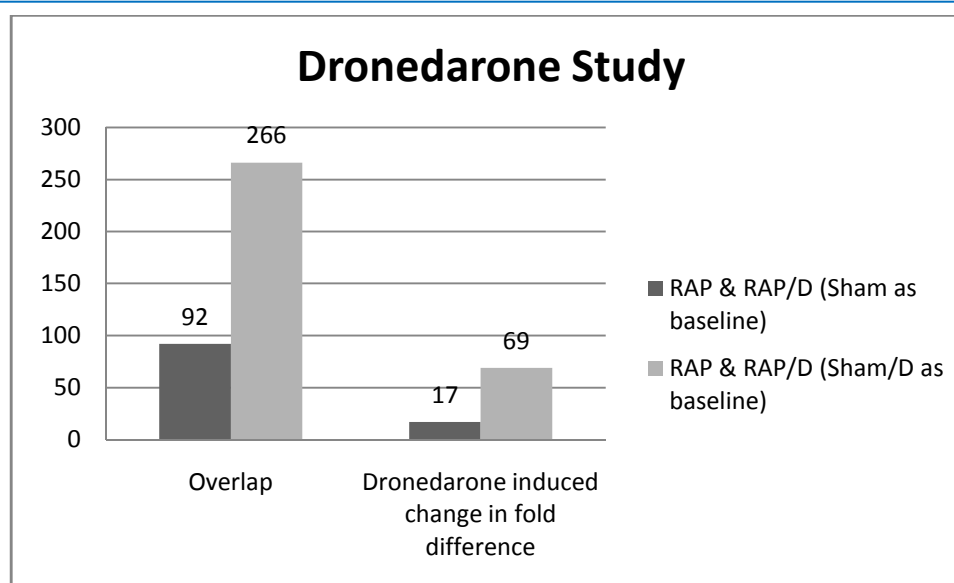


Figure 10C: The number of gene-specific probe sets indicating significantly different gene expression that were commonly regulated in the RAP and RAP/D groups with Sham (92) and Sham/D (266) as baselines. Dronedarone treatment caused an at least 15% dronedarone-mediated attenuation in RAP/D in 17 gene-specific probe sets with Sham as baseline and 69 with Sham/D as baseline, respectively.

Of note, dronedarone, as indicated by the transcriptome data, was not effective in preventing RAP-induced differential gene expression.

4.5. FUNCTIONAL CATEGORIZATION OF IMPORTANT GENE EXPRESSION SIGNATURES IN RESPONSE TO RAP AND RAP/I

As shown in the heat-map in *figure 11*, the detailed analysis of the list of differentially expressed genes from the irbesartan study allowed identification of three pronounced functional categories of regulated genes. Accordingly, RAP caused a change in the overall gene expression profile reflecting:

- **Oxidative stress** as indicated by increased expression of *HMOX1*, *MAFF*, *MAFG*, *SOD2*, *TXNRD1*, *TXNDC1*, *MAP2K3*, *CP*, *DNAJA4*, *DNAJB9*, *DNAJC1*, *DNAJC3*, *HSPA4*, *HSPA13*, *HSPA14*, and *HSPH1*,
- **Tissue remodeling** as indicated by differential expression of *TNFRSF12A*, *ADAMTS6*, *ADAMTS7*, *ADAMTS9*, *ADAMTS20*, *MMP2*, *MMP8*, *MMP11*, *COL1A1*, *COL5A1*, *COL11A1*, *COL14A1*, *COL15A*, *LAMA2*, *LAMB2*, and
- **Cellular energy depletion** as indicated by higher mRNA amounts of *PRKAG2*, *PPARGC1A*, *HK2*, and *SLC25A25*.

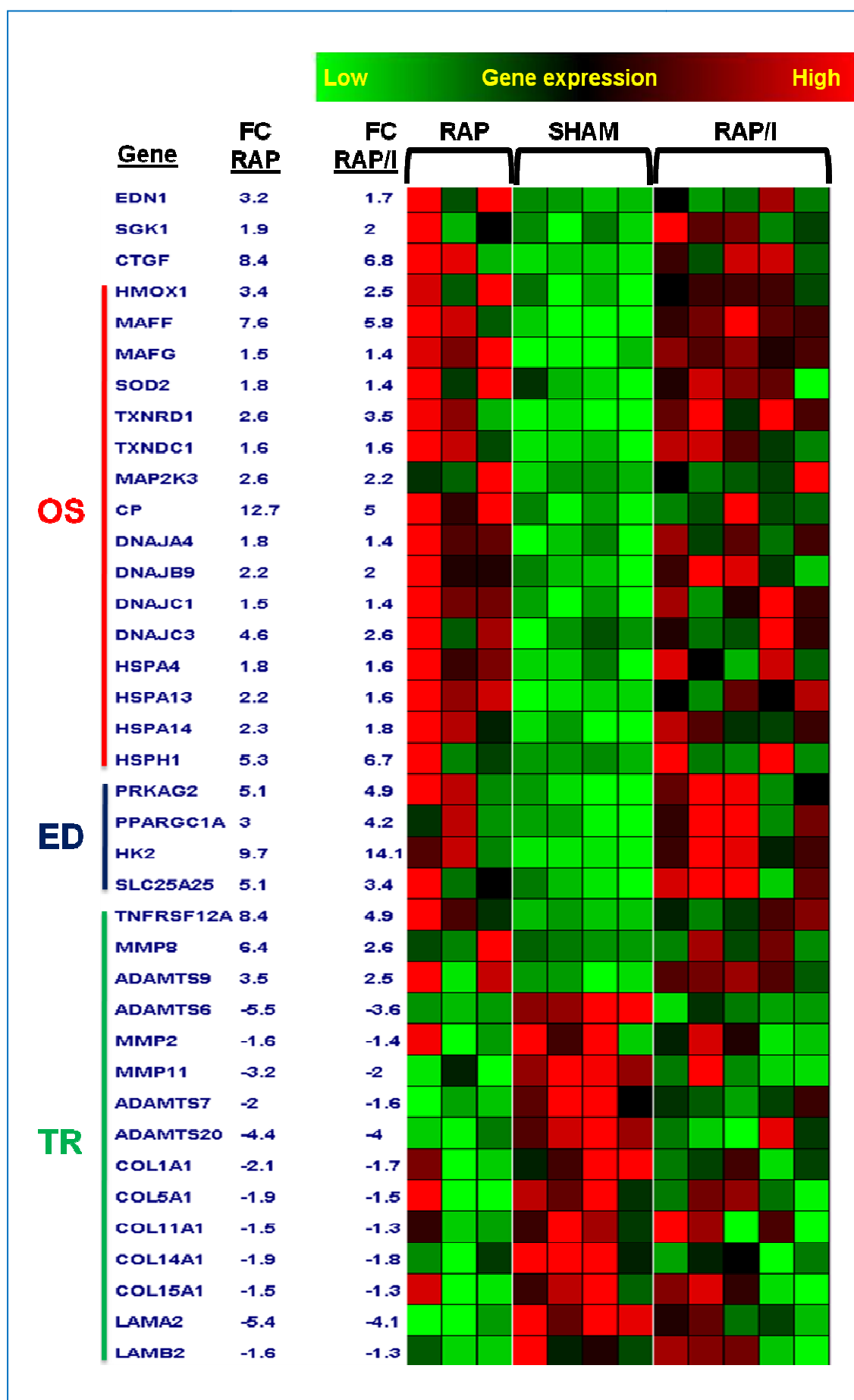


Figure 11: Heat-map displaying differential gene expression signatures including “oxidative stress” (**OS**), tissue remodeling (**TR**), and energy depletion (**ED**) in the left atrium (LA) tissue of animals under conditions of rapid atrial pacing (RAP), RAP in presence of irbesartan (RAP/I), and animals instrumented without further interventions (sham, control group). The heat-map was generated using the k-NN classifier algorithm with Euclidean distance similarity measure. FC (RAP): Averaged expressions fold change in RAP. FC (RAP/I): Averaged expressions fold change in RAP/I.

Details concerning the interpretation of the differential regulation of these marker genes are given in the **Discussion** section.

The results from the dronedarone study also indicated similar effects of RAP on the expression of these genes. Of note, as shown in table 4, the expression changes in the RAP or RAP/D groups were in the same direction in the dronedarone study, but some of the results were not significant when all cut-off thresholds were applied as mentioned in *figure 6*. One possible reason might be that the duration of RAP was only 6h in the dronedarone study while it was 7h in the irbesartan study. Furthermore, the inter-animal variation in RAP animals was higher in the dronedarone study as compared to the irbesartan study and greater variation was seen in the RAP/D group animals as well, that might have a larger impact.

Table 4: Differential gene expression signatures including Oxidative stress (OS), Tissue remodeling (TR), and Energy Depletion (ED) in left atrium (LA) tissue of animals under conditions of RAP and RAP/D compared with that of sham group animals. The non-significant p-values are colored in light grey, >1.5-fold increase was indicated by Bold **Red** color, where as >1.5-fold decrease was indicated by Bold **Green** color.

Gene Symbol	Category	RAP (Dron project)			RAP/D (Dron project)		
		RB_P-value_Shams vs. RP	ANOVA_P-value_Shams vs. RP	Sham vs. RP_Fold Change	RB_P-value_Shams vs. RP	ANOVA_P-value_Shams vs. RP	Sham vs. RP_Fold Change
<i>EDN1</i>	ET1-SGK1-CTGF axis	0.58203	0.9999	-1.16	0.86345	0.99992	-1.05
<i>SGK1</i>	ET1-SGK1-CTGF axis	0.01461	0.22466	1.47	0.83741	0.99992	-1.04
<i>CTGF</i>	ET1-SGK1-CTGF axis	0.00086	0.01987	5.52	0.04706	0.42846	3.62
<i>HMOX1</i>	Oxidative stress	0.61605	0.81949	1.43	0.05531	0.11754	4.81
<i>MAFF</i>	Oxidative stress	1.12E-07	3.33E-07	5.03	0.00225	0.08065	4.14
<i>MAFG</i>	Oxidative stress	0.0483	0.37157	1.30	0.20654	0.85096	1.19

Gene Symbol	Category	RAP (Dron project)			RAP/D (Dron project)		
		RB_P- value_Sham vs. RP	ANOVA_P - value_Sha m vs. RP	Sham vs. RP_Fold Change	RB_P- value_Sham vs. RP	ANOVA_P - value_Sha m vs. RP	Sham vs. RP- Dron_Fold Change
<i>SOD2</i>	Oxidative stress	0.5555	0.9999	1.19	0.30663	0.99992	1.35
<i>TXNRD1</i>	Oxidative stress	0.00273	0.08168	1.79	0.04449	0.53931	1.58
<i>TXNDC1</i>	Oxidative stress	4.72E-12	6.07E-07	1.67	1.08E-10	3.59E-07	1.53
<i>MAP2K3</i>	Oxidative stress	0.02676	0.15408	1.34	0.04069	0.38702	1.44
<i>CP</i>	Oxidative stress	0.48288	0.96791	1.30	0.18451	0.81342	1.79
<i>DNAJA4</i>	Oxidative stress	0.00005	0.00539	2.18	1.69E-07	0.00003	2.37
<i>DNAJB9</i>	Oxidative stress	0.0358	0.50806	1.65	0.07711	0.6625	1.50
<i>DNAJC1</i>	Oxidative stress	0.2712	0.93738	1.29	0.92821	0.99992	-1.02
<i>DNAJC3</i>	Oxidative stress	0.05724	0.77983	1.73	0.47965	0.99992	1.24
<i>HSPA4</i>	Oxidative stress	0.00006	0.01373	1.81	4.37E-06	0.00266	2.02
<i>HSPA13</i>	Oxidative stress	0.01544	0.2052	1.49	0.04303	0.58653	1.47
<i>HSPA14</i>	Oxidative stress	0.00355	0.13517	1.46	0.32748	0.99992	1.15
<i>HSPH1</i>	Oxidative stress	0.02321	0.07195	4.77	0.01605	0.26121	7.84
<i>CACNA1C</i>	Oxidative stress	0.0223	0.33531	1.63	0.0846	0.57875	1.45
<i>PRKAG2</i>	Energy Depletion	3.91E-09	2.27E-06	3.46	0.00004	0.00762	2.70
<i>PPARGC1A</i>	Energy Depletion	3.31E-07	0.00012	2.92	0.00165	0.01499	2.00
<i>HK2</i>	Energy Depletion	3.13E-06	0.0013	7.78	0.0001	0.00007	4.49
<i>SLC25A25</i>	Energy Depletion	0.0003	0.00653	3.91	0.02606	0.35655	2.65
<i>TNFRSF12A</i>	Tissue remodeling	0.00046	0.07372	4.74	4.52E-06	0.00018	5.03
<i>MMP8</i>	Tissue remodeling	0.60668	0.9999	-1.34	0.26557	0.86189	-1.59
<i>ADAMTS9</i>	Tissue remodeling	0.03301	0.40472	1.89	0.00561	0.22367	2.29
<i>ADAMTS6</i>	Tissue remodeling	0.31213	0.97903	-1.35	0.43538	0.99992	-1.25
<i>MMP2</i>	Tissue remodeling	0.07681	0.58287	-1.27	0.33407	0.99992	-1.14
<i>MMP11</i>	Tissue remodeling	0.0158	0.26375	-1.81	0.03887	0.44706	-1.69
<i>ADAMTS7</i>	Tissue remodeling	0.2178	0.88114	-1.39	0.30903	0.99992	-1.32
<i>ADAMTS20</i>	Tissue remodeling	0.71327	0.9999	1.10	0.35838	0.99992	1.32
<i>COL1A1</i>	Tissue remodeling	0.17332	0.73426	-1.42	0.28971	0.99992	-1.32
<i>COL5A1</i>	Tissue remodeling	0.11361	0.567	-1.50	0.12152	0.80068	-1.51
<i>COL11A1</i>	Tissue remodeling	0.00993	0.07998	-1.64	0.33374	0.99992	-1.22
<i>COL14A1</i>	Tissue remodeling	0.89851	0.9999	1.04	0.13077	0.70659	-1.69
<i>COL15A1</i>	Tissue remodeling	0.95271	0.9999	1.00	0.78257	0.99992	1.02
<i>LAMA2</i>	Tissue remodeling	0.48944	0.98799	-1.39	0.3644	0.99992	-1.65
<i>LAMB2</i>	Tissue remodeling	0.09352	0.67021	-1.16	0.22972	0.99992	-1.12

4.6. DRONEDARONE PREVENTS RAP-INDUCED MICROCIRCULATORY ABNORMALITIES AND OXIDATIVE STRESS/ISCHAEMIA-RELATED GENE EXPRESSION

CFR, a combined measure of flow reserve in epicardial arteries and microcirculation, was comparatively similar across the different treatment groups at baseline and was decreased 6h after RAP initiation, but was higher in RAP/D and dronedarone-treated Sham animals. This suggested microcirculatory disturbance during RAP which is prevented by dronedarone (data was shown in table 3B).

4.6.1. Dronedarone prevents RAP-induced oxidative stress

Oxidative stress and calcium overload appear to be the major underlying mechanisms of microcirculatory abnormalities. Hence, expression of the oxidative stress molecular marker proteins NOX1/2/4, which represent members of the NADPH oxidase and are responsible for the catalytic one-electron transfer of oxygen to generate superoxide or hydrogen peroxide, major sources of ROS in cardiac tissue, was assessed by Western blotting. As shown in *figure 12A*, expression of these NADPH oxidase members was induced 6h after RAP initiation as compared with sham levels, suggesting the generation of ROS and indicating oxidative stress during RAP. Dronedarone significantly reduced this RAP-induced up-regulation of NOX2 in RAP/D animals, and there was a similar but not significant effect on NOX1. RAP-induced NOX4 up-regulation was not affected by Dronedarone. *The data was generated in Prof.Dr.Uwe Lendeckel's lab.*

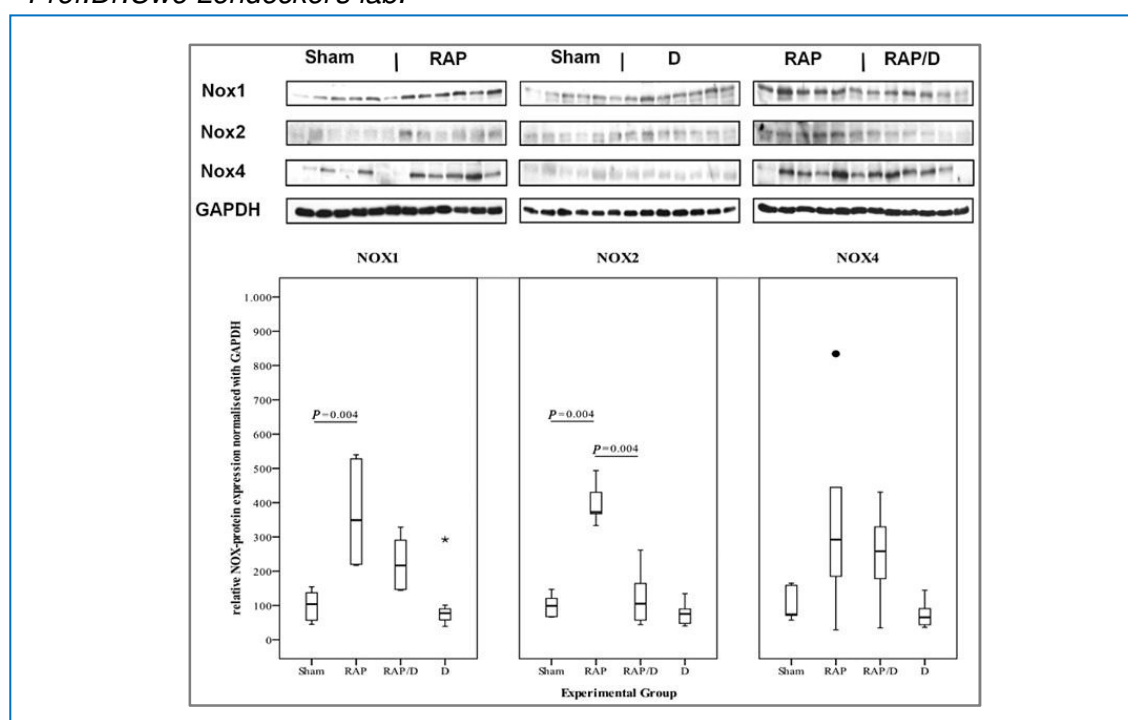


Figure 12A: Dronedarone (D) partly prevented the RAP-induced expression of NADPH oxidase subunit (NOX) isoforms 1, 2 and 4 in the left ventricle 6 h after RAP initiation.

The members of the protein kinase C (PKC) family represent serine- and threonine-specific protein kinases that can be activated by calcium and have been shown to contribute to the phosphorylation and, thus, activation of NOX subunits. The isoform PKC α is itself activated by phosphorylation. Hence, phosphorylation of PKC α was analyzed. As shown in the *Figure 12B*, phosphorylation of PKC α increased during RAP ($P=0.025$) compared with sham. Dronedarone markedly prevented this RAP-induced phosphorylation of PKC α that was nearly significant ($P=0.055$).

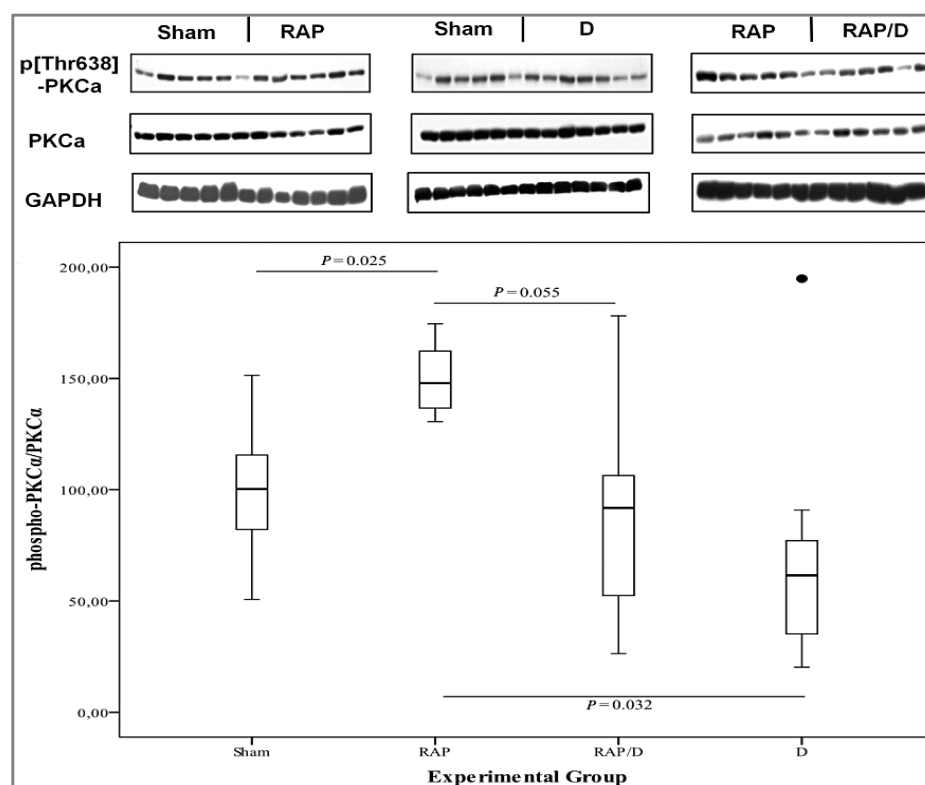


Figure 12B: Dronedarone (D) partially inhibited the RAP-induced phosphorylation of Thr⁶³⁸ in PKC α .

Shown are treatment-induced changes in the NOX:GAPDH ratio. Sham ratios were set to 100. ●: outlier; *: extreme value

To further confirm that the observed RAP-dependent increase of NADPH oxidase levels cause increased cardiac ROS (oxidative stress), left ventricular concentrations

of F_2 -isoprostanes were determined. F_2 -isoprostanes are a group of prostaglandin F (2 α)-like compounds formed *in vivo* via non-enzymatic oxidation of arachidonic acid, involving the free radical (ROS)-initiated peroxidation of arachidonic acid. Hence, F_2 -isoprostanes were shown to represent the most reliable index of *in vivo* oxidative stress (Milne et al., 2007, 2005). As shown in *figure 13A*, the level of F_2 -isoprostanes was elevated by 76% after RAP compared with sham, and was significantly reduced in the RAP/D group, indicating RAP-dependent increase in cardiac ROS (oxidative stress), which was reduced by Dronedarone. *The data was generated in Prof.Dr.Uwe Lendeckel's lab.*

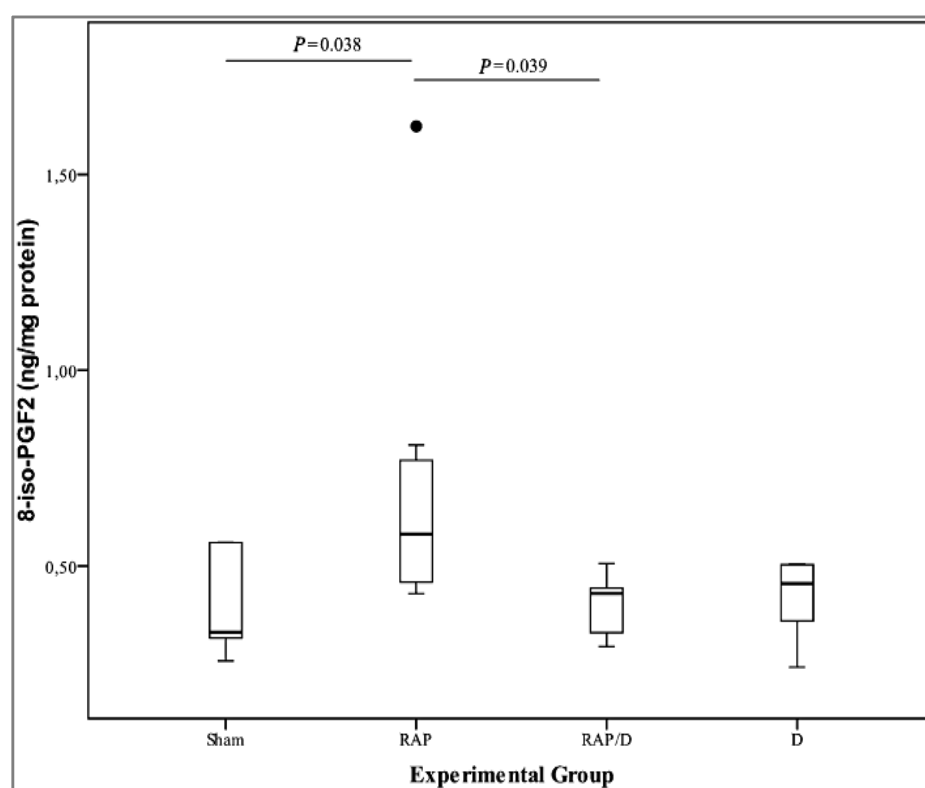


Figure 13A: Effect of RAP and dronedarone (D) on F_2 -isoprostane levels in left ventricular tissue. Samples were taken 15min after the termination of RAP (6h) and F_2 -isoprostanes measured by GC-MS.

Results shown are the changes, induced by treatments, in the $plkB\alpha$:GAPDH ratio. Sham ratios were set to 100. •: outlier; *: extreme value.

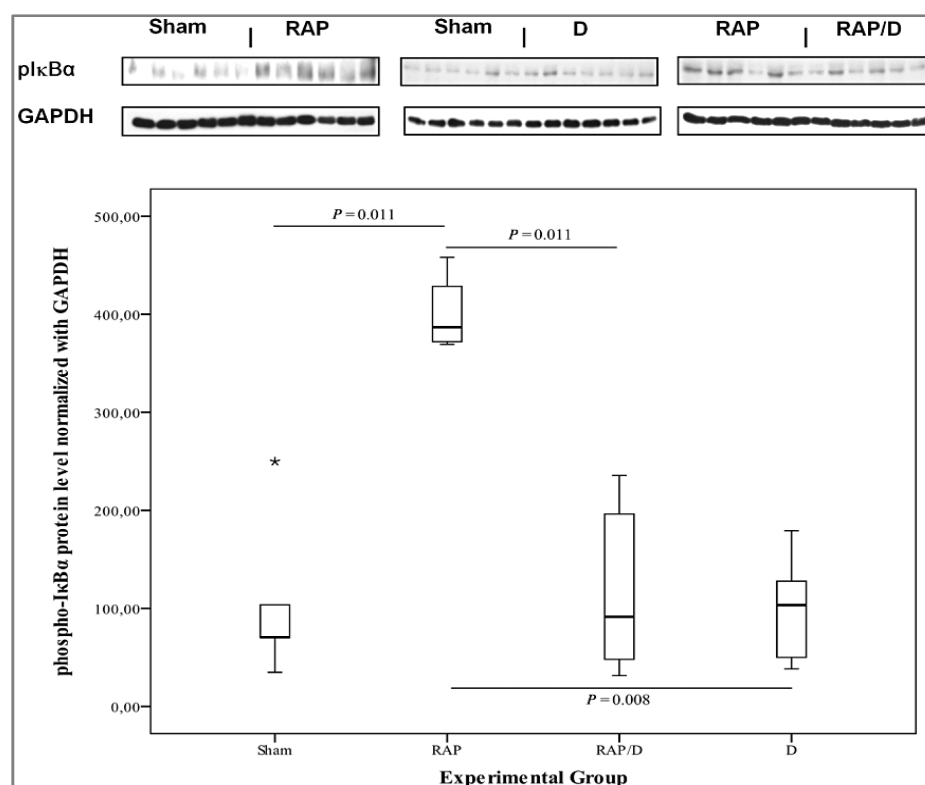


Figure 13B: Dronedarone (D) prevented the RAP-induced phosphorylation of IkBα.

Results shown are the changes, induced by treatments, in the pIkBα:GAPDH ratio. Sham ratios were set to 100. ●: outlier; *: extreme value.

4.6.2. Effect of Dronedarone on the RAP-induced redox-sensitive transcription factor NFκB

To evaluate if the observed RAP-induced oxidative stress involves the activation of redox-sensitive signalling molecules such as the transcriptional factor NF-κB, the phosphorylation of its endogenous inhibitor (IkBα) was analyzed by Western blot analysis. The first step in the activation of NF-κB in response to oxidative stress is the phosphorylation of its endogenous inhibitors. IkBα (NFKBIA) is a member of the NF-kappa-B inhibitor family. In the cytoplasm, this protein inhibits the activity of dimeric NF-κB/REL complexes by trapping them. Under conditions of oxidative stress, IkBα is inactivated by phosphorylation, promoting its ubiquitination and degradation, thereby enabling the dimeric NF-κB/REL complexes to translocate to the nucleus and activate transcription of downstream targets. As shown in *figure 13B*, phosphorylation of IkBα was increased during RAP compared with Sham animals, indicating a response to increased amounts of cardiac ROS. This effect was prevented by dronedarone

indicating lower levels of ROS in dronedarone-treated animals as compared with Sham.

4.6.3. Dronedarone attenuates RAP-induced changes in ischaemia/oxidative stress-related gene expression of left ventricular tissue samples

To evaluate if the microcirculatory disturbance during RAP was associated with ischaemia or altered cellular energy metabolism due to shortage of oxygen/glucose, a comprehensive transcriptome analysis was performed using left atrium tissue samples. As shown in Table 5 and 6, 6h of RAP resulted in significant changes in the expression of several marker genes of oxidative stress/ischaemia. The functional categories of these genes included **energy/glycogen metabolism** (*HK2*, *GSK3B*, *PYGM*, and *PPARGC1* encoding hexokinase 2, glycogen synthase kinase3 β , the muscle isoform of glycogen phosphorylase, and PPAR γ coactivator 1- α , respectively), **hypoxia/ischaemia** (*HIF1A* and *VEGFA* encoding hypoxia-inducible factor-1 α and vascular endothelial growth factor A, respectively) and **oxidative stress** (*DNAJB9*, *PRX3*, and *CCL2* encoding the DnaJ homolog family member B9, peroxiredoxin 3, and the chemokine CCL-2, respectively). Dronedarone treatment did not significantly attenuate these RAP-induced changes.

Table 5: RAP-induced changes in the expression of marker genes indicative for energy/glycogen metabolism, hypoxia/ischaemia, and oxidative stress as determined by microarray-based transcriptome analysis of left atrial tissue samples, under conditions of sham, RAP and RAP/D

energy/glycogen metabolism/ hypoxia/ischaemia/ oxidative stress-related	Sham vs. RAP (n= 4)		RAP vs. RAP/D (n= 6)	
	Fold change	P-value (ANOVA)	Fold change	P-value (ANOVA)
<i>HK2</i>	7.8	0.001	-1.7	N.S.
<i>GSK3B</i>	1.6	0.25	1.2	N.S.
<i>PYGM</i>	-1.4	0.08	1.1	N.S.
<i>PPARGC1A</i>	3.4	<0.001	-1.4	N.S.
<i>HIF1A</i>	-1.2	N.S.	-1.2	N.S.
<i>VEGFA</i>	1.6	0.03	-1.3	N.S.

energy/glycogen metabolism/ hypoxia/ischaemia/ oxidative stress-related	Sham vs. RAP (n= 4)		RAP vs. RAP/D (n= 6)	
	Fold change	P-value (ANOVA)	Fold change	P-value (ANOVA)
<i>CCL2</i>	2.2	0.005	-1.9	N.S.
<i>PRKAG2</i>	3.5	<0.001	-1.3	N.S.
<i>ACADL</i>	-1.3	0.12	1.1	N.S.

HK2, hexokinase 2; **GSK3B**, glycogen synthase 3 B; **PYGM**, muscle isoform of glycogen phosphorylase **AGL**, anti-glycogen debranching enzyme; **VEGFA**, Vascular Endothelial Growth Factor A; **CCL2**, Chemokine (C-C motif) ligand 2; **PRKAG2**, 5'-AMP-activated protein kinase subunit gamma-2; **PPARGC1A**, Peroxisome proliferator-activated receptor gamma coactivator 1-alpha; **ACADL**, acyl-coenzyme A dehydrogenase locus; **HIF1A**, Hypoxia-induced factor 1 alpha.

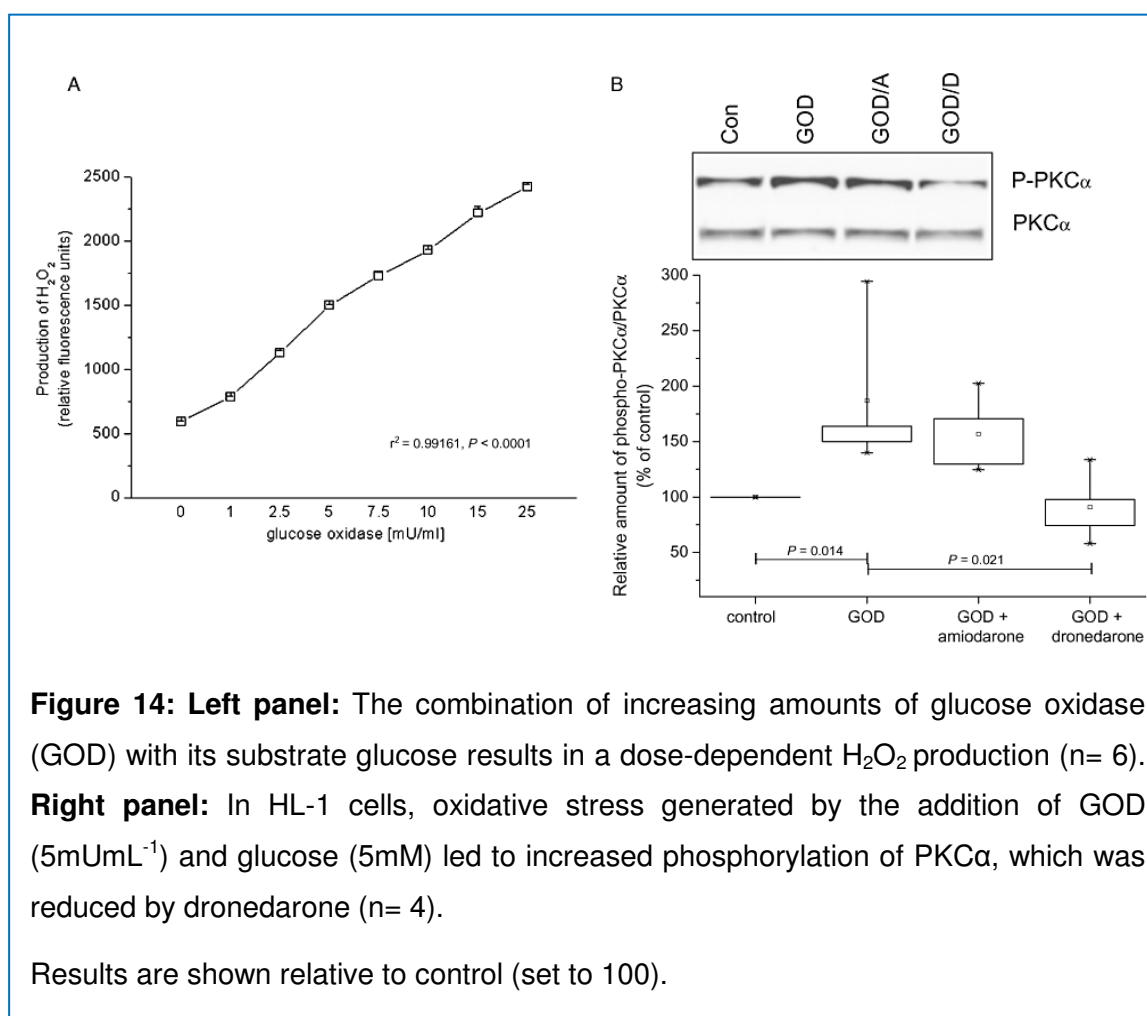
By reverse transcription-quantitative PCR (RT-qPCR), expression of several genes identified to be differentially expressed in left atrial tissue was also analyzed in left ventricular tissue samples (Table 6). In line with the results for left atrial tissue, RAP significantly increased the mRNA amounts of *VEGFA*, *PRKAG2*, *DNAJB9* and *PRX3* as compared with the sham group. For *PPARGC1*, a trend towards increased expression was detected. Treatment with dronedarone significantly reduced the RAP-dependent up-regulation of *VEGFA*, *PRKAG2*, *PPARGC1* and *CCL2*. In contrast to dronedarone, amiodarone was not able to prevent the RAP-dependent increase in *CCL2*, but led to a further increase. Amiodarone was also less effective in attenuating the RAP-dependent induction of *PPARGC1* (Table 6).

Table 6: Significant changes in the expression of marker genes indicating hypoxia/ischaemia and oxidative stress in left ventricular tissue samples under conditions of sham, RAP and RAP/D as determined by RT-qPCR.

	Sham (n= 5)	RAP (n= 6)	RAP/D (n= 6)	D (n= 7)	RAP/A (n= 4)	P-value (Kruskal– Wallis)	P-value (Sham vs. RAP)	P-value (RAP vs. RAP/D)	P-value (RAP vs. RAP/A)	P-value (RAP/D vs. RAP/A)	P-value (Sham vs. D)	P-value (RAP vs. D)
	Median	Median	Median	Median	Median							
	(Q1; Q3)	(Q1; Q3)	(Q1; Q3)	(Q1; Q3)	(Q1; Q3)							
HIF1A	106.87 (63.66; 124.55)	204.90 (153.58; 436.57)	121.39 (105.26; 129.69)	71.65 (28.51; 104.72)	91.80 (61.20; 123.00)	0.017	0.016	0.037	0.033	0.522	0.253	0.004
VEGFA	70.50 (47.50; 93.50)	240.00 (175.00; 262.50)	53.00 (33.00; 56.00)	66.00 (59.00; 70.00)	49.94 (32.44; 63.74)	0.008	0.037	0.01	0.038	0.571	0.391	0.038
CCL2	113.50 (82.50; 130.50)	296.00 (202.00; 303.50)	74.60 (70.00; 93.00)	86.00 (59.00; 106.00)	479.33 (366.88; 647.44)	0.005	0.2	0.025	0.055	0.011	0.143	0.025
PRKAG2	87.95 (67.60; 195.20)	374.30 (311.30; 772.75)	120.20 (99.80; 158.70)	133.60 (107.00; 137.90)	157.93 (143.35; 178.32)	0.01	0.047	0.004	0.014	0.131	0.116	0.009
PRKCa	97.90 (93.40; 106.40)	236.60 (215.75; 280.50)	152.20 (107.80; 221.50)	122.30 (120.70; 122.50)	81.90 (69.57; 97.26)	0.011	0.086	0.273	0.027	0.033	0.011	0.361
DNAJB9	92.50 (78.00; 116.00)	211.00 (177.00; 317.00)	114.00 (101.00; 143.00)	77.00 (73.00; 102.00)	113.81 (97.49; 120.13)	0.004	0.008	0.055	0.011	0.394	0.423	0.004
PRX3	96.85 (81.35; 109.40)	171.10 (150.85; 221.80)	92.80 (87.50; 153.80)	90.10 (74.80; 94.10)	145.86 (144.28; 148.39)	0.01	0.037	0.116	0.394	0.257	0.046	0.007
PPARGC1	84.85 (61.20; 96.75)	267.60 (226.10; 373.90)	66.20 (48.40; 89.20)	70.80 (61.80; 85.10)	136.94 (123.72; 142.28)	0.01	0.076	0.018	0.142	0.033	0.201	0.028

Analyzed genes and encoded proteins: **HIF1A**, hypoxia-induced factor 1 α ; **VEGFA**, vascular endothelial growth factor A; **CCL2**, Chemokine (C-C Motif) Ligand 2; **PRKAG2**, PKA subunit γ -2; **PRKCa**, PKC α ; **DNAJB9**, DnaJ homolog subfamily B member 9; **Prx3**, peroxiredoxin 3; **PPARGC1**, PPAR γ coactivator 1- α ; **Q1**, 1st quartile; **Q3**, 3rd quartile.

To confirm the effects of oxidative stress on the activation of PKC α and its sensitivity to dronedarone *in vitro*, the murine cardiomyocyte cell line HL1 was used. In order to simulate the model of oxidative stress during RAP, HL1-cells were exposed to a combination of glucose oxidase (GOD) and its substrate, glucose, in a dose-dependent manner. As shown in *figure 14 (left panel)*, this exposure resulted in a corresponding dose-dependent increase in the production of H₂O₂, indicating oxidative stress. Using an intermediate concentration of GOD (5 mU·mL⁻¹), there was a ROS-dependent 1.6-fold increase in PKC α activation as indicated by phosphorylation which was prevented by dronedarone (*figure 14, right panel*).



To check the activation of PKC α in response to 7 h of *in vitro* rapid pacing, HL1-cells were paced for 7h and the amount of phospho-PKC α was analyzed by immunoblot. As shown in *figure 15 (left panel)*, a significant increase in the extent of PKC α phosphorylation was observed after 7h of pacing. Dronedarone showed a strong tendency to attenuate this RAP-dependent increased amount of pPKC α . Furthermore, dose-dependent treatment with dronedarone, under basal conditions, exhibited a

tendency to decrease the amounts of phospho-PKC α at higher concentrations (>0.1mM), but this was not consistent (*figure 15, right lower panel*).

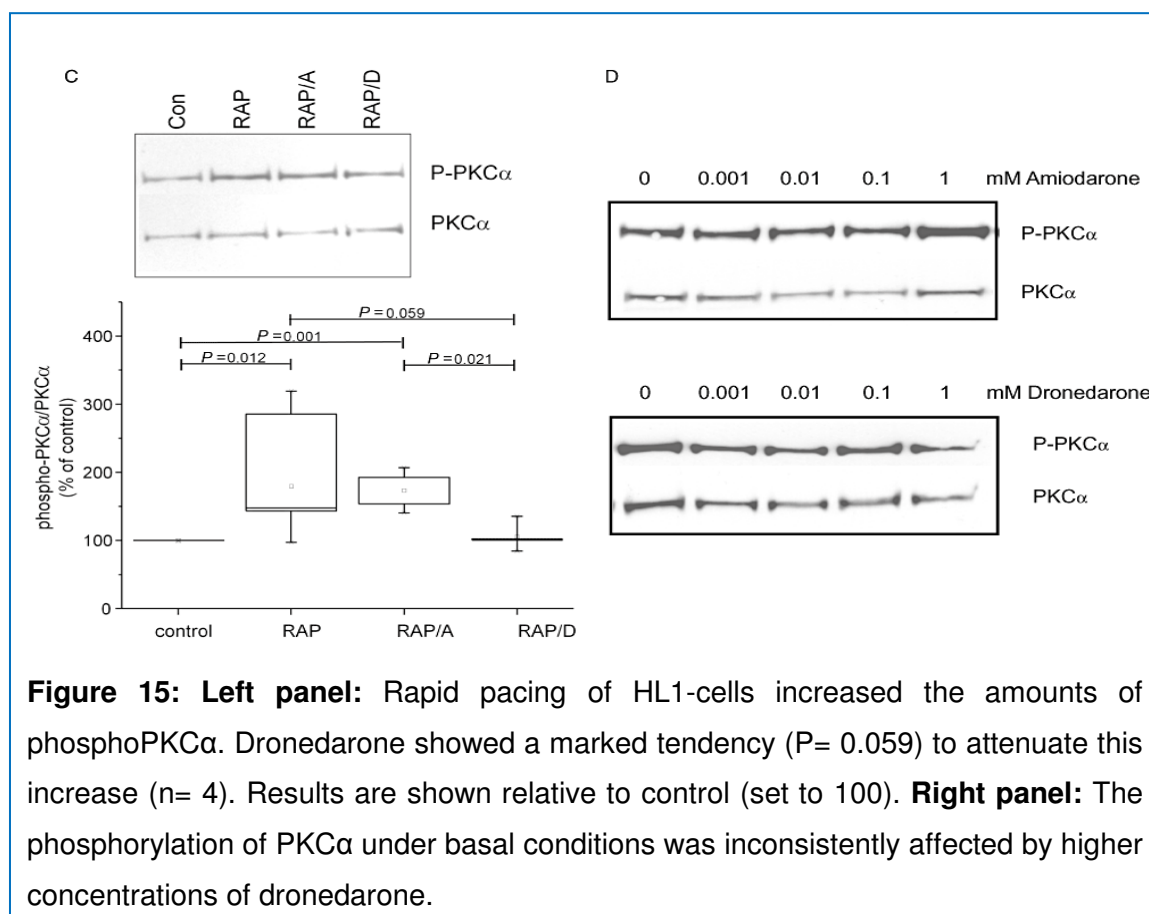


Figure 15: Left panel: Rapid pacing of HL1-cells increased the amounts of phosphoPKC α . Dronedarone showed a marked tendency ($P=0.059$) to attenuate this increase ($n=4$). Results are shown relative to control (set to 100). **Right panel:** The phosphorylation of PKC α under basal conditions was inconsistently affected by higher concentrations of dronedarone.

Taken together, these results from the dronedarone study confirmed that RAP causes flow abnormalities in the microcirculation as well as oxidative stress, both prevented by dronedarone. Additionally, dronedarone was capable of attenuating most of the RAP-induced changes in ischaemia/oxidative stress-related gene expression.

4.7. CANONICAL PATHWAYS INFLUENCED BY IRBESARTAN

In the context of the ibesartan study, Ingenuity Pathway Analysis (IPA) of the RAP-dependent gene expression signatures revealed that several canonical IPA pathways that have already been associated with pathological conditions of the cardiovascular system, including AF, were significantly influenced. These pathways included *myocardial hypertrophy*, *integrin signaling*, *ERK/EMPK signaling* and *cardiac fibrosis*. As shown in table 7, most of these RAP-dependent expression changes were partially attenuated by irbesartan. The mRNA amounts of the genes

CTGF, EDN1, F3, GNAO1, GNG7, GNL3, HMOX1, IGFBP5, MAPK12, MYC, PPP2R5B, PYGM, RASSF1, TDP2, TSC22D1 and TSPAN2 which belong to the IPA-pathways *cardiac hypertrophy signaling, ERK/EMPK signaling, integrin signaling, HIF1- α signaling, PKA signaling* and *cardiac fibrosis* were strongly influenced by irbesartan, with 16-82% change in the RAP-dependent expression values.

Table 7: Genes representing gene-ontology based cardiac-specific canonical IPA pathways that are significantly altered during RAP. The RAP-dependent changes were partially attenuated by irbesartan (RAP/I). ‘% Change by irbesartan’ represents the effect of irbesartan on RAP-dependent gene expression.

IPA Canonical Pathway	Gene Symbol	Entrez Gene Name	RAP	RAP/I	% Change by Irbesartan (with direction)
Cardiac Hypertrophy Signaling	<i>CACNA1C</i>	calcium channel, voltage-dependent, L type, alpha 1C subunit	2.20	2.00	9.3
	<i>CALM1 (includes others)</i>	CALM1 (includes others)	2.05	1.86	9.3
	<i>EIF4E</i>	eukaryotic translation initiation factor 4E	1.72	1.72	-0.1
	<i>ELK1</i>	ELK1, member of ETS oncogene family	1.62	1.75	-7.4
	<i>GNAO1</i>	guanine nucleotide binding protein (G protein), alpha activating activity polypeptide O	-2.74	-1.89	45.0
	<i>GNG7</i>	guanine nucleotide binding protein (G protein), gamma 7	-1.91	-1.58	21.2
	<i>IGF1</i>	insulin-like growth factor 1 (somatomedin C)	-2.01	-2.22	10.8
	<i>MAPK12</i>	mitogen-activated protein kinase 12	-1.95	-1.62	20.5
	<i>PIK3C2B</i>	phosphatidylinositol-4-phosphate 3-kinase, catalytic subunit type 2 beta	-1.66	-1.59	4.5
	<i>PIK3R1</i>	phosphoinositide-3-kinase, regulatory subunit 1 (alpha)	-1.61	-1.60	0.4
	<i>PRKAG2</i>	protein kinase, AMP-activated, gamma 2 non-catalytic subunit	5.07	4.88	3.7
	<i>RHOJ</i>	ras homolog family member J	-2.47	-2.61	5.8
Nitric Oxide Signaling in the Cardio Vascular System	<i>CACNA1C</i>	calcium channel, voltage-dependent, L type, alpha 1C subunit	2.20	2.00	9.3
	<i>CALM1 (includes others)</i>	CALM1 (includes others)	2.05	1.86	9.3
	<i>PIK3C2B</i>	phosphatidylinositol-4-phosphate 3-kinase, catalytic subunit type 2 beta	-1.66	-1.59	4.5
	<i>PIK3R1</i>	phosphoinositide-3-kinase, regulatory subunit 1 (alpha)	-1.61	-1.60	0.4
	<i>PRKAG2</i>	protein kinase, AMP-activated, gamma 2 non-catalytic subunit	5.07	4.88	3.7

IPA Canonical Pathway	Gene Symbol	Entrez Gene Name	RAP	RAP/I	% Change by Irbesartan (with direction)
	<i>SLC7A1</i>	solute carrier family 7 (cationic amino acid transporter, y+ system), member 1	2.25	2.16	4.0
ERK/EMPK Signaling	<i>ATF4</i>	activating transcription factor 4	1.50	1.66	-9.3
	<i>EIF4E</i>	eukaryotic translation initiation factor 4E	1.72	1.72	-0.1
	<i>ELK1</i>	ELK1, member of ETS oncogene family	1.62	1.75	-7.4
	<i>ETS2</i>	ETS2	2.05	2.21	-7.2
	<i>MYC</i>	v-myc myelocytomatosis viral oncogene homolog (avian)	3.21	2.09	34.8
	<i>PIK3C2B</i>	phosphatidylinositol-4-phosphate 3-kinase, catalytic subunit type 2 beta	-1.66	-1.59	4.5
	<i>PIK3R1</i>	phosphoinositide-3-kinase, regulatory subunit 1 (alpha)	-1.61	-1.60	0.4
	<i>PPP2R5B</i>	protein phosphatase 2, regulatory subunit B', beta	-4.10	-3.15	30.3
	<i>PRKAG2</i>	protein kinase, AMP-activated, gamma 2 non-catalytic subunit	5.07	4.88	3.7
	<i>RPS6KA5</i>	RPS6KA5	-2.18	-2.08	4.9
	<i>STAT3</i>	signal transducer and activator of transcription 3 (acute-phase response factor)	2.21	2.29	-3.5
Integrin Signaling	<i>ARF6</i>	ADP-ribosylation factor 6	1.55	1.71	-9.3
	<i>ARHGAP26</i>	Rho GTPase activating protein 26	-2.53	-2.21	14.6
	<i>ARPC1A</i>	ARPC1A	2.06	2.05	0.8
	<i>PIK3C2B</i>	phosphatidylinositol-4-phosphate 3-kinase, catalytic subunit type 2 beta	-1.66	-1.59	4.5
	<i>PIK3R1</i>	phosphoinositide-3-kinase, regulatory subunit 1 (alpha)	-1.61	-1.60	0.4
	<i>RHOJ</i>	ras homolog family member J	-2.47	-2.61	5.8
	<i>TSPAN2</i>	tetraspanin 2	-3.76	-3.13	20.3
IGF1 Signaling	<i>CTGF</i>	connective tissue growth factor	8.45	6.85	18.9
	<i>ELK1</i>	ELK1, member of ETS oncogene family	1.62	1.75	-7.4
	<i>IGF1</i>	insulin-like growth factor 1 (somatomedin C)	-2.01	-2.22	10.8
	<i>IGFBP5</i>	insulin-like growth factor binding protein 5	-2.53	-2.14	18.6
	<i>PIK3C2B</i>	phosphatidylinositol-4-phosphate 3-kinase,	-1.66	-1.59	4.5

IPA Canonical Pathway	Gene Symbol	Entrez Gene Name	RAP	RAP/I	% Change by Irbesartan (with direction)
		catalytic subunit type 2 beta			
	<i>PIK3R1</i>	phosphoinositide-3-kinase, regulatory subunit 1 (alpha)	-1.61	-1.60	0.4
	<i>PRKAG2</i>	protein kinase, AMP-activated, gamma 2 non-catalytic subunit	5.07	4.88	3.7
	<i>STAT3</i>	signal transducer and activator of transcription 3 (acute-phase response factor)	2.21	2.29	-3.5
HIF1a Signaling	<i>APEX1</i>	APEX nuclease (multifunctional DNA repair enzyme) 1	1.61	1.52	5.7
	<i>EDN1</i>	endothelin 1	3.20	1.68	47.7
	<i>EGLN3</i>	egl nine homolog 3 (C. elegans)	-2.35	-2.06	13.8
	<i>MAPK12</i>	mitogen-activated protein kinase 12	-1.95	-1.62	20.5
	<i>PIK3C2B</i>	phosphatidylinositol-4-phosphate 3-kinase, catalytic subunit type 2 beta	-1.66	-1.59	4.5
	<i>PIK3R1</i>	phosphoinositide-3-kinase, regulatory subunit 1 (alpha)	-1.61	-1.60	0.4
PKA Signaling	<i>AKAP7</i>	A kinase (PRKA) anchor protein 7	-1.96	-1.93	1.6
	<i>APEX1</i>	APEX nuclease (multifunctional DNA repair enzyme) 1	1.61	1.52	5.7
	<i>ATF4</i>	activating transcription factor 4	1.50	1.66	-9.3
	<i>CALM1 (includes others)</i>	CALM1 (includes others)	2.05	1.86	9.3
	<i>CAMK2G</i>	calcium/calmodulin-dependent protein kinase II gamma	-2.07	-1.89	9.4
	<i>ELK1</i>	ELK1, member of ETS oncogene family	1.62	1.75	-7.4
	<i>GNG7</i>	guanine nucleotide binding protein (G protein), gamma 7	-1.91	-1.58	21.2
	<i>PRKAG2</i>	protein kinase, AMP-activated, gamma 2 non-catalytic subunit	5.07	4.88	3.7
	<i>PYGM</i>	phosphorylase, glycogen, muscle	-3.64	-2.00	82.6
	<i>TDP2</i>	tyrosyl-DNA phosphodiesterase 2	-2.01	-1.52	32.3
	<i>IL33</i>	interleukin 33	-1.56	-1.63	5.1
	<i>PIK3C2B</i>	phosphatidylinositol-4-phosphate 3-kinase, catalytic subunit type 2 beta	-1.66	-1.59	4.5

IPA Canonical Pathway	Gene Symbol	Entrez Gene Name	RAP	RAP/I	% Change by Irbesartan (with direction)
	<i>PIK3R1</i>	phosphoinositide-3-kinase, regulatory subunit 1 (alpha)	-1.61	-1.60	0.4
	<i>TDP2</i>	tyrosyl-DNA phosphodiesterase 2	-2.01	-1.52	32.3
Cardiac Fibrosis	<i>CACNA1C</i>	calcium channel, voltage-dependent, L type, alpha 1C subunit	2.20	2.00	9.3
	<i>DAG1</i>	dystroglycan 1 (dystrophin-associated glycoprotein 1)	-2.06	-2.11	2.6
	<i>F3</i>	coagulation factor III (thromboplastin, tissue factor)	-2.34	-1.79	30.5
	<i>HMOX1</i>	heme oxygenase (decycling) 1	3.38	2.52	25.2
	<i>NR3C2</i>	nuclear receptor subfamily 3, group C, member 2	-1.97	-1.89	4.3
	<i>RASSF1</i>	Ras association (RalGDS/AF-6) domain family member 1	1.84	1.53	16.8
	<i>RRM2B</i>	ribonucleotide reductase M2 B (TP53 inducible)	-1.52	-1.54	1.4
	<i>STAT3</i>	signal transducer and activator of transcription 3 (acute-phase response factor)	2.21	2.29	-3.5
	<i>TRDN</i>	triadin	-1.78	-1.71	4.1
	<i>TSC22D1</i>	TSC22 domain family, member 1	-2.29	-1.60	43.6
	<i>XIRP1</i>	xin actin-binding repeat containing 1	1.86	2.04	-8.7
Increased Cardiac Proliferaion	<i>EDN1</i>	endothelin 1	3.20	1.68	47.7
	<i>GNL3</i>	guanine nucleotide binding protein-like 3 (nucleolar)	2.60	1.92	26.0
	<i>HMOX1</i>	heme oxygenase (decycling) 1	3.38	2.52	25.2
	<i>IGF1</i>	insulin-like growth factor 1 (somatomedin C)	-2.01	-2.22	10.8
	<i>NRG1</i>	neuregulin 1	-2.15	-2.31	7.1

4.8. IMPACT OF RAPID ATRIAL PACING (RAP) ON EXPRESSION OF *CTGF*

CTGF encoding connective tissue growth factor has been frequently implicated as an important effector gene during cardiac remodeling and extensively associated with cardiac fibrosis in previous studies, although causality has not been proven, yet. *CTGF* has also been reported to have diverse functions in cellular activities including ECM production, cell adhesion, cell proliferation, apoptosis and angiogenesis. A number of studies have reported that *CTGF* production by myocytes and fibroblasts significantly increases after myocardial infarction (Ahmed et al., 2004; Chen et al., 2000; Hishikawa et al., 1999, p. -7; Shimo et al., 1999). Consistent with previous data from the literature, our transcriptome data from the irbesartan study demonstrated 8.4-fold up-regulation of *CTGF* in LA tissue samples under conditions of RAP as compared to sham animals ($p < 0.001$), as shown in *figure 16A*. Administration of irbesartan significantly diminished this RAP-dependent induction of *CTGF* (6.4-fold vs. sham; $p < 0.001$). Subsequently, RT-qPCR analyses were performed to confirm the *CTGF* induction in LA and also to check the expression pattern of *CTGF* in other tissues (RA and LV) as well. As shown in *figure 16A*, the RT-qPCR analyses confirmed the microarray data by showing a 7.8-fold increase of left atrial *CTGF* mRNA amounts in the RAP group ($p = 0.029$), which was partly prevented by irbesartan (RAP/I: 4.4-fold vs. sham, $p = 0.11/\text{n.s.}$). Similar but less pronounced changes were observed in RA tissue, whereas in LV no increase of *CTGF* mRNA levels could be detected.

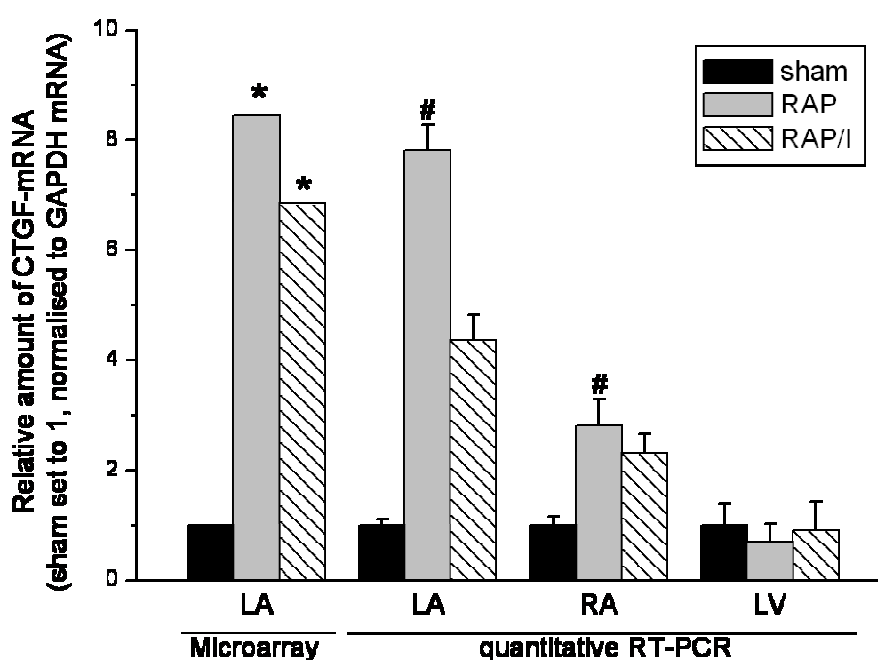


Figure 16A: Transcriptome and RT-qPCR analyses of *CTGF* expression in LA, RA and LV under conditions of RAP and RAP/I. The amount of *CTGF* mRNA was strongly increased by RAP in LA and similar, but less pronounced in RA. This RAP-dependent induction was partially attenuated by irbesartan (RAP/I). There was no corresponding change in *CTGF* expression in LV. *GAPDH* mRNA was used as internal control. Results are shown relative to control (Sham) (* $p < 0.001$; # $p < 0.05$). **LA:** left atrium; **RA:** right atrium; **LV:** left ventricle.

The strong induction of *CTGF* at the mRNA level was additionally correlated with CTGF protein abundance. Western blot analysis demonstrated that, in accordance with the observed RAP-dependent increase in *CTGF* mRNA, there was also a tendency towards increased CTGF protein levels in LA and RA, but most consistent in LV tissue samples. Administration of irbesartan also showed a similar trend to attenuate the RAP-induced increases in level (*figure 16B*).

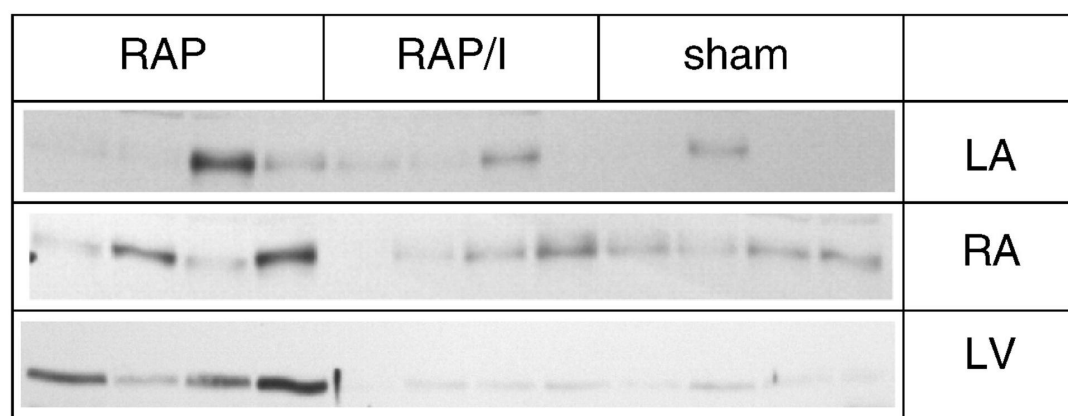


Figure 16B: Comparison of the CTGF protein abundance in left atria (LA), right atria (RA) and left ventricles (LV) using Western blotting. RAP induced increase in CTGF amounts was attenuated by irbesartan in LA, RA and LV. Equal loading of proteins was confirmed by verifying equal amounts of β -actin on the same blots (data not shown).

These results indicate that RAP substantially induces mRNA and protein amounts of CTGF and that irbesartan is capable of attenuating most of these changes.

4.9. RAP-DEPENDENT REGULATION OF *EDN1* AND *SGK1*

The microarray data was explored to identify casual regulators of *CTGF* expression under AF conditions. Intriguingly, the data revealed expression changes of two specific candidate genes that have been previously associated with *CTGF* induction, in particular *EDN1* and *SGK1* encoding endothelin 1 and stress and glucocorticoid induced kinase-1, respectively. *EDN1* and *SGK1* are known to be highly expressed in fibrosing tissue and both of them have inter-relationship with ANGII while modulating the expression of CTGF.

Although the p-values for *EDN1* and *SGK1* derived from the variance analysis of the microarray experiment were slightly higher than the standard value of significance (0.05) when RAP or RAP/I conditions were compared to sham, these targets were successfully validated by RT-qPCR in both groups. As shown in *figure17A*, microarray analysis revealed a significant RAP-dependent increase in left atrial (LA) *EDN1* mRNA amounts (3.2-fold, $p < 0.01$). Interestingly, confirmatory RT-qPCR analyses revealed similar effects in LA (4.84-fold, $p = 0.029$), RA (4.2-fold, $p = 0.014$), and LV samples (3.0-fold, $p = 0.014$). In the left atrium, irbesartan significantly prevented this *EDN1* induction (LA: 55%, $p = 0.048$; RA: 54%, $p = n. s$).

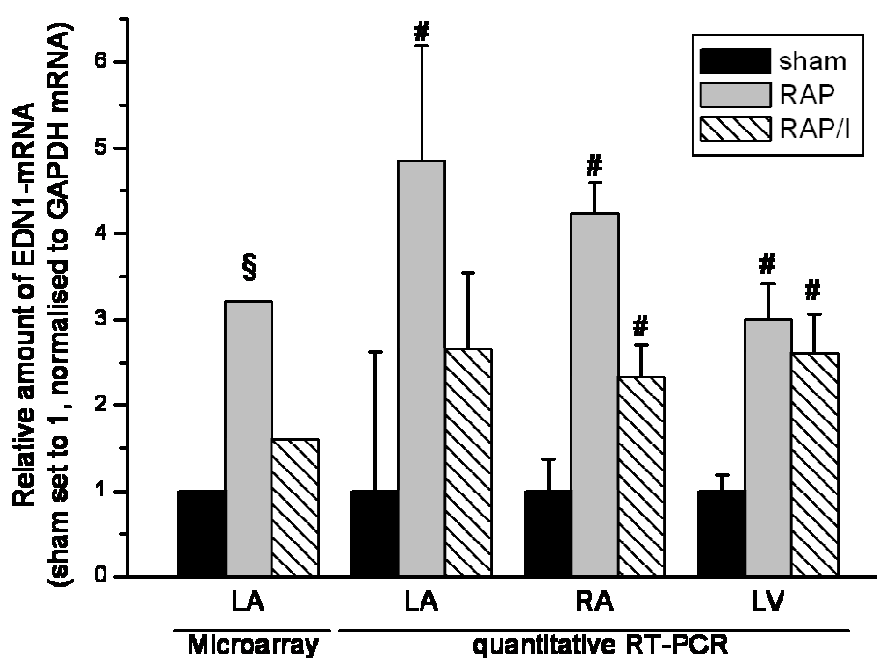


Figure 17A: Transcriptome and RT-qPCR analyses of *EDN1* expression in LA, RA and LV under conditions of RAP and RAP/I. The amount of *EDN1* mRNA was increased under conditions of RAP in LA, RA and LV. This RAP-dependent induction was partially attenuated by irbesartan (RAP/I) in the atrial tissues, whereas in left ventricle, there was a slight trend towards attenuation. *GAPDH* mRNA was used as internal control. Results are shown relative to control (Sham) (* $p < 0.001$; § $p < 0.01$; # $p < 0.05$). **LA:** left atrium; **RA:** right atrium; **LV:** left ventricle.

Likewise, RAP *in vivo* caused a significant increase in LA tissue levels of *SGK1* mRNA (2.1-fold; $p < 0.05$). A similar response could be observed in LV (1.72-fold vs. sham, $p = 0.029$), but the increase was less pronounced in RA (1.37-fold). Interestingly, irbesartan had no effect on the RAP-dependent changes in *SGK1* mRNA in either tissue (*figure 17B*).

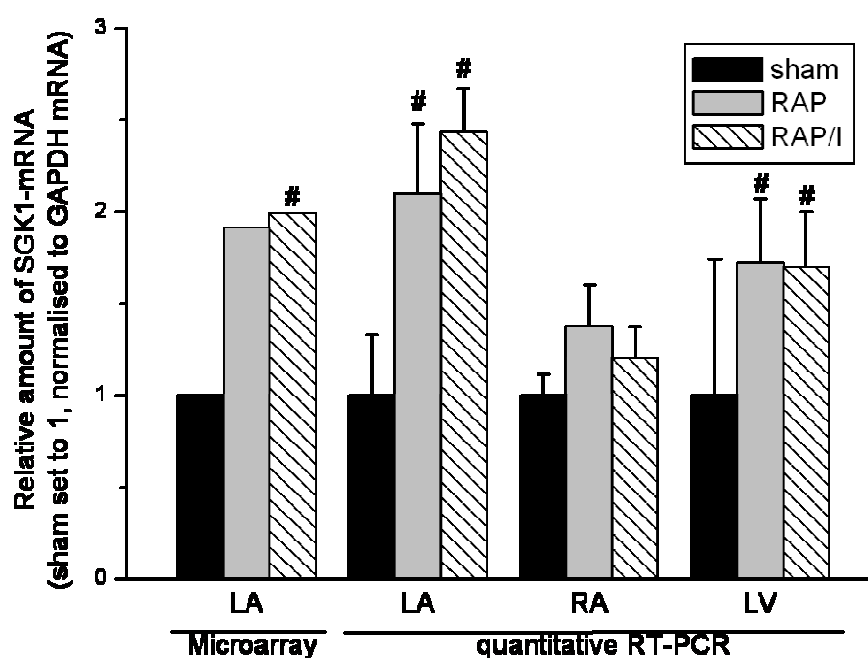


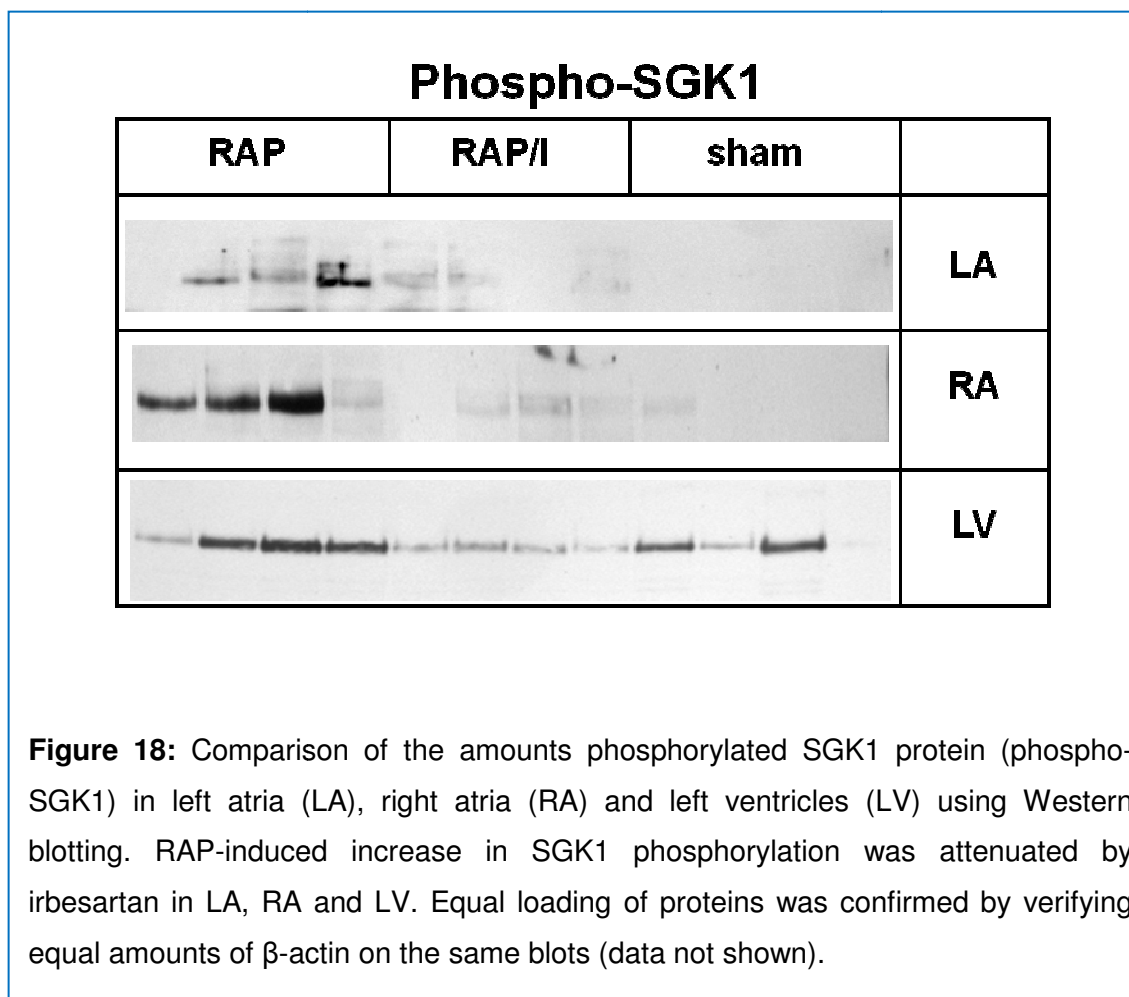
Figure 17B: Transcriptome and RT-qPCR analyses of *SGK1* expression in LA, RA and LV under conditions of RAP and RAP/I. The amount of *SGK1* mRNA was increased under conditions of RAP in LA and LV. There was a trivial increase of *SGK1* mRNA in RA. Administration of irbesartan did not show any effect on RAP-dependent change of *SGK1* in any of the tissue sample (RAP/I). *GAPDH* mRNA was used as internal control. Results are shown relative to control (Sham) (# $p < 0.05$). **LA:** left atrium; **RA:** right atrium; **LV:** left ventricle.

These results indicate that RAP induces the expression of *EDN1* and *SGK1* which were subsequently correlated with *CTGF* induction. Irbesartan was capable of attenuating RAP-induced changes in *EDN1* mRNA, whereas *SGK1* was not affected at the transcriptional level.

4.10. RAP-INDUCED SGK1 PHOSPHORYLATION IS PARTLY PREVENTED BY IRBESARTAN

In order to investigate the lack of irbesartan's effect on *SGK1* mRNA amounts, the regulation of SGK1 activity was explored based on previous published data. Reversible phosphorylation of SGK1 represents a key step in the regulation of its activity. Therefore, to determine the activation state of SGK1, the amounts of

phospho-SGK1 were determined by immunoblot analyses in LA, RA, and LV tissue samples. As shown in *figure 18*, there was a significant increase of p-SGK1 amounts in all tissues during RAP when compared to sham (LA: 3.1-fold, $p = 0.05$; RA: 2.78-fold, $p = 0.02$; LV: 2.8-fold, $p = 0.041$). Irbesartan significantly attenuated the RAP-dependent increase of phospho-SGK1 amounts in LA, RA and LV.



Recent studies performed using smooth muscle cells (Wolf et al., 2006, p. -1) and human and mouse fibroblasts (Hussain et al., 2008) demonstrated that on the one hand, *SGK1* expression is positively regulated by ET1 and that on the other hand, ANG II-dependent *CTGF* induction depends on this transcriptional SGK1 induction. Therefore, the simultaneous RAP-dependent increase in *EDN1*, *SGK1*, and *CTGF* mRNA as observed in the irbesartan study suggested a mechanism involving ANG II-dependent up-regulation of *EDN1* and subsequent auto- or/and paracrine ET1-mediated activation of *SGK1* by enhanced *SKG1* transcription as well as phosphorylation of the encoded protein, finally resulting in the induction of *CTGF* expression.

4.11. EXPRESSION OF RAS COMPONENTS DURING RAP

The renin–angiotensin system (RAS), one of the most important physiological systems involved in blood pressure regulation, has been shown to be involved in many cardiovascular diseases and is activated in the fibrillating atria. AF is associated with activation of the RAS, in particular tissue levels of angiotensin-converting enzyme (ACE) were elevated in the atria of patients with a history of paroxysmal or persistent AF compared with those in sinus rhythm. Atrial ANG II concentration was demonstrated to be increased in a ventricular tachypacing-induced congestive heart failure animal model of AF. In a sheep model, the development of AF by atrial tachypacing was associated with an increase in plasma levels of ANG II (Goette et al., 2000; Li et al., 2001; Tsai, 2004; Willems et al., 2001). Hence, with this background and the observation that irbesartan attenuated most of the RAP-dependent expression changes in the present study, the array-based expression data for *ACE*, *AT1R*, and *AT2R* was analyzed to investigate the effects of RAP on the left atrial classical RAS components. In the irbesartan study, expression of *AT2R* and *ACE* did not appear to be different between the different groups, but there was a strong tendency towards lower *AT1R*-mRNA levels in response to RAP (54% of sham; ratio build p-value= 0.02, ANOVA p = 0.08, table 8). This finding was verified by RT-qPCR for LA and RA, and there was a similar tendency for LV (data not shown). A similar tendency towards reduced *AT1R*-mRNA levels in response to RAP was observed in the dronedarone study as well (table 8, Dronedarone).

Table 8: Microarray analyses of LA tissue samples revealed that 7 h of RAP caused a strong tendency towards reduced *AGTR1* mRNA amounts, whereas no significant expression changes of other RAS components encoding genes were observed between the groups. Data from sham, RAP, RAP/I and RAP/D groups were used. The non-significant p-values are colored in light grey, >1.5-fold increase was indicated by Bold **Red** color, where as >1.5-fold decrease was indicated by Bold **Green** color.

Irbesartan							
		RAP			RAP/I		
Gene Symbol	Name	ANOVA_P-value	RB_P-value	Fold Change	ANOVA_P-value	RB_P-value	Fold Change
<i>AGTR1</i>	Type-1 angiotensin II receptor (AT1) (AT1AR)	0.08053	0.02217	-1.61	0.42174	0.09116	-1.38
<i>ACE</i>	Angiotensin-converting enzyme	0.84978	0.40293	1.09	0.62825	0.19994	1.12
<i>AGTR2</i>	Type-2 angiotensin II receptor (AT2)	0.94638	0.8376	-1.24	0.97854	0.8699	1.16
Dronedarone							
		RAP (Dron project)			RAP/D (Dron project)		
Gene Symbol	Name	RB_P-value	ANOVA_P-value	Fold Change	RB_P-value	ANOVA_P-value	Fold Change
<i>AGTR1</i>	Type-1 angiotensin II receptor (AT1) (AT1AR)	0.01169	0.26312	-1.92	0.03247	0.31762	-1.70
<i>ACE</i>	Angiotensin-converting enzyme	0.33582	0.97476	1.27	0.96821	0.99992	1.01
<i>AGTR2</i>	Type-2 angiotensin II receptor (AT2)	0.7909	0.75998	1.14	0.94055	0.99992	-1.04

4.12. CONFIRMATORY EXPERIMENTS WITH THE MURINE HL-1 CARDIOMYOCYTE-LIKE CELL LINE

Many of the RAP-dependent gene expression changes indicated structural alterations of the myocardial tissue in terms of 'myocardial remodeling' which are known to be fundamental for the development of heart failure. In particular, a number of studies demonstrated that CTGF production majorly by cardiomyocytes and fibroblasts significantly increased in post-myocardial infarction conditions (Ahmed et al., 2004; Chen et al., 2000; Hishikawa et al., 1999, p. -7; Shimo et al., 1999). Cardiomyocytes constitute 20% to 30% of the total number of cells present in the adult heart, but they constitute the vast majority of the heart's total mass and are assumed to represent a major target of ANGII (Rubart and Field, 2006). Hence, we used the murine cardiomyocyte cell line HL-1 as a well-defined model system to validate the hypothesized model of CTGF regulation *via* ET1 and SGK1.

4.12.1. RAP-induced ERK1/2 phosphorylation is partially prevented by irbesartan in the HL-1 cell line

The experimental set-up was verified by demonstrating that HL-1 cells adequately respond to the pacing procedure. It has been published previously that the extracellular signal-regulated kinase (ERK) pathway is activated by ANG II during atrial pacing. Activated ERK1/2 induces cellular differentiation processes and fibroblast activation, thereby causing the development of interstitial fibrosis (Goette et al., 2000). Hence, the levels of phosphorylated Erk2 were analyzed by immunoblotting to confirm successful *in vitro* pacing of HL-1 cells. As shown in *figure 19*, in response to 7 h of rapid-pacing *in vitro*, HL-1 cells exhibited the typical AF-dependent activating Erk2-phosphorylation (Goette et al., 2000), which was partly prevented when pacing was performed in the presence of irbesartan.

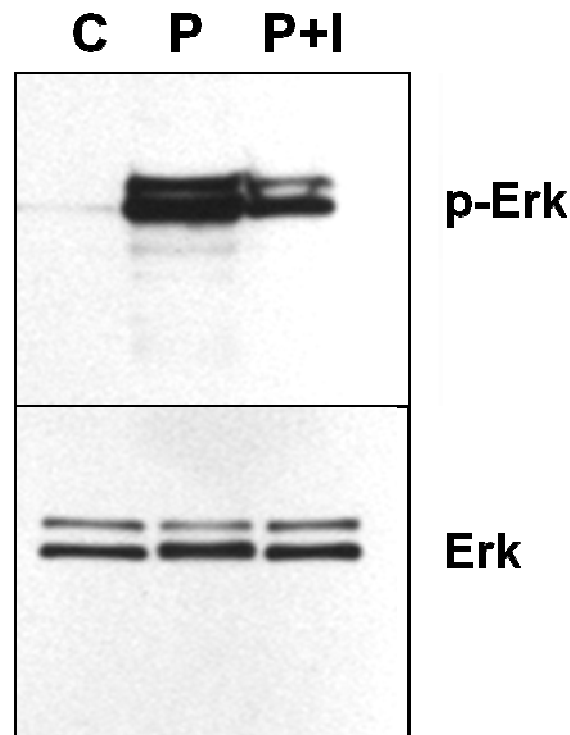


Figure 19: Rapid pacing for 7 h resulted in a strong increase in the amount of phosphorylated Erk1/2 (p-Erk) under conditions of rapid pacing (P), which was significantly attenuated in the presence of irbesartan (P + I). The total amount of Erk2 (Erk) protein was comparable between the groups. Non-treated cells served as the control (C).

4.12.2. Frequency-dependent down-regulation of *CACNA1C* mRNA amounts in HL-1 cells subjected to rapid pacing *in vitro*.

HL-1 cells subjected to rapid pacing *in vitro* showed a frequency-dependent decrease in *CACNA1C*-specific mRNA (figure 20). Down-regulation of this gene, which encodes the L-type Ca^{2+} -channel subunit, represents a key mechanism of electrical remodeling during AF (Schotten et al., 2011). It has been demonstrated that AF induces cellular calcium overload *via* the L-type Ca^{2+} channel. This further triggers cytoprotective mechanisms causing Ca^{2+} -concentration-dependent inactivation of the L-type Ca^{2+} current which in turn enhances the likelihood of AF. If arrhythmia persists, this might lead to reduced levels of L-type Ca^{2+} channel protein, possibly *via* activation of Ca^{2+} overload-induced proteases like calpain, further followed by a decrease in the L-type Ca^{2+} channel mRNA levels. Finally, these

events might result in structural myocyte remodeling such as myolysis and nuclear condensation (Bosch et al., 2003; Brundel, 2004; Brundel et al., 2001a, 1999, 2002).

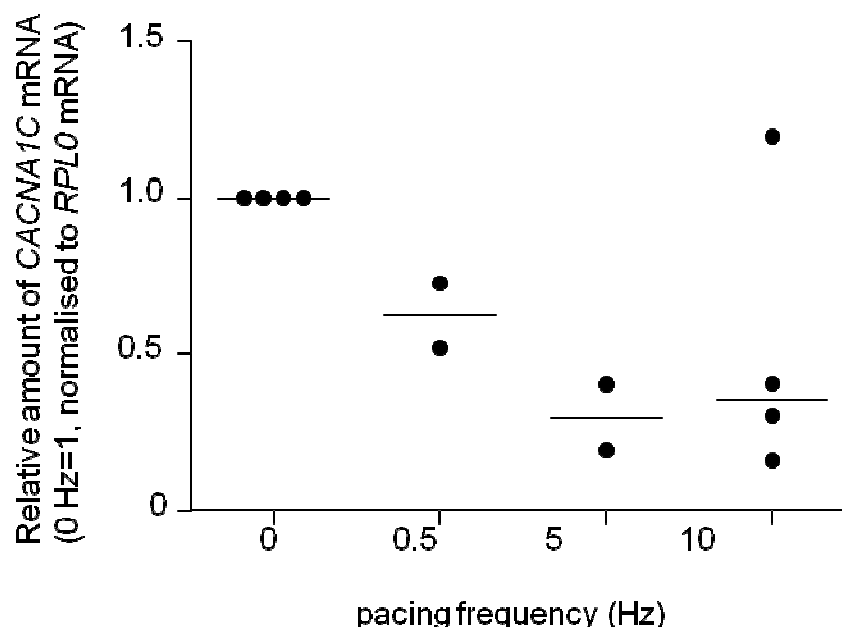


Figure 20: Frequency-dependent down-regulation of *CACNA1C* in HL-1 cells. The amount of *CACNA1C* specific mRNA in HL-1 cells paced at different electrical field stimulation frequencies (0, 0.5, 5, and 10 Hz) for 7 h was determined by RT-qPCR. *RPLP0* mRNA was used as internal control (data provided by Christoph Aderkast, IMBM).

4.12.3. Comparison of *in vivo* transcriptome results from the irbesartan study with previous transcriptome data of paced HL-1 cells reveals similar regulation of most prominent genes

The transcriptome results from the irbesartan study were compared with recently published data from a genome-wide array-based expression analysis describing the comparison of the transcriptomes of HL-1 cells either paced for 24 h or representing non-paced controls (Mace et al., 2009). In this analysis, altogether 758 genes exhibited significantly altered expression under RAP conditions where 626 genes were up-regulated and 132 genes were down-regulated. Of these, 32 (up-regulated) and 7 (down-regulated) genes exhibited the same direction of regulation in our analysis. The group of overlapping genes includes some of the most prominent

genes identified in our study: *CTGF*, *MAP2K3*, *MAFF*, *MAFG*, *TXNRD1*, *SLC25A25*, *TNFRSF12A*, and *CP* (table 9). The relatively low number of significantly overlapping genes was not too surprising considering the fact that our *in vivo* model represents a complex system consisting of several different cell types like cardiomyocytes, fibroblasts, endothelial cells and resident immune cells. Furthermore, the statistical analysis identified only genes that reproducibly demonstrated similar regulation in all animals of a respective experimental sub-group. In contrast, in case of the HL-1 cells, cultures consisting of only one cell type were analyzed *in vitro*. In this study as well, HL-1 cells were confirmed as a suitable *in vitro* model of atrial fibrillation.

Table 9: Comparison of *in vivo* transcriptome analyses results from left atrial tissue samples of a porcine model with the transcriptome analyses results of rapidly stimulated HL-1 atrial myocytes (Mace et al., 2009). *In vivo* results are shown as the amount of transcripts under conditions of RAP and RAP/I relative to control (Sham). HL-1 cells were subjected to rapid pacing at 300 bpm for 24h and results were compared with control (spontaneously-beating, non-paced cells).

		RAP		RAP/I		HL-1 atrial myocytes
Gene Symbol	Name	ANOVA_P-value	Fold Change	ANOVA_P-value	Fold Change	Fold change
CP	ceruloplasmin	9.83E-07	12.73	0.22	5.04	2.64
WARS	Tryptophanyl-tRNA synthetase, tryptophan metabolism	8.33E-06	8.89	0.01	4.39	1.63
CTGF	connective tissue growth factor	0.00018	8.45	1.51E-06	6.85	9.11
TNFRSF12A	tumor necrosis factor receptor superfamily, member 12a	0.00016	8.44	0.00716	4.94	3.75
MAFF	v-maf musculoaponeurotic fibrosarcoma oncogene family, protein F (avian)	1.56E-12	7.63	2.94E-06	5.77	7.24
SLC25A25	solute carrier family 25 (mitochondrial carrier, phosphate carrier), member 25	0.00027	5.08	0.01744	3.40	1.59
IFRD1	interferon-related developmental regulator 1	0.00033	4.87	0.0031	3.35	2.32
CTH	cystathionase (cystathionine gamma-lyase)	2.54E-06	3.21	4.62E-12	3.97	4.07
PPAN	peter pan homolog (Drosophila)	0.00028	2.74	0.00186	2.17	2.16
NOLA1	nucleolar protein family A, member 1 (H/ACA small nucleolar RNPs)	2.04E-09	2.72	0.23	1.75	1.64
TXNRD1	thioredoxin reductase 1	0.0074	2.62	1.02E-11	3.54	1.48
EEF1E1	eukaryotic translation elongation factor 1 epsilon 1	5.41E-06	2.60	0.00869	1.84	1.61
MAP2K3	mitogen activated protein kinase kinase 3	0.02234	2.58	0.08	2.25	2.08
PAK1IP1	PAK1 interacting protein 1	5.02E-12	2.43	0.03629	1.86	1.62
DDIT3	DNA-damage inducible transcript 3	0.01149	2.34	5.35E-13	2.79	6.14
GAR1	nucleolar protein family A, member 1 (H/ACA small nucleolar RNPs)	0.01487	2.24	0.14	1.78	1.64
RNMT	RNA (guanine-7-) methyltransferase	1.23E-08	2.17	0.00017	1.92	1.55

		RAP		RAP/I		HL-1 atrial myocytes
Gene Symbol	Name	ANOVA_P-value	Fold Change	ANOVA_P-value	Fold Change	Fold change
<i>CHKA</i>	choline kinase alpha	0.01271	2.17	0.00616	2.93	2.39
<i>NOL5A</i>	nucleolar protein 5A	0.03327	1.89	0.21	1.70	1.67
<i>SLC20A1</i>	solute carrier family 20, member 1	7.34E-06	1.87	0.00235	1.57	2.06
<i>TAF4B</i>	Myeloid/lymphoid or mixed-lineage leukemia 3	0.00764	1.86	0.04539	1.77	1.72
<i>TAF5</i>	TAF5 RNA polymerase II, TATA box binding protein (TBP)-associated factor	0.02327	1.86	0.04815	1.60	1.62
<i>ODC1</i>	ornithine decarboxylase, structural 1	0.00003	1.84	0.00177	1.66	1.92
<i>WDR43</i>	WD repeat domain 43	0.00012	1.83	0.00033	1.91	1.95
<i>EAF1</i>	ELL associated factor 1	0.00852	1.81	0.0029	1.66	1.97
<i>NUP153</i>	nucleoporin 153	0.00008	1.80	0.00172	1.63	1.88
<i>NARS</i>	asparaginyl-tRNA synthetase	9.51E-06	1.75	0.00001	1.59	2.31
<i>EIF4E</i>	Eukaryotic translation initiation factor 4E	1.23E-06	1.72	0.00003	1.72	1.72
<i>TBC1D15</i>	TBC1 domain family, member 15	0.01021	1.71	0.01546	1.70	1.56
<i>EIF5</i>	eukaryotic translation initiation factor 5	0.00024	1.70	0.00058	1.59	2.25
<i>ZCCHC7</i>	zinc finger, CCHC domain containing 7	0.01827	1.57	0.054	1.58	2.11
<i>ARF6</i>	ADP-ribosylation factor 6	0.01225	1.55	0.00003	1.71	1.54
<i>DSG2</i>	desmoglein 2	3.43E-07	-2.91	2.43E-07	-2.44	-2.65
<i>CIB4</i>	potassium channel, subfamily K, member 3	0.00577	-1.92	0.00959	-1.86	-1.95
<i>NCAM1</i>	neural cell adhesion molecule 1	1.46E-06	-1.86	0.11	-1.54	-1.69
<i>CCNG2</i>	cyclin G2	0.00083	-1.84	0.00875	-1.63	-2.90
<i>IVNS1ABP</i>	influenza virus NS1A binding protein	0.00063	-1.70	0.01088	-1.35	-2.02
<i>KIF13A</i>	Kinesin Family member 13a, microtubule-based process	0.02979	-1.64	0.37	-1.56	-1.77
<i>PIK3R1</i>	phosphatidylinositol 3-kinase, regulatory subunit, polypeptide 1(p85 alpha)	0.04851	-1.61	0.00029	-1.60	-2.18

4.12.4. *CTGF* expression is transiently induced in HL-1 cells by exogenous administration of ET1.

In order to validate *CTGF* regulation *via* ET1 and SGK1, *CTGF* expression was first examined in HL-1 cells at different time points after addition of exogenous ET1 (0.1 μ M). As shown in *figure 21*, this resulted in a rapid transient increase in *CTGF* mRNA. In this experiment, maximum *CTGF* expression was observed 2 h after ET1 addition (6.8-fold, $p < 0.001$), but was nearly at baseline after 6 h ($p = \text{n.s.}$), indicating a transient course of *CTGF* induction under these conditions. These results confirmed that *CTGF* is induced *via* ET1.

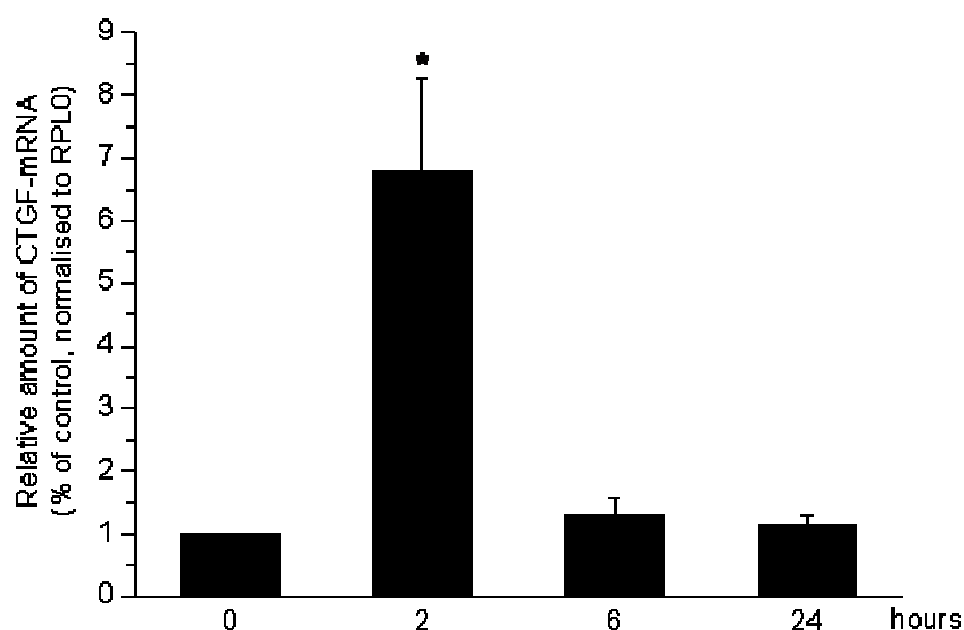
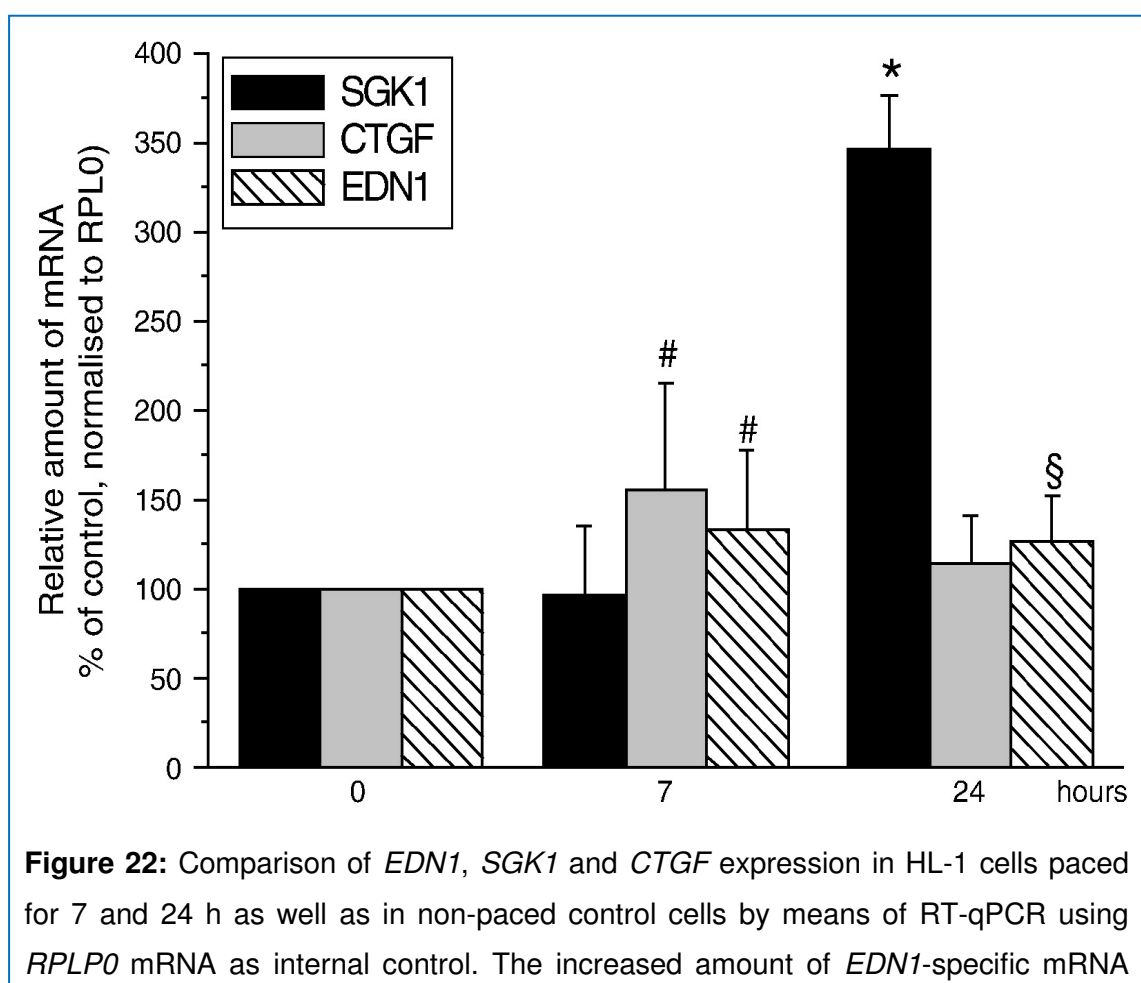


Figure 21: Transient induction of *CTGF* expression in HL-1 cells after addition of exogenous ET1 (0.1 μ M) as determined by RT-qPCR. Samples for RNA preparation were collected at 2, 6, and 24 h after ET1 addition, and the amount of *CTGF* specific mRNA was compared to non-treated cultures. *RPLP0* mRNA was used as internal control ($n = 6$; * $p < 0.001$).

4.12.5. Rapid pacing of HL-1 cells induces *CTGF* expression via the ET1-SGK1-axis.

To test the hypothesis that rapid pacing of HL-1 cells *in vitro* also leads to increased *CTGF* expression via the ET1-SGK1-axis, the mRNA amounts of *EDN1*, *SGK1*, and *CTGF* in HL-1 cells before and at different time points (7 h and 24 h) after initiation of rapid pacing were analyzed by RT-qPCR. As shown in *figure 22*, there was an increase in the amount of *EDN1* specific mRNA after 7 h (1.33-fold, $p < 0.05$), and this increased level was still observed after 24 h (1.26-fold, $p < 0.05$). As predicted, *EDN1* induction was followed by delayed transcriptional up-regulation of *SGK1* after 24 h (3.46-fold, $p < 0.001$) (Fig. 6). The finding that the amount of *CTGF* mRNA was already increased after 7 h (1.55-fold, $p < 0.05$) can be explained by activation of pre-existing SGK1 by ET1-mediated phosphorylation. After 24 h, the level of *CTGF* mRNA was already significantly decreased, again indicating the transient nature of the *CTGF* induction. Taken together, the experimental results obtained with the HL-1 cardiomyocyte cell line confirmed the predicted *CTGF* regulation via the proposed ET1-SGK1-axis.



after 7 h was still observed after 24 h. This *EDN1* induction was followed by a delayed up-regulation of *SGK1* after 24 h, whereas *CTGF* expression already increased after 7 h (n= 12; * p< 0.001; § p< 0.01; # p< 0.05).

5. DISCUSSION

AF is the most common sustained cardiac arrhythmia in clinical practice, causing an increasing number of complications and deaths in humans. AF can markedly impair quality of life through symptoms such as palpitations, fatigue and dyspnea and is independently associated with an increased risk of stroke, heart failure and death. However, AF remains an enigmatic disease arising from multiple, mutually interacting mechanisms. The pathophysiology of AF is very complex and incompletely understood. Though, the management of AF has evolved greatly in the past few years, therapeutic success rates in AF patients treated with either antiarrhythmic drug therapy or catheter-based ablation or both remain highly variable, in part because of incomplete understanding of the mechanisms underlying AF (Authors/Task Force Members et al., 2006; Heist et al., 2012; Kirchhof et al., 2009).

Few genome-wide gene expression analyses have been performed in humans and animal models to characterize gene expression changes related to the pathophysiology of arrhythmia. Complementary DNA (cDNA) microarrays were used to evaluate the expression of 1,152 known genes in right atrial appendages from 26 permanent AF patients and compared with 26 normal sinus rhythm control patients (Kim et al., 2003). This allowed identification of 55 significantly regulated genes related to generation of ROS (Kim et al., 2003). Atrial-specific changes in the expression of several genes encoding potassium channels, especially *TWIK-1* (*KCNK1*), were revealed by comparing left atrial and left ventricular myocardium of 6 patients with heart failure from chronic AF using high-density oligonucleotide arrays (Ellinghaus et al., 2005). Another study evaluated the ion-channel gene expression profile of valvular heart disease (VHD) patients with AF using spotted arrays. They observed cardiac ion-channel and transporter remodeling in those patients with permanent AF (AF-VHD) when compared with VHD patients in sinus rhythm (SR-VHD), reflected by increased mRNA amounts of *PLN*, *KCNE1*, *KCNE3*, and *KCNK1* encoding phospholamban, the β -subunit MinK, MIRP2, and the 2-pore potassium channel TWIK-1, respectively, and decreased mRNA amounts of *CACNA1G* and *KCND3* encoding T-type calcium-channel Cav3.1 and the transient-outward potassium channel Kv4.3 (Gaborit et al., 2005).

The limitation of transcriptome analyses in humans is that the profiles of AF patients reflect both underlying heart-disease and changes because of AF-induced atrial-tachycardia remodeling. It is very difficult to differentiate between AF-promoting changes caused by AF and those resulting from underlying cardiac diseases. The analyses are further complicated by systematic inter-group differences in drug therapy, age, atrial size,

and other cardiac phenotype variables. Hence, animal models to simulate AF are very important to understand the underlying mechanisms of atrial-tachycardia remodeling largely independent from other existing heart diseases or risk factors. Furthermore, animal models of AF allow for greater control over study conditions to diminish the inter-group variations and permit the time course analyses of any alterations.

The time course transcriptome analyses of a dog model of atrial tachypacing (ATP, 400 bpm \times 24 h, 1 or 6 weeks) and ventricular tachypacing (VTP, 240 bpm \times 24 h or 2 weeks) revealed prominent time-dependent effects of VTP, over ATP, on the mRNA amounts of genes encoding proteins related to ECM, represented by induced expression of such coding for collagens, fibrillin-1, MMP2, fibronectin, and lysine oxidase-like 2 (Cardin et al., 2007). Another study, by using a porcine model with continuous rapid atrial pacing for 3-4 weeks, demonstrated that the excess deposition of ECM in right and left atrial appendages was correlated with altered expression of the genes encoding FN1, fibrillin-1 and fibromodulin (Lin et al., 2007).

Earlier studies using a porcine *in vivo* model with acute rapid pacing have documented the impact of RAP on endocardial expression of adhesion molecules (VCAM and ICAM), on asymmetric dimethyl arginine (ADMA) levels, eNOS expression, and on renal expression of neutral endopeptidase (NEP). RAP was further associated with subsequent renal stimulation of TGF- β 1 signaling, AngII-mediated oxidative stress, and microvascular flow abnormalities in the ventricles. The effect of AT1R blockade by irbesartan in preventing the RAP-dependent increase of endocardial VCAM-1 expression was also documented (Bukowska et al., 2008a; Goette et al., 2009a, 2008a). The studies described in the present thesis are the first to demonstrate the comprehensive impact and efficacy of irbesartan and dronedarone in modifying RAP-dependent transcriptional changes on a genome-wide level.

The results from the current irbesartan study demonstrate that acute RAP *in vivo* for seven hours results in profound changes in the global gene expression pattern of left atrial tissue. The transcriptome analysis revealed a RAP-induced overall expression profile that reflects increased ROS production and induction of redox-regulated pathways, tissue remodeling, and energy depletion. As explained below, most of these signatures can be largely explained to be caused by an RAP-induced increase in the tissue levels of AngII. Blockade of AT1-receptors with irbesartan partially attenuated these maladaptive alterations emphasizing the key role of AngII-signaling as a major underlying pathomechanism. In addition to the global expression signatures, the results indicate specific positive regulation of CTGF *via* the AngII-ET1-SGK1 axis. Interestingly, the observed RAP-dependent changes in gene expression were not restricted to the LA, but could be observed in RA and LV samples, too, although to different extents.

The dronedarone study focused on RAP-induced microvascular flow abnormalities. The results show that dronedarone reduces microvascular flow abnormalities and oxidative stress that were induced by RAP. This was evidenced by significantly reduced expression of genes encoding ROS-generating enzymes (e. g. NADPH oxidase) and proteins involved in redox signaling (PKC, NF- κ B) in response to dronedarone.

5.1. DRONEDARONE PREVENTS AF-(RAP)-INDUCED MICROCIRCULATORY FLOW ABNORMALITIES

Despite exclusion of coronary artery disease (CAD), AF is frequently associated with symptoms of myocardial ischemia (MI). With the onset of AF, chest discomfort indicating typical angina pectoris sometimes develops in patients without previously documented CAD. Recent studies have shown that patients with AF have impaired myocardial perfusion, ventricular-flow abnormalities and higher incidence of cardiac events such as cardiac death. Consistent with this notion, coronary vascular resistance (CVR, indicating vasoconstriction if increased) is markedly elevated by 62% and myocardial blood flow (MBF) is substantially reduced in AF patients (Abidov et al., 2004; Fineschi et al., 2008; Range et al., 2007). These findings are supported by another line of evidence; Doppler-derived CVR index has been shown to be increased in experimental models of AF (Kochiadakis, 2002). Previous studies have clearly shown that AF increases systemic AngII levels, indicating a potential link between AF and increased CVR/decreased MBF/LV malperfusion. In line with this observation, 7 h of RAP has also been demonstrated to almost double the systemic AngII levels (Cardin et al., 2003; Goette et al., 2009b, 2008a). In accordance with these findings, the results from the dronedarone study presented here showed that 6 h of RAP reduced the Coronary flow reserve(CFR), indicating myocardial ischemia if reduced but not FFR (Fractional flow reserve), indicating coronary artery stenosis, thereby demonstrating that there was a ventricular microcirculatory disturbance during pacing without significant obstruction of blood flow. This effect was abolished by dronedarone by increasing the CFR, suggesting that dronedarone prevented RAP-induced microcirculatory flow disturbances. In support of this, in a recent study using a porcine model of ischaemia/reperfusion, dronedarone reduced the infarct size that was independent of the actual sub-endocardial blood flow. This clearly demonstrates that blockade of ion channels, in particular sodium-calcium exchangers, by dronedarone might reduce calcium overload and thus contribute to direct cardioprotective action during myocardial ischemia/reperfusion (Skyschally and Heusch, 2011).

5.2. “OXIDATIVE STRESS” AND AF: IMPACT OF DRONEDARONE AND IRBESARTAN

“Oxidative stress” was historically defined as an imbalance between the generation of ROS and the capacity of the corresponding defense systems (Cadenas et al., 1982). The contemporary definition of oxidative stress has been refined as an imbalance between pro-oxidant and anti-oxidant reactions with two different mechanistic outcomes: free radical intermediate ($\bullet\text{O}_2^-$, $\bullet\text{OH}$ and $\text{NO}\bullet$ etc.)-mediated macromolecular damage and non-radical oxidant (H_2O_2 , ONOO^- , disulfides, aldehydes, epoxides, quinines etc.)-based disruption of thiol redox circuits, which leads to aberrant cell signaling and dysfunctional redox control (Fink, 2000; Ghezzi et al., 2005; Jones, 2008, 2006).

ROS are constantly generated under physiological conditions in the cardiovascular system as a result of numerous metabolic processes, including oxidation of NADPH by NADPH oxidase, uncoupling of the mitochondrial electron transport chain, and oxidation of xanthine by xanthine oxidase. But under pathophysiological conditions, chronically elevated amounts of ROS or a decline in antioxidant defenses may exert oxidative stress (Sayre et al., 2001; Schafer and Buettner, 2001). This elevated production of different ROS affects distinct presets of target proteins through oxidant-specific and site specific modifications. Most frequently, thiols of cysteines are subject to oxidative modifications to form cysteinyl side chains. Thiol oxidation of the same protein or other proteins results in conformation changes and various types of post-translational modifications (PTMs). In addition, protein carbonylation was identified as a novel mechanism in redox signaling. Protein carbonyls are quite stable products formed on proline, arginine, lysine or threonine residues (Grimsrud et al., 2008; Wang et al., 2012; Wong et al., 2008). A variety of antioxidant enzymes and other proteins in different cellular compartments, so-called antioxidant redox systems, e.g., glutathione, NADPH, thioredoxin (Trx), and peroxidases such as the peroxiredoxins (Prx), are, however, not in equilibrium and independently maintained at distinct redox potentials. Hence, oxidative stress may be defined as the chronic disturbance of redox circuits and redox-responsive signal transduction pathways (Fink, 2000; Ghezzi et al., 2005; Grimsrud et al., 2008; Jones, 2006).

Oxidative stress has been closely associated with AF and implicated as playing a critical role in the pathophysiology of heart and other cardiovascular diseases such as heart failure, LV hypertrophy, and coronary heart disease. It appears that oxidative damage initiates the disease-dependent tissue remodeling and promotes its propagation. Oxidative stress is associated with microvascular flow abnormalities and arises immediately after initiation of even short periods of AF. Accordingly, it likely represents a

key mechanism to initiate ventricular remodeling in patients with lone recurrent AF and rapid atrial pacing models. Increased mRNA amounts of genes encoding proteins involved in the protection against ROS were previously described under these conditions (Bukowska et al., 2008b; Carnes et al., 2001; Goette et al., 2009b; Huang et al., 2009; Kochiadakis, 2002; Korantzopoulos et al., 2007; Mihm et al., 2001).

5.2.1. Panel of oxidative stress-related genes: Mechanistic insights into the actions of dronedarone and irbesartan

Tachycardia-induced imbalances of myocardial oxygen supply and myocardial oxygen demand due to compromised microcirculation in ventricles lead to the specific activation of redox-sensitive signaling pathways. The resulting oxidative stress might be triggered by tachycardia-induced intracellular calcium and sodium overload due to increased NCX currents and spontaneous Ca^{2+} -release events (Nishida et al., 2011). Also, the RAP-induced increase in ROS observed both in the dronedarone and irbesartan studies is mediated *via* AngII-dependent nicotinamide adenine dinucleotide phosphate oxidase (NADPH oxidase, NOX) activation. In this context, as already mentioned, it has been shown earlier that 7h of RAP almost doubles systemic AngII levels (Reilly et al., 2011). Increased expression and activity of ACE (Goette et al., 2000) contribute to elevated systemic as well as atrial AngII levels (Ko et al., 2011).

Thus, impaired intracellular Ca^{2+} -handling together with elevated cardiac and systemic AngII levels are two important factors which very likely contribute to RAP-dependent activation of protein kinase C (PKC) *via* phosphorylation. Dronedarone partially prevented this RAP-induced effect as shown in *figure 12B*. PKC regulates the function of calcium and potassium channels, and phosphorylates the regulatory p47^{phox} NOX subunit. Phosphorylated p47^{phox} , when physically bound to another regulatory subunit, namely p67^{phox} , plays a pivotal role in the activation of the NOX family of proteins (NOX2/NOX1/NOX5) (Fontayne et al., 2002).

Furthermore, the genes encoding NOX1 and NOX2 are up-regulated 6 h after RAP. Dronedarone, as shown in *figure 12A*, clearly reduced this RAP-induced up-regulation of *NOX2* and there was a similar but not significant effect on *NOX1*. Blockade of AT1-receptors by irbesartan has also been shown to prevent this RAP-induced *NOX2* expression (Goette et al., 2009b).

AF-induced NADPH oxidase activity has been shown to contribute to elevated ROS production, protein modification, and redox-related gene expression patterns (Carnes et al., 2001). In the murine heart, AngII increased superoxide generation and cardiac hypertrophy involving NOX2 (Bendall et al., 2002). In support of this view, 6 h RAP

elevated the level of oxidative stress markers, F_2 -isoprostanes, by 76%, and dronedarone significantly reduced this RAP-dependent increase (*figure 13A*). Irbesartan also showed a similar effect of preventing RAP-dependent elevation of F_2 -isoprostane concentrations (Goette et al., 2009b).

The results of the transcriptome analysis from the irbesartan study presented here showed significantly elevated mRNA amounts (between 2.6- and 12.7-fold) of several prominent genes known to be induced by increased ROS levels, like *HMOX1*, *MAFF*, *MAFG*, *SOD2*, *TXNRD1*, *TXNDC1*, *MAP2K3*, and *CP*, encoding heme oxygenase 1, two basic leucine zipper (bZIP) transcription factors, mitochondrial manganese-dependent superoxide dismutase, thioredoxin reductase 1, a thioredoxin family transmembrane oxidoreductase, mitogen-activated protein kinase kinase 3 (MKK3), and the ferroxidase ceruloplasmin, respectively (*figure 11*), clearly indicating that 7 h of acute pacing obviously induces increased intracellular ROS production. With the exception of MKK3 which is part of a phosphorylation cascade involved in transcriptional activation of *HMOX1* (Kietzmann et al., 2003), all the encoded proteins mediate protection against increased amounts of ROS (Fukai and Ushio-Fukai, 2011; Katsuoka et al., 2005; Matsui and Sadoshima, 2004; Shukla et al., 2006; Suvorova et al., 2009; Wu et al., 2011). In addition, induction of the heat-shock genes *DNAJA4*, *DNAJB9*, *DNAJC1*, *DNAJC3*, *HSPA4*, *HSPA13*, *HSPA14* and *HSPH1* (between 1.51- and 4.64-fold) encoding molecular co-chaperones and chaperones pointed towards ROS production; it has already been demonstrated that the common regulatory transcription factor of those genes, HSF1, is not only activated by temperature up-shift but also by oxidative stress (Ahn, 2003).

Among the ROS generating NADPH oxidases, NOX5 represents a Ca^{2+} /calmodulin-stimulated homologue that is regulated by AngII and Endothelin-1 (ET-1). ET-1 is a peptide with strong vasoconstrictory activity. Atrial stretch is a potent factor promoting the production and release of ET-1 (Bruneau et al., 1997). As shown in schematic flowchart *figure 23*, binding of the vasoactive peptides AngII and ET-1 to their respective receptors AT1R and ETRB causes Ca^{2+} influx via L-type Ca^{2+} channels and subsequent calmodulin activation, thereby enabling the resulting Ca^{2+} /calmodulin complex to interact with specific binding domains of NOX5, thus activating the enzyme. Furthermore, ET-1 activates PKC and MAP kinases (Sugden, 2003). Finally, this regulation results in subsequent ROS generation and ERK1/2 signaling. Therefore, it might be hypothesized that AngII/EDN1-mediated NOX5 activation contributes to oxidative stress, which is reflected in the gene expression pattern that is observed in the irbesartan study presented here (Bánfi et al., 2004; Brandes and

Schröder, 2008; Clempus et al., 2007; Dammanahalli and Sun, 2008; Honjo et al., 2008; Kim et al., 2003, 2008).

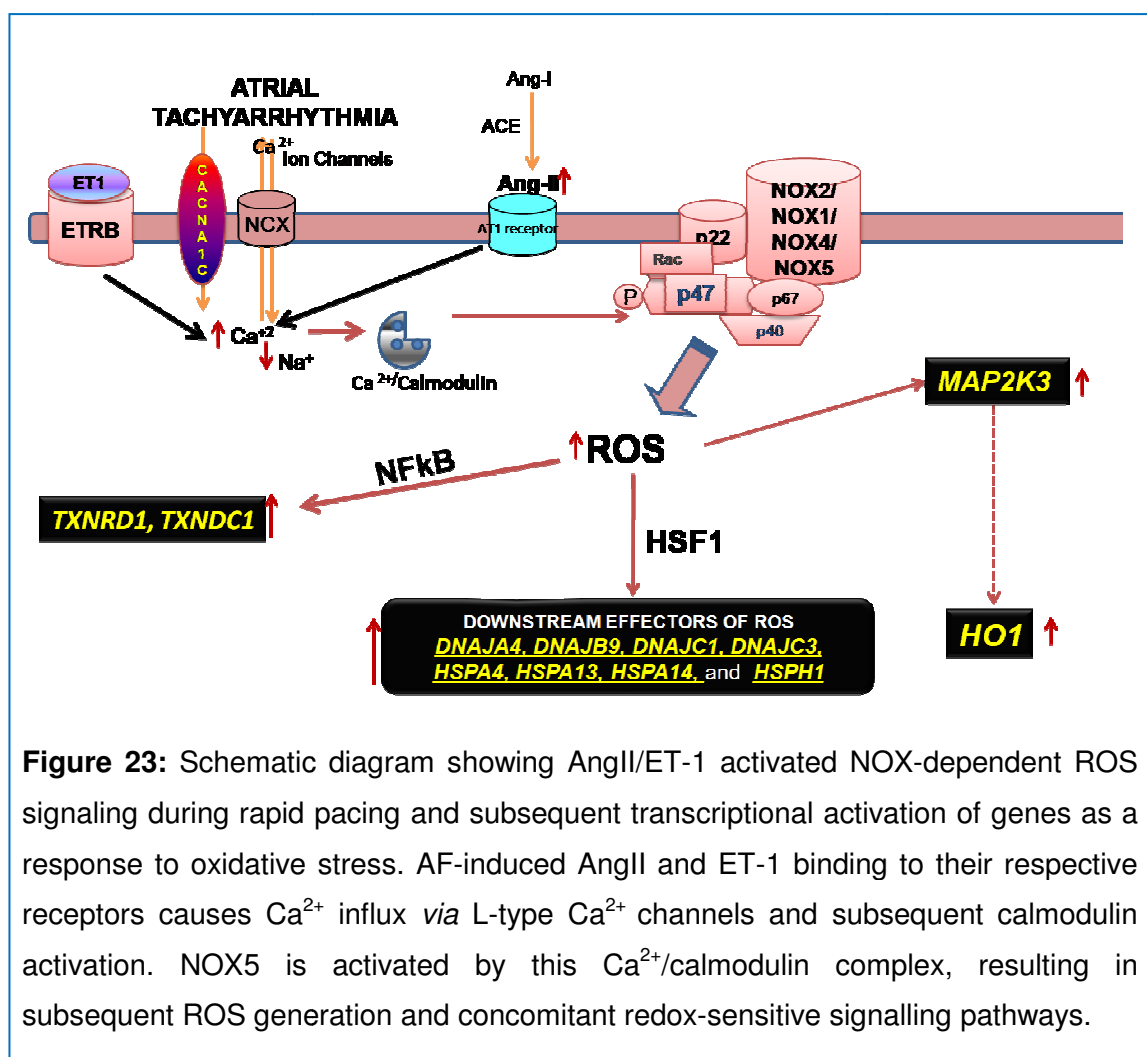


Figure 23: Schematic diagram showing AngII/ET-1 activated NOX-dependent ROS signaling during rapid pacing and subsequent transcriptional activation of genes as a response to oxidative stress. AF-induced AngII and ET-1 binding to their respective receptors causes Ca²⁺ influx via L-type Ca²⁺ channels and subsequent calmodulin activation. NOX5 is activated by this Ca²⁺/calmodulin complex, resulting in subsequent ROS generation and concomitant redox-sensitive signalling pathways.

The induction of atrial NADPH oxidase activity or subunit expression in the natural course of AF development and progression, however, indicated a transient mechanism. ROS production by NADPH oxidases is effective in acute models of AF and in patients with post-operative AF. Later, with increasing duration of AF, ROS production is shifted from NADPH oxidase to mitochondrial oxidases and uncoupled eNOS in the right atrium (Antoniades et al., 2012; Reilly et al., 2011).

In the presented dronedarone study as well, increased mRNA levels of oxidative stress/ischaemia-related genes was observed in left atrial tissue 6 h after RAP (Table 5) initiation. This RAP-dependent induction of oxidative stress-related gene expression was also detected in left ventricular tissue by RT-qPCR (Table 6), which was associated with flow abnormalities in left ventricles. Dronedarone showed protective effects reflected by attenuation of RAP-dependent gene expression. NFκB is a redox-sensitive transcription factor and appears to represent another key

mediator of ROS-induced inflammatory effects, mediating expression of adhesion molecules and inflammatory gene products in vascular cells (Alexander, 1995; Berliner et al., 1995; Bowie and O'Neill, 2000; Flohé et al., 1997; Lee et al., 1999; Rahman, 2003; Schreck et al., 1992). ROS induce redox-sensitive protein kinases by modulating the phosphorylation of I κ B α (*figure 13B*) which in turn initiates nuclear translocation of NF κ B and subsequent induction of its target genes, e. g. *VEGF-A* (Kiriakidis et al., 2003, p. 2; Martin et al., 2009), *CCL2* (Lawrence et al., 2006), and *HIF1A* (Bonello et al., 2007; Kunsch and Medford, 1999), as well as those for the DnaJ family proteins (Table 5 and 6).

ROS-induced activation of NF κ B, together with compromised microvascular blood flow during rapid pacing, increases the expression of *HIF1A*, the gene encoding hypoxia-inducible factor 1 (HIF-1 α), a key component of the eukaryotic oxygen-response system. HIF-1 α in turn activates expression of *VEGFA* encoding vascular endothelial growth factor (VEGF-A) (Forsythe et al., 1996, p. 1). VEGF increases intracellular calcium levels in endothelial cells, which in turn increases NO by eNOS and ROS with subsequent limitation of NO. PRKAG2 (gamma subunit of cAMP activated protein kinase) sense the increased ROS and is activated by Ca²⁺/calmodulin-dependent kinase and in turn increase the expression of ROS-limiting enzymes (Banumathi et al., 2011; Evans et al., 2005; Mungai et al., 2011; Zaha and Young, 2012). Thus, VEGF and PRKAG2 are indirectly involved in regulating NO and together play a role in the production of nitric oxide (NO) in the vascular system by endothelial NO synthase (eNOS), a Ca²⁺/calmodulin-dependent enzyme. NO reacts with ROS, especially superoxide, to produce peroxynitrite (.OONO⁻), thereby reducing NO bioavailability and elevating vascular resistance and promoting vasoconstriction (Dusting et al., 1998; Zicha et al., 2001). As a result, expression of *PRDX3* encoding the anti-oxidant peroxiredoxin 3 is induced (Wolf et al., 2010). NO may also act to suppress the vascular NADPH oxidase activity (Dusting et al., 2005), hence, reduced NO bioavailability may in turn increase ROS generation by NADPH oxidase as well.

Besides HIF1 α , other factors are also crucially involved in the regulation of oxidative and metabolic programs to sense and respond to local oxygen concentrations and metabolic conditions. One of these systems involves the peroxisome proliferator-activated receptor coactivator 1- α (PGC-1 α), encoded by *PPARGC1A*, a key transcriptional regulator of mitochondrial biogenesis and oxidative phosphorylation (Shoag and Arany, 2010). Increased expression of *PPARGC1A* has been observed under hypoxia/ischaemia-like conditions, which in turn acts protectively by increasing the expression of ROS-limiting and scavenging genes including *Prx3* and

mitochondrial detoxification enzymes like superoxide dismutase 2 (encoded by *SOD2*). In addition, PGC-1 α is involved in induction of a broad angiogenic program, in response to ischemia, which includes VEGF (Arany et al., 2008; Gutsaeva et al., 2008; Storey, 2003). Therefore, increased expression of *PPARGC1A* observed in the dronedarone and irbesartan studies is consistent with a compromised coronary flow as shown for the RAP group. *CFR* and *PPARGC1A* expression were more efficiently attenuated by dronedarone. Since further differences were observed in the response to dronedarone or irbesartan with respect to oxidative stress/hypoxia-related gene expression, it is reasonable to assume that different but partly overlapping adaptation reactions aimed on limiting stress-mediated tissue damage are influenced by both compounds. Besides attenuating the RAP-induced expression of *HIF1 α* and *VEGFA*, in particular *PPARGC1A* was more strongly affected by dronedarone. This might suggest that dronedarone (in addition to limiting ROS production) interfered with both angiogenic and oxidative-metabolic response pathways.

The established association of RAP with oxidative stress together with *in vivo* data of the dronedarone study was further confirmed *in vitro* by exposing HL-1 cardiomyocytes to glucose oxidase (GOD)+glucose and rapid pacing *in vitro*, with and without dronedarone, to analyse the effects of ROS or RAP *in vitro* on PKC α activation, respectively. Under both conditions, an increase in phospho-PKC α was observed (*figure 15*). The amounts of ROS generated by GOD/glucose are not likely to be affected by dronedarone. Thus, dronedarone is supposed to act on targets downstream of oxidative stress, including the antioxidative stress response. It is likely that similar mechanisms occurred during RAP, where dronedarone showed a strong and nearly significant activity to attenuate PKC α activation ($P=0.059$).

These findings clearly demonstrate that dronedarone and irbesartan are capable of attenuating most of the RAP-induced changes in oxidative stress-related atrial gene expression.

5.3. ENERGY DEPLETION

AF has been demonstrated by a number of *in vivo* and *in vitro* studies to be associated with a higher demand of energy of cardiomyocytes resulting in transiently decreased concentrations of high-energy phosphates and mitochondrial NADH. Mitochondria are key players in cardiomyocyte energy metabolism, redox state control, and apoptosis. Tachycardia-induced alterations in the mitochondrial morphology of cardiomyocytes have also been demonstrated (Ausma, 2000; Brown

and O'Rourke, 2010; Seppet et al., 2005; Tsuboi et al., 2001; White and Wittenberg, 2000).

The dynamics of cardiac metabolism are reflected by adenosine-5'-triphosphate (ATP), which is a high-energy phosphate and the source of energy for maintenance of ion homeostasis as well as repetitive mechanical contraction and relaxation (Knowles, 1980). Apart from the ATP utilization in anabolic processes, in the context of cardiac metabolism, approximately 60–70% of ATP is used for cardiac muscle contraction. The remaining 30–40% is used by SERCA (sarco/endoplasmic reticulum Ca^{2+} -ATPase) for Ca^{2+} uptake into the sarcoplasmic reticulum (SR) to initiate diastolic relaxation and to sustain ion current homeostasis including the maintenance of Na^+ and K^+ gradients across the plasma membrane (Gibbs, 1978; Martonosi, 1984; Suga, 1990). Energy utilization, for contraction by these ATPases, leads to the hydrolysis of high-energy phosphate bonds in ATP, leading to the formation of adenosine diphosphate (ADP) or adenosine monophosphate (AMP), respectively. Therefore, a high ADP/ATP or AMP/ATP ratio implies falling energy stores, leading to signals that activate pathways to restore energy homeostasis. Functioning of an organism depends on the maintenance of this delicate energy homeostasis.

Energy deficits also include decreased activity of phosphor transfer enzyme and adenine nucleotide pool size. Duration of sustained AF has been shown to be linearly correlated with reduced ATP levels, as well as the reduced activities of the phosphotransfer enzymes creatine kinase (CK) and adenylate kinase (AK). These two phosphotransfer enzymes facilitate ATP delivery from sites of production to sites of utilization and promote removal of ADP, P_i , and H^+ from cellular ATPases. Tissue content of creatine phosphate (CrP), another high-energy phosphate formed by CK *via* ATP consumption, is also known to be transiently lowered during AF. These changes suggest an increased ATP consumption and depletion of intra-cellular high-energy phosphoryl pool (ATP, CrP etc.) with subsequent increase in energy demand during the early phase of AF (Ausma, 2000; Cha et al., 2003; Dzeja et al., 1999; Mihm et al., 2001; Neubauer et al., 1992).

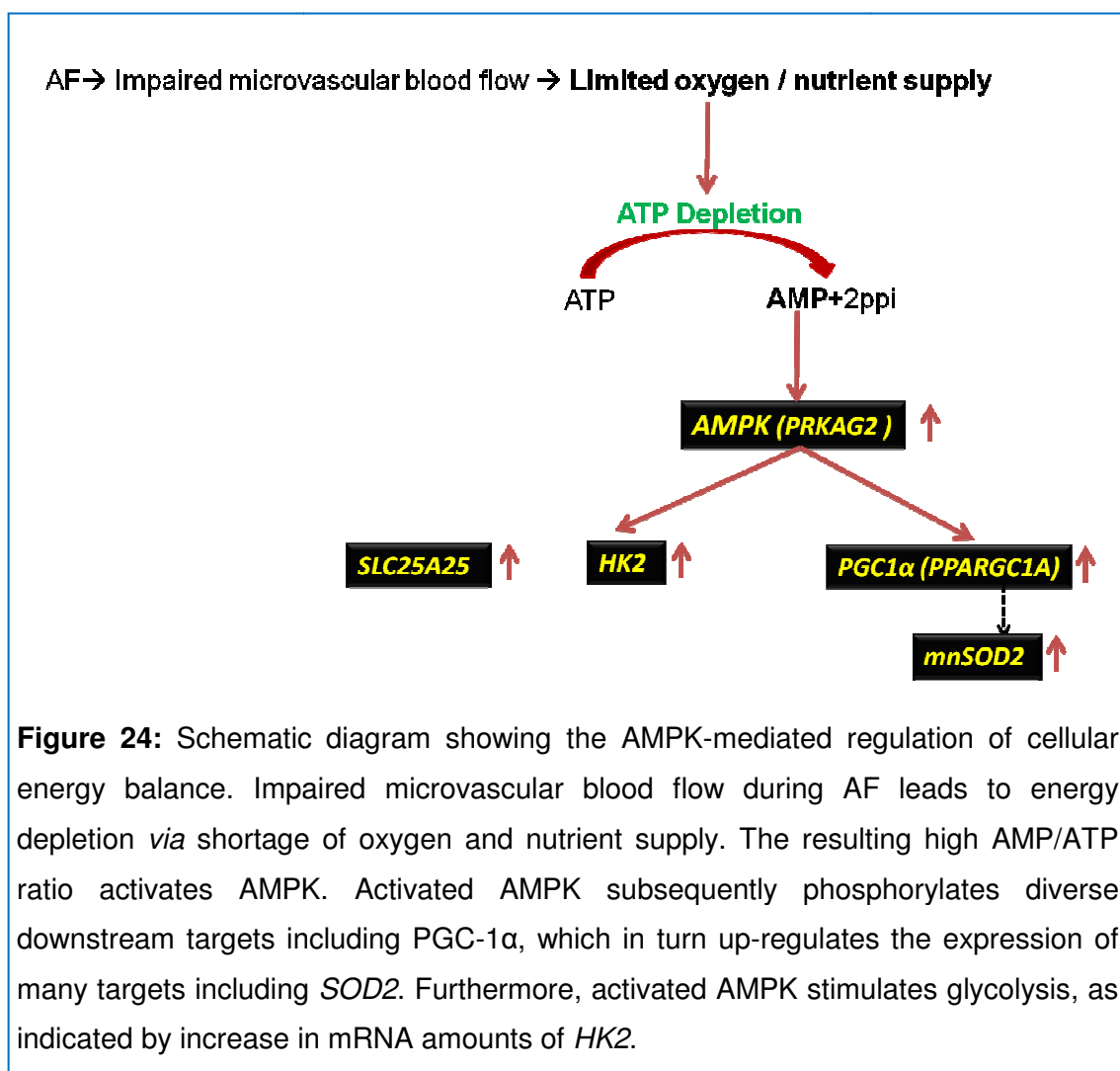
In favor of a status of high-energy demand during AF Barbey et al. (Barbey et al., 2000) confirmed that after 100 min of AF a high-demand metabolic state translated into an increased mitochondrial ATPase synthase (FOF1-ATPase) activity. Concomitantly, there was no change in the sarcolemmal Na^+/K^+ -ATPase activity, a plasma membrane-bound enzyme that needs high energy expenditure to maintain Na^+ and K^+ gradients during the cardiac action potential (Barbey et al., 2000). On the other hand, increased expression and activity of Na^+/K^+ -ATPase (sodium pump) has been shown in a sheep model of AF and in aortic smooth muscle cells with short-

term cyclic stretch (Maixent et al., 2002; Songu-Mize et al., 2001). In the irbesartan study as well the gene encoding the beta subunit of this pump (*ATP1B1*) showed an increase at transcriptional level (2.38-fold) during RAP, which was attenuated by irbesartan.

Accumulating evidence suggests that high levels of ROS, either by AngII/EDN1-induced NADPH oxidase or uncoupled NOS or electron leakage from complex I and III during mitochondria/OXPHOS, induce cardiac mitochondrial dysfunction, which may also contribute to the impaired energy production (Barth and Tomaselli, 2009; Liu et al., 2010). AngII/EDN1-induced NADPH oxidase-dependent ROS, produced in acute AF, were furthermore described to react rapidly with nitric oxide (NO) resulting in the formation of peroxynitrite. This in turn causes reduced NO availability and as a consequence impaired microvascular blood flow due to endothelial dysfunction (Dusting et al., 1998; Zicha et al., 2001). Thus, ROS-induced compromised microvascular blood flow during AF may also contribute to energy depletion in the myocardium *via* both oxygen- and nutrient shortage.

Indeed, the significant increase in *PRKAG2*- and *PPARGC1A*-specific mRNA under RAP-conditions (5.1- and 2.3-fold, respectively) in the irbesartan study might indeed reflect the hypothesized energy depletion. Both genes encode key proteins involved in regulation of cellular energy balance, namely a γ -subunit of the AMP-activated protein kinase (AMPK) and the aforementioned transcriptional co-activator PGC-1 α , respectively. Similarly, the up-regulation (5.1-fold) of *SLC25A25* encoding the mitochondrial ATP-Mg/Pi carrier protein (phosphate carrier) thought to be involved in the control of ATP homeostasis (Anunciado-Koza et al., 2011) also indicates the onset of energy depletion.

As shown in schematic *figure 24*, hypoxia/ischemia-induced ATP depletion, implied by a high AMP/ATP ratio (high levels of AMP and low levels of ATP), cause activation of AMPK by AMP (Cantó and Auwerx, 2009; Steinberg and Kemp, 2009). Activated AMPK subsequently phosphorylates diverse downstream targets including PGC-1 α causing among other effects a transcriptional response that boosts mitochondrial activity (Jeninga et al., 2009). As already mentioned, PGC-1 α plays an important role in regulating mitochondrial biogenesis. These effects are mediated *via* direct PGC-1 α phosphorylation by AMPK (Jäger et al., 2007; Zong et al., 2002) and, as also observed in the irbesartan study, by increased expression of its encoding gene *PPARGC1A* (Suwa et al., 2003). In this context, it is also noteworthy that PGC-1 α positively regulates the expression of *SOD2* encoding the antioxidant enzyme mitochondrial superoxide dismutase 2 (*figure 11*) that was also detected to be up-regulated during RAP in the irbesartan study (Lu et al., 2010).



In addition, AMPK activation enhances insulin sensitivity, inhibits glucose production, stimulates glucose uptake and glycolysis, and inhibits fatty acid synthesis and esterification, and diminishes pro-inflammatory changes (Ruderman and Prentki, 2004). With regard to stimulation of glycolysis, a further target gene described to be transcriptionally up-regulated in response to activation of AMPK, *HK2* encoding hexokinase 2 (Holmes et al., 1999; Stoppani et al., 2002), also exhibited significantly higher mRNA levels under RAP conditions (9.7-fold) in the irbesartan study. Localization of HK2 to the outer mitochondrial membrane is associated with increased phosphorylation of glucose to form glucose-6-phosphate, which can be metabolized *via* either glycolysis or the pentose phosphate pathway (PPP). Mitochondria-associated HK2 is further associated with maintenance of mitochondrial membrane potential, and may link glycolytic glucose metabolism to oxidative phosphorylation *via* the use of intra-mitochondrial ATP to phosphorylate glucose (Robey and Hay, 2006). Stimulation of glycolysis in ischemic hearts has also been shown to be mediated by AMPK *via* the activation of another cardiac specific glycolytic enzyme, phosphofructo kinase 2 (PFK2) (Marsin et al., 2002). Another

paradigm of AMPK regulation of glycolysis is that AMPK activation up-regulates HIF-1 α and VEGF expression in hypoxia, which can also drive transcription of nearly all glycolysis-related enzymes, including pyruvate kinase (PK) and lactate dehydrogenase (LDH) (Hwang et al., 2004; Lee et al., 2006). There are several studies demonstrating that AMPK activation is preceded HIF-1 α expression under oxygen- and glucose-deprived conditions and in turn, regulates the expression of VEGF in a HIF-1 α --dependent or -independent manner (Hwang et al., 2004; Lee et al., 2006; Ouchi et al., 2005).

Taken together, it can be concluded that under conditions of RAP, the obtained transcriptional profile of left atrial tissue indicates an increase in AngII-mediated ROS production, as well as cellular energy depletion. These RAP induced changes are partially attenuated by irbesartan.

5.4. TISSUE REMODELING

Alterations in atrial tissue structure (tissue/structural remodeling) have been proposed as a “second factor,” after electrical remodeling, contributing to the high susceptibility to the self-perpetuation of arrhythmia in patients with AF. Unlike electrical remodeling, tissue/structural remodeling takes place in a slower time frame of weeks to months and contributes synergistically with electrical remodeling to AF (Allessie, 2002; Todd, 2004). Structural alterations that develop progressively in the atria are not exclusively related to AF, but at least to the same degree as the existence of structural heart disease present in an individual patient. However, increased amounts of fibrous tissue were observed in patients with lone AF as well. The kind of structural alterations are highly diverse, including atrial dilatation, myocyte hypertrophy, myocyte necrosis, fibrosis, loss of sarcomeres, accumulation of glycogen, and mitochondrial abnormalities (Ausma et al., 1997; Frustaci, 1991; Frustaci et al., 1997; Morillo et al., 1995; Shi, 2001). The molecular mechanism of atrial structural remodeling is largely unknown.

Atrial fibrosis is a hallmark feature of arrhythmogenic structural remodeling in clinical AF. Several *in vivo* as well as *in vitro* studies using animal models and atrial-derived cardiomyocytes suggested a positive correlation between the amount of fibrosis and the persistence of AF. In general, fibrosis is characterized by excessive deposition of extracellular matrix (ECM) proteins synthesized by fibroblast-related cells, particularly myofibroblasts, upon stimulation (Manabe et al., 2002; Xu et al., 2004). The volume of extracellular matrix (ECM) per myocyte increases during months of

AF, mimicking a similar pattern to interstitial fibrosis or “microfibrosis” observed during aging, which can lead to slow, discontinuous conduction during transverse propagation (Ausma et al., 2003; Spach and Boineau, 1997). Though fibroblasts account for 75% of all cells in the myocardium, they comprise only 5–10% of the total mammalian heart volume because of their small size. However, in the sinoatrial node, up to 75% of total volume is comprised of fibroblasts. Cardiac fibroblasts are electrically non-excitable (Banerjee et al., 2007; Carver et al., 1991; I Shiraishi et al., 1992; I. Shiraishi et al., 1992).

Under physiological conditions, myofibroblasts are rarely found in normal cardiac tissue. They are represented as the principal ECM-secretory cell type (Sun, 2000). Under pathophysiological conditions such as myocardial injury, oxidative stress, mechanical stretch, and inflammation, myofibroblasts are majorly derived from fibroblasts, but also from cardiac endothelial cells. In response to these pathological stimuli, the fibroblasts proliferate, migrate, and undergo phenotypic changes involving differentiation into myofibroblasts (Goumans et al., 2008; Swynghedauw, 1999; Weber, 1994).

Myofibroblasts play a pivotal role in the fibrotic process by producing growth factors, cytokines, chemokines, ECM proteins, and proteases. Fibroblasts can be further stimulated by the cytokines and other growth factors produced by myofibroblasts, perpetuating a fibrogenic cascade. Two types of fibrosis are induced by fibroblasts, reactive and reparative. Reparative (replacement) fibrosis replaces degenerating myocardial cells and accompanies myocyte death, but maintain the structural integrity after cardiomyocyte death, whereas reactive fibrosis is a response to excessive myocardial loads or inflammation and appears as “interstitial” or “perivascular” fibrosis that causes ECM expansion between muscle bundles (Burstein and Nattel, 2008; Powell et al., 1999; Tomasek et al., 2002; Weber et al., 1989).

Several cytokines and growth factors, such as platelet-derived growth factor (PDGF), basic fibroblast growth factor (bFGF), angiotensin II (AngII), endothelin-1 (EDN1), transforming growth factor beta1 (TGF- β 1), and CTGF, stimulate fibro-proliferative signaling pathways, and often work in concert in the clinical setting. The results from the irbesartan and dronedarone studies indicated pronounced induction of *CTGF* (8.4-fold and 5.5-fold, respectively) under the conditions of RAP, whereas *EDN1* mRNA amounts showed a significant increase of 3.2-fold in the irbesartan study only (figure 11 and table 4). Blockade of AngII receptors by irbesartan partially reversed these effects. *CTGF* is induced by AngII, EDN1 or TGF- β 1. *CTGF* is a major

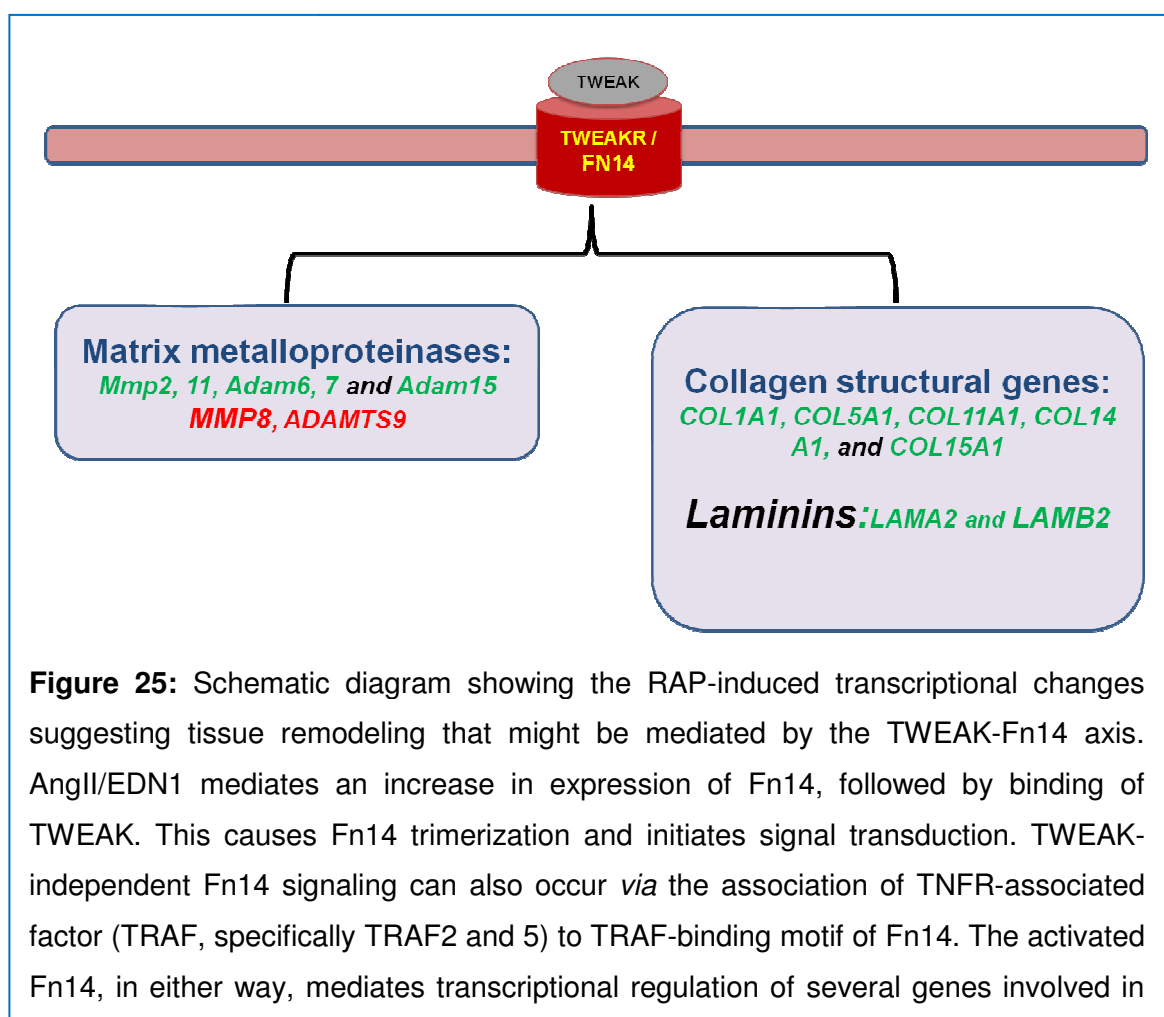
downstream effector of TGF- β 1 fibrosis promotion and it directly activates fibroblasts (Ahmed et al., 2004; Recchia et al., 2009).

Elevated levels of Angiotensin II (Ang II) during AF or RAP play a key role in the pathogenesis of atrial fibrosis *via* the activation of many downstream signal transduction pathways, such as mitogen-activated protein kinase (MAPK) pathways (Burstein and Nattel, 2008; Nattel et al., 2008; Sugden and Clerk, 1998; Yano et al., 1998), Janus kinase (JAK)/signal transducers and activators of transcription (STAT) pathways (Tsai et al., 2008b), and TGF- β 1 pathways (Rosenkranz, 2004; Verheule et al., 2004, p. 1). AngII mediates these profibrotic effects *via* the activation of its type 1 receptors (AT1Rs). The results from the irbesartan study indicated that the activation of the MAPK (ERK/EMPK) pathway as typically observed in AF / RAP is associated with increased mRNA amounts of *MAP2K3 (MKK3)*, *ATF4*, *ELK1*, *EIF4E*, *ETS2* and *STAT3* (*figure 11* and table 7). AngII-induced AT1R signaling activates the small GTPase protein Ras, which initiates MAPK phosphorylation cascades that are centrally involved in remodeling (Hunyady and Catt, 2006). The MAP kinases activate transcription factors (ELK1, ATF4, c-jun, and c-fos) that modulate expression of genes that regulate fibroblast proliferation, differentiation and tissue remodeling by ECM synthesis. In addition, Ras/Rac1 may activate NF κ B (Sulciner et al., 1996) and STAT3, both of these signaling pathways can be activated by AngII as well, to play important roles in atrial fibrosis. Increased mRNA amounts of *RASSF1* encoding the Ras association domain-containing protein 1, was observed in the irbesartan study (table 7). Signal transduction through the JAK/STAT pathway activates transcription factors such as activator protein-1 (AP-1) and NF κ B. EDN1 also triggers signal transduction cascades through the formation of the AP-1 complex. In this regard, it is noteworthy that different studies have demonstrated an increase in myocardial AP-1 DNA binding activity, which is involved in cardiac hypertrophic signaling (Izumi et al., 2000; Motte et al., 2006; Yano et al., 1998).

AngII has also been reported to mediate cardiac remodeling indirectly by inducing the synthesis of TGF- β 1 which then acts locally *via* auto-/paracrine mechanisms. TGF- β 1 is secreted by both cardiomyocytes and fibroblasts and considered as a primary downstream mediator of AngII (Rosenkranz, 2004; Jo El J Schultz et al., 2002). Primarily, TGF- β 1 acts through the SMAD signaling pathway to stimulate collagen production (Hao et al., 2000). In addition, AngII-stimulated up-regulation of TGF- β 1 has been documented by several studies during cardiac hypertrophy in patients with dilated cardiomyopathy and in animal models of myocardial infarction, progressive coronary artery occlusion, and pressure overload (Byrne*, 2003; Pauschinger et al., 1999; Jo El J. Schultz et al., 2002). TGF- β 1 activates a

serine/threonine kinase that causes phosphorylation of SMAD3 which in turn forms a hetero oligomer with SMAD4 and this complex moves to nucleus and binds with activating transcription factor-2 (ATF-2) to enhance its transcription activity, which is responsible for overexpression of hypertrophic genes (Sano et al., 1999). It is worth to note that 7h RAP induced the mRNA amount of *ATF4* in the irbesartan study.

As shown in the schematic *figure 25*, another important mediator involved in pathological tissue remodeling is the TWEAK/Fn14 axis (Blanco-Colio, 2014). Fn14 expression is rapidly and highly upregulated under pathological conditions as demonstrated in experimental models of myocardial infarction (Mustonen et al., 2010), denervation-induced skeletal muscle atrophy (Mittal et al., 2010), restenosis after balloon injury (Wiley et al., 2001), atherosclerosis (Munoz-Garcia et al., 2006), and cardiac dysfunction (Jain et al., 2009). In this context and in line with previous findings the transcriptome analysis of the irbesartan study showed pronounced induction of *TNFRSF12A* (8.4-fold) on the mRNA level. This gene encodes member 12A of the tumor necrosis factor receptor superfamily, also known as the TWEAK (tumor necrosis factor-like WEAK inducer of apoptosis) receptor or as Fn14



aberrant remodeling of the extracellular matrix, such as matrix metalloproteinases, collagens, laminins etc.

(FGF-inducible 14-kDa protein). AngII-mediated induction of this gene has already been described earlier (Chorianopoulos et al., 2010). Strong activation of *Fn14* gene expression was shown in neonatal rat ventricular myocytes when treated with EDN1 or AngII, whereas *TWEAK* mRNA levels remained unchanged, suggesting the potential role of these hypertrophic agonists in regulating the TWEAK/*Fn14*-axis during cardiac remodeling (Mustonen et al., 2010). Once *Fn14* is present at higher levels, TWEAK binds and causes *Fn14* trimerization and initiates signal transduction (Brown et al., 2003). Indeed, it is known that TWEAK/*Fn14* activation of intracellular signaling pathways requires the association of TNFR-associated factor (TRAF, specifically TRAF2 and 5) to the *Fn14* TRAF-binding motif (Han et al., 2003; Harada et al., 2002; Saitoh et al., 2003). This motif is likely responsible for activating different signaling pathways such as NF κ B and mitogen-activated protein kinases (MAPK) and likely mediates *Fn14*–RAC1 interaction (Brown et al., 2003; Saitoh et al., 2003). Ectopic *Fn14* overexpression studies conducted *in vitro* have indicated that TWEAK-independent *Fn14* signaling can also occur when cellular *Fn14* levels are elevated to a certain threshold value. It is likely that if TWEAK expression is low, but *Fn14* expression is high, *Fn14* on the cell surface induces monomer trimerization and trimer multimerization, which then triggers TRAF association and the subsequent molecular and cellular events. However, it is not yet known if this happens *in vivo* (Brown et al., 2003; Tran et al., 2006, 2003; Winkles, 2008).

Furthermore, it has been demonstrated in a murine system (C2C12 myoblasts) that activation of the TWEAK/*Fn14*-axis results in transcriptional regulation of several genes encoding matrix metalloproteinases, namely in significant up-regulation of *MMP3*, *MMP9*, *MMP14*, and *MMP17* and down-regulation of *MMP2*, *MMP7*, *MMP11*, and *MMP24*, *ADAM6B*, and *ADAM15*. TWEAK/*Fn14*-induced NF κ B activation mediated this remodeling of the extracellular matrix (Li et al., 2009). In agreement with this notion, the transcriptome analysis of the irbesartan study revealed significant down-regulation of *ADAMTS6* (5.5-fold), *MMP2* (1.6-fold), and *MMP11* (3.2-fold) as well as up-regulation of *MMP8* (6.4-fold) and *ADAMTS9* (3.6-fold), further members of this gene family, in the porcine atrial model. Additional matrix metalloproteinase encoding genes, namely *ADAMTS7* (1.96-fold) and *ADAMTS20* (4.4-fold) turned out to be down-regulated under RAP conditions. The differential regulation of these genes, together with the observed down-regulation of collagen structural genes (*COL1A1*, *COL5A1*, *COL11A1*, *COL14A1*, and *COL15A1*, between

1.5- and 2.1-fold), and genes encoding extracellular matrix component proteins, in particular laminins (*LAMA2* and *LAMB2*, 5.4- and 1.6-fold) under conditions of RAP might indicate the onset of structural cardiac remodeling, a hallmark of atrial fibrillation (Schotten et al., 2011). Of note, irbesartan was capable of attenuating the observed differential regulation of genes involved in tissue remodeling.

The most abundant structural components of the ECM are collagens. Connective tissue consists mainly of collagen, and to a much lesser extent of fibronectin, laminin, and elastic fibers (Bowers and Baudino, 2012; Jugdutt, 2003). Presently, more than 20 collagen types have been identified. Among them, collagen I, II, III, V, and XI form fibrils and provide the structural framework of tissues. Type I collagen makes up approximately 85% and type III collagen 11% of total collagen in the heart and coexist in the ECM (de Souza, 2002). Laminins which represent extracellular proteins are a major component of the basement membrane. The balance of ECM remodeling *via* collagen ECM synthesis and degradation is tightly controlled by matrix metalloproteinases (MMPs) and tissue inhibitors of metalloproteinases (TIMPs). This balance finally determines cardiac remodeling (Ahmed et al., 2006; Benjamin and Khalil, 2012; Jugdutt, 2003). MMPs are an endogenous family of proteolytic enzymes that degrade various components of ECM proteins. There are 24 MMPs that have been identified in humans and categorized into collagenases, gelatinases, stromelysins, matrilysins, membrane-type MMPs, and others. MMP-1, -8 and -13 belong to collagenases. TIMPs are natural inhibitors of the MMPs (Awad et al., 2009; Benjamin and Khalil, 2012). Hence, the induction of *MMP8* in the irbesartan study is correlated with decreased expression of collagens (*COL1A1*, *COL5A1*, *COL11A1*, *COL14A1*, and *COL15A1*), indicating aberrant remodeling of the extracellular matrix. ADAMTS (A Disintegrin-like And Metalloprotease domain with ThromboSpondin-type 1 Motifs) family of enzymes belongs to the proteoglycanases and cleaves the large aggregating proteoglycans, aggrecan and versican. There is accumulating evidence that elastin–versican interactions play a role in ECM homeostasis. Versican interferes with elastic fiber assembly, and versican loss of function promotes elastogenesis. MMP activity is modulated by versican, because of its interactions with elastin, for example MMP9, an elastin degrading MMP. Also, versican has diverse binding partners including ECM components such as type I collagen, tenascin-R, fibulin-1, and -2, fibrillin-1 and fibronectin (Huang, 2006; Wu et al., 2005). Furthermore, cardiac and aortic anomalies were observed in a *ADAMTS9* deficient mouse (Kern et al., 2010). Hence, these findings suggest that there may be a potential feedback mechanism whereby remodeling enzymes and proteoglycans are inversely regulated to maintain ECM

homeostasis. Dysregulation of these enzymes causes ECM remodeling abnormalities that may well affect myocardial function and stability.

5.5. REGULATION OF *CTGF*

As mentioned in the previous section, data from the irbesartan study show that even short episodes of rapid pacing *in vivo* cause an increase of *CTGF* expression on mRNA and protein level. *CTGF* is a member of the CNN (Cysteine rich protein 61, Connective tissue growth factor, and Nephroblastoma overexpressed gene) family of cysteine-rich secreted proteins that participate in the proliferation, migration, adhesion, and differentiation of fibroblasts. *CTGF* is described as a “multifunctional matricellular protein” in fibroblasts (Leask and Abraham, 2003) because of its ability to interact with cytokines such as bone morphogenetic proteins (BMPs) or TGF- β (Abreu et al., 2002) or the binding to proteoglycans like heparin (Brigstock, 1997) and different cell surface receptors like integrins (Heng et al., 2006; Jedsadayanmata et al., 1999). *CTGF* frequently has been associated with cardiac fibrosis in previous studies, although causality has not been proven, yet. Increased expression of *CTGF* has been demonstrated in the atrial tissues of AF patients and animal models as well (Ahmed et al., 2005; Lavall et al., 2014; Song et al., 2014). *CTGF* is generally regarded as an immediate early gene and downstream mediator of the profibrotic effects of TGF- β (Biernacka et al., 2011; Grotendorst, 2005, 1997). However, TGF- β -independent induction of *CTGF* has also been shown in a recent study using a canine AF model, with subsequent induction of other fibrosis-associated genes, and the appearance of fibrosis after 6 weeks of pacing *in vivo*. This is likely considered to be mediated by AngII (Kiryu et al., 2012). Furthermore, AngII has been shown to increase the expression of *CTGF* in the kidney (Rup  rez et al., 2003) or heart (Adam et al., 2010; Ko et al., 2011). Thus, the exact mode of signaling mechanisms of *CTGF* induction remains largely unclear. Accordingly, in the irbesartan study, RAP-dependent induction of *CTGF* was attenuated to a significant extent by irbesartan. However, *CTGF* induction was not completely abolished, indicating the involvement of additional factors.

The irbesartan study demonstrates that concomitant to the RAP-dependent increase in *CTGF* mRNA amounts, there is a sequential transcriptional induction of *EDN1* (*ET-1*) and *SGK1*. This suggests that ET-1, after or in addition to AngII-mediated transcriptional up-regulation, modulates *CTGF* induction in an auto- and paracrine fashion *via* SGK1 activation by increased transcription of its encoding gene and by specific phosphorylation of the protein (as shown in hypothetical flow chart *figure 26*).

This view is supported by two lines of evidence provided by previous work: (I) ET-1 promotes increased *CTGF* expression in rat ventricular cardiomyocytes (Kemp et al., 2004) and VSMC (Rodriguez-Vita et al., 2005) as well as in HL-1 cells (Recchia et al., 2009), and (II) the mineralocorticoid-dependent induction of *CTGF* and cardiac fibrosis is severely compromised in *Sgk1*^{-/-} mice (Vallon et al., 2006). Thus, the irbesartan study adds another piece of evidence by demonstrating the efficacy of ET-1 to induce both *SGK1* and *CTGF* expression. Further, it provides another supporting evidence for TGF- β -independent regulation of *CTGF*.

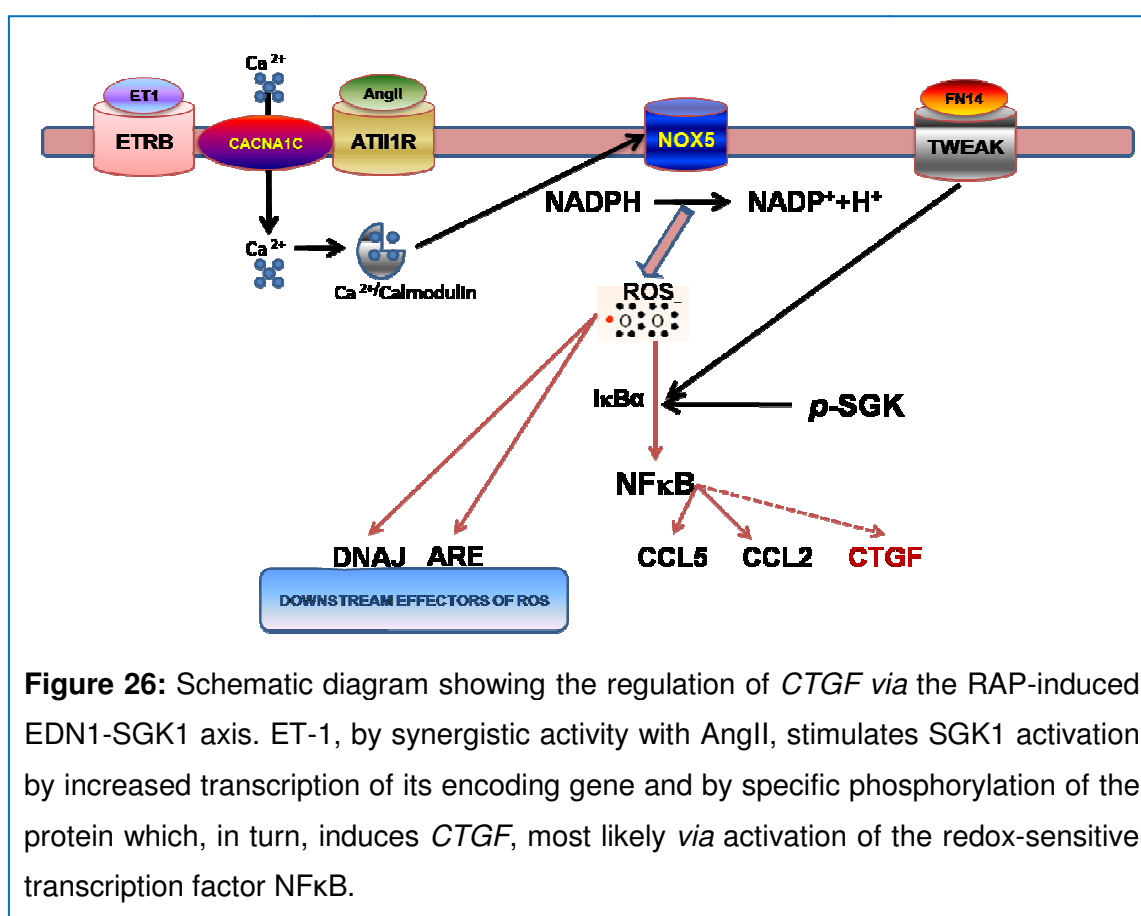


Figure 26: Schematic diagram showing the regulation of *CTGF* via the RAP-induced EDN1-SGK1 axis. ET-1, by synergistic activity with AngII, stimulates SGK1 activation by increased transcription of its encoding gene and by specific phosphorylation of the protein which, in turn, induces *CTGF*, most likely via activation of the redox-sensitive transcription factor NFκB.

Endothelin-1 (ET-1) is a 21 amino acid peptide with potent vasoconstrictory activity. This peptide is released from the endothelium, epithelium, and vascular smooth muscle cells (Yanagisawa et al., 1988). ET-1 elicits its downstream effects via two main receptor subtypes, ET_A and ET_B. Though both receptors share approximately 60% sequence homology and bind ET-1 with similar affinities, ET_A is predominantly expressed in human cardiomyocytes (Kirkby et al., 2009). Increased ET-1 expression has been observed previously in AF patients in presence of underlying valve disease (Brundel et al., 2001b). Plasma ET-1 levels are reported to be elevated in AF patients with congestive heart failure (Tuinenburg et al., 1998) and in

patients with chronic heart failure (HF). In HF patients, plasma ET-1 level was reported to be a strong and independent predictor of AF (Masson et al., 2006). Recent work showed a positive correlation of elevated left atrial ET-1 content with increased LA size, AF persistence, and fibrosis in AF patients with structural heart disease (Mayyas et al., 2010). In human and porcine cardiomyocytes, ET_A and ET_B receptors are synthesized in 85:15 ratios under physiological conditions (Modesti et al., 1999). Differential regulation of these receptors was demonstrated in patients with AF, depending on AF duration and underlying disease. Expression of the ET_B receptor was shown to be decreased in patients with persistent AF compared to sinus rhythm, whereas ET_A mRNA amounts remained unchanged (Brundel et al., 2001b). Acute pacing *in vivo* or *in vitro*, respectively, as performed in the irbesartan study did not alter *ETR* expression (data not shown). Nevertheless, induction of *ET-1* in response to RAP appears to be sufficient to induce *SGK1* and *CTGF*. In support of this view, exogenous addition of ET-1 rapidly and strongly induced *CTGF* in HL-1 cardiomyocytes (Figure. 21). Again, *CTGF* induction was preceded by increased *SGK1* mRNA levels and activation (phosphorylation) of SGK1 (figure 18).

SGK1 is a serine/threonine protein kinase and its activity is regulated at two different levels, i.e. induction of transcription and subsequent activation by phosphorylation. *SGK1* transcription has been shown to be stimulated by various growth factors (Lang et al., 2000), nitric oxide (Turpaev et al., 2005), as well as increased cytosolic Ca^{2+} concentration (Klingel et al., 2000) and oxidative stress (Leong, 2002). Moreover, a striking increase of *SGK1* expression is observed during cardiac fibrosis (Vallon et al., 2006). Although the mechanisms of *SGK1* induction remained poorly understood, ET-1 was shown to trigger *SGK1* expression as well in A-10 smooth muscle cells and intact aortas of adult rats (Wolf et al., 2006, p. -1). Described mechanisms linking CTGF and SGK1 involve NF κ B, because the promoter of rat *Sgk1* carries several putative and confirmed transcription factor binding sites including such for NF κ B (Firestone et al., 2003). *CTGF* has been identified as an NF κ B target gene (Blom et al., 2002; Lang et al., 2006). Furthermore, SGK1 activates and triggers nuclear translocation of NF κ B through phosphorylation and activation of IKK β which subsequently phosphorylates I κ B. Since the *CTGF* promoter contains NF κ B binding sites, this in turn results in increased expression of *CTGF*. Activation of NF κ B during AF and RAP has been previously described (Bukowska et al., 2008b; Chen et al., 2013; Qu et al., 2009). Therefore, it is reasonable to conceive that NF κ B mediates the finally observed transcriptional up-regulation of *CTGF* under RAP conditions.

In summary, the transcriptome data show that acute pacing for seven hours is able to induce significant changes in the expression of several left atrial genes, including

those reflecting AngII-mediated oxidative stress, tissue remodeling, and energy depletion.

Further, the results from the dronedarone study demonstrated that dronedarone is capable of attenuating most of the RAP-induced changes in oxidative stress-related gene expression. The findings are indicative of a significant reduction of ROS production itself rather than an improved handling of ROS, because both mediators of ROS (such as HIF-1 α) and anti-oxidative response genes (Prxs and chaperones) are affected by dronedarone to the same extent and within the same time frame. Accordingly, the hemodynamic parameters also show that dronedarone reduced the RAP-induced microvascular flow abnormalities. This view is supported by the observation that in our model of acute AF, dronedarone decreased RAP-dependent PKC phosphorylation, NADPH isoform expression, F₂-isoprostane release, and I κ B α phosphorylation.

Additionally, the results of the irbesartan study indicate that ET-1 contributes to AF-dependent atrial fibrosis by synergistic activity with AngII to stimulate *SGK1* expression and enhance phosphorylation of the SGK1 protein which, in turn, induces *CTGF*. The latter has been consistently associated with tissue fibrosis. In support of this view, *in vitro* analyses using HL-1 cells verify *CTGF* induction after short episodes of rapid pacing and also, in response to exogenous addition of ET1. Thus, the results demonstrate that regulation of *CTGF* occurs in response to AngII and ET1, is mediated *via* SGK1, and possibly involves activation of redox-sensitive transcription factor NF κ B. Accordingly, irbesartan was shown to be able to attenuate most of the RAP-dependent changes in atrial or ventricular gene expression profiles.

6. REFERENCES

- Abidov, A., Hachamovitch, R., Rozanski, A., Hayes, S.W., Santos, M.M., Sciammarella, M.G., Cohen, I., Gerlach, J., Friedman, J.D., Germano, G., Berman, D.S., 2004. Prognostic implications of atrial fibrillation in patients undergoing myocardial perfusion single-photon emission computed tomography. *J. Am. Coll. Cardiol.* 44, 1062–1070. doi:10.1016/j.jacc.2004.05.076
- Abreu, J.G., Ketpura, N.I., Reversade, B., De Robertis, E.M., 2002. Connective-tissue growth factor (CTGF) modulates cell signalling by BMP and TGF- β . *Nature Cell Biology.* doi:10.1038/ncb826
- Adam, O., Lavall, D., Theobald, K., Hohl, M., Grube, M., Ameling, S., Sussman, M.A., Rosenkranz, S., Kroemer, H.K., Schäfers, H.-J., Böhm, M., Laufs, U., 2010. Rac1-induced connective tissue growth factor regulates connexin 43 and N-cadherin expression in atrial fibrillation. *J. Am. Coll. Cardiol.* 55, 469–480. doi:10.1016/j.jacc.2009.08.064
- Ahmed, M.S., Øie, E., Vinge, L.E., Yndestad, A., Øystein Andersen, G., Andersson, Y., Attramadal, T., Attramadal, H., 2004. Connective tissue growth factor--a novel mediator of angiotensin II-stimulated cardiac fibroblast activation in heart failure in rats. *J. Mol. Cell. Cardiol.* 36, 393–404. doi:10.1016/j.yjmcc.2003.12.004
- Ahmed, M.S., von Lueder, T.G., Øie, E., Kjekshus, H., Attramadal, H., 2005. Induction of myocardial connective tissue growth factor in pacing-induced heart failure in pigs. *Acta Physiol. Scand.* 184, 27–36. doi:10.1111/j.1365-201X.2005.01416.x
- Ahmed, S.H., Clark, L.L., Pennington, W.R., Webb, C.S., Bonnema, D.D., Leonardi, A.H., McClure, C.D., Spinale, F.G., Zile, M.R., 2006. Matrix metalloproteinases/tissue inhibitors of metalloproteinases: relationship between changes in proteolytic determinants of matrix composition and structural, functional, and clinical manifestations of hypertensive heart disease. *Circulation* 113, 2089–2096. doi:10.1161/CIRCULATIONAHA.105.573865
- Ahn, S.-G., 2003. Redox regulation of mammalian heat shock factor 1 is essential for Hsp gene activation and protection from stress. *Genes & Development* 17, 516–528. doi:10.1101/gad.1044503
- Alexander, R.W., 1995. Theodore Cooper Memorial Lecture. Hypertension and the pathogenesis of atherosclerosis. Oxidative stress and the mediation of arterial inflammatory response: a new perspective. *Hypertension* 25, 155–161.
- Allessie, M., 2002. Electrical, contractile and structural remodeling during atrial fibrillation. *Cardiovascular Research* 54, 230–246. doi:10.1016/S0008-6363(02)00258-4
- Anne, W., Willems, R., Roskams, T., Sergeant, P., Herijgers, P., Holemans, P., Ector, H., Heidbuchel, H., 2005. Matrix metalloproteinases and atrial remodeling in patients with mitral valve disease and atrial fibrillation. *Cardiovascular Research* 67, 655–666. doi:10.1016/j.cardiores.2005.04.016
- Antoniades, C., Demosthenous, M., Reilly, S., Margaritis, M., Zhang, M.-H., Antonopoulos, A., Marinou, K., Nahar, K., Jayaram, R., Tousoulis, D., Bakogiannis, C., Sayeed, R., Triantafyllou, C., Koumallos, N., Psarros, C., Miliou, A., Stefanadis, C., Channon, K.M., Casadei, B., 2012. Myocardial redox state predicts in-hospital clinical outcome after cardiac surgery effects of short-term pre-operative statin treatment. *J. Am. Coll. Cardiol.* 59, 60–70. doi:10.1016/j.jacc.2011.08.062
- Anunciado-Koza, R.P., Zhang, J., Ukropec, J., Bajpeyi, S., Koza, R.A., Rogers, R.C., Cefalu, W.T., Mynatt, R.L., Kozak, L.P., 2011. Inactivation of the mitochondrial carrier SLC25A25 (ATP-Mg²⁺/Pi transporter) reduces physical endurance and metabolic efficiency in mice. *J. Biol. Chem.* 286, 11659–11671. doi:10.1074/jbc.M110.203000
- Arany, Z., Foo, S.-Y., Ma, Y., Ruas, J.L., Bommi-Reddy, A., Girnun, G., Cooper, M., Laznik, D., Chinsomboon, J., Rangwala, S.M., Baek, K.H., Rosenzweig, A., Spiegelman, B.M., 2008. HIF-independent regulation of VEGF and angiogenesis by the

- transcriptional coactivator PGC-1 α . *Nature* 451, 1008–1012. doi:10.1038/nature06613
- Arndt, M., Lendeckel, U., Röcken, C., Nepple, K., Wolke, C., Spiess, A., Huth, C., Ansorge, S., Klein, H.U., Goette, A., 2002. Altered expression of ADAMs (A Disintegrin And Metalloproteinase) in fibrillating human atria. *Circulation* 105, 720–725.
- Ausma, J., 2000. Atrial high energy phosphate content and mitochondrial enzyme activity during chronic atrial fibrillation. *Cardiovascular Research* 47, 788–796. doi:10.1016/S0008-6363(00)00139-5
- Ausma, J., van der Velden, H.M.W., Lenders, M.-H., van Ankeren, E.P., Jongsma, H.J., Ramaekers, F.C.S., Borgers, M., Allessie, M.A., 2003. Reverse structural and gap-junctional remodeling after prolonged atrial fibrillation in the goat. *Circulation* 107, 2051–2058. doi:10.1161/01.CIR.0000062689.04037.3F
- Ausma, J., Wijffels, M., Thoné, F., Wouters, L., Allessie, M., Borgers, M., 1997. Structural changes of atrial myocardium due to sustained atrial fibrillation in the goat. *Circulation* 96, 3157–3163.
- Authors/Task Force Members, Fuster, V., Ryden, L.E., Cannom, D.S., Crijns, H.J., Curtis, A.B., Ellenbogen, K.A., Halperin, J.L., Le Heuzey, J.-Y., Kay, G.N., Lowe, J.E., Olsson, S.B., Prystowsky, E.N., Tamargo, J.L., Wann, S., ESC Committee for Practice Guidelines, Priori, S.G., Blanc, J.-J., Budaj, A., Camm, A.J., Dean, V., Deckers, J.W., Despres, C., Dickstein, K., Lekakis, J., McGregor, K., Metra, M., Morais, J., Osterspey, A., Tamargo, J.L., Zamorano, J.L., ACC/AHA (Practice Guidelines) Task Force Members, Smith, S.C., Jacobs, A.K., Adams, C.D., Anderson, J.L., Antman, E.M., Halperin, J.L., Hunt, S.A., Nishimura, R., Ornato, J.P., Page, R.L., Riegel, B., 2006. ACC/AHA/ESC 2006 guidelines for the management of patients with atrial fibrillation executive summary: A report of the American College of Cardiology/American Heart Association Task Force on practice guidelines and the European Society of Cardiology Committee for Practice Guidelines (Writing Committee to Revise the 2001 Guidelines for the Management of Patients with Atrial Fibrillation) Developed in collaboration with the European Heart Rhythm Association and the Heart Rhythm Society. *European Heart Journal* 27, 1979–2030. doi:10.1093/eurheartj/ehl176
- Awad, A.E., Kandam, V., Chakrabarti, S., Wang, X., Penninger, J.M., Davidge, S.T., Oudit, G.Y., Kassiri, Z., 2009. Tumor necrosis factor induces matrix metalloproteinases in cardiomyocytes and cardiofibroblasts differentially via superoxide production in a PI3K -dependent manner. *AJP: Cell Physiology* 298, C679–C692. doi:10.1152/ajpcell.00351.2009
- Banerjee, I., Fuseler, J.W., Price, R.L., Borg, T.K., Baudino, T.A., 2007. Determination of cell types and numbers during cardiac development in the neonatal and adult rat and mouse. *AJP: Heart and Circulatory Physiology* 293, H1883–H1891. doi:10.1152/ajpheart.00514.2007
- Bánfi, B., Tirone, F., Durussel, I., Knisz, J., Moskwa, P., Molnár, G.Z., Krause, K.-H., Cox, J.A., 2004. Mechanism of Ca²⁺ activation of the NADPH oxidase 5 (NOX5). *J. Biol. Chem.* 279, 18583–18591. doi:10.1074/jbc.M310268200
- Banumathi, E., O'Connor, A., Gurunathan, S., Simpson, D.A., McGeown, J.G., Curtis, T.M., 2011. VEGF-induced retinal angiogenic signaling is critically dependent on Ca²⁺ signaling by Ca²⁺/calmodulin-dependent protein kinase II. *Invest. Ophthalmol. Vis. Sci.* 52, 3103–3111. doi:10.1167/iov.10-6574
- Barbey, O., Pierre, S., Duran, M.J., Sennoune, S., Lévy, S., Maixent, J.M., 2000. Specific up-regulation of mitochondrial F0F1-ATPase activity after short episodes of atrial fibrillation in sheep. *J. Cardiovasc. Electrophysiol.* 11, 432–438.
- Barth, A.S., Tomaselli, G.F., 2009. Cardiac Metabolism and Arrhythmias. *Circulation: Arrhythmia and Electrophysiology* 2, 327–335. doi:10.1161/CIRCEP.108.817320
- Bassani, J.W., Bassani, R.A., Bers, D.M., 1994. Relaxation in rabbit and rat cardiac cells: species-dependent differences in cellular mechanisms. *J. Physiol. (Lond.)* 476, 279–293.

- Bendall, J.K., Cave, A.C., Heymes, C., Gall, N., Shah, A.M., 2002. Pivotal role of a gp91(phox)-containing NADPH oxidase in angiotensin II-induced cardiac hypertrophy in mice. *Circulation* 105, 293–296.
- Benjamin, E.J., Levy, D., Vaziri, S.M., D'Agostino, R.B., Belanger, A.J., Wolf, P.A., 1994. Independent risk factors for atrial fibrillation in a population-based cohort. The Framingham Heart Study. *JAMA* 271, 840–844.
- Benjamin, E.J., Wolf, P.A., D'Agostino, R.B., Silbershatz, H., Kannel, W.B., Levy, D., 1998. Impact of atrial fibrillation on the risk of death: the Framingham Heart Study. *Circulation* 98, 946–952.
- Benjamin, M.M., Khalil, R.A., 2012. Matrix metalloproteinase inhibitors as investigative tools in the pathogenesis and management of vascular disease. *EXS* 103, 209–279. doi:10.1007/978-3-0348-0364-9_7
- Berger, M., Schweitzer, P., 1998. Timing of thromboembolic events after electrical cardioversion of atrial fibrillation or flutter: a retrospective analysis. *Am. J. Cardiol.* 82, 1545–1547, A8.
- Berliner, J.A., Navab, M., Fogelman, A.M., Frank, J.S., Demer, L.L., Edwards, P.A., Watson, A.D., Lusis, A.J., 1995. Atherosclerosis: basic mechanisms. Oxidation, inflammation, and genetics. *Circulation* 91, 2488–2496.
- Bers, D.M., 2008. Calcium Cycling and Signaling in Cardiac Myocytes. *Annual Review of Physiology* 70, 23–49. doi:10.1146/annurev.physiol.70.113006.100455
- Biernacka, A., Dobaczewski, M., Frangogiannis, N.G., 2011. TGF- β signaling in fibrosis. *Growth Factors* 29, 196–202. doi:10.3109/08977194.2011.595714
- Black, I.W., Fatkin, D., Sagar, K.B., Khandheria, B.K., Leung, D.Y., Galloway, J.M., Feneley, M.P., Walsh, W.F., Grimm, R.A., Stollberger, C., 1994. Exclusion of atrial thrombus by transesophageal echocardiography does not preclude embolism after cardioversion of atrial fibrillation. A multicenter study. *Circulation* 89, 2509–2513.
- Blanco-Colio, L.M., 2014. TWEAK/Fn14 Axis: A Promising Target for the Treatment of Cardiovascular Diseases. *Front Immunol* 5, 3. doi:10.3389/fimmu.2014.00003
- Blom, I.E., Goldschmeding, R., Leask, A., 2002. Gene regulation of connective tissue growth factor: new targets for antifibrotic therapy? *Matrix Biology* 21, 473–482. doi:10.1016/S0945-053X(02)00055-0
- Bode, F., Sachs, F., Franz, M.R., 2001. Tarantula peptide inhibits atrial fibrillation. *Nature* 409, 35–36. doi:10.1038/35051165
- Boldt, A., Wetzel, U., Lauschke, J., Weigl, J., Gummert, J., Hindricks, G., Kottkamp, H., Dhein, S., 2004. Fibrosis in left atrial tissue of patients with atrial fibrillation with and without underlying mitral valve disease. *Heart* 90, 400–405.
- Bonello, S., Zähringer, C., BelAiba, R.S., Djordjevic, T., Hess, J., Michiels, C., Kietzmann, T., Görlach, A., 2007. Reactive oxygen species activate the HIF-1 α promoter via a functional NF κ B site. *Arterioscler. Thromb. Vasc. Biol.* 27, 755–761. doi:10.1161/01.ATV.0000258979.92828.bc
- Bootman, M.D., Higazi, D.R., Coombes, S., Roderick, H.L., 2006. Calcium signalling during excitation-contraction coupling in mammalian atrial myocytes. *J. Cell. Sci.* 119, 3915–3925. doi:10.1242/jcs.03223
- Bosch, R.F., Scherer, C.R., Rüb, N., Wöhr, S., Steinmeyer, K., Haase, H., Busch, A.E., Seipel, L., Kühlkamp, V., 2003. Molecular mechanisms of early electrical remodeling: transcriptional downregulation of ion channel subunits reduces I(Ca,L) and I(to) in rapid atrial pacing in rabbits. *J. Am. Coll. Cardiol.* 41, 858–869.
- Bowers, S.L.K., Baudino, T.A., 2012. Cardiac myocyte-fibroblast interactions and the coronary vasculature. *J Cardiovasc Transl Res* 5, 783–793. doi:10.1007/s12265-012-9407-2
- Bowie, A., O'Neill, L.A., 2000. Oxidative stress and nuclear factor-kappaB activation: a reassessment of the evidence in the light of recent discoveries. *Biochem. Pharmacol.* 59, 13–23.
- Boyden, P.A., Hoffman, B.F., 1981. The effects on atrial electrophysiology and structure of surgically induced right atrial enlargement in dogs. *Circ. Res.* 49, 1319–1331.

- Brand, T., Schneider, M.D., 1996. Transforming growth factor-beta signal transduction. *Circ. Res.* 78, 173–179.
- Brandes, R.P., Schröder, K., 2008. Differential vascular functions of Nox family NADPH oxidases. *Curr. Opin. Lipidol.* 19, 513–518. doi:10.1097/MOL.0b013e32830c91e3
- Brigstock, D.R., 1997. Purification and Characterization of Novel Heparin-binding Growth Factors in Uterine Secretory Fluids. IDENTIFICATION AS HEPARIN-REGULATED Mr 10,000 FORMS OF CONNECTIVE TISSUE GROWTH FACTOR. *Journal of Biological Chemistry* 272, 20275–20282. doi:10.1074/jbc.272.32.20275
- Brown, D.A., O'Rourke, B., 2010. Cardiac mitochondria and arrhythmias. *Cardiovascular Research* 88, 241–249. doi:10.1093/cvr/cvq231
- Brown, S.A.N., Richards, C.M., Hanscom, H.N., Feng, S.-L.Y., Winkles, J.A., 2003. The Fn14 cytoplasmic tail binds tumour-necrosis-factor-receptor-associated factors 1, 2, 3 and 5 and mediates nuclear factor- κ B activation. *Biochemical Journal* 371, 395. doi:10.1042/BJ20021730
- Brundel, B., 2004. Calpain inhibition prevents pacing-induced cellular remodeling in a HL-1 myocyte model for atrial fibrillation. *Cardiovascular Research* 62, 521–528. doi:10.1016/j.cardiores.2004.02.007
- Brundel, B.J., Van Gelder, I.C., Henning, R.H., Tieleman, R.G., Tuinenburg, A.E., Wietes, M., Grandjean, J.G., Van Gilst, W.H., Crijns, H.J., 2001a. Ion channel remodeling is related to intraoperative atrial effective refractory periods in patients with paroxysmal and persistent atrial fibrillation. *Circulation* 103, 684–690.
- Brundel, B.J., van Gelder, I.C., Henning, R.H., Tuinenburg, A.E., Deelman, L.E., Tieleman, R.G., Grandjean, J.G., van Gilst, W.H., Crijns, H.J., 1999. Gene expression of proteins influencing the calcium homeostasis in patients with persistent and paroxysmal atrial fibrillation. *Cardiovasc. Res.* 42, 443–454.
- Brundel, B.J., Van Gelder, I.C., Tuinenburg, A.E., Wietes, M., Van Veldhuisen, D.J., Van Gilst, W.H., Crijns, H.J., Henning, R.H., 2001b. Endothelin system in human persistent and paroxysmal atrial fibrillation. *J. Cardiovasc. Electrophysiol.* 12, 737–742.
- Brundel, B.J.J.M., Henning, R.H., Kampinga, H.H., Van Gelder, I.C., Crijns, H.J.G.M., 2002. Molecular mechanisms of remodeling in human atrial fibrillation. *Cardiovasc. Res.* 54, 315–324.
- Bruneau, B.G., Piazza, L.A., de Bold, A.J., 1997. BNP gene expression is specifically modulated by stretch and ET-1 in a new model of isolated rat atria. *Am. J. Physiol.* 273, H2678–2686.
- Bukowska, A., Hammwöhner, M., Sixdorf, A., Schild, L., Wiswedel, I., Röhl, F.-W., Wolke, C., Lendeckel, U., Aderkast, C., Bochmann, S., Chilukoti, R.K., Mostertz, J., Bramlage, P., Goette, A., 2011. Dronedronone prevents microcirculatory abnormalities in the left ventricle during atrial tachypacing. *Br. J. Pharmacol.* doi:10.1111/j.1476-5381.2011.01784.x
- Bukowska, A., Lendeckel, U., Krohn, A., Keilhoff, G., ten Have, S., Neumann, K.H., Goette, A., 2008a. Atrial fibrillation down-regulates renal neutral endopeptidase expression and induces profibrotic pathways in the kidney. *Europace* 10, 1212–1217. doi:10.1093/europace/eun206
- Bukowska, A., Schild, L., Keilhoff, G., Hirte, D., Neumann, M., Gardemann, A., Neumann, K.H., Röhl, F.-W., Huth, C., Goette, A., Lendeckel, U., 2008b. Mitochondrial dysfunction and redox signaling in atrial tachyarrhythmia. *Exp. Biol. Med.* (Maywood) 233, 558–574. doi:10.3181/0706-RM-155
- Burstein, B., Comtois, P., Michael, G., Nishida, K., Villeneuve, L., Yeh, Y.-H., Nattel, S., 2009. Changes in connexin expression and the atrial fibrillation substrate in congestive heart failure. *Circ. Res.* 105, 1213–1222. doi:10.1161/CIRCRESAHA.108.183400
- Burstein, B., Libby, E., Calderone, A., Nattel, S., 2008. Differential behaviors of atrial versus ventricular fibroblasts: a potential role for platelet-derived growth factor in atrial-ventricular remodeling differences. *Circulation* 117, 1630–1641. doi:10.1161/CIRCULATIONAHA.107.748053

- Burstein, B., Nattel, S., 2008. Atrial Fibrosis: Mechanisms and Clinical Relevance in Atrial Fibrillation. *Journal of the American College of Cardiology* 51, 802–809. doi:10.1016/j.jacc.2007.09.064
- Byrne*, J.A., 2003. Contrasting Roles of NADPH Oxidase Isoforms in Pressure-Overload Versus Angiotensin II-Induced Cardiac Hypertrophy. *Circulation Research* 93, 802–805. doi:10.1161/01.RES.0000099504.30207.F5
- Cabrera, C., Bohr, D., 1995. The role of nitric oxide in the central control of blood pressure. *Biochem. Biophys. Res. Commun.* 206, 77–81. doi:10.1006/bbrc.1995.1011
- Cai, H., Li, Z., Goette, A., Mera, F., Honeycutt, C., Feterik, K., Wilcox, J.N., Dudley, S.C., Jr, Harrison, D.G., Langberg, J.J., 2002. Downregulation of endocardial nitric oxide synthase expression and nitric oxide production in atrial fibrillation: potential mechanisms for atrial thrombosis and stroke. *Circulation* 106, 2854–2858.
- Cantó, C., Auwerx, J., 2009. PGC-1 α , SIRT1 and AMPK, an energy sensing network that controls energy expenditure. *Curr. Opin. Lipidol.* 20, 98–105. doi:10.1097/MOL.0b013e328328d0a4
- Cardin, S., Li, D., Thorin-Trescases, N., Leung, T.-K., Thorin, E., Nattel, S., 2003. Evolution of the atrial fibrillation substrate in experimental congestive heart failure: angiotensin-dependent and -independent pathways. *Cardiovasc. Res.* 60, 315–325.
- Cardin, S., Libby, E., Pelletier, P., Le Bouter, S., Shiroshita-Takeshita, A., Le Meur, N., Léger, J., Demolombe, S., Ponton, A., Glass, L., Nattel, S., 2007. Contrasting gene expression profiles in two canine models of atrial fibrillation. *Circ. Res.* 100, 425–433. doi:10.1161/01.RES.0000258428.09589.1a
- Carey, R.M., 2003. Newly Recognized Components of the Renin-Angiotensin System: Potential Roles in Cardiovascular and Renal Regulation. *Endocrine Reviews* 24, 261–271. doi:10.1210/er.2003-0001
- Carnes, C.A., Chung, M.K., Nakayama, T., Nakayama, H., Baliga, R.S., Piao, S., Kanderian, A., Pavia, S., Hamlin, R.L., McCarthy, P.M., Bauer, J.A., Van Wagoner, D.R., 2001. Ascorbate attenuates atrial pacing-induced peroxynitrite formation and electrical remodeling and decreases the incidence of postoperative atrial fibrillation. *Circ. Res.* 89, E32–38.
- Caron, K.M.I., James, L.R., Kim, H.-S., Knowles, J., Uhler, R., Mao, L., Hagaman, J.R., Cascio, W., Rockman, H., Smithies, O., 2004. Cardiac hypertrophy and sudden death in mice with a genetically clamped renin transgene. *Proc. Natl. Acad. Sci. U.S.A.* 101, 3106–3111. doi:10.1073/pnas.0307333101
- Carver, W., Nagpal, M.L., Nachtigal, M., Borg, T.K., Terracio, L., 1991. Collagen expression in mechanically stimulated cardiac fibroblasts. *Circulation Research* 69, 116–122. doi:10.1161/01.RES.69.1.116
- Cha, Y.-M., Dzeja, P.P., Shen, W.K., Jahangir, A., Hart, C.Y.T., Terzic, A., Redfield, M.M., 2003. Failing atrial myocardium: energetic deficits accompany structural remodeling and electrical instability. *Am. J. Physiol. Heart Circ. Physiol.* 284, H1313–1320. doi:10.1152/ajpheart.00337.2002
- Chahal, C.A.A., Ali, O., Hunter, R.J., Schilling, R.J., 2012. Impact of controlling atrial fibrillation on outcomes relevant to the patient: focus on dronedarone. *Patient Relat Outcome Meas* 3, 95–103. doi:10.2147/PROM.S16678
- Chen, L., Zhang, W., Fang, C., Jiang, S., Shu, C., Cheng, H., Li, F., Li, H., 2011. Polymorphism H558R in the human cardiac sodium channel SCN5A gene is associated with atrial fibrillation. *J. Int. Med. Res.* 39, 1908–1916.
- Chen, L.-P., Liu, H., Huang, Y., Zhang, X.-Y., Alexander, R.E., Cheng, L., 2013. Expression of NF κ B, ICAM1, and VCAM1 in rheumatic heart disease with atrial fibrillation. *Anal. Quant. Cytol. Histol.* 35, 249–252.
- Chen, M.M., Lam, A., Abraham, J.A., Schreiner, G.F., Joly, A.H., 2000. CTGF expression is induced by TGF- β in cardiac fibroblasts and cardiac myocytes: a potential role in heart fibrosis. *J. Mol. Cell. Cardiol.* 32, 1805–1819. doi:10.1006/jmcc.2000.1215
- Chomczynski, P., Sacchi, N., 1987. Single-step method of RNA isolation by acid guanidinium thiocyanate-phenol-chloroform extraction. *Anal. Biochem.* 162, 156–159. doi:10.1006/abio.1987.9999

- Chorianopoulos, E., Heger, T., Lutz, M., Frank, D., Bea, F., Katus, H.A., Frey, N., 2010. FGF-inducible 14-kDa protein (Fn14) is regulated via the RhoA/ROCK kinase pathway in cardiomyocytes and mediates nuclear factor-kappaB activation by TWEAK. *Basic Res. Cardiol* 105, 301–313. doi:10.1007/s00395-009-0046-y
- Chung, M.K., Martin, D.O., Sprecher, D., Wazni, O., Kanderian, A., Carnes, C.A., Bauer, J.A., Tchou, P.J., Niebauer, M.J., Natale, A., Van Wagoner, D.R., 2001. C-reactive protein elevation in patients with atrial arrhythmias: inflammatory mechanisms and persistence of atrial fibrillation. *Circulation* 104, 2886–2891.
- Claycomb, W.C., Lanson, N.A., Stallworth, B.S., Egeland, D.B., Delcarpio, J.B., Bahinski, A., Izzo, N.J., 1998. HL-1 cells: a cardiac muscle cell line that contracts and retains phenotypic characteristics of the adult cardiomyocyte. *Proc. Natl. Acad. Sci. U.S.A* 95, 2979–2984.
- Cleland, J., 2003. The EuroHeart Failure survey programme—a survey on the quality of care among patients with heart failure in Europe Part 1: patient characteristics and diagnosis. *European Heart Journal* 24, 442–463. doi:10.1016/S0195-668X(02)00823-0
- Clempus, R.E., Sorescu, D., Dikalova, A.E., Pounkova, L., Jo, P., Sorescu, G.P., Schmidt, H.H.H., Lassègue, B., Griendling, K.K., 2007. Nox4 is required for maintenance of the differentiated vascular smooth muscle cell phenotype. *Arterioscler. Thromb. Vasc. Biol.* 27, 42–48. doi:10.1161/01.ATV.0000251500.94478.18
- Connolly, S.J., Crijns, H.J.G.M., Torp-Pedersen, C., van Eickels, M., Gaudin, C., Page, R.L., Hohnloser, S.H., for the ATHENA Investigators, 2009. Analysis of Stroke in ATHENA: A Placebo-Controlled, Double-Blind, Parallel-Arm Trial to Assess the Efficacy of Dronedarone 400 mg BID for the Prevention of Cardiovascular Hospitalization or Death From Any Cause in Patients With Atrial Fibrillation/Atrial Flutter. *Circulation* 120, 1174–1180. doi:10.1161/CIRCULATIONAHA.109.875252
- Conway, D.S.G., Buggins, P., Hughes, E., Lip, G.Y.H., 2004. Relationship of interleukin-6 and C-reactive protein to the prothrombotic state in chronic atrial fibrillation. *J. Am. Coll. Cardiol.* 43, 2075–2082. doi:10.1016/j.jacc.2003.11.062
- Courtemanche, M., Ramirez, R.J., Nattel, S., 1998. Ionic mechanisms underlying human atrial action potential properties: insights from a mathematical model. *Am. J. Physiol.* 275, H301–321.
- Couture, O., Callenberg, K., Koul, N., Pandit, S., Younes, R., Hu, Z.-L., Dekkers, J., Reecy, J., Honavar, V., Tuggle, C., 2009. ANEXdb: an integrated animal ANnotation and microarray EXpression database. *Mamm. Genome* 20, 768–777. doi:10.1007/s00335-009-9234-1
- Cuspidi, C., Rescaldani, M., Sala, C., 2013. Prevalence of echocardiographic left-atrial enlargement in hypertension: a systematic review of recent clinical studies. *Am. J. Hypertens.* 26, 456–464. doi:10.1093/ajh/hpt001
- Da Cunha, V., Tham, D.M., Martin-McNulty, B., Deng, G., Ho, J.J., Wilson, D.W., Rutledge, J.C., Vergona, R., Sullivan, M.E., Wang, Y.-X.J., 2005. Enalapril attenuates angiotensin II-induced atherosclerosis and vascular inflammation. *Atherosclerosis* 178, 9–17. doi:10.1016/j.atherosclerosis.2004.08.023
- Dammanahalli, K.J., Sun, Z., 2008. Endothelins and NADPH oxidases in the cardiovascular system. *Clin. Exp. Pharmacol. Physiol.* 35, 2–6. doi:10.1111/j.1440-1681.2007.04830.x
- De Git, K.C.G., de Boer, T.P., Vos, M.A., van der Heyden, M.A.G., 2013. Cardiac ion channel trafficking defects and drugs. *Pharmacol. Ther.* doi:10.1016/j.pharmthera.2013.03.008
- De Souza, R.R., 2002. Aging of myocardial collagen. *Biogerontology* 3, 325–335.
- De Winther, M.P.J., 2005. Nuclear Factor B Signaling in Atherogenesis. *Arteriosclerosis, Thrombosis, and Vascular Biology* 25, 904–914. doi:10.1161/01.ATV.0000160340.72641.87
- Developed with the special contribution of the European Heart Rhythm Association (EHRA), Endorsed by the European Association for Cardio-Thoracic Surgery (EACTS), Authors/Task Force Members, Camm, A.J., Kirchhof, P., Lip, G.Y.H., Schotten, U.,

- Savelieva, I., Ernst, S., Van Gelder, I.C., Al-Attar, N., Hindricks, G., Prendergast, B., Heidbuchel, H., Alfieri, O., Angelini, A., Atar, D., Colonna, P., De Caterina, R., De Sutter, J., Goette, A., Gorenek, B., Haldal, M., Hohloser, S.H., Kolh, P., Le Heuzey, J.-Y., Ponikowski, P., Rutten, F.H., ESC Committee for Practice Guidelines (CPG), Vahanian, A., Auricchio, A., Bax, J., Ceconi, C., Dean, V., Filippatos, G., Funck-Brentano, C., Hobbs, R., Kearney, P., McDonagh, T., Popescu, B.A., Reiner, Z., Sechtem, U., Sirnes, P.A., Tendera, M., Vardas, P.E., Widimsky, P., Document Reviewers, Vardas, P.E., Agladze, V., Aliot, E., Balabanski, T., Blomstrom-Lundqvist, C., Capucci, A., Crijns, H., Dahlof, B., Folliguet, T., Glikson, M., Goethals, M., Gulba, D.C., Ho, S.Y., Klautz, R.J.M., Kose, S., McMurray, J., Perrone Filardi, P., Raatikainen, P., Salvador, M.J., Schalij, M.J., Shpektor, A., Sousa, J., Stepinska, J., Uuetoa, H., Zamorano, J.L., Zupan, I., 2010. Guidelines for the management of atrial fibrillation: The Task Force for the Management of Atrial Fibrillation of the European Society of Cardiology (ESC). *Europace* 12, 1360–1420. doi:10.1093/europace/euq350
- Donato, A.J., Eskurza, I., Silver, A.E., Levy, A.S., Pierce, G.L., Gates, P.E., Seals, D.R., 2007. Direct evidence of endothelial oxidative stress with aging in humans: relation to impaired endothelium-dependent dilation and upregulation of nuclear factor-kappaB. *Circ. Res.* 100, 1659–1666. doi:10.1161/01.RES.0000269183.13937.e8
- Dostal, D.E., Baker, K.M., 1999. The cardiac renin-angiotensin system: conceptual, or a regulator of cardiac function? *Circ. Res.* 85, 643–650.
- Dragović, T., Igić, R., Erdős, E.G., Rabito, S.F., 1993. Metabolism of Bradykinin by Peptidases in the Lung. *American Review of Respiratory Disease* 147, 1491–1496. doi:10.1164/ajrccm/147.6_Pt_1.1491
- Dudley, S.C., Jr, Hoch, N.E., McCann, L.A., Honeycutt, C., Diamandopoulos, L., Fukai, T., Harrison, D.G., Dikalov, S.I., Langberg, J., 2005. Atrial fibrillation increases production of superoxide by the left atrium and left atrial appendage: role of the NADPH and xanthine oxidases. *Circulation* 112, 1266–1273. doi:10.1161/CIRCULATIONAHA.105.538108
- Dusting, G.J., Fennessy, P., Yin, Z.L., Gurevich, V., 1998. Nitric oxide in atherosclerosis: vascular protector or villain? *Clin Exp Pharmacol Physiol Suppl* 25, S34–41.
- Dusting, G.J., Selemidis, S., Jiang, F., 2005. Mechanisms for suppressing NADPH oxidase in the vascular wall. *Mem. Inst. Oswaldo Cruz* 100 Suppl 1, 97–103. doi:/S0074-02762005000900016
- Dzeja, P.P., Vitkevicius, K.T., Redfield, M.M., Burnett, J.C., Terzic, A., 1999. Adenylate Kinase Catalyzed Phosphotransfer in the Myocardium: Increased Contribution in Heart Failure. *Circulation Research* 84, 1137–1143. doi:10.1161/01.RES.84.10.1137
- Ehrlich, J.R., Biliczki, P., Hohloser, S.H., Nattel, S., 2008. Atrial-selective approaches for the treatment of atrial fibrillation. *J. Am. Coll. Cardiol.* 51, 787–792. doi:10.1016/j.jacc.2007.08.067
- El-Armouche, A., Boknik, P., Eschenhagen, T., Carrier, L., Knaut, M., Ravens, U., Dobrev, D., 2006. Molecular determinants of altered Ca²⁺ handling in human chronic atrial fibrillation. *Circulation* 114, 670–680. doi:10.1161/CIRCULATIONAHA.106.636845
- Elenes, S., Rubart, M., Moreno, A.P., 1999. Junctional communication between isolated pairs of canine atrial cells is mediated by homogeneous and heterogeneous gap junction channels. *J. Cardiovasc. Electrophysiol.* 10, 990–1004.
- Ellinghaus, P., Scheubel, R.J., Dobrev, D., Ravens, U., Holtz, J., Huetter, J., Nielsch, U., Morawietz, H., 2005. Comparing the global mRNA expression profile of human atrial and ventricular myocardium with high-density oligonucleotide arrays. *J. Thorac. Cardiovasc. Surg.* 129, 1383–1390. doi:10.1016/j.jtcvs.2004.08.031
- European Heart Rhythm Association, European Association for Cardio-Thoracic Surgery, Camm, A.J., Kirchhof, P., Lip, G.Y.H., Schotten, U., Savelieva, I., Ernst, S., Van Gelder, I.C., Al-Attar, N., Hindricks, G., Prendergast, B., Heidbuchel, H., Alfieri, O., Angelini, A., Atar, D., Colonna, P., De Caterina, R., De Sutter, J., Goette, A., Gorenek, B., Haldal, M., Hohloser, S.H., Kolh, P., Le Heuzey, J.-Y., Ponikowski, P., Rutten, F.H., 2010. Guidelines for the management of atrial fibrillation: the Task Force

- for the Management of Atrial Fibrillation of the European Society of Cardiology (ESC). *Eur. Heart J.* 31, 2369–2429. doi:10.1093/eurheartj/ehq278
- Evans, A.M., Mustard, K.J.W., Wyatt, C.N., Peers, C., Dipp, M., Kumar, P., Kinnear, N.P., Hardie, D.G., 2005. Does AMP-activated Protein Kinase Couple Inhibition of Mitochondrial Oxidative Phosphorylation by Hypoxia to Calcium Signaling in O₂-sensing Cells? *Journal of Biological Chemistry* 280, 41504–41511. doi:10.1074/jbc.M510040200
- Fatkin, D., Kuchar, D.L., Thorburn, C.W., Feneley, M.P., 1994. Transesophageal echocardiography before and during direct current cardioversion of atrial fibrillation: evidence for “atrial stunning” as a mechanism of thromboembolic complications. *J. Am. Coll. Cardiol.* 23, 307–316.
- Ferrario, C.M., Strawn, W.B., 2006. Role of the renin-angiotensin-aldosterone system and proinflammatory mediators in cardiovascular disease. *Am. J. Cardiol.* 98, 121–128. doi:10.1016/j.amjcard.2006.01.059
- Fineschi, M., Bravi, A., Gori, T., 2008. The “slow coronary flow” phenomenon: evidence of preserved coronary flow reserve despite increased resting microvascular resistances. *Int. J. Cardiol.* 127, 358–361. doi:10.1016/j.ijcard.2007.06.010
- Fink, G., 2000. *Encyclopedia of Stress Three-Volume Set*. Elsevier, Burlington.
- Firestone, G., Giampaolo, J., O’Keeffe, B., 2003. Stimulus-Dependent Regulation of Serum and Glucocorticoid Inducible Protein Kinase (SGK) Transcription, Subcellular Localization and Enzymatic Activity. *Cellular Physiology and Biochemistry* 13, 1–12. doi:10.1159/000070244
- Flohé, L., Brigelius-Flohé, R., Saliou, C., Traber, M.G., Packer, L., 1997. Redox regulation of NF-kappa B activation. *Free Radic. Biol. Med.* 22, 1115–1126.
- Fontayne, A., Dang, P.M.-C., Gougerot-Pocidalo, M.-A., El-Benna, J., 2002. Phosphorylation of p47phox sites by PKC alpha, beta II, delta, and zeta: effect on binding to p22phox and on NADPH oxidase activation. *Biochemistry* 41, 7743–7750.
- Forsythe, J.A., Jiang, B.H., Iyer, N.V., Agani, F., Leung, S.W., Koos, R.D., Semenza, G.L., 1996. Activation of vascular endothelial growth factor gene transcription by hypoxia-inducible factor 1. *Mol. Cell. Biol.* 16, 4604–4613.
- Frustaci, A., 1991. Cardiac biopsy in patients with “primary” atrial fibrillation. Histologic evidence of occult myocardial diseases. *CHEST Journal* 100, 303. doi:10.1378/chest.100.2.303
- Frustaci, A., Chimenti, C., Bellocci, F., Morgante, E., Russo, M.A., Maseri, A., 1997. Histological substrate of atrial biopsies in patients with lone atrial fibrillation. *Circulation* 96, 1180–1184.
- Fukai, T., Ushio-Fukai, M., 2011. Superoxide dismutases: role in redox signaling, vascular function, and diseases. *Antioxid. Redox Signal.* 15, 1583–1606. doi:10.1089/ars.2011.3999
- Fuster, V., Rydén, L.E., Cannom, D.S., Crijns, H.J., Curtis, A.B., Ellenbogen, K.A., Halperin, J.L., Le Heuzey, J.-Y., Kay, G.N., Lowe, J.E., Olsson, S.B., Prystowsky, E.N., Tamargo, J.L., Wann, S., Smith, S.C., Jr, Jacobs, A.K., Adams, C.D., Anderson, J.L., Antman, E.M., Hunt, S.A., Nishimura, R., Ornato, J.P., Page, R.L., Riegel, B., Priori, S.G., Blanc, J.-J., Budaj, A., Camm, A.J., Dean, V., Deckers, J.W., Despres, C., Dickstein, K., Lekakis, J., McGregor, K., Metra, M., Morais, J., Osterspey, A., Zamorano, J.L., 2006. ACC/AHA/ESC 2006 guidelines for the management of patients with atrial fibrillation--executive summary: a report of the American College of Cardiology/American Heart Association Task Force on Practice Guidelines and the European Society of Cardiology Committee for Practice Guidelines (Writing Committee to Revise the 2001 Guidelines for the Management of Patients With Atrial Fibrillation). *J. Am. Coll. Cardiol.* 48, 854–906. doi:10.1016/j.jacc.2006.07.009
- Gaborit, N., Steenman, M., Lamirault, G., Le Meur, N., Le Bouter, S., Lande, G., Léger, J., Charpentier, F., Christ, T., Dobrev, D., Escande, D., Nattel, S., Demolombe, S., 2005. Human atrial ion channel and transporter subunit gene-expression remodeling associated with valvular heart disease and atrial fibrillation. *Circulation* 112, 471–481. doi:10.1161/CIRCULATIONAHA.104.506857

- Gaspo, R., Bosch, R.F., Talajic, M., Nattel, S., 1997. Functional mechanisms underlying tachycardia-induced sustained atrial fibrillation in a chronic dog model. *Circulation* 96, 4027–4035.
- Gautier, P., Guillemare, E., Marion, A., Bertrand, J.-P., Tourneur, Y., Nisato, D., 2003. Electrophysiologic characterization of dronedarone in guinea pig ventricular cells. *J. Cardiovasc. Pharmacol.* 41, 191–202.
- Ghezzi, P., Bonetto, V., Fratelli, M., 2005. Thiol-disulfide balance: from the concept of oxidative stress to that of redox regulation. *Antioxid. Redox Signal.* 7, 964–972. doi:10.1089/ars.2005.7.964
- Gibbs, C.L., 1978. Cardiac energetics. *Physiol. Rev.* 58, 174–254.
- Giles, T.D., Sander, G.E., Nossaman, B.D., Kadowitz, P.J., 2012. Impaired vasodilation in the pathogenesis of hypertension: focus on nitric oxide, endothelial-derived hyperpolarizing factors, and prostaglandins. *J Clin Hypertens (Greenwich)* 14, 198–205. doi:10.1111/j.1751-7176.2012.00606.x
- Go, A.S., Hylek, E.M., Phillips, K.A., Chang, Y., Henault, L.E., Selby, J.V., Singer, D.E., 2001. Prevalence of diagnosed atrial fibrillation in adults: national implications for rhythm management and stroke prevention: the AnTicoagulation and Risk Factors in Atrial Fibrillation (ATRIA) Study. *JAMA* 285, 2370–2375.
- Goette, A., Bukowska, A., Dobrev, D., Pfeifferberger, J., Morawietz, H., Strugala, D., Wiswedel, I., Röhl, F.-W., Wolke, C., Bergmann, S., Bramlage, P., Ravens, U., Lendeckel, U., 2009a. Acute atrial tachyarrhythmia induces angiotensin II type 1 receptor-mediated oxidative stress and microvascular flow abnormalities in the ventricles. *Eur. Heart J.* 30, 1411–1420. doi:10.1093/eurheartj/ehp046
- Goette, A., Bukowska, A., Dobrev, D., Pfeifferberger, J., Morawietz, H., Strugala, D., Wiswedel, I., Röhl, F.-W., Wolke, C., Bergmann, S., Bramlage, P., Ravens, U., Lendeckel, U., 2009b. Acute atrial tachyarrhythmia induces angiotensin II type 1 receptor-mediated oxidative stress and microvascular flow abnormalities in the ventricles. *Eur. Heart J* 30, 1411–1420. doi:10.1093/eurheartj/ehp046
- Goette, A., Bukowska, A., Lendeckel, U., Erxleben, M., Hammwöhner, M., Strugala, D., Pfeifferberger, J., Röhl, F.-W., Huth, C., Ebert, M.P.A., Klein, H.U., Röcken, C., 2008a. Angiotensin II receptor blockade reduces tachycardia-induced atrial adhesion molecule expression. *Circulation* 117, 732–742. doi:10.1161/CIRCULATIONAHA.107.730101
- Goette, A., D'Alessandro, A., Bukowska, A., Kropf, S., Mewis, C., Stellbrink, C., Tebbenjohanns, J., Weiss, C., Lendeckel, U., 2008b. Rationale for and design of the CREATIVE-AF trial: randomized, double-blind, placebo-controlled, crossover study of the effect of irbesartan on oxidative stress and adhesion molecules in patients with persistent atrial fibrillation. *Clin Drug Investig* 28, 565–572.
- Goette, A., Staack, T., Röcken, C., Arndt, M., Geller, J.C., Huth, C., Ansorge, S., Klein, H.U., Lendeckel, U., 2000. Increased expression of extracellular signal-regulated kinase and angiotensin-converting enzyme in human atria during atrial fibrillation. *J. Am. Coll. Cardiol.* 35, 1669–1677.
- Goumans, M.-J., van Zonneveld, A.J., ten Dijke, P., 2008. Transforming Growth Factor β –Induced Endothelial-to-Mesenchymal Transition: A Switch to Cardiac Fibrosis? *Trends in Cardiovascular Medicine* 18, 293–298. doi:10.1016/j.tcm.2009.01.001
- Greiser, M., Lederer, W.J., Schotten, U., 2011. Alterations of atrial Ca^{2+} handling as cause and consequence of atrial fibrillation. *Cardiovascular Research* 89, 722–733. doi:10.1093/cvr/cvq389
- Greiser, M., Neuberger, H.-R., Harks, E., El-Armouche, A., Boknik, P., de Haan, S., Verheyen, F., Verheule, S., Schmitz, W., Ravens, U., Nattel, S., Allesie, M.A., Dobrev, D., Schotten, U., 2009. Distinct contractile and molecular differences between two goat models of atrial dysfunction: AV block-induced atrial dilatation and atrial fibrillation. *J. Mol. Cell. Cardiol.* 46, 385–394. doi:10.1016/j.yjmcc.2008.11.012
- Griendling, K.K., Murphy, T.J., Alexander, R.W., 1993. Molecular biology of the renin-angiotensin system. *Circulation* 87, 1816–1828.

- Grimsrud, P.A., Xie, H., Griffin, T.J., Bernlohr, D.A., 2008. Oxidative Stress and Covalent Modification of Protein with Bioactive Aldehydes. *Journal of Biological Chemistry* 283, 21837–21841. doi:10.1074/jbc.R700019200
- Grotendorst, G.R., 1997. Connective tissue growth factor: a mediator of TGF- β action on fibroblasts. *Cytokine & Growth Factor Reviews* 8, 171–179. doi:10.1016/S1359-6101(97)00010-5
- Grotendorst, G.R., 2005. Individual domains of connective tissue growth factor regulate fibroblast proliferation and myofibroblast differentiation. *The FASEB Journal* 19, 729–738. doi:10.1096/fj.04-3217com
- Gutsaeva, D.R., Carraway, M.S., Suliman, H.B., Demchenko, I.T., Shitara, H., Yonekawa, H., Piantadosi, C.A., 2008. Transient hypoxia stimulates mitochondrial biogenesis in brain subcortex by a neuronal nitric oxide synthase-dependent mechanism. *J. Neurosci.* 28, 2015–2024. doi:10.1523/JNEUROSCI.5654-07.2008
- Haïssaguerre, M., Jaïs, P., Shah, D.C., Takahashi, A., Hocini, M., Quiniou, G., Garrigue, S., Le Mouroux, A., Le Métayer, P., Clémenty, J., 1998. Spontaneous Initiation of Atrial Fibrillation by Ectopic Beats Originating in the Pulmonary Veins. *New England Journal of Medicine* 339, 659–666. doi:10.1056/NEJM199809033391003
- Han, S., Yoon, K., Lee, K., Kim, K., Jang, H., Lee, N.K., Hwang, K., Young Lee, S., 2003. TNF-related weak inducer of apoptosis receptor, a TNF receptor superfamily member, activates NF-kappa B through TNF receptor-associated factors. *Biochem. Biophys. Res. Commun.* 305, 789–796.
- Hao, J., Wang, B., Jones, S.C., Jassal, D.S., Dixon, I.M., 2000. Interaction between angiotensin II and Smad proteins in fibroblasts in failing heart and in vitro. *Am. J. Physiol. Heart Circ. Physiol.* 279, H3020–3030.
- Harada, N., Nakayama, M., Nakano, H., Fukuchi, Y., Yagita, H., Okumura, K., 2002. Pro-inflammatory effect of TWEAK/Fn14 interaction on human umbilical vein endothelial cells. *Biochem. Biophys. Res. Commun.* 299, 488–493.
- Harkcom, W.T., Abbott, G.W., 2010. Emerging concepts in the pharmacogenomics of arrhythmias: ion channel trafficking. *Expert Rev Cardiovasc Ther* 8, 1161–1173. doi:10.1586/erc.10.89
- Heeringa, J., van der Kuip, D.A.M., Hofman, A., Kors, J.A., van Herpen, G., Stricker, B.H.C., Stijnen, T., Lip, G.Y.H., Witteman, J.C.M., 2006. Prevalence, incidence and lifetime risk of atrial fibrillation: the Rotterdam study. *Eur. Heart J.* 27, 949–953. doi:10.1093/eurheartj/ehi825
- Heist, E.K., Chalhoub, F., Barrett, C., Danik, S., Ruskin, J.N., Mansour, M., 2012. Predictors of atrial fibrillation termination and clinical success of catheter ablation of persistent atrial fibrillation. *Am. J. Cardiol.* 110, 545–551. doi:10.1016/j.amjcard.2012.04.028
- Heng, E.C.K., Huang, Y., Black, S.A., Jr, Trackman, P.C., 2006. CCN2, connective tissue growth factor, stimulates collagen deposition by gingival fibroblasts via α 3 and α 6- and β 1 integrins. *J. Cell. Biochem.* 98, 409–420. doi:10.1002/jcb.20810
- Henry, W.L., Morganroth, J., Pearlman, A.S., Clark, C.E., Redwood, D.R., Itscoitz, S.B., Epstein, S.E., 1976. Relation between echocardiographically determined left atrial size and atrial fibrillation. *Circulation* 53, 273–279.
- Hishikawa, K., Oemar, B.S., Tanner, F.C., Nakaki, T., Lüscher, T.F., Fujii, T., 1999. Connective tissue growth factor induces apoptosis in human breast cancer cell line MCF-7. *J. Biol. Chem.* 274, 37461–37466.
- Hobbs, F.D.R., Fitzmaurice, D.A., Mant, J., Murray, E., Jowett, S., Bryan, S., Raftery, J., Davies, M., Lip, G., 2005. A randomised controlled trial and cost-effectiveness study of systematic screening (targeted and total population screening) versus routine practice for the detection of atrial fibrillation in people aged 65 and over. *The SAFE study. Health Technol Assess* 9, iii–iv, ix–x, 1–74.
- Hohnloser, S.H., Crijns, H.J.G.M., van Eickels, M., Gaudin, C., Page, R.L., Torp-Pedersen, C., Connolly, S.J., 2009. Effect of Dronedarone on Cardiovascular Events in Atrial Fibrillation. *New England Journal of Medicine* 360, 668–678. doi:10.1056/NEJMoa0803778

- Holmes, B.F., Kurth-Kraczek, E.J., Winder, W.W., 1999. Chronic activation of 5'-AMP-activated protein kinase increases GLUT-4, hexokinase, and glycogen in muscle. *J. Appl. Physiol.* 87, 1990–1995.
- Honjo, T., Otsui, K., Shiraki, R., Kawashima, S., Sawamura, T., Yokoyama, M., Inoue, N., 2008. Essential role of NOXA1 in generation of reactive oxygen species induced by oxidized low-density lipoprotein in human vascular endothelial cells. *Endothelium* 15, 137–141. doi:10.1080/10623320802125433
- Huang, C.-X., Liu, Y., Xia, W.-F., Tang, Y.-H., Huang, H., 2009. Oxidative stress: a possible pathogenesis of atrial fibrillation. *Med. Hypotheses* 72, 466–467. doi:10.1016/j.mehy.2008.08.031
- Huang, R., 2006. Inhibition of Versican Synthesis by Antisense Alters Smooth Muscle Cell Phenotype and Induces Elastic Fiber Formation In Vitro and in Neointima After Vessel Injury. *Circulation Research* 98, 370–377. doi:10.1161/01.RES.0000202051.28319.c8
- Hunt, M.J., Aru, G.M., Hayden, M.R., Moore, C.K., Hoit, B.D., Tyagi, S.C., 2002. Induction of oxidative stress and disintegrin metalloproteinase in human heart end-stage failure. *Am. J. Physiol. Lung Cell Mol. Physiol.* 283, L239–245. doi:10.1152/ajplung.00001.2002
- Hunter, R., Chahal, Ali, O., Schilling, 2012. Impact of controlling atrial fibrillation on outcomes relevant to the patient: focus on dronedarone. *Patient Related Outcome Measures* 95. doi:10.2147/PROM.S16678
- Hunyady, L., Catt, K.J., 2006. Pleiotropic AT1 receptor signaling pathways mediating physiological and pathogenic actions of angiotensin II. *Mol. Endocrinol.* 20, 953–970. doi:10.1210/me.2004-0536
- Hussain, A., Wyatt, A.W., Wang, K., Bhandaru, M., Biswas, R., Avram, D., Föller, M., Rexhepaj, R., Friedrich, B., Ullrich, S., Müller, G., Kuhl, D., Risler, T., Lang, F., 2008. SGK1-dependent upregulation of connective tissue growth factor by angiotensin II. *Kidney Blood Press. Res* 31, 80–86. doi:10.1159/000119703
- Hwang, J.-T., Lee, M., Jung, S.-N., Lee, H.-J., Kang, I., Kim, S.-S., Ha, J., 2004. AMP-activated protein kinase activity is required for vanadate-induced hypoxia-inducible factor 1 α expression in DU145 cells. *Carcinogenesis* 25, 2497–2507. doi:10.1093/carcin/bgh253
- Israel, C.W., Grönfeld, G., Ehrlich, J.R., Li, Y.-G., Hohnloser, S.H., 2004. Long-term risk of recurrent atrial fibrillation as documented by an implantable monitoring device. *Journal of the American College of Cardiology* 43, 47–52. doi:10.1016/j.jacc.2003.08.027
- Izumi, Y., Kim, S., Zhan, Y., Namba, M., Yasumoto, H., Iwao, H., 2000. Important Role of Angiotensin II-Mediated c-Jun NH2-Terminal Kinase Activation in Cardiac Hypertrophy in Hypertensive Rats. *Hypertension* 36, 511–516. doi:10.1161/01.HYP.36.4.511
- Jabbari, J., Olesen, M.S., Holst, A.G., Nielsen, J.B., Haunso, S., Svendsen, J.H., 2011. Common polymorphisms in KCNJ5 [corrected] are associated with early-onset lone atrial fibrillation in Caucasians. *Cardiology* 118, 116–120. doi:10.1159/000323840
- Jäger, S., Handschin, C., St-Pierre, J., Spiegelman, B.M., 2007. AMP-activated protein kinase (AMPK) action in skeletal muscle via direct phosphorylation of PGC-1 α . *Proc. Natl. Acad. Sci. U.S.A.* 104, 12017–12022. doi:10.1073/pnas.0705070104
- Jain, M., Jakubowski, A., Cui, L., Shi, J., Su, L., Bauer, M., Guan, J., Lim, C.C., Naito, Y., Thompson, J.S., Sam, F., Ambrose, C., Parr, M., Crowell, T., Lincecum, J.M., Wang, M.Z., Hsu, Y.-M., Zheng, T.S., Michaelson, J.S., Liao, R., Burkly, L.C., 2009. A Novel Role for Tumor Necrosis Factor-Like Weak Inducer of Apoptosis (TWEAK) in the Development of Cardiac Dysfunction and Failure. *Circulation* 119, 2058–2068. doi:10.1161/CIRCULATIONAHA.108.837286
- Jedsadayanmata, A., Chen, C.C., Kireeva, M.L., Lau, L.F., Lam, S.C., 1999. Activation-dependent adhesion of human platelets to Cyr61 and Fisp12/mouse connective tissue growth factor is mediated through integrin α (IIb) β (3). *J. Biol. Chem.* 274, 24321–24327.

- Jenninga, E.H., Gurnell, M., Kalkhoven, E., 2009. Functional implications of genetic variation in human PPARgamma. *Trends Endocrinol. Metab.* 20, 380–387. doi:10.1016/j.tem.2009.04.005
- Jones, D.P., 2006. Redefining oxidative stress. *Antioxid. Redox Signal.* 8, 1865–1879. doi:10.1089/ars.2006.8.1865
- Jones, D.P., 2008. Radical-free biology of oxidative stress. *Am. J. Physiol., Cell Physiol.* 295, C849–868. doi:10.1152/ajpcell.00283.2008
- Jugdutt, B.I., 2003. Remodeling of the myocardium and potential targets in the collagen degradation and synthesis pathways. *Curr Drug Targets Cardiovasc Haematol Disord* 3, 1–30.
- Kannel, W.B., Wolf, P.A., Benjamin, E.J., Levy, D., 1998. Prevalence, incidence, prognosis, and predisposing conditions for atrial fibrillation: population-based estimates. *Am. J. Cardiol.* 82, 2N–9N.
- Kathofer, S., Thomas, D., Karle, C.A., 2005. The novel antiarrhythmic drug dronedarone: comparison with amiodarone. *Cardiovasc Drug Rev* 23, 217–230.
- Kato, T., Yamashita, T., Sagara, K., Iinuma, H., Fu, L.-T., 2004. Progressive Nature of Paroxysmal Atrial Fibrillation. *Circulation Journal* 68, 568–572. doi:10.1253/circj.68.568
- Katsuoka, F., Motohashi, H., Ishii, T., Aburatani, H., Engel, J.D., Yamamoto, M., 2005. Genetic evidence that small maf proteins are essential for the activation of antioxidant response element-dependent genes. *Mol. Cell. Biol.* 25, 8044–8051. doi:10.1128/MCB.25.18.8044-8051.2005
- Kemp, T.J., Aggeli, I.-K., Sugden, P.H., Clerk, A., 2004. Phenylephrine and endothelin-1 upregulate connective tissue growth factor in neonatal rat cardiac myocytes. *J. Mol. Cell. Cardiol.* 37, 603–606. doi:10.1016/j.yjmcc.2004.04.022
- Kern, C.B., Wessels, A., McGarity, J., Dixon, L.J., Alston, E., Argraves, W.S., Geeting, D., Nelson, C.M., Menick, D.R., Apte, S.S., 2010. Reduced versican cleavage due to Adamts9 haploinsufficiency is associated with cardiac and aortic anomalies. *Matrix Biol.* 29, 304–316. doi:10.1016/j.matbio.2010.01.005
- Kietzmann, T., Samoylenko, A., Immenschuh, S., 2003. Transcriptional regulation of heme oxygenase-1 gene expression by MAP kinases of the JNK and p38 pathways in primary cultures of rat hepatocytes. *J. Biol. Chem.* 278, 17927–17936. doi:10.1074/jbc.M203929200
- Kim, Y.H., Lim, D.S., Lee, J.H., Lim, D.-S., Shim, W.J., Ro, Y.M., Park, G.H., Becker, K.G., Cho-Chung, Y.S., Kim, M.-K., 2003. Gene expression profiling of oxidative stress on atrial fibrillation in humans. *Exp. Mol. Med.* 35, 336–349.
- Kim, Y.M., Kattach, H., Ratnatunga, C., Pillai, R., Channon, K.M., Casadei, B., 2008. Association of atrial nicotinamide adenine dinucleotide phosphate oxidase activity with the development of atrial fibrillation after cardiac surgery. *J. Am. Coll. Cardiol.* 51, 68–74. doi:10.1016/j.jacc.2007.07.085
- Kirchhof, P., Bax, J., Blomstrom-Lundquist, C., Calkins, H., Camm, A.J., Cappato, R., Cosio, F., Crijns, H., Diener, H.-C., Goette, A., Israel, C.W., Kuck, K.-H., Lip, G.Y.H., Nattel, S., Page, R.L., Ravens, U., Schotten, U., Steinbeck, G., Vardas, P., Waldo, A., Wegscheider, K., Willems, S., Breithardt, G., 2009. Early and comprehensive management of atrial fibrillation: executive summary of the proceedings from the 2nd AFNET-EHRA consensus conference “research perspectives in AF”. *European Heart Journal* 30, 2969–2980. doi:10.1093/eurheartj/ehp235
- Kiriakidis, S., Andreacos, E., Monaco, C., Foxwell, B., Feldmann, M., Paleolog, E., 2003. VEGF expression in human macrophages is NF-kappaB-dependent: studies using adenoviruses expressing the endogenous NF-kappaB inhibitor IkappaBalpha and a kinase-defective form of the IkappaB kinase 2. *J. Cell. Sci.* 116, 665–674.
- Kirkby, N.S., Hadoke, P.W.F., Bagnall, A.J., Webb, D.J., 2009. The endothelin system as a therapeutic target in cardiovascular disease: great expectations or bleak house?: Therapeutic targeting of the endothelin system. *British Journal of Pharmacology* 153, 1105–1119. doi:10.1038/sj.bjp.0707516

- Kiryu, M., Niwano, S., Niwano, H., Kishihara, J., Aoyama, Y., Fukaya, H., Masaki, Y., Izumi, T., 2012. Angiotensin II-mediated up-regulation of connective tissue growth factor promotes atrial tissue fibrosis in the canine atrial fibrillation model. *Europace: European pacing, arrhythmias, and cardiac electrophysiology: journal of the working groups on cardiac pacing, arrhythmias, and cardiac cellular electrophysiology of the European Society of Cardiology*. doi:10.1093/europace/eus052
- Klingel, K., Wärntges, S., Bock, J., Wagner, C.A., Sauter, M., Waldegger, S., Kandolf, R., Lang, F., 2000. Expression of cell volume-regulated kinase h-sgk in pancreatic tissue. *American Journal of Physiology - Gastrointestinal and Liver Physiology* 279, G998–G1002.
- Knowles, J.R., 1980. Enzyme-catalyzed phosphoryl transfer reactions. *Annu. Rev. Biochem.* 49, 877–919. doi:10.1146/annurev.bi.49.070180.004305
- Ko, W.-C., Hong, C.-Y., Hou, S.-M., Lin, C.-H., Ong, E.-T., Lee, C.-F., Tsai, C.-T., Lai, L.-P., 2011. Elevated expression of connective tissue growth factor in human atrial fibrillation and angiotensin II-treated cardiomyocytes. *Circ. J.* 75, 1592–1600.
- Kochiadakis, G., 2002. Effect of acute atrial fibrillation on phasic coronary blood flow pattern and flow reserve in humans. *European Heart Journal* 23, 734–741. doi:10.1053/euhj.2001.2894
- Korantzopoulos, P., Kolettis, T.M., Galaris, D., Goudevenos, J.A., 2007. The role of oxidative stress in the pathogenesis and perpetuation of atrial fibrillation. *Int. J. Cardiol.* 115, 135–143. doi:10.1016/j.ijcard.2006.04.026
- Kostin, S., 2002. Structural correlate of atrial fibrillation in human patients. *Cardiovascular Research* 54, 361–379. doi:10.1016/S0008-6363(02)00273-0
- Kunsch, C., Medford, R.M., 1999. Oxidative stress as a regulator of gene expression in the vasculature. *Circ. Res.* 85, 753–766.
- Lai, L.P., Su, M.J., Lin, J.L., Lin, F.Y., Tsai, C.H., Chen, Y.S., Huang, S.K., Tseng, Y.Z., Lien, W.P., 1999. Down-regulation of L-type calcium channel and sarcoplasmic reticular Ca(2+)-ATPase mRNA in human atrial fibrillation without significant change in the mRNA of ryanodine receptor, calsequestrin and phospholamban: an insight into the mechanism of atrial electrical remodeling. *J. Am. Coll. Cardiol.* 33, 1231–1237.
- Lang, F., Böhmer, C., Palmada, M., Seeböhm, G., Strutz-Seeböhm, N., Vallon, V., 2006. (Patho)physiological significance of the serum- and glucocorticoid-inducible kinase isoforms. *Physiol. Rev* 86, 1151–1178. doi:10.1152/physrev.00050.2005
- Lang, F., Klingel, K., Wagner, C.A., Stegen, C., Warntges, S., Friedrich, B., Lanzendorfer, M., Melzig, J., Moschen, I., Steuer, S., Waldegger, S., Sauter, M., Paulmichl, M., Gerke, V., Risler, T., Gamba, G., Capasso, G., Kandolf, R., Hebert, S.C., Massry, S.G., Broer, S., 2000. Deranged transcriptional regulation of cell-volume-sensitive kinase hSGK in diabetic nephropathy. *Proceedings of the National Academy of Sciences* 97, 8157–8162. doi:10.1073/pnas.97.14.8157
- Lau, Y.-F., Yiu, K.-H., Siu, C.-W., Tse, H.-F., 2012. Hypertension and atrial fibrillation: epidemiology, pathophysiology and therapeutic implications. *J Hum Hypertens* 26, 563–569. doi:10.1038/jhh.2011.105
- Lavall, D., Selzer, C., Schuster, P., Lenski, M., Adam, O., Schaefers, H.-J., Boehm, M., Laufs, U., 2014. The mineralocorticoid receptor promotes fibrotic remodeling in atrial fibrillation. *Journal of Biological Chemistry*. doi:10.1074/jbc.M113.519256
- Lawrence, D.M.P., Seth, P., Durham, L., Diaz, F., Boursiquot, R., Ransohoff, R.M., Major, E.O., 2006. Astrocyte differentiation selectively upregulates CCL2/monocyte chemoattractant protein-1 in cultured human brain-derived progenitor cells. *Glia* 53, 81–91. doi:10.1002/glia.20261
- Leask, A., Abraham, D.J., 2003. The role of connective tissue growth factor, a multifunctional matricellular protein, in fibroblast biology. *Biochemistry and Cell Biology* 81, 355–363. doi:10.1139/o03-069
- Lee, J.S., Kahlon, S.S., Culbreth, R., Cooper, A.D., Jr, 1999. Modulation of monocyte chemokine production and nuclear factor kappa B activity by oxidants. *J. Interferon Cytokine Res.* 19, 761–767. doi:10.1089/107999099313613

- Lee, M., Hwang, J.-T., Yun, H., Kim, E.J., Kim, M.-J., Kim, S.-S., Ha, J., 2006. Critical roles of AMP-activated protein kinase in the carcinogenic metal-induced expression of VEGF and HIF-1 proteins in DU145 prostate carcinoma. *Biochem. Pharmacol.* 72, 91–103. doi:10.1016/j.bcp.2006.03.021
- Leong, M.L.L., 2002. Expression of the Serum- and Glucocorticoid-inducible Protein Kinase, Sgk, Is a Cell Survival Response to Multiple Types of Environmental Stress Stimuli in Mammary Epithelial Cells. *Journal of Biological Chemistry* 278, 5871–5882. doi:10.1074/jbc.M211649200
- Li, D., Fareh, S., Leung, T.K., Nattel, S., 1999. Promotion of atrial fibrillation by heart failure in dogs: atrial remodeling of a different sort. *Circulation* 100, 87–95.
- Li, D., Shinagawa, K., Pang, L., Leung, T.K., Cardin, S., Wang, Z., Nattel, S., 2001. Effects of angiotensin-converting enzyme inhibition on the development of the atrial fibrillation substrate in dogs with ventricular tachypacing-induced congestive heart failure. *Circulation* 104, 2608–2614.
- Li, H., Mittal, A., Paul, P.K., Kumar, M., Srivastava, D.S., Tyagi, S.C., Kumar, A., 2009. Tumor necrosis factor-related weak inducer of apoptosis augments matrix metalloproteinase 9 (MMP-9) production in skeletal muscle through the activation of nuclear factor-kappaB-inducing kinase and p38 mitogen-activated protein kinase: a potential role of MMP-9 in myopathy. *J. Biol. Chem.* 284, 4439–4450. doi:10.1074/jbc.M805546200
- Lie, J.T., Hammond, P.I., 1988. Pathology of the senescent heart: anatomic observations on 237 autopsy studies of patients 90 to 105 years old. *Mayo Clin. Proc.* 63, 552–564.
- Lin, C.-S., Lai, L.-P., Lin, J.-L., Sun, Y.-L., Hsu, C.-W., Chen, C.-L., Mao, S.J.T., Huang, S.K.S., 2007. Increased expression of extracellular matrix proteins in rapid atrial pacing-induced atrial fibrillation. *Heart Rhythm* 4, 938–949. doi:10.1016/j.hrthm.2007.03.034
- Liu, M., Liu, H., Dudley, S.C., 2010. Reactive Oxygen Species Originating From Mitochondria Regulate the Cardiac Sodium Channel. *Circulation Research* 107, 967–974. doi:10.1161/CIRCRESAHA.110.220673
- Löbe, S., Salmáš, J., John, S., Kornej, J., Husser, D., Hindricks, G., Bollmann, A., 2013. Usefulness of Dronedarone in Patients With Atrial Arrhythmias. *Am. J. Cardiol.* doi:10.1016/j.amjcard.2012.12.057
- Lu, Z., Xu, X., Hu, X., Fassett, J., Zhu, G., Tao, Y., Li, J., Huang, Y., Zhang, P., Zhao, B., Chen, Y., 2010. PGC-1 alpha regulates expression of myocardial mitochondrial antioxidants and myocardial oxidative stress after chronic systolic overload. *Antioxid. Redox Signal.* 13, 1011–1022. doi:10.1089/ars.2009.2940
- Luo, M.H., Li, Y.S., Yang, K.P., 2007. Fibrosis of collagen I and remodeling of connexin 43 in atrial myocardium of patients with atrial fibrillation. *Cardiology* 107, 248–253. doi:10.1159/000095501
- Mace, L.C., Yermalitskaya, L.V., Yi, Y., Yang, Z., Morgan, A.M., Murray, K.T., 2009. Transcriptional remodeling of rapidly stimulated HL-1 atrial myocytes exhibits concordance with human atrial fibrillation. *J. Mol. Cell. Cardiol.* 47, 485–492. doi:10.1016/j.yjmcc.2009.07.006
- Maixent, J.-M., Duran, M.-J., Pierre, S., Sennoune, S., Robert, K., Bernard, M., Lévy, S., 2002. Remodeling of Na,K-ATPase, and membrane fluidity after atrial fibrillation in sheep. *J. Recept. Signal Transduct. Res.* 22, 201–211. doi:10.1081/RRS-120014596
- Malishevskii, M.V., 2012. [Irbesartan in clinical practice]. *Kardiologiya* 52, 66–74.
- Malmqvist, K., Kahan, T., Edner, M., Bergfeldt, L., 2007. Cardiac repolarization and its relation to ventricular geometry and rate in reverse remodelling during antihypertensive therapy with irbesartan or atenolol: results from the SILVHIA study. *Journal of Human Hypertension* 21, 956–965. doi:10.1038/sj.jhh.1002250
- Manabe, I., Shindo, T., Nagai, R., 2002. Gene Expression in Fibroblasts and Fibrosis: Involvement in Cardiac Hypertrophy. *Circulation Research* 91, 1103–1113. doi:10.1161/01.RES.0000046452.67724.B8
- Marsin, A.-S., Bouzin, C., Bertrand, L., Hue, L., 2002. The stimulation of glycolysis by hypoxia in activated monocytes is mediated by AMP-activated protein kinase and

- inducible 6-phosphofructo-2-kinase. *J. Biol. Chem.* 277, 30778–30783. doi:10.1074/jbc.M205213200
- Martin, D., Galisteo, R., Gutkind, J.S., 2009. CXCL8/IL8 stimulates vascular endothelial growth factor (VEGF) expression and the autocrine activation of VEGFR2 in endothelial cells by activating NFkappaB through the CBM (Carma3/Bcl10/Malt1) complex. *J. Biol. Chem.* 284, 6038–6042. doi:10.1074/jbc.C800207200
- Martonosi, A.N., 1984. Mechanisms of Ca²⁺ release from sarcoplasmic reticulum of skeletal muscle. *Physiol. Rev.* 64, 1240–1320.
- Masson, S., Latini, R., Anand, I.S., Barlera, S., Judd, D., Salio, M., Perticone, F., Perini, G., Tognoni, G., Cohn, J.N., 2006. The Prognostic Value of Big Endothelin-1 in More Than 2,300 Patients With Heart Failure Enrolled in the Valsartan Heart Failure Trial (Val-HeFT). *Journal of Cardiac Failure* 12, 375–380. doi:10.1016/j.cardfail.2006.02.013
- Matsui, Y., Sadoshima, J., 2004. Rapid upregulation of CTGF in cardiac myocytes by hypertrophic stimuli: implication for cardiac fibrosis and hypertrophy. *J. Mol. Cell. Cardiol* 37, 477–481. doi:10.1016/j.yjmcc.2004.05.012
- Mayyas, F., Niebauer, M., Zurick, A., Barnard, J., Gillinov, A.M., Chung, M.K., Van Wagoner, D.R., 2010. Association of left atrial endothelin-1 with atrial rhythm, size, and fibrosis in patients with structural heart disease. *Circ Arrhythm Electrophysiol* 3, 369–379. doi:10.1161/CIRCEP.109.924985
- Mihm, M.J., Yu, F., Carnes, C.A., Reiser, P.J., McCarthy, P.M., Van Wagoner, D.R., Bauer, J.A., 2001. Impaired myofibrillar energetics and oxidative injury during human atrial fibrillation. *Circulation* 104, 174–180.
- Milne, G.L., Musiek, E.S., Morrow, J.D., 2005. F2-isoprostanes as markers of oxidative stress in vivo: an overview. *Biomarkers* 10 Suppl 1, S10–23. doi:10.1080/13547500500216546
- Milne, G.L., Sanchez, S.C., Musiek, E.S., Morrow, J.D., 2007. Quantification of F2-isoprostanes as a biomarker of oxidative stress. *Nat Protoc* 2, 221–226. doi:10.1038/nprot.2006.375
- Mittal, A., Bhatnagar, S., Kumar, A., Lach-Trifilieff, E., Wauters, S., Li, H., Makonchuk, D.Y., Glass, D.J., Kumar, A., 2010. The TWEAK-Fn14 system is a critical regulator of denervation-induced skeletal muscle atrophy in mice. *The Journal of Cell Biology* 188, 833–849. doi:10.1083/jcb.200909117
- Miyasaka, Y., 2005. Time Trends of Ischemic Stroke Incidence and Mortality in Patients Diagnosed With First Atrial Fibrillation in 1980 to 2000: Report of a Community-Based Study. *Stroke* 36, 2362–2366. doi:10.1161/01.STR.0000185927.63746.23
- Modesti, P.A., Vanni, S., Panicia, R., Perna, A., Maccherini, M., Lisi, G., Sani, G., Neri Serneri, G.G., 1999. Endothelin receptors in adult human and swine isolated ventricular cardiomyocytes. *Biochem. Pharmacol.* 58, 369–374.
- Moreno, I., 2003. Effects of Irbesartan on Cloned Potassium Channels Involved in Human Cardiac Repolarization. *Journal of Pharmacology and Experimental Therapeutics* 304, 862–873. doi:10.1124/jpet.102.042325
- Morillo, C.A., Klein, G.J., Jones, D.L., Guiraudon, C.M., 1995. Chronic Rapid Atrial Pacing□: Structural, Functional, and Electrophysiological Characteristics of a New Model of Sustained Atrial Fibrillation. *Circulation* 91, 1588–1595. doi:10.1161/01.CIR.91.5.1588
- Motte, S., McEntee, K., Naeije, R., 2006. Endothelin receptor antagonists. *Pharmacology & Therapeutics* 110, 386–414. doi:10.1016/j.pharmthera.2005.08.012
- Müller, D.N., Bohlender, J., Hilgers, K.F., Dragun, D., Costerousse, O., Ménard, J., Luft, F.C., 1997. Vascular angiotensin-converting enzyme expression regulates local angiotensin II. *Hypertension* 29, 98–104.
- Mungai, P.T., Waypa, G.B., Jairaman, A., Prakriya, M., Dokic, D., Ball, M.K., Schumacker, P.T., 2011. Hypoxia Triggers AMPK Activation through Reactive Oxygen Species-Mediated Activation of Calcium Release-Activated Calcium Channels. *Molecular and Cellular Biology* 31, 3531–3545. doi:10.1128/MCB.05124-11

- Munoz-Garcia, B., Martin-Ventura, J.L., Martinez, E., Sanchez, S., Hernandez, G., Ortega, L., Ortiz, A., Egido, J., Blanco-Colio, L.M., 2006. Fn14 Is Upregulated in Cytokine-Stimulated Vascular Smooth Muscle Cells and Is Expressed in Human Carotid Atherosclerotic Plaques: Modulation by Atorvastatin. *Stroke* 37, 2044–2053. doi:10.1161/01.STR.0000230648.00027.00
- Mustonen, E., Säkkinen, H., Tokola, H., Isopoussu, E., Aro, J., Leskinen, H., Ruskoaho, H., Rysä, J., 2010. Tumour necrosis factor-like weak inducer of apoptosis (TWEAK) and its receptor Fn14 during cardiac remodelling in rats. *Acta Physiologica* 199, 11–22. doi:10.1111/j.1748-1716.2010.02080.x
- Nabauer, M., Gerth, A., Limbourg, T., Schneider, S., Oeff, M., Kirchhof, P., Goette, A., Lewalter, T., Ravens, U., Meinertz, T., Breithardt, G., Steinbeck, G., 2008. The Registry of the German Competence NETwork on Atrial Fibrillation: patient characteristics and initial management. *Europace* 11, 423–434. doi:10.1093/europace/eun369
- Nattel, S., 1998. Experimental evidence for proarrhythmic mechanisms of antiarrhythmic drugs. *Cardiovasc. Res.* 37, 567–577.
- Nattel, S., 2002. New ideas about atrial fibrillation 50 years on. *Nature* 415, 219–226. doi:10.1038/415219a
- Nattel, S., 2004. Defining “culprit mechanisms” in arrhythmogenic cardiac remodeling. *Circ. Res.* 94, 1403–1405. doi:10.1161/01.RES.0000133229.19586.bb
- Nattel, S., Burstein, B., Dobrev, D., 2008. Atrial remodeling and atrial fibrillation: mechanisms and implications. *Circ Arrhythm Electrophysiol* 1, 62–73. doi:10.1161/CIRCEP.107.754564
- Nattel, S., Carlsson, L., 2006. Innovative approaches to anti-arrhythmic drug therapy. *Nature Reviews Drug Discovery* 5, 1034–1049. doi:10.1038/nrd2112
- Nerbonne, J.M., Kass, R.S., 2005. Molecular physiology of cardiac repolarization. *Physiol. Rev.* 85, 1205–1253. doi:10.1152/physrev.00002.2005
- Neubauer, S., Newell, J.B., Ingwall, J.S., 1992. Metabolic consequences and predictability of ventricular fibrillation in hypoxia. A ³¹P- and ²³Na-nuclear magnetic resonance study of the isolated rat heart. *Circulation* 86, 302–310. doi:10.1161/01.CIR.86.1.302
- Nieuwlaet, R., 2005. Atrial fibrillation management: a prospective survey in ESC Member Countries: The Euro Heart Survey on Atrial Fibrillation. *European Heart Journal* 26, 2422–2434. doi:10.1093/eurheartj/ehi505
- Nieuwlaet, R., Prins, M.H., Le Heuzey, J.-Y., Vardas, P.E., Aliot, E., Santini, M., Cobbe, S.M., Widdershoven, J.W.M.G., Baur, L.H., Levy, S., Crijns, H.J.G.M., 2008. Prognosis, disease progression, and treatment of atrial fibrillation patients during 1 year: follow-up of the Euro Heart Survey on Atrial Fibrillation. *European Heart Journal* 29, 1181–1189. doi:10.1093/eurheartj/ehn139
- Nishida, K., Qi, X.Y., Wakili, R., Comtois, P., Chartier, D., Harada, M., Iwasaki, Y., Romeo, P., Maguy, A., Dobrev, D., Michael, G., Talajic, M., Nattel, S., 2011. Mechanisms of atrial tachyarrhythmias associated with coronary artery occlusion in a chronic canine model. *Circulation* 123, 137–146. doi:10.1161/CIRCULATIONAHA.110.972778
- Ohtani, K., Yutani, C., Nagata, S., Koretsune, Y., Hori, M., Kamada, T., 1995. High prevalence of atrial fibrosis in patients with dilated cardiomyopathy. *J. Am. Coll. Cardiol.* 25, 1162–1169.
- Olesen, M.S., Jespersen, T., Nielsen, J.B., Liang, B., Møller, D.V., Hedley, P., Christiansen, M., Varró, A., Olesen, S.-P., Haunsø, S., Schmitt, N., Svendsen, J.H., 2011. Mutations in sodium channel β -subunit SCN3B are associated with early-onset lone atrial fibrillation. *Cardiovascular Research* 89, 786–793. doi:10.1093/cvr/cvq348
- Ouchi, N., Shibata, R., Walsh, K., 2005. AMP-activated protein kinase signaling stimulates VEGF expression and angiogenesis in skeletal muscle. *Circ. Res.* 96, 838–846. doi:10.1161/01.RES.0000163633.10240.3b
- Panek, A.N., Posch, M.G., Alenina, N., Ghadge, S.K., Erdmann, B., Popova, E., Perrot, A., Geier, C., Dietz, R., Morano, R.D.I., Morano, I., Bader, M., Ozcelik, C., 2009. Connective tissue growth factor overexpression in cardiomyocytes promotes cardiac

- hypertrophy and protection against pressure overload. *PLoS ONE* 4, e6743. doi:10.1371/journal.pone.0006743
- Patterson, E., Jackman, W.M., Beckman, K.J., Lazzara, R., Lockwood, D., Scherlag, B.J., Wu, R., Po, S., 2007. Spontaneous Pulmonary Vein Firing in Man: Relationship to Tachycardia-Pause Early Afterdepolarizations and Triggered Arrhythmia in Canine Pulmonary Veins In Vitro. *Journal of Cardiovascular Electrophysiology* 18, 1067–1075. doi:10.1111/j.1540-8167.2007.00909.x
- Paul, M., Poyan Mehr, A., Kreutz, R., 2006. Physiology of local renin-angiotensin systems. *Physiol. Rev.* 86, 747–803. doi:10.1152/physrev.00036.2005
- Pauschinger, M., Knopf, D., Petschauer, S., Doerner, A., Poller, W., Schwimmbeck, P.L., Kuhl, U., Schultheiss, H.-P., 1999. Dilated Cardiomyopathy Is Associated With Significant Changes in Collagen Type I/III ratio. *Circulation* 99, 2750–2756. doi:10.1161/01.CIR.99.21.2750
- Pham, T.D., Fenoglio, J.J., Jr, 1982. Right atrial ultrastructural in chronic rheumatic heart disease. *Int. J. Cardiol.* 1, 289–304.
- Pierce, G.L., Lesniewski, L.A., Lawson, B.R., Beske, S.D., Seals, D.R., 2009. Nuclear factor- κ B activation contributes to vascular endothelial dysfunction via oxidative stress in overweight/obese middle-aged and older humans. *Circulation* 119, 1284–1292. doi:10.1161/CIRCULATIONAHA.108.804294
- Powell, D.W., Mifflin, R.C., Valentich, J.D., Crowe, S.E., Saada, J.I., West, A.B., 1999. Myofibroblasts. I. Paracrine cells important in health and disease. *Am. J. Physiol.* 277, C1–9.
- Proteases in tissue remodelling of lung and heart, 2003. , *Proteases in biology and disease.* Kluwer Academic/Plenum Publishers, New York.
- Qu, Y.-C., Du, Y.-M., Wu, S.-L., Chen, Q.-X., Wu, H.-L., Zhou, S.-F., 2009. Activated nuclear factor-kappaB and increased tumor necrosis factor-alpha in atrial tissue of atrial fibrillation. *Scand. Cardiovasc. J.* 43, 292–297. doi:10.1080/14017430802651803
- Rahman, I., 2003. Oxidative stress, chromatin remodeling and gene transcription in inflammation and chronic lung diseases. *J. Biochem. Mol. Biol.* 36, 95–109.
- Range, F.T., Schäfers, M., Acil, T., Schäfers, K.P., Kies, P., Paul, M., Hermann, S., Brisse, B., Breithardt, G., Schober, O., Wichter, T., 2007. Impaired myocardial perfusion and perfusion reserve associated with increased coronary resistance in persistent idiopathic atrial fibrillation. *Eur. Heart J.* 28, 2223–2230. doi:10.1093/eurheartj/ehm246
- Recchia, A.G., Filice, E., Pellegrino, D., Dobrina, A., Cerra, M.C., Maggiolini, M., 2009. Endothelin-1 induces connective tissue growth factor expression in cardiomyocytes. *J. Mol. Cell. Cardiol* 46, 352–359. doi:10.1016/j.yjmcc.2008.11.017
- Reil, J.-C., Hohl, M., Selejan, S., Lipp, P., Drautz, F., Kazakow, A., Münz, B.M., Müller, P., Steendijk, P., Reil, G.-H., Allessie, M.A., Böhm, M., Neuberger, H.-R., 2012. Aldosterone promotes atrial fibrillation. *Eur. Heart J.* 33, 2098–2108. doi:10.1093/eurheartj/ehr266
- Reilly, S.N., Jayaram, R., Nahar, K., Antoniadis, C., Verheule, S., Channon, K.M., Alp, N.J., Schotten, U., Casadei, B., 2011. Atrial sources of reactive oxygen species vary with the duration and substrate of atrial fibrillation: implications for the antiarrhythmic effect of statins. *Circulation* 124, 1107–1117. doi:10.1161/CIRCULATIONAHA.111.029223
- Robey, R.B., Hay, N., 2006. Mitochondrial hexokinases, novel mediators of the antiapoptotic effects of growth factors and Akt. *Oncogene* 25, 4683–4696. doi:10.1038/sj.onc.1209595
- Rodriguez-Vita, J., Ruiz-Ortega, M., Rupérez, M., Esteban, V., Sanchez-López, E., Plaza, J.J., Egido, J., 2005. Endothelin-1, via ETA receptor and independently of transforming growth factor-beta, increases the connective tissue growth factor in vascular smooth muscle cells. *Circ. Res.* 97, 125–134. doi:10.1161/01.RES.0000174614.74469.83
- Rosenkranz, S., 2004. TGF-beta1 and angiotensin networking in cardiac remodeling. *Cardiovasc. Res.* 63, 423–432. doi:10.1016/j.cardiores.2004.04.030

- Rostock, T., Steven, D., Lutomsky, B., Servatius, H., Drewitz, I., Klemm, H., Müllerleile, K., Ventura, R., Meinertz, T., Willems, S., 2008. Atrial fibrillation begets atrial fibrillation in the pulmonary veins on the impact of atrial fibrillation on the electrophysiological properties of the pulmonary veins in humans. *J. Am. Coll. Cardiol.* 51, 2153–2160. doi:10.1016/j.jacc.2008.02.059
- Rubart, M., Field, L.J., 2006. CARDIAC REGENERATION: Repopulating the Heart. *Annual Review of Physiology* 68, 29–49. doi:10.1146/annurev.physiol.68.040104.124530
- Ruderman, N., Prentki, M., 2004. AMP kinase and malonyl-CoA: targets for therapy of the metabolic syndrome. *Nat Rev Drug Discov* 3, 340–351. doi:10.1038/nrd1344
- Rupérez, M., Ruiz-Ortega, M., Esteban, V., Lorenzo, O., Mezzano, S., Plaza, J.J., Egido, J., 2003. Angiotensin II increases connective tissue growth factor in the kidney. *Am. J. Pathol.* 163, 1937–1947. doi:10.1016/S0002-9440(10)63552-3
- Saitoh, T., Nakayama, M., Nakano, H., Yagita, H., Yamamoto, N., Yamaoka, S., 2003. TWEAK induces NF-kappaB2 p100 processing and long lasting NF-kappaB activation. *J. Biol. Chem.* 278, 36005–36012. doi:10.1074/jbc.M304266200
- Sanfilippo, A.J., Abascal, V.M., Sheehan, M., Oertel, L.B., Harrigan, P., Hughes, R.A., Weyman, A.E., 1990. Atrial enlargement as a consequence of atrial fibrillation. A prospective echocardiographic study. *Circulation* 82, 792–797.
- Sano, Y., Harada, J., Tashiro, S., Gotoh-Mandeville, R., Maekawa, T., Ishii, S., 1999. ATF-2 is a common nuclear target of Smad and TAK1 pathways in transforming growth factor-beta signaling. *J. Biol. Chem.* 274, 8949–8957.
- Sayre, L.M., Smith, M.A., Perry, G., 2001. Chemistry and biochemistry of oxidative stress in neurodegenerative disease. *Curr. Med. Chem.* 8, 721–738.
- Schafer, F.Q., Buettner, G.R., 2001. Redox environment of the cell as viewed through the redox state of the glutathione disulfide/glutathione couple. *Free Radic. Biol. Med.* 30, 1191–1212.
- Schlöndorff, J., Blobel, C.P., 1999. Metalloprotease-disintegrins: modular proteins capable of promoting cell-cell interactions and triggering signals by protein-ectodomain shedding. *J. Cell. Sci.* 112 (Pt 21), 3603–3617.
- Schotten, U., Ausma, J., Stellbrink, C., Sabatschus, I., Vogel, M., Frechen, D., Schoendube, F., Hanrath, P., Allessie, M.A., 2001. Cellular mechanisms of depressed atrial contractility in patients with chronic atrial fibrillation. *Circulation* 103, 691–698.
- Schotten, U., de Haan, S., Neuberger, H.-R., Eijsbouts, S., Blaauw, Y., Tieleman, R., Allessie, M., 2004. Loss of atrial contractility is primary cause of atrial dilatation during first days of atrial fibrillation. *Am. J. Physiol. Heart Circ. Physiol.* 287, H2324–H2331. doi:10.1152/ajpheart.00581.2004
- Schotten, U., Verheule, S., Kirchhof, P., Goette, A., 2011. Pathophysiological mechanisms of atrial fibrillation: a translational appraisal. *Physiol. Rev.* 91, 265–325. doi:10.1152/physrev.00031.2009
- Schreck, R., Albermann, K., Baeuerle, P.A., 1992. Nuclear factor kappa B: an oxidative stress-responsive transcription factor of eukaryotic cells (a review). *Free Radic. Res. Commun.* 17, 221–237.
- Schroeder, A., Mueller, O., Stocker, S., Salowsky, R., Leiber, M., Gassmann, M., Lightfoot, S., Menzel, W., Granzow, M., Ragg, T., 2006. The RIN: an RNA integrity number for assigning integrity values to RNA measurements. *BMC Mol. Biol.* 7, 3. doi:10.1186/1471-2199-7-3
- Schultz, J.E.J., Witt, S.A., Glascock, B.J., Nieman, M.L., Reiser, P.J., Nix, S.L., Kimball, T.R., Doetschman, T., 2002. TGF-beta1 mediates the hypertrophic cardiomyocyte growth induced by angiotensin II. *J. Clin. Invest.* 109, 787–796. doi:10.1172/JCI14190
- Schultz, J.E.J., Witt, S.A., Glascock, B.J., Nieman, M.L., Reiser, P.J., Nix, S.L., Kimball, T.R., Doetschman, T., 2002. TGF-β1 mediates the hypertrophic cardiomyocyte growth induced by angiotensin II. *Journal of Clinical Investigation* 109, 787–796. doi:10.1172/JCI14190
- Seppet, E., Eimre, M., Peet, N., Paju, K., Orlova, E., Ress, M., Kõvask, S., Piirsoo, A., Saks, V.A., Gellerich, F.N., Zierz, S., Seppet, E.K., 2005. Compartmentation of energy

- metabolism in atrial myocardium of patients undergoing cardiac surgery. *Mol. Cell. Biochem.* 270, 49–61.
- Shaw, R.M., Rudy, Y., 1997. Ionic mechanisms of propagation in cardiac tissue. Roles of the sodium and L-type calcium currents during reduced excitability and decreased gap junction coupling. *Circ. Res.* 81, 727–741.
- Shi, Y., 2001. Remodeling of atrial dimensions and emptying function in canine models of atrial fibrillation. *Cardiovascular Research* 52, 217–225. doi:10.1016/S0008-6363(01)00377-7
- Shimo, T., Nakanishi, T., Nishida, T., Asano, M., Kanyama, M., Kuboki, T., Tamatani, T., Tezuka, K., Takemura, M., Matsumura, T., Takigawa, M., 1999. Connective tissue growth factor induces the proliferation, migration, and tube formation of vascular endothelial cells in vitro, and angiogenesis in vivo. *J. Biochem.* 126, 137–145.
- Shiraishi, I., Takamatsu, T., Minamikawa, T., Fujita, S., 1992. 3-D observation of actin filaments during cardiac myofibrinogenesis in chick embryo using a confocal laser scanning microscope. *Anat. Embryol.* 185, 401–408.
- Shiraishi, I., Takamatsu, T., Minamikawa, T., Onouchi, Z., Fujita, S., 1992. Quantitative histological analysis of the human sinoatrial node during growth and aging. *Circulation* 85, 2176–2184. doi:10.1161/01.CIR.85.6.2176
- Shoag, J., Arany, Z., 2010. Regulation of hypoxia-inducible genes by PGC-1 alpha. *Arterioscler. Thromb. Vasc. Biol.* 30, 662–666. doi:10.1161/ATVBAHA.108.181636
- Shukla, N., Maher, J., Masters, J., Angelini, G.D., Jeremy, J.Y., 2006. Does oxidative stress change ceruloplasmin from a protective to a vasculopathic factor? *Atherosclerosis* 187, 238–250. doi:10.1016/j.atherosclerosis.2005.11.035
- Sinner, M.F., Ellinor, P.T., Meitinger, T., Benjamin, E.J., Kääb, S., 2011. Genome-wide association studies of atrial fibrillation: past, present, and future. *Cardiovascular Research* 89, 701–709. doi:10.1093/cvr/cvr001
- Sinner, M.F., Pfeufer, A., Akyol, M., Beckmann, B.-M., Hinterseer, M., Wacker, A., Perz, S., Sauter, W., Illig, T., Näbauer, M., Schmitt, C., Wichmann, H.-E., Schömig, A., Steinbeck, G., Meitinger, T., Kääb, S., 2008. The non-synonymous coding IKr-channel variant KCNH2-K897T is associated with atrial fibrillation: results from a systematic candidate gene-based analysis of KCNH2 (HERG). *Eur. Heart J.* 29, 907–914. doi:10.1093/eurheartj/ehm619
- Skyschally, A., Heusch, G., 2011. Reduction of myocardial infarct size by dronedarone in pigs--a pleiotropic action? *Cardiovasc Drugs Ther* 25, 197–201. doi:10.1007/s10557-011-6300-1
- Song, Z.-P., Liu, X., Zhang, D.-D., 2014. Connective Tissue Growth Factor: A Predictor of Recurrence after Catheter Ablation in Patients with Nonparoxysmal Atrial Fibrillation: CTGF PREDICTS AF RECURRENCE. *Pacing and Clinical Electrophysiology* n/a–n/a. doi:10.1111/pace.12345
- Songu-Mize, E., Sevieux, N., Liu, X., Jacobs, M., 2001. Effect of short-term cyclic stretch on sodium pump activity in aortic smooth muscle cells. *Am. J. Physiol. Heart Circ. Physiol.* 281, H2072–2078.
- Soubrier, F., Wei, L., Hubert, C., Clauser, E., Alhenc-Gelas, F., Corvol, P., 1993. Molecular biology of the angiotensin I converting enzyme: II. Structure-function. Gene polymorphism and clinical implications. *J. Hypertens.* 11, 599–604.
- Spach, M.S., Boineau, J.P., 1997. Microfibrosis produces electrical load variations due to loss of side-to-side cell connections: a major mechanism of structural heart disease arrhythmias. *Pacing Clin Electrophysiol* 20, 397–413.
- Spach, M.S., Heidlage, J.F., Barr, R.C., Dolber, P.C., 2004. Cell size and communication: role in structural and electrical development and remodeling of the heart. *Heart Rhythm* 1, 500–515. doi:10.1016/j.hrthm.2004.06.010
- Spach, M.S., Heidlage, J.F., Dolber, P.C., Barr, R.C., 2007. Mechanism of origin of conduction disturbances in aging human atrial bundles: experimental and model study. *Heart Rhythm* 4, 175–185. doi:10.1016/j.hrthm.2006.10.023
- Steinberg, G.R., Kemp, B.E., 2009. AMPK in Health and Disease. *Physiol. Rev.* 89, 1025–1078. doi:10.1152/physrev.00011.2008

- Stoner, L., Erickson, M.L., Young, J.M., Fryer, S., Sabatier, M.J., Faulkner, J., Lambrick, D.M., McCully, K.K., 2012. There's more to flow-mediated dilation than nitric oxide. *J. Atheroscler. Thromb.* 19, 589–600.
- Stoppani, J., Hildebrandt, A.L., Sakamoto, K., Cameron-Smith, D., Goodyear, L.J., Neufer, P.D., 2002. AMP-activated protein kinase activates transcription of the UCP3 and HKII genes in rat skeletal muscle. *Am. J. Physiol. Endocrinol. Metab.* 283, E1239–1248. doi:10.1152/ajpendo.00278.2002
- Storey, K.B., 2003. Mammalian hibernation. Transcriptional and translational controls. *Adv. Exp. Med. Biol.* 543, 21–38.
- Suga, H., 1990. Ventricular energetics. *Physiol. Rev.* 70, 247–277.
- Sugden, P.H., 2003. An overview of endothelin signaling in the cardiac myocyte. *J. Mol. Cell. Cardiol.* 35, 871–886.
- Sugden, P.H., Clerk, A., 1997. Regulation of the ERK subgroup of MAP kinase cascades through G protein-coupled receptors. *Cell. Signal.* 9, 337–351.
- Sugden, P.H., Clerk, A., 1998. "Stress-responsive" mitogen-activated protein kinases (c-Jun N-terminal kinases and p38 mitogen-activated protein kinases) in the myocardium. *Circ. Res.* 83, 345–352.
- Sulciner, D.J., Irani, K., Yu, Z.X., Ferrans, V.J., Goldschmidt-Clermont, P., Finkel, T., 1996. rac1 regulates a cytokine-stimulated, redox-dependent pathway necessary for NF-kappaB activation. *Mol. Cell. Biol.* 16, 7115–7121.
- Sun, Y., 2000. Infarct scar: a dynamic tissue. *Cardiovascular Research* 46, 250–256. doi:10.1016/S0008-6363(00)00032-8
- Suvorova, E.S., Lucas, O., Weisend, C.M., Rollins, M.F., Merrill, G.F., Capecchi, M.R., Schmidt, E.E., 2009. Cytoprotective Nrf2 pathway is induced in chronically txnrd 1-deficient hepatocytes. *PLoS ONE* 4, e6158. doi:10.1371/journal.pone.0006158
- Suwa, M., Nakano, H., Kumagai, S., 2003. Effects of chronic AICAR treatment on fiber composition, enzyme activity, UCP3, and PGC-1 in rat muscles. *J. Appl. Physiol.* 95, 960–968. doi:10.1152/jappphysiol.00349.2003
- Swynghedauw, B., 1999. Molecular mechanisms of myocardial remodeling. *Physiol. Rev.* 79, 215–262.
- Takaoka, H., Funabashi, N., Takahashi, M., Uchimura, Y., Sairaku, A., Kobayashi, Y., 2013. Left-atrial wall thickening may be an important-response in systemic hypertension as well as left-ventricular hypertrophy and more remarkable than left-ventricular diastolic dysfunction and left-atrial enlargement. *Int. J. Cardiol.* doi:10.1016/j.ijcard.2013.01.232
- Targher, G., Valbusa, F., Bonapace, S., Bertolini, L., Zenari, L., Rodella, S., Zoppini, G., Mantovani, W., Barbieri, E., Byrne, C.D., 2013. Non-alcoholic Fatty liver disease is associated with an increased incidence of atrial fibrillation in patients with type 2 diabetes. *PLoS ONE* 8, e57183. doi:10.1371/journal.pone.0057183
- Todd, D.M., 2004. Repetitive 4-Week Periods of Atrial Electrical Remodeling Promote Stability of Atrial Fibrillation: Time Course of a Second Factor Involved in the Self-Perpetuation of Atrial Fibrillation. *Circulation* 109, 1434–1439. doi:10.1161/01.CIR.0000124006.84596.D9
- Tomasek, J.J., Gabbiani, G., Hinz, B., Chaponnier, C., Brown, R.A., 2002. Myofibroblasts and mechano-regulation of connective tissue remodelling. *Nature Reviews Molecular Cell Biology* 3, 349–363. doi:10.1038/nrm809
- Tran, N.L., McDonough, W.S., Donohue, P.J., Winkles, J.A., Berens, T.J., Ross, K.R., Hoelzinger, D.B., Beaudry, C., Coons, S.W., Berens, M.E., 2003. The human Fn14 receptor gene is up-regulated in migrating glioma cells in vitro and overexpressed in advanced glial tumors. *Am. J. Pathol.* 162, 1313–1321. doi:10.1016/S0002-9440(10)63927-2
- Tran, N.L., McDonough, W.S., Savitch, B.A., Fortin, S.P., Winkles, J.A., Symons, M., Nakada, M., Cunliffe, H.E., Hostetter, G., Hoelzinger, D.B., Rennert, J.L., Michaelson, J.S., Burkly, L.C., Lipinski, C.A., Loftus, J.C., Mariani, L., Berens, M.E., 2006. Increased fibroblast growth factor-inducible 14 expression levels promote glioma cell

- invasion via Rac1 and nuclear factor-kappaB and correlate with poor patient outcome. *Cancer Res.* 66, 9535–9542. doi:10.1158/0008-5472.CAN-06-0418
- Tsai, C.-T., 2004. Renin-Angiotensin System Gene Polymorphisms and Atrial Fibrillation. *Circulation* 109, 1640–1646. doi:10.1161/01.CIR.0000124487.36586.26
- Tsai, C.-T., Chiang, F.-T., Chen, W.-P., Hwang, J.-J., Tseng, C.-D., Wu, C.-K., Yu, C.-C., Wang, Y.-C., Lai, L.-P., Lin, J.-L., 2011a. Angiotensin II induces complex fractionated electrogram in a cultured atrial myocyte monolayer mediated by calcium and sodium-calcium exchanger. *Cell Calcium* 49, 1–11. doi:10.1016/j.ceca.2010.10.005
- Tsai, C.-T., Lai, L.-P., Hwang, J.-J., Chen, W.-P., Chiang, F.-T., Hsu, K.-L., Tseng, C.-D., Tseng, Y.-Z., Lin, J.-L., 2008a. Renin-angiotensin system component expression in the HL-1 atrial cell line and in a pig model of atrial fibrillation. *J. Hypertens.* 26, 570–582. doi:10.1097/HJH.0b013e3282f34a4a
- Tsai, C.-T., Lai, L.-P., Kuo, K.-T., Hwang, J.-J., Hsieh, C.-S., Hsu, K.-L., Tseng, C.-D., Tseng, Y.-Z., Chiang, F.-T., Lin, J.-L., 2008b. Angiotensin II activates signal transducer and activators of transcription 3 via Rac1 in atrial myocytes and fibroblasts: implication for the therapeutic effect of statin in atrial structural remodeling. *Circulation* 117, 344–355. doi:10.1161/CIRCULATIONAHA.107.695346
- Tsai, C.-T., Tseng, C.-D., Hwang, J.-J., Wu, C.-K., Yu, C.-C., Wang, Y.-C., Chen, W.-P., Lai, L.-P., Chiang, F.-T., Lin, J.-L., 2011b. Tachycardia of atrial myocytes induces collagen expression in atrial fibroblasts through transforming growth factor β 1. *Cardiovascular Research* 89, 805–815. doi:10.1093/cvr/cvq322
- Tsuboi, M., Hisatome, I., Morisaki, T., Tanaka, M., Tomikura, Y., Takeda, S., Shimoyama, M., Ohtahara, A., Ogino, K., Igawa, O., Shigemasa, C., Ohgi, S., Nanba, E., 2001. Mitochondrial DNA deletion associated with the reduction of adenine nucleotides in human atrium and atrial fibrillation. *Eur. J. Clin. Invest.* 31, 489–496.
- Tuinenburg, A.E., Van Veldhuisen, D.J., Boomsma, F., Van Den Berg, M.P., De Kam, P.J., Crijns, H.J.G., 1998. Comparison of Plasma Neurohormones in Congestive Heart Failure Patients With Atrial Fibrillation Versus Patients With Sinus Rhythm. *The American Journal of Cardiology* 81, 1207–1210. doi:10.1016/S0002-9149(98)00092-7
- Turpaev, K., Bouton, C., Diet, A., Glatigny, A., Drapier, J.-C., 2005. Analysis of differentially expressed genes in nitric oxide-exposed human monocytic cells. *Free Radical Biology and Medicine* 38, 1392–1400. doi:10.1016/j.freeradbiomed.2005.02.002
- Vallon, V., Wyatt, A.W., Klingel, K., Huang, D.Y., Hussain, A., Berchtold, S., Friedrich, B., Grahmmer, F., Belaiba, R.S., Görlach, A., Wulff, P., Daut, J., Dalton, N.D., Ross, J., Flögel, U., Schrader, J., Osswald, H., Kandolf, R., Kuhl, D., Lang, F., 2006. SGK1-dependent cardiac CTGF formation and fibrosis following DOCA treatment. *J. Mol. Med* 84, 396–404. doi:10.1007/s00109-005-0027-z
- Van Veen, T.A.B., van Rijen, H.V.M., Jongsma, H.J., 2006. Physiology of cardiovascular gap junctions. *Adv Cardiol* 42, 18–40. doi:10.1159/000092560
- Veenhuizen, G.D., Simpson, C.S., Abdollah, H., 2004. Atrial fibrillation. *CMAJ* 171, 755–760. doi:10.1503/cmaj.1031364
- Verheule, S., Sato, T., Everett, T., 4th, Engle, S.K., Otten, D., Rubart-von der Lohe, M., Nakajima, H.O., Nakajima, H., Field, L.J., Olgin, J.E., 2004. Increased vulnerability to atrial fibrillation in transgenic mice with selective atrial fibrosis caused by overexpression of TGF-beta1. *Circ. Res.* 94, 1458–1465. doi:10.1161/01.RES.0000129579.59664.9d
- Wakili, R., Voigt, N., Käb, S., Dobrev, D., Nattel, S., 2011. Recent advances in the molecular pathophysiology of atrial fibrillation. *Journal of Clinical Investigation* 121, 2955–2968. doi:10.1172/JCI46315
- Wang, H.D., Xu, S., Johns, D.G., Du, Y., Quinn, M.T., Cayatte, A.J., Cohen, R.A., 2001. Role of NADPH oxidase in the vascular hypertrophic and oxidative stress response to angiotensin II in mice. *Circ. Res.* 88, 947–953.
- Wang, Y., Yang, J., Yi, J., 2012. Redox sensing by proteins: oxidative modifications on cysteines and the consequent events. *Antioxid. Redox Signal.* 16, 649–657. doi:10.1089/ars.2011.4313

- Watanabe, T., Kawasaki, M., Tanaka, R., Ono, K., Nishigaki, K., Takemura, G., Arai, M., Noda, T., Watanabe, S., Minatoguchi, S., 2013. Association among blood pressure control in elderly patients with hypertension, left atrial structure and function and new-onset atrial fibrillation: a prospective 2-year study in 234 patients. *Hypertens. Res.* doi:10.1038/hr.2013.25
- Watson, T., Karthikeyan, V.J., Lip, G.Y.H., Beevers, D.G., 2009. Atrial fibrillation in primary aldosteronism. *J Renin Angiotensin Aldosterone Syst* 10, 190–194. doi:10.1177/1470320309342734
- Weber, K., 1994. Collagen Network of the Myocardium: Function, Structural Remodeling and Regulatory Mechanisms. *Journal of Molecular and Cellular Cardiology* 26, 279–292. doi:10.1006/jmcc.1994.1036
- Weber, K.T., Pick, R., Jalil, J.E., Janicki, J.S., Carroll, E.P., 1989. Patterns of myocardial fibrosis. *J. Mol. Cell. Cardiol.* 21 Suppl 5, 121–131.
- Wegener, F.T., Ehrlich, J.R., Hohnloser, S.H., 2006. Dronedarone: an emerging agent with rhythm- and rate-controlling effects. *J. Cardiovasc. Electrophysiol.* 17 Suppl 2, S17–20. doi:10.1111/j.1540-8167.2006.00583.x
- Welikovich, L., Lafreniere, G., Burggraf, G.W., Sanfilippo, A.J., 1994. Change in atrial volume following restoration of sinus rhythm in patients with atrial fibrillation: a prospective echocardiographic study. *Can J Cardiol* 10, 993–996.
- White, R.L., Wittenberg, B.A., 2000. Mitochondrial NAD(P)H, ADP, oxidative phosphorylation, and contraction in isolated heart cells. *Am. J. Physiol. Heart Circ. Physiol.* 279, H1849–1857.
- Wiegerinck, R.F., Verkerk, A.O., Belterman, C.N., van Veen, T.A.B., Baartscheer, A., Opthof, T., Wilders, R., de Bakker, J.M.T., Coronel, R., 2006. Larger cell size in rabbits with heart failure increases myocardial conduction velocity and QRS duration. *Circulation* 113, 806–813. doi:10.1161/CIRCULATIONAHA.105.565804
- Wiley, S.R., Cassiano, L., Lofton, T., Davis-Smith, T., Winkles, J.A., Lindner, V., Liu, H., Daniel, T.O., Smith, C.A., Fanslow, W.C., 2001. A Novel TNF Receptor Family Member Binds TWEAK and Is Implicated in Angiogenesis. *Immunity* 15, 837–846. doi:10.1016/S1074-7613(01)00232-1
- Willems, R., Sipido, K.R., Holemans, P., Ector, H., Van de Werf, F., Heidbüchel, H., 2001. Different patterns of angiotensin II and atrial natriuretic peptide secretion in a sheep model of atrial fibrillation. *J. Cardiovasc. Electrophysiol.* 12, 1387–1392.
- Winkles, J.A., 2008. The TWEAK-Fn14 cytokine-receptor axis: discovery, biology and therapeutic targeting. *Nat Rev Drug Discov* 7, 411–425. doi:10.1038/nrd2488
- Wolf, G., Aumann, N., Michalska, M., Bast, A., Sonnemann, J., Beck, J.F., Lendeckel, U., Newsholme, P., Walther, R., 2010. Peroxiredoxin III protects pancreatic β cells from apoptosis. *J. Endocrinol.* 207, 163–175. doi:10.1677/JOE-09-0455
- Wolf, S.C., Schultze, M., Risler, T., Rieg, T., Lang, F., Schulze-Osthoff, K., Brehm, B.R., 2006. Stimulation of serum- and glucocorticoid-regulated kinase-1 gene expression by endothelin-1. *Biochem. Pharmacol* 71, 1175–1183. doi:10.1016/j.bcp.2006.01.001
- Wong, C.M., Cheema, A.K., Zhang, L., Suzuki, Y.J., 2008. Protein Carbonylation as a Novel Mechanism in Redox Signaling. *Circulation Research* 102, 310–318. doi:10.1161/CIRCRESAHA.107.159814
- Wu, M.-L., Ho, Y.-C., Lin, C.-Y., Yet, S.-F., 2011. Heme oxygenase-1 in inflammation and cardiovascular disease. *Am J Cardiovasc Dis* 1, 150–158.
- Wu, Y.J., Pierre, D.P.L., Wu, J., Yee, A.J., Yang, B.B., 2005. The interaction of versican with its binding partners. *Cell Research* 15, 483–494. doi:10.1038/sj.cr.7290318
- Xiao, H.D., Fuchs, S., Campbell, D.J., Lewis, W., Dudley, S.C., Jr, Kasi, V.S., Hoit, B.D., Keshelava, G., Zhao, H., Capecchi, M.R., Bernstein, K.E., 2004. Mice with cardiac-restricted angiotensin-converting enzyme (ACE) have atrial enlargement, cardiac arrhythmia, and sudden death. *Am. J. Pathol.* 165, 1019–1032. doi:10.1016/S0002-9440(10)63363-9
- Xu, J., Cui, G., Esmailian, F., Plunkett, M., Marelli, D., Ardehali, A., Odum, J., Laks, H., Sen, L., 2004. Atrial extracellular matrix remodeling and the maintenance of atrial fibrillation. *Circulation* 109, 363–368. doi:10.1161/01.CIR.0000109495.02213.52

- Yanagisawa, M., Kurihara, H., Kimura, S., Tomobe, Y., Kobayashi, M., Mitsui, Y., Yazaki, Y., Goto, K., Masaki, T., 1988. A novel potent vasoconstrictor peptide produced by vascular endothelial cells. *Nature* 332, 411–415. doi:10.1038/332411a0
- Yano, M., Kim, S., Izumi, Y., Yamanaka, S., Iwao, H., 1998. Differential activation of cardiac c-jun amino-terminal kinase and extracellular signal-regulated kinase in angiotensin II-mediated hypertension. *Circ. Res.* 83, 752–760.
- Yue, L., Feng, J., Gaspo, R., Li, G.R., Wang, Z., Nattel, S., 1997. Ionic remodeling underlying action potential changes in a canine model of atrial fibrillation. *Circ. Res.* 81, 512–525.
- Yue, L., Melnyk, P., Gaspo, R., Wang, Z., Nattel, S., 1999. Molecular mechanisms underlying ionic remodeling in a dog model of atrial fibrillation. *Circ. Res.* 84, 776–784.
- Yusuf, S., Healey, J.S., Pogue, J., Chrolavicius, S., Flather, M., Hart, R.G., Hohnloser, S.H., Joyner, C.D., Pfeffer, M.A., Connolly, S.J., 2011. Irbesartan in patients with atrial fibrillation. *N. Engl. J. Med.* 364, 928–938. doi:10.1056/NEJMoa1008816
- Zaha, V.G., Young, L.H., 2012. AMP-Activated Protein Kinase Regulation and Biological Actions in the Heart. *Circulation Research* 111, 800–814. doi:10.1161/CIRCRESAHA.111.255505
- Zicha, J., Dobesová, Z., Kunes, J., 2001. Relative deficiency of nitric oxide-dependent vasodilation in salt-hypertensive Dahl rats: the possible role of superoxide anions. *J. Hypertens.* 19, 247–254.
- Zong, H., Ren, J.M., Young, L.H., Pypaert, M., Mu, J., Birnbaum, M.J., Shulman, G.I., 2002. AMP kinase is required for mitochondrial biogenesis in skeletal muscle in response to chronic energy deprivation. *Proc. Natl. Acad. Sci. U.S.A.* 99, 15983–15987. doi:10.1073/pnas.252625599
- Zou, Y., Komuro, I., Yamazaki, T., Kudoh, S., Aikawa, R., Zhu, W., Shiojima, I., Hiroi, Y., Tobe, K., Kadowaki, T., Yazaki, Y., 1998. Cell type-specific angiotensin II-evoked signal transduction pathways: critical roles of Gbetagamma subunit, Src family, and Ras in cardiac fibroblasts. *Circ. Res.* 82, 337–345.

7. APPENDIX

7.1. PUBLICATIONS

1. **Chilukoti RK**, Mostertz J, Bukowska A, Aderkast C, Felix SB, Busch M, Völker U, Goette A, Wolke C, Homuth G, Lendeckel U. Effects of irbesartan on gene expression revealed by transcriptome analysis of left atrial tissue in a porcine model of acute rapid pacing *in vivo*. *Int J Cardiol.* **2013 Oct 3;168(3):2100-8. doi: 10.1016/j.ijcard.2013.01.007. Epub 2013 Feb 12.**
2. Subramaniam S, Sreenivas P, Cheedipudi S, Reddy VR, Shashidhara LS, **Chilukoti RK**, Mylavarapu M, Dhawan J. Distinct transcriptional networks in quiescent myoblasts: a role for Wnt signaling in reversible vs. irreversible arrest. *PLoS One.* **2013 Jun 3;8(6):e65097. doi: 10.1371/journal.pone.0065097. Print 2013.**
3. Warsow G, Endlich N, Schordan E, Schordan S, **Chilukoti RK**, Homuth G, Moeller MJ, Fuellen G, Endlich K. PodNet, a protein-protein interaction network of the podocyte. *Kidney Int.* **2013 Jul;84(1):104-15. doi: 10.1038/ki.2013.64. Epub 2013 Apr 3.**
4. Bis JC, Kavousi M, Franceschini N, Isaacs A, Abecasis GR, Schminke U, Post WS, Smith AV, Cupples LA, Markus HS, Schmidt R, Huffman JE, Lehtimäki T, Baumert J, Münzel T, Heckbert SR, Dehghan A, North K, Oostra B, Bevan S, Stoegeger EM, Hayward C, Raitakari O, Meisinger C, Schillert A, Sanna S, Völzke H, Cheng YC, Thorsson B, Fox CS, Rice K, Rivadeneira F, Nambi V, Halperin E, Petrovic KE, Peltonen L, Wichmann HE, Schnabel RB, Dörr M, Parsa A, Aspelund T, Demissie S, Kathiresan S, Reilly MP, Taylor K, Uitterlinden A, Couper DJ, Sitzer M, Kähönen M, Illig T, Wild PS, Orru M, Lüdemann J, Shuldiner AR, Eiriksdottir G, White CC, Rotter JI, Hofman A, Seissler J, Zeller T, Usala G, Ernst F, Launer LJ, D'Agostino RB Sr, O'Leary DH, Ballantyne C, Thiery J, Ziegler A, Lakatta EG, **Chilukoti RK**, Harris TB, Wolf PA, Psaty BM, Polak JF, Li X, Rathmann W, Uda M, Boerwinkle E, Klopp N, Schmidt H, Wilson JF, Viikari J, Koenig W, Blankenberg S, Newman AB, Witteman J, Heiss G, Duijn C, Scuteri A, Homuth G, Mitchell BD, Gudnason V, O'Donnell CJ; CARDIoGRAM Consortium. Meta-analysis of genome-wide association studies from the CHARGE consortium identifies common variants associated with carotid intima media thickness and plaque. *Nat Genet.* **2011 Sep 11;43(10):940-7. doi:10.1038/ng.920.**
5. Bukowska A, Hammwöhner M, Sixdorf A, Schild L, Wiswedel I, Röhl FW, Wolke C, Lendeckel U, Aderkast C, Bochmann S, **Chilukoti RK**, Mostertz J, Bramlage P, Goette A. Dronedarone prevents microcirculatory abnormalities in the left ventricle during atrial tachypacing in pigs. *Br J Pharmacol.* **2012 Jun;166(3):964-80. doi: 10.1111/j.1476-5381.2011.01784.x.**
6. Kabgani N, Grigoleit T, Schulte K, Sechi A, Sauer-Lehnen S, Tag C, Boor P, Kuppe C, Warsow G, Schordan S, Mostertz J, **Chilukoti RK**, Homuth G, Endlich N, Tacke F, Weiskirchen R, Fuellen G, Endlich K, Floege J, Smeets B, Moeller MJ. Primary cultures of glomerular parietal epithelial cells or podocytes with proven origin. *PLoS One.* **2012;7(4):e34907. doi: 10.1371/journal.pone.0034907. Epub 2012 Apr 18.**

7. **Ravi Kumar Chilukoti**, Josefine Linke, Christian Scharf, Kirsten Utpatel, Katja Evert, Alicja Bukowska, Barbara Peters, Daniel Galla, Uwe Völker, Andreas Goette, Carmen Wolke, Georg Homuth, and Uwe Lendeckel. Transcriptome and Proteome Characterization of Dronedarone-Treated Myocardium in a Porcine Model of Myocardial Infarction: Role of matricellular protein Periostin as the trigger of the feedback mechanisms in the ongoing infarct healing process. *In preparation*.
8. Jessica Mühlhaus, Juliane Dinter, Daniela Nürnberg, Maren Rehders, **Ravi Kumar Chilukoti**, Georg Homuth, Chun-Xia Yi, Silke Morin, Josef Köhrle, Klaudia Brix, Matthias Tschöp, Gunnar Kleinau, Heike Biebermann. Analysis of trace amine-associated receptor 8 (TAAR8) mediated signaling pathways. *Submitted to International Journal of Molecular Sciences*.
9. Ravi Kumar Chilukoti, Carolin Malsch, Sabine Ameling, Tim Kacprowski, Elke Hammer, Ulrike Lissner, Stefan Weiß, Georg Homuth, Volkmar Liebscher and Uwe Völker. Circulating microRNA profiling for identification of potential biomarkers of BMI, age and sex according to continuous variables in SHIP-Trend cohort. *In preparation*.
10. Erik Richter, Manuela Harms, Katharina Ventz, Philipp Gierok, **Ravi Kumar Chilukoti**, Jan-Peter Hildebrandt, Jörg Mostertz, Falko Hochgräfe. A multi-omics approach revealed cell-specific effects of Hla-mediated cytotoxicity in airway epithelial cells. *In preparation*

7.2. CONTRIBUTIONS TO SCIENTIFIC MEETINGS

Effects of irbesartan on gene expression revealed by transcriptome analysis of left atrial tissue in a porcine model of acute rapid pacing in vivo

U. Lendeckel, **R.K. Chilukoti**, J. Mostertz, A. Bukowska, S.B. Felix, M. Busch, U. Völker, A. Goette, C. Wolke, and G. Homuth

POSTER SESSION ON BEHALF OF THE WORKING GROUP ON CARDIACCELLULAR ELECTROPHYSIOLOGY.EHRA EUROPACE 2013, 23 Jun 2013–26 Jun 2013, Athens–Greece.

7.3. ORIGINAL ARTICLES

7.4.

Hiermit erkläre ich, dass diese Arbeit bisher von mir weder an der Mathematisch-Naturwissenschaftlichen Fakultät der Ernst-Moritz-Arndt-Universität Greifswald noch einer anderen wissenschaftlichen Einrichtung zum Zwecke der Promotion eingereicht wurde.

Ferner erkläre ich, dass ich diese Arbeit selbständig verfasst und keine anderen als die darin angegebenen Hilfsmittel und Hilfen benutzt und keine Textabschnitte eines Dritten ohne Kennzeichnung übernommen habe.

Ravi Kumar Chilukoti

7.5. CURRICULUM VITAE



Ravi Kumar Chilukoti

Phone: 03834 86 5883

Fax: 03834 86 795871

e-mail: ravi@uni-greifswald.de

Official address:	Universitätsmedizin Greifswald (University of Greifswald) Department of Functional Genomics, Friedrich-Ludwig-Jahn-Straße 15 17487 Greifswald
Date of birth:	20.11.1978
Place of birth:	Peteru, India
Marital status:	Married

Career (Education, Training, Employment)

1996-1999	Bachelor of Science in Microbiology, Bio-Chemistry and Nutrition from Acharya Nagarjuna University, Nagarjuna Nagar, Guntur, India.
1999-2001	Master of Science in Microbiology from Acharya Nagarjuna University, Nagarjuna Nagar, Guntur, India.
2002-2006	Project Research Fellow at Center for Cellular and Molecular Biology (CCMB), Hyderabad, India
2006-2007	Scientist in VIMTA Life Sciences, Hyderabad, India
2007-2008	Group Leader-Genomics in VIMTA Life Sciences, Hyderabad, India
Since 2008	Department of Functional Genomics, University of Greifswald, Germany

Main Research Focus

Research Interests	
Cardiovascular research (Molecular mechanisms of Atrial fibrillation), Biomarker Screening/validation using genomics approaches and Personalized Medicine	
Skills & Expertise	
Genomics:	Transcriptome/miRNA profiling analysis using Affymetrix/Agilent arrays, GWAS/SNP genotyping/CNV analysis using Affymetrix/SEQUENOM MassARRAY/DNA sequencing/TaqMan/Exiqon LNA
Proteomics:	Gel-free/gel-based Protein expression analysis using LC-MSMS/ABI 4800 MALDI TOF-TOF
Cell culture:	HL-1, HUVEC, SMC, Primary Cardiac Fibroblasts, HEK 293
Data Analysis tools:	Rosetta Resolver, Gene data, Expression Console & Genotyping Console (Affymetrix), Rosetta Elucidator, Proteome Discoverer, Scaffold3, PDQUEST Advanced, GPS Explorer, MASCOT, Proteome Discoverer 1.2, SOURCERER, PLINK, Quicktest, SNPTTEST, Metal, Haploview, WGAVIEWER, R (basic script writing knowledge), TIGR-MIDAS, TIGR-MeV, Copy Caller, Array Assist (Avadis), Data Assist, AGCC, GCOS v1.4, GTYPE, Netaffix, CNAT, Sequencing Analysis 5.2, Gene tool, Bioedit, Graph Pad Prism, MS-office (Excellent command over MS-Excel, MS-Access)
Pathway Profiling:	IPA (Ingenuity Pathway Analysis), GenMAPP v2.1, Panther
Independent Coursework (Post Graduate Diploma in Computer Applications)	
Front and back end (RDBMS):	C, C++, FORTRAN, COBOL, and ORACLE 8i.
Professional Memberships	
HNCIG (Head and Neck Cancer Interest Group)	

7.6. ACKNOWLEDGEMENTS

First and foremost, my sincere thanks to Prof. Dr. Uwe Völker for granting me the chance to pursue my doctoral studies. I express my sincere gratitude to him for allowing me to use the excellent technical equipment in the Department of Functional Genomics.

I would like to express my sincere thanks and gratitude to Prof. Dr. Uwe Lendeckel from the bottom of my heart for providing the chance to work on the AF-related topics and notably, for the mentoring and valuable discussions. In particular, I can not forget his support, motivation and kind help extended to me in challenging times.

Further, I'm thankful to Dr. Georg Homuth for his invaluable support provided within and beyond the lab, especially during the life threatening troubles in my personal life. In addition, for assigning me projects on variety of topics that have broadened my knowledge.

Another person who has to be mentioned with special note Mr. Marc Schaffer, a god given brother to me. I do not have words to mention his support and care. I cannot even imagine where I would be today if Marc is not behind me. I'll remember his support throughout my life. In this regard, I thank Anja and Florian-Sandra Ernst as well for the kind support.

I'm thankful to Dr. Elke Hammer for helping me in performing *in vitro* studies using HL-1, L929 and fibroblasts. Additionally, she kindly extended her constant support and encouragement in other projects too. In this regard, I'm thankful to Sophie, Ulrike Lissner and Katrin Darm as well.

I'm thankful to Dr. Jörg Mostertz and Dr. Alexander Teumer for the timely guidance and support.

I'd like to thank all colleagues from Prof. Dr. Uwe Lendeckel's lab, in particular, Dr. Carmen Wolke, Josephine Linke and Christian Anderkast for the kind help in validating *in vivo* and *in vitro* results.

I like to thank all all supervisors and colleagues of co-operation projects, in particular to Professor Dr. Jens Kockskämper, Professor Andreas Goette, Prof. Dr. rer. nat. habil. Reinhard Walther, Prof. Dr. med. Stephan Felix, Prof. Dr. Nicole Endlich and Prof. Dr. Karlhans Endlich.

Furthermore, I thank all my friends and colleagues of AG Functional Genomics, in particular Praveen, Rasmita, Nicholas Ehlers, Claudia, Dr. Leif Steil, Dr. Ulrike Maider, Hermann, Carolin, Janine, Priyanka, Ramesh, Kumar, Dhople, Tej, Gaurav, Nanda, Nithya, Maren, Sabine, Anna, Tanja, Stephan Michalik and Tim... for the nice working atmosphere

that made my six years tenure a memorable one with many joyful moments. I thank to Dr. Ronny Michel for taking care of my health.

I like to thank with a special note to my grandfather Mr. Janam Viswanatha Rao, Ex-Director, CITD, Hyderabad and Dr. Ramesh K. Aggarwal, Group Leader, CCMB, Hyderabad for the timely encouragement and suggestions that helped me to grow-up in my career.

And last but not least, sincere thanks are given to my parents, for the encouragement and care in every moment of my life.

7.7. SUPPLEMENTARY TABLES OF IRBESARTAN STUDY

The following supplemental data is included in the form of a digital appendix (CD):

7.7.1. Supplementary table 1 (RAP)

List of probe sets indicating significantly different gene expression under Rapid atrial pacing (RAP) conditions as compared to control (sham) conditions. ANOVA p-values are given in column “ANOVA P-value”, results of the signal correction statistics of the “Ratio Builder” software are given in the column “RB P-value”, and expression fold changes in the column “Fold Change”. The following significance criteria were applied: ANOVA p-value ≤ 0.05 ; signal correction statistics of the “Ratio Builder” software: $p \leq 0.05$; expression fold-change ≥ 1.5 .

7.7.2. Supplementary table 2 (RAP/I)

List of probe sets indicating significantly different gene expression under rapid atrial pacing in the presence of irbesartan (RAP/I) conditions as compared to control (sham) conditions. ANOVA p-values are given in column “ANOVA P-value”, results of the signal correction statistics of the “Ratio Builder” software are given in the column “RB P-value”, and expression fold changes in the column “Fold Change”. The following significance criteria were applied: ANOVA p-value ≤ 0.05 ; signal correction statistics of the “Ratio Builder” software: $p \leq 0.05$; expression fold-change ≥ 1.5 .

7.7.3. Supplementary table 3 (Overlap)

List of probe sets indicating overlap between RAP and RAP/I conditions as compared to control (sham) conditions. ANOVA p-values are given in column “ANOVA P-value”, results of the signal correction statistics of the “Ratio Builder” software are given in the column “RB P-value”, and expression fold changes in the column “Fold Change”. The following significance criteria were applied: ANOVA p-value ≤ 0.05 ; signal correction statistics of the “Ratio Builder” software: $p \leq 0.05$; expression fold-change ≥ 1.5 .

7.7.4. Supplementary table 4 (genes affected by Irbesartan)

List of probe sets indicating irbesartan-mediated attenuation of RAP-induced differential gene expression (151 gene-specific probe sets = 144 genes = 25.7%).

ANOVA p-values are given in column “ANOVA P-value”, results of the signal correction statistics of the “Ratio Builder” software are given in the column “RB P-value”, expression fold changes in the column “Fold Change” and percentage of RAP-induced attenuation in the column “% of irbesartan-mediated attenuation”. The following significance criteria were applied in both conditions: ANOVA p-value ≤ 0.05 ; signal correction statistics of the “Ratio Builder” software: $p \leq 0.05$; expression fold-change ≥ 1.5 ; a minimum of 15% attenuation of RAP-induced change by irbesartan in RAP/I.